# DESIGN AND ANALYSIS OF A FRICTION STIR WELDING MACHINE FOR TUBE TO TUBE-SHEET WELDING APPLICATION

BY

**Mohammedanas Ibrahim Tuffaha**

A Thesis Presented to the

DEANSHIP OF GRADUATE STUDIES

**KING FAHD UNIVERSITY OF PETROLEUM & MINERALS**

DHAHRAN, SAUDI ARABIA

In Partial Fulfillment of the
Requirements for the Degree of

## MASTER OF SCIENCE

In

**MECHANICAL ENGINEERING**

**December 2017**

KING FAHD UNIVERSITY OF PETROLEUM & MINERALS
DHAHRAN- 31261, SAUDI ARABIA
**DEANSHIP OF GRADUATE STUDIES**

This thesis, written by **Mohammedanas Tuffaha** under the direction of his thesis advisor and approved by his thesis committee, has been presented and accepted by the Dean of Graduate Studies, in partial fulfillment of the requirements for the degree of **MASTER OF SCIENCE IN MECHANICAL ENGINEERING.**

Dr. Abdelaziz Bazoune
(Advisor)

Dr. Zuhair Gasem
Department Chairman

Dr. Nesar Merah
(Member)

Dr. Salam A. Zummo
Dean of Graduate Studies

Dr. Fadi Al-Badour
(Member)

6/5/18
Date

# *Dedication*

بسم الله الرحمن الرحيم

قُلْ إِنَّ صَلَاتِي وَنُسُكِي وَمَحْيَايَ وَمَمَاتِي لِلَّهِ رَبِّ الْعَالَمِينَ

*To the dearest to my heart, my mother, father, brothers, and sisters*

*To the woman that raised me, my grandmother*

*To those I think about even though they left this world, my dear grandfather*

*and my cousin Mahmoud*

*To all those who have helped me*

*To all my friends and colleagues*

*To all of them,*

*I dedicate this work*

# ACKNOWLEDGMENTS

To begin with, I thank the one and only Almighty Allah for giving me more than I can ever deserve and for guiding me in my life journey to where I have reached.

I would like to start out my acknowledgement by expressing my deep appreciation to my thesis advisor **Dr. Abdelaziz Bazoune** for helping me with advice and guidance to complete this work. I thank him for all the effort and valuable time he spent helping me and his patience.

I would like to send a special thanks to the Mechanical Engineering Department represented by the chairman **Dr. Zuhair Gasem**. I would also like to thank the committee members, **Dr. Nesar Merah** and **Dr. Fadi Al-Badour** for their suggestions and interest in my work, and their help and advice.

Furthermore, I would also like to thank **Dr. AbdelRahman Shuaib** for all his help and support.

I appreciate and honor KFUPM for accepting me and for giving me the opportunity of a life time. I am pleased to have studied in this great university.

Last of all, I can never thank enough my family and friends for always standing by my side and being there, I will always cherish this feeling. I will always be in debt to them for all the hardships they had to go through in order for me to succeed. I would never have reached to where I am without their prayers and their help.

# TABLE OF CONTENTS

# LIST OF TABLES

# LIST OF FIGURES

# LIST OF ABBREVIATIONS

| | | |
|---|---|---|
| **FSW** | : | Friction Stir Welding |
| **FSWM** | : | Friction Stir Welding Machine |
| **GTAW** | : | Gas Tungsten Arc Welding |
| **HEX** | : | Heat Exchanger |
| **CNC** | : | Computer Numerical Control |
| **CAD** | : | Computer Aided Design |
| **CAM** | : | Computer Aided Manufacturing |
| **FEA** | : | Finite Element Analysis |
| **FBD** | : | Free Body Diagram |
| **EOM** | : | Equation of Motion |
| **GUI** | : | Guided User Interface |
| **VFD** | : | Variable Frequency Drive |
| **FEM** | : | Finite Element Method |

# ABSTRACT

Full Name : Mohammedanas Tuffaha
Thesis Title : Design and Analysis of a Friction Stir Welding Machine for Tube to Tube-Sheet Welding Application
Major Field : Mechanical Engineering
Date of Degree : [December 2017]

In this work, a design and analysis of a Friction Stir Welding (FSW) machine is performed for tubes to tube-sheet welding applications. The design accounts for machine mobility, ability to perform straight and contour welding, as well as welding precision. The designed machine is then studied in terms of static, dynamic and frequency variations using SOLIDWORKS' finite element analysis. Static analysis is performed for various loading conditions to investigate the critical stresses and displacements of the machine. The machine life and damage under cyclic loading are inspected for fatigue analysis. Frequency analysis is carried out providing the resonant frequencies and mode shapes. Dynamic analysis is also simulated providing dynamic motion of a point on the machine under cyclic forces/torque and under different frequencies. These studies were performed for two spindle positions while the machine is either plunging or traversing. A mathematical lumped model of the machine is derived using Lagrange's equation. With the aid of MATLAB software, the natural frequencies as well as the output motion of the machine structure are plotted and compared with those provided by SOLIDWORKS. Very good agreement is found between the two methods of solution.

# ملخص الرسالة

**الاسم الكامل**: محمدأنس ابراهيم فتحي تفاحه

**عنوان الرسالة:** تصميم الة لحام تعمل على مبدأ الاحتكاك و التدوير مخصصة على لحام الانابيب بصفائح الانابيب

**التخصص: هندسة ميكانيك**

**تاريخ الدرجة العلمية**: كانون الاول 2017

تم تصميم الة لحام تعمل على مبدأ الاحتكاك و التدوير لتطبيق لحام الانابيب بصفائح الانابيب. يقوم هذا التصميم على مبدأ متانة الالة و قدرتها على التنقل. بالاضافة الى ذلك يأخذ بالحسبان قدرتها على لحام الاشكال المطلوبة بالسرعات المرغوبة. كما تم القيام بعدة تحاليل باستخدام طريقة العناصر المحددة بمساعدة المتوفرة في برنامج سوليدوركس. ذلك للتأكد من متانة الالة و قدرتها على التحمل كإيجاد الاجهاد و الازاحات على الالة و هي محملة بقوى ساكنة. تم ايضا ايجاد العمر المفترض للآلة. كما تم تحليل و ايجاد الترددات التي قد تسبب في التجاوب وعدم استقرار الالة . أخيرا تم تحليل حركة قاعدة المغزل بوضع الحركي للتأكد انها تعمل باستقرار ضمن الترددات الطبيعية. يستخدم ايضا نموذج رياضي تم انشائه باستخدام معادلة لاجرانج لايجاد ترددات الالة الطبيعية و حركتها بمساعدة من برنامج ماتلاب.

# INTRODUCTION

Friction Stir Welding (FSW) is an attractive relatively new technique invented by the welding institute in 1991. It is used to join two or more parts together using a solid-state environment friendly process. The FSW process is performed by penetrating material (in the joint area) via non-consumable rotating tool comprising a pin and a shoulder and traversing along the joint direction afterwards. Friction caused by the interaction between the tool and the material produces sufficient amount of heat to soften the material. The rotating tool stirs the soft material in the direction of the pin rotation. Throughout this process no fusion or filler material is used and the heat does not reach to the melting temperature of the material. This technique's unique process eliminates a major predicament by facilitating aluminum alloy welding (which is hard to weld by conventional fusion welding). In addition, FSW can be employed to join dissimilar materials. FSW has been proven successful in welding high strength steel, stainless steel, and titanium [1].

## 1.1 Problem Statement

In common practice today, tube to tube-sheet welding is performed by gas tungsten arc welding (GTAW). Special tools and equipment are used for this welding process, which is considered a non-continuous welding process. This means that after welding, a tube to the tube-sheet, as well as the location of the machine needs to be manually adjusted for another welding, which is time consuming when someone has hundreds of welds to be performed. In addition, GTAW means that the parent metals

will reach melting point to bond together. This may cause high stresses in the joint, which requires extra care to prevent cracking.

FSW can be a good alternative to this commonly used welding method. FSW is easily automated and can be used for continuous welding. At the same time, no preheating or post heating is required because friction stir welding operates in solid state, in return resulting in less energy consumption.

Another attribute that FSW can offer is the wide range of controlled parameters. For example, tool rotation and traverse speeds can be controlled easily, to allow material flow and temperature easy to control. There is also a wide range of tool shapes used to enhance weld quality. Last, friction stir weldments do not require grinding, polishing, or straightening[1].

## 1.2 Advantages of Friction Stir Welding

FSW has many advantages that the conventional fusion welding does not provide. One of the main advantages is the low residual stresses found in the weld joint. This may help making the joint harder to crack compared to the conventional fusion welding. Cracks in the weld joint area are considered a challenging problem in heat exchangers industry. FSW may alleviate this problem.

New developments depend on the newly asserted attributes attained by FSW, such as high strength joints, ability to add alloys, high precision of the automated process, and ability to weld complex patterns. These attributes can be utilized by designers to replace (for example) screw-nut fixed joints to friction stir welded joints especially on hard to weld material, widening the range of design flexibility and also granting them an opportunity to simplify their design while maintaining robustness.

In addition, FSW is considered as a quick welding method, that is time saving in many cases. This is due to the fact that material does not have to reach melting point in order to be joined and does not require post heat treatment. Other advantages such as excellent mechanical properties in the joint area and no loss in alloy element mass fraction makes FSW more attractive. Last, it is important to mention that FSW is an environmentally friendly technique that consumes less energy compared to the other welding methods.

## 1.3 Applications of FSW Machine

FSW can be used in many applications. Other than the conventional use of FSW in ship building and aerospace applications, it can also be tested to weld tubes to tube-sheet. Utilizing FSW for welding tubes to tube-sheets provides a new extended look into the wide range of opportunities FSW provides.

FSW showed its superiority in many fields such as pipe line welding, marine applications, material welding, and even aerospace material welding. For example, in pipeline welding, companies such as Orbitalum [2] and Axxair [3] are selling commercial orbital welding mechanisms using TIG welding as a solution. On the other hand, companies like MegaStir [4] and Gatwick Technologies [5] provide FSW machines as an alternative to conventional fusion welding for pipeline welding and many other applications.

Another application that FSW can be used for is joining rails. Masithulela [6] designed a friction stir welding machine for this particular purpose. As the author mentions, the railway business in South Africa can reduce tremendous repair costs by using FSW for sound weld quality and easy labor training.

## 1.4 Tube to Tube-sheet Welding

One of the main uses of the tube to tube-sheet layout is for heat exchangers (HEX). HEX's have a wide range of use in many industries such as chemical plants and power production. Each HEX has a number of tubes which are primarily welded to the tube-sheet. Murali *et al.*[7] worked on providing a layout program that provides the tube count in the HEX.

Tube to tube-sheet welding is performed using gas tungsten arc welding (GTAW). GTAW process needs both electrical supply and an inert gas to operate efficiently. This welding process joins two materials by melting them together.

Several studies are performed today to increase weld quality of the tube to tube-sheet joint. For example, Kim *et al.*[8] studied the effect of the inert gas used to increase corrosion resistance. Moorthy *et al.*[9] evaluated the post weld heat treatment on the welded joint. Unlike FSW, GTAW requires the parent metals to reach melting point (liquid state) to bond together, requiring inert gas to shield this liquefied metal so that it does not react with the environment. In addition to that, due to high temperature, the joint will have a new crystal structure that is relatively hard, requiring post heating. FSW does not necessarily require post heating since material joined using FSW does not reach melting temperature.

# LITERATURE REVIEW

Many heavy duty FSW machines were designed and manufactured by companies such as MTI, TWI, Esab and Gatwick and the number is increasing rapidly in order to respond to the high demand on FSW machines for automated welding in order to minimize the time and cost of welding. Some of these machines perform straight welding while others were built for contour welding.

Most of the FSW machines are computer controlled enabling optimum control over the welding parameters. Companies including MegaStir [4], and Gatwick Technologies Ltd [5] (as mentioned before) worked on designing particular application of FSW machines. These machines are used for specific purposes. They are designed and tested to operate in certain environment conditions (e.g. outdoors) for a specific job. For example, pipeline welding is performed through orbital machines in outdoor environmental conditions. Whereas sheet and plate welding are performed by a three to six axes CNC vertical bridge machine indoors. In addition, researchers are contributing in the design of widespread FSW special application machines. Masithulela's [6] work was based on designing a FSW machine where rail welding is performed by a mobile module that can be transported easily to the operating site.

Gibson *et al*. [10] pointed out that computer numerically controlled milling machines can be used for FSW. However, due to the large required forces, large milling machines would be preferable, providing higher rigidity thus decreasing vibration amplitudes. In addition, special force sensors and data acquisition devices are needed to monitor and control the welding process. The force sensors monitor the three acting

forces in the welding process and the rotational torque induced by the tool rotation. Usually, dynamometers are used for monitoring the forces.

Burford *et al*. [11] provided a FSW assembly with an associated system, controller, and method for the operation. The FSW assembly is like a milling machine with a CNC controller capable of driving the machine tool for FSW. The torque of the FSW is monitored and controlled, therefore, the machine operates at steady torque throughout the welding process by varying the tool's travel and rotational speeds.

## 2.1 FSW Robotic Implementations

FSW control scheme is categorized as either position control, force control, or a combination of both. When the machine is rigid and has the ability to withstand high forces, position control is considered advantageous for the high accuracy it provides. It is important to notice that the material being welded must be clamped and supported securely.

Gibson *et al*. [10] pointed out the attractiveness in using robotics for FSW to obtain flexibility. The authors advised to use commercially available robots rather than custom built machines due to cost effectiveness. Axial force must be accounted for while choosing the compatible robot. One of the disadvantages presented in robots for this specific application is the bend and deflection in the linkages due to the high endured forces. This cannot be detected by the encoders while welding, thus affecting the contact accuracy between the tool and the work piece.

Cook *et al.*[12] showed that force feedback is essential for successful FSW even when using industrial robots with high stiffness. The authors also examined forces and torques associated with FSW. Furthermore, they pointed out that robotic implementation cannot be assumed to be rigid like a milling machine, thus; enabling a

force control scheme. This control scheme would be a closed loop control system with the feedback as a Jacobian relationship between actuator torques and forces.

Backer *et al*.[13] outlined important steps in implementing robotic FSW in industry. They presented robot deflections during FSW using several methods. Force control (which is one of the methods) is needed for a fine welding process to eliminate the effect of deflection inaccuracy. They discussed two types of force control, namely; the direct and indirect force control. Direct force control depends mainly on sending force sensor measurements to a closed loop force controller around the position control loop. This additional force control loop overwrites the position values where force input can be varied. Indirect force control relies basically on the torque-deflection model as demonstrated by Smith [14].

Results from Backer *et al*.[13] and Cook *et al*.[12] commonly depicted a decrease in axial force when spindle speed is increased noting that this is a result of increased heat input causing an increase in material softness. This is considered important because increasing spindle speed (to a certain permitted extent) can be utilized to decrease robot joint deflection. The authors performed tests and found that path deviation increases as side forces increase in value. The deviation was measured by both a camera system and a laser system.

Kusuda [15] shed the light on Honda's new developed FSW technology, which utilizes robotic FSW. A Fanuc M-700 with a C-type FSW gun was applied by Honda to fabricate a sub-frame on the Accord 2013 car model. The produced sub-frame was lighter than previous models possibly because of use of Aluminum instead of steel, in turn contributing to an increase fuel efficiency. The new model was also more rigid than previous models. The new technology adopted by Honda proved advantageous in

productivity in many ways. This includes less electrical energy consumption, no consumables, space saving, and resulting in high strength welding with no distortion.

## 2.2 Machine Modeling and Analysis

Published work in modeling three to five axes operating machines are reviewed [16-25]. Fan *et al*. [16] analyzed a turn milling machine tool using modal analysis in order to investigate the dynamic characteristics of the machine. The results of the study showed that the turn milling machine tool resonant frequencies are much higher than the maximum operating frequency. Ebrahimi *et al*. [17] analyzed the stiffness in machine tool drives, using different approaches to simulate the linear and nonlinear models of the tool drive. In addition, a comparison was made between the two models. The drives analyzed by the authors can be compared with the analysis of the drive modules in the FSWM. Each drive in the machine can be mathematically modeled separately such as the work published by Carbajal *et al*. [18] and Leonard-Cristian Pop [19]. These mathematical models [17-18] represent a single axis motion of the machine assuming that no deflection occurs in the beams carrying these drives. This study can be performed for the sole reason of controlling the power input to obtain the desired speed and torque output.

Dynamic analysis on a FSWM is scarce in literature even for plain bridge type machines. Bridge type FSWM can be modeled similarly to milling machines as stated before but forces cannot be considered alike. In this proposed work, the analysis will be performed on a uniquely oriented FSWM where the orientation will have significant changes in the mathematical model since the spindle is mounted horizontally.

Many researchers modeled different types of systems with a variety of configurations in order to obtain equations of motion, natural frequencies, mode shapes,

and simulate the output response [20-25]. Authors such as Sciavicco *et al.*[20] and Chen [21] used Lagrange's equation to derive the equations of motion for robot manipulators. Le *et al*. [22] modeled a parallel-mechanism-based meso-milling machine tool using Lagrange's equation. Huo *et al*. [23] performed integrated dynamic design and modeling on ultra-precision micro-milling machines to find the natural frequencies using the block Lanczos method. Mode shapes were described based on the motion of the x, y, or z sliding components. The authors also noted that in conventional precision machine design, the first natural frequency is expected to be higher than the machine operating frequency. This indicates that the machine will operate in a safe region below resonance.

Hung *et al*. [24] modeled the spindle of a vertical milling machine using the finite element method. The model considered ball screw as a shaft and the rolling guide to have two ball grooves (instead of four). Estimated frequencies were close to the experimental ones. Modal analysis was also conducted for both pitch and yaw rotational coordinates showing the amplitude of each at natural frequency. The results of the FEA was used to determine the dynamic performance of the machine and its stability.

Tian *et al*.[25] compared simulated and experimental natural frequencies for a virtual material fixed joint interface. The investigated case in the author's work was a milling machine tool gantry beam-column specimen. The natural frequencies were identified by modal hammering impact testing experimental method and two simulated models. It was shown that the material natural frequency slightly changed with increase in in hammering torque. Furthermore, it was observed that element natural frequencies slightly decrease with the increase of the elements thickness. The authors were also able to obtain the mode shapes for the specimen by using the virtual material and the experimental specimen.

One of the basic goals desired from modeling is the prediction of output response under specified reference input according to certain functional requirements. Output response can be shown as a time-amplitude relation. Amplitude can be displacement, velocity, or acceleration depending on the desired study. Change in amplitude can vary with change in input forces or initial conditions. It is important that the response amplitude range is acceptable under a certain force range that the machine operates in. This ensures that the machine is designed according to functional requirements or specifications (such as precision).

## 2.3 Machines Used For FSW

FSW machines are classified based on their capabilities. These capabilities must be found according to the application FSW is used for. For example, welding two metallic pieces with different thicknesses requires the machine to provide a tilt angle while welding. Mendes *et al*. [26] stated six classifications for the machine namely:

1- Force capability

2- Stiffness and accuracy capability

3- Sensing capability

4- Decision making capability

5- Flexibility capability

6- Application of use

The above classifications give a clear idea of the machine capabilities needed to perform the required welding. There are some factors that must be known before choosing the classifications of the machine. These include workpiece material type, weld joint geometry complications, tool geometry and material, distance of penetration needed, and automation scheme. For example, if the geometry of the joint is

complicated, then high machine flexibility is required. It should be noted that sometimes concentrating on a certain classification can impact negatively on another. In some cases, high flexibility means that machine accuracy is decreased due to lower stiffness. This makes selecting the classifications a trade-off.

Moreover, Mendes *et al*. [26] mentioned three types of FSWMs reported in literature. The first type is the conventional machine tool or milling machine. These milling machines may be modified to improve several of its classifications. Mainly, stiffness, flexibility, and force control are improved. One main disadvantage is that this type of FSWMs cannot be used for mass production. They are advantageous when it comes to welding different lengths and thicknesses and are recommended for low flexibility high stiffness applications.

The second type of FSWMs are the dedicated type which are built for special purposes and applications. When large mass production is needed, this type is the optimum solution. Classifications of these machines are designed according to the application and the specific task it needs to perform. Many studies nowday concentrate on making this type of machines portable.

The third type of FSWMs are the robotic type which are highly flexible but has very low stiffness. Robotic FSWMs are categorized as either articulated arm robots or parallel kinematic robots. Articulated arm robots are more flexible and lower in cost, and have higher work volume than the parallel kinematic robot. On the other hand, they withstand less loads, and have lower stiffness.

Okawa *et al*. [27] developed a 5-axis FSWM that can be categorized as a dedicated type. The main upgrades that were introduced is the use of air cylinders to maintain pressure on the tools, and the software that reads the path of the weld joint to later perform welding on the same line. The machine proposed by the author had two heads,

a 2-D and a 3-D head. The author reported specifications of both heads and their applications.

The software developed by Okawa *et al*. [27] stores the readings of the 3-D points obtained by a 3-D coordinates measuring instrument. These readings will then be fed to the NC program that will move the FSWM tool on this same path. The software was tested showing welding results on a 3-D plane.

Lijin *et al*. [28] presented a new design for a robotic arm for FSW purposes. The main addition is this design is the parallelogram structure for the arms, where the goal is to increase the stiffness. The author also mentioned backlash minimization by using feedforward compensation. The structure of the electric cylinder actuators were described in detail, in addition to the rotary unit, and the robot wrist. In the design, the stiffness of the robot was evaluated through FEA, and by using Castilliano's theorem.

Lijin *et al*. [28] calculated the stiffness of the arms at four different positions. The author's design had much higher stiffness compared with the FANUCS 900iBl400 robot. The disadvantage of the design proposed by Lijin *et al.* [28] is that it weighs 1000kgs more than the FANUC robot arm.

## 2.4 Tube to Tube-Sheet Welding Methods

Currently, tube to tube-sheet welding is performed by repositioning the GTAW welding device on to each separate tube manually. This is a time-consuming process that relies on the operator work speed, skills and experience. New alternatives that can eliminate this manual process is sought. Batistoni *et al.* [29] provided a method for automatically welding tubes to tube-sheet by moving the torch continuously between the joint contours without turning it off. While the torch is traveling between the joint contours, its current is decreased to produce partial fading of the arc.

Monley [30] provided a continuous method for arc welding tubes to a tube-sheet. The torch is moved in a certain direction based on a probe that provides the location of each tube and its diameter. The movement will be contoured on the welded joint then straight till the next tube is reached. Monley [30] shows the apparatus that can be utilized for continuous welding in addition to the various continuous weld paths that can be encountered. His method of motion feedforwarding can be combined with Batistoni *et al*. [29] method of lowering the current while traveling between welding joints.

Eller *et al*. [31] proposed a method for friction stir welding tube ends for a heat exchanger. Basically, what the authors introduced was an anvil that is situated inside the tube then jammed by and anchor and a washer. This method is especially useful for ensuring that the tube is fixed while enduring the plunging force of the FSW tool.

Al-Badour *et al* [32] experimented friction stir seal welding on tube to tube-sheet joints using 6xxx-series aluminum. The author pointed out that parameters such as weld speed and tool offset affect the weld quality, where low weld speeds increased the size of the HAZ, while high weld speeds increase weld defects. Furthermore, increasing weld quality is obtained when the center of the pin tool is offset from the tube–tubesheet interface by an amount lower than 40% of the pin diameter.

Shuaib *et al* [33] investigated friction stir seal welding tube-tubesheet joints made of steel. The tube material is ASTM 179 seamless cold-drawn carbon steel while the tube-sheet material is ASTM A516 Grade 70. Sound welds were achieved, and tool wear was documented. Shuaib *et al* [34] also provided an apparatus for joint sealing using tube expansion and friction welding

## 2.5 Objectives

The main objective of this work is to design a FSW mobile automated machine that enables the FSW of tubes to the tube-sheet joints. The design process consists of several steps to make certain of the machine's performance and endurance. These steps include the design approach, analysis, and modifications.

The design approach focused on the concept of assembling a preliminary machine from smaller units (sub-assemblies) based on importance. The machine components are specified in terms of type and brand.

Four types of analyses are then conducted on the preliminary design using SOLIDWORKS' finite element method. They are static, fatigue, frequency, and dynamic analysis. The machine's strength and deformation under static loads are inspected, while the fatigue investigation predicts the machine's life under cyclic loads. Frequency analysis provides the natural frequencies of the model and the dynamic study shows the machine's behavior while observing loads with forced frequencies.

Based on the results obtained from the analyses, the design undergoes modifications to make the machine function more accurately at specified loads in a safe frequency range.

A mathematical model was developed to further study the dynamic behavior of the machine under different loading conditions. The resonant frequencies are identified to avoid resonant conditions of the machine. The dynamic response is compared to the simulated one obtained from the SOLIDWORKS' finite element model to validate the actual findings.

# MACHINE DESIGN

This work proposes a new dedicated type machine utilizing FSW to join tubes to tube-sheets. This machine is designed to operate and perform welding of tube to tube-sheet with curved contours while maintaining robustness. Proper design stages and performing the required analysis ensures the machine's ability to perform the desired welding. Necessary modifications made whenever possible based on the analysis results to increase robustness.

## 3.1 Design Approach

The machine design approach followed in the study is based on the analysis of the design parameters and the functional requirements of each component of the machine. Machine components were selected and assembled to perform the proper tasks. These components are geometrically synchronous and properly assembled.

### 3.1.1 Machine Visualization and Design Parameters

The proposed machine must fit for welding tubes to tube-sheets. It is oriented and operated to travel in the same plane (parallel) as the work piece. Meanwhile, plunging will be perpendicular to the travel plane.

Welding process requires the tool to rotate and traverse in three axes to weld a contoured joint. For the tool to rotate, a spinning spindle and a motor are required. For traverse motion, modular linear actuators with motors are required in the x, y, and z-

directions. These parts and modules are mounted and coupled properly to satisfy functional requirements of the machine. Figure 3-1 shows the main parts and modules of the machine operating in the working plane.

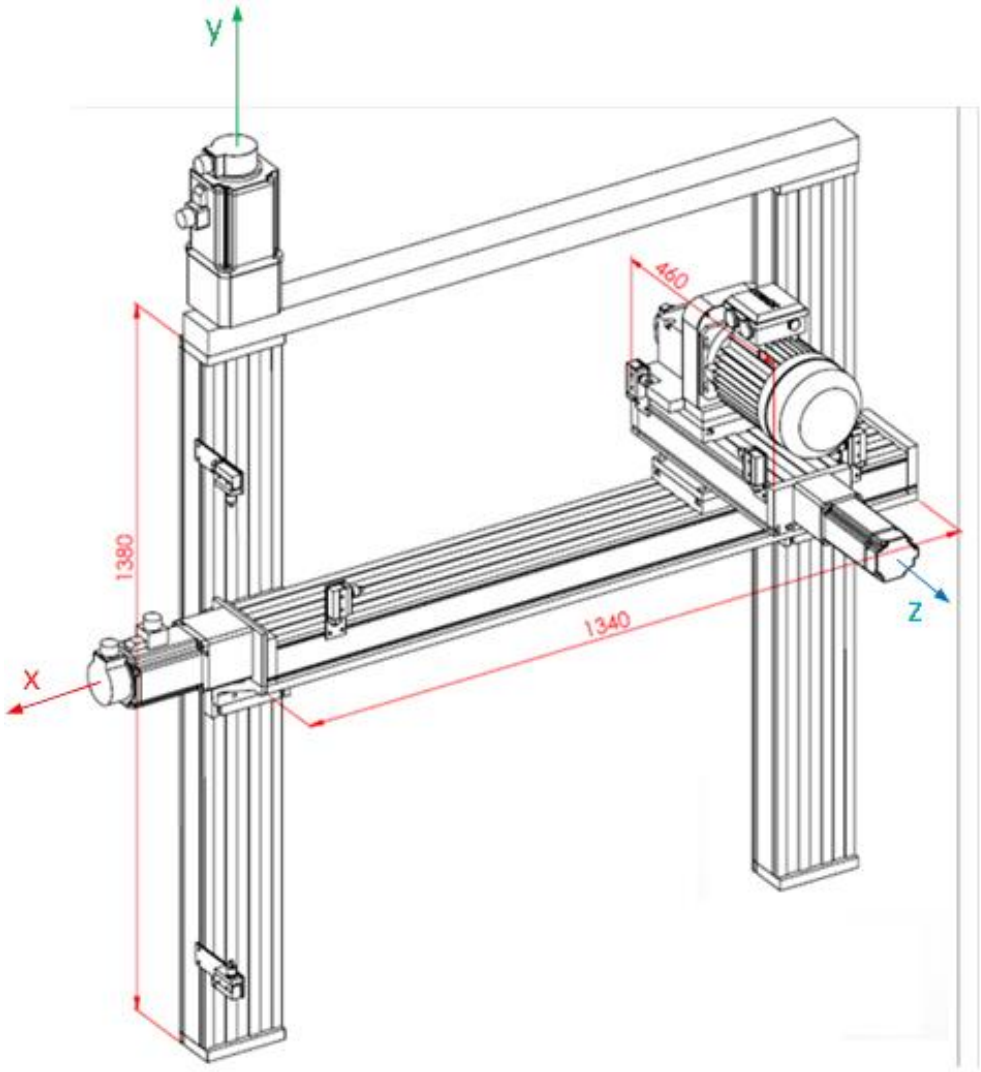


**Figure 3-1: Horizontal Spindle Mount Machine**

Figure 3-1 represents the main sub-assembly of the proposed machine comprising the main components that transmit linear and rotary motion. This dynamic sub-assembly moves the rotating spindle in linear x, y, and z-directions using linear modular actuators. The actuators convert the rotating motion provided from the electric

motors to the desired linear motion by a ball screw mechanism. Furthermore, this dynamic sub-assembly is mounted on a rigid mobile chassis (will be shown in detail later in this chapter). This sub-assembly, will be further mounted with others, resembling a full machine designed for welding tubes to tube-sheets.

Preliminary design parameters shown in Table 3-1 are based on observations and previously conducted studies and analyses performed at KFUPM [35] [36], and literature [37].

**Table 3-1: Machine Design Parameters [32-33]**

| **Parameter** | **Unit** | **Process** |
|---|---|---|
| **Forces** | [N] | $F_x > 650$ (x-direction)<br>$F_y > 750$ (y-direction)<br>$F_z > 1800$ (z-direction) |
| **Torque** | [N. m] | $T_z > 40$ (about z-axis) |
| **Traverse Distance** | [mm] | $S_x = 550$ (x-direction)<br>$S_y = 750$ (y-direction)<br>$S_z = 150$ (z-direction) |
| **Traverse Speed** | [mm/s] | **Loaded** |
| | | $V_{xmax} = 10$ (x-direction)<br>$V_{ymax} = 10$ (y-direction)<br>$V_{zmax} = 5$ (z-direction) |
| | | **Idle** |
| | | $V_{xmax} = 100$ (x-direction)<br>$V_{ymax} = 100$ (y-direction)<br>$V_{zmax} = 100$ (z-direction) |
| **Spindle Rotational Speed** | [rpm] | $200 < SS < 2000$ [34] |
| **Temperature** | [°C] | Tool tip temperature may exceed 1200 degree Celsius |

The inputs and outputs of the machine are specified to meet these required parameters. As for the inputs, the machine will run as a CNC machine using G-code as

input commands. Additional inputs are switches, push buttons, and calibration tools. The outputs are the machine feed speeds, the ability to penetrate and traverse along the material, spindle speed, and travel path.

The minimum force/torque requirements for the machine were obtained by testing out a tube to tube-sheet sample at KFUPM FSW machine with an attached load cell (MTI Inc.) showing the maximum forces ($F_{xmax}, F_{ymax}, F_{zmax}$) in x, y, and z-directions respectively in addition to the maximum spindle torque used. Spindle speed is also selected to have a range compatible with welding of steel components.

Throughout the design stage, parameter values have been accounted. These values were utilized to obtain the desired output with minimum error.

### 3.1.2 Machine Components (Module Specification and Design)

The designed machine consists of six main sub-assemblies. These sub-assemblies are properly mounted and coupled together enabling the machine to work properly and efficiently. Some are of greater significance than others for machine operation. These are mentioned below (Figure 3-2) with the dependency factor differentiating between the most important ones (which is first mentioned).

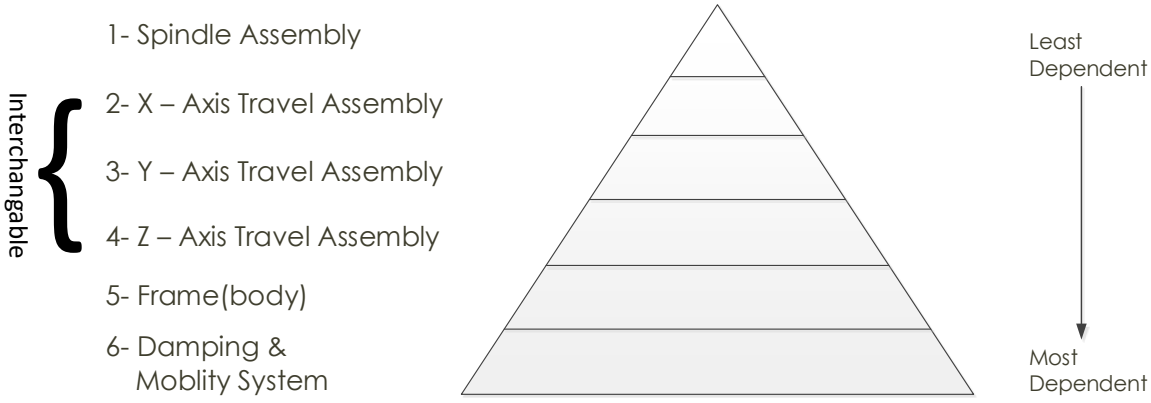


**Figure 3-2: Dependency Diagram**

**Module 1: Spindle Assembly**

Figure 3-3 represents the first sub-assembly for the proposed FSW machine. It comprises the spindle (fixed on the z-axis linear actuator). The spindle is the most important module because all other sub-assemblies depend on its function, geometry, and load endurance. The spindle has an approximate maximum diameter of 30 cm and a total length ranging between 40-50 cm working on nearly 4 kW power. The torque at rated speed of 1500 rpm will be around 24 N.m with maximum torque reaching 40 N.m (as shown in Table 3-1).

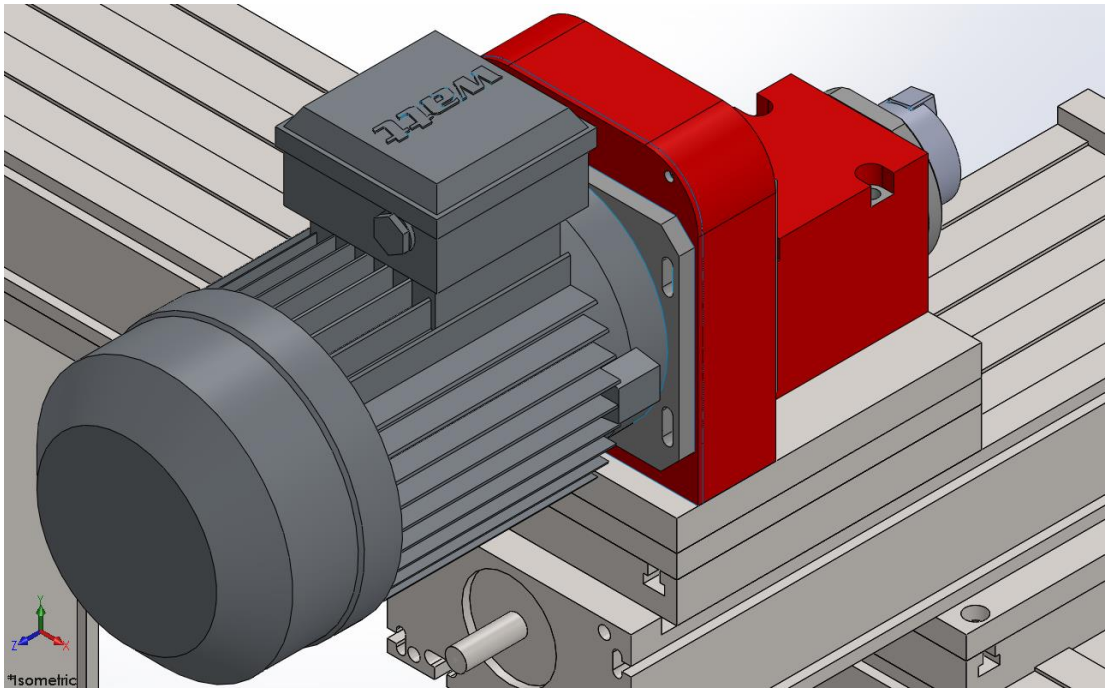


**Figure 3-3: Spindle Assembly**

**Module 2: Travel Assembly**

In Figure 3-4, the x, y, and z axes mechanical linear modular actuators are shown. These actuators are ball screw driven where rotational screw motion is converted into translational carriage motion. Special parts and equipment including bolts, spring washers, and mounting blocks are used for fixing these mechanical

actuators on the frame. A flange and coupling are also used to tie them with the motors reducing the effects of eccentricity and motor vibrations. A timing belt (with pulleys) is used to rotate the two y-axis modular linear actuators at the same speed.

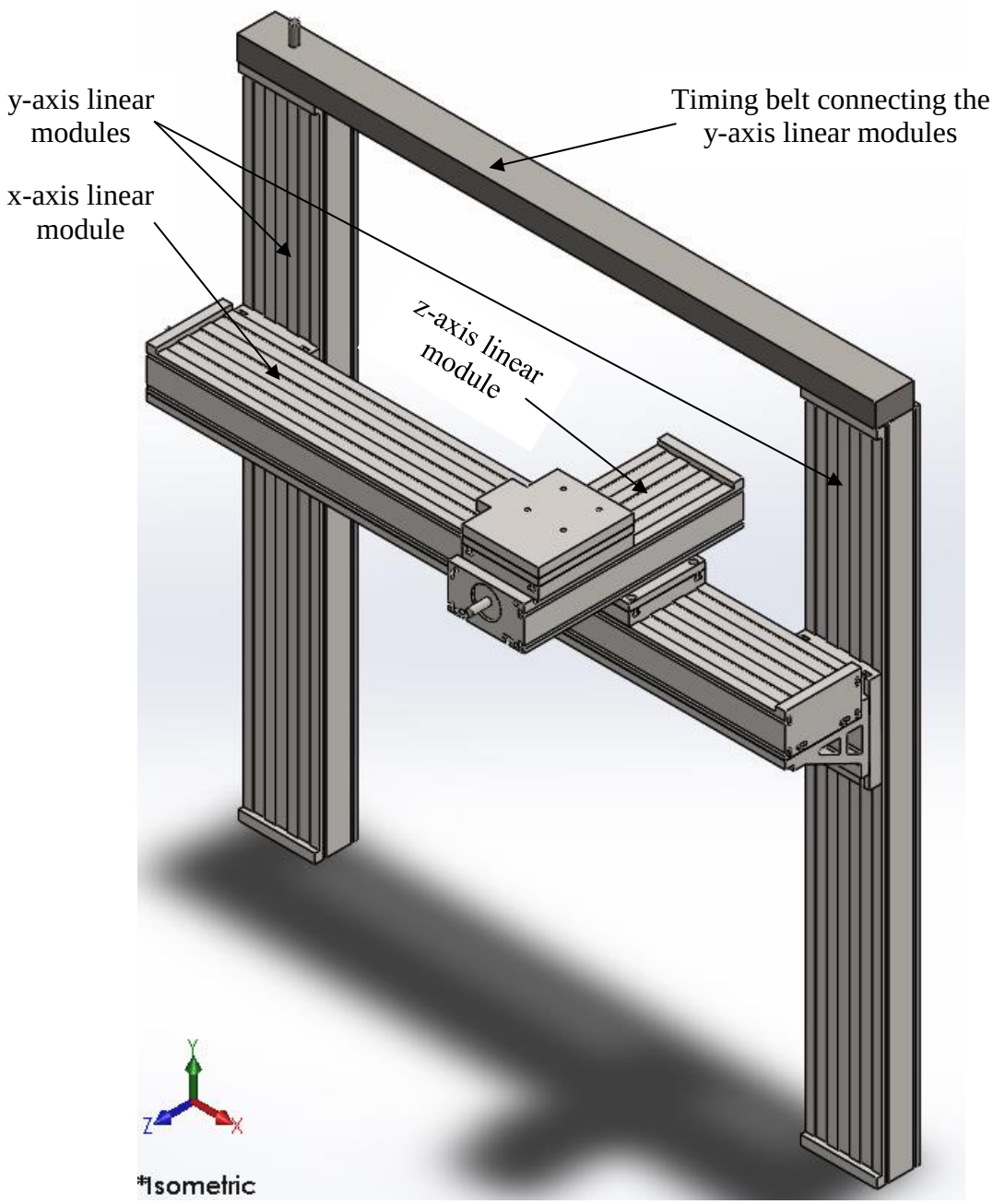


**Figure 3-4: Travel Assembly**

**Module 3: Frame (Chassis)**

Figure 3-5 shows the main frame assembly that contains rectangular profiles, bars, angles, and plates used to hold the machine giving it its rigidity and weight. All the sub-assemblies will be mounted on this frame for machine operation. The triangular geometry construction strengthens the machine load endurance. Component materials used are carbon steel alloy except for the base plates which will be Aluminum 6061 alloy because of its lightweight (compared to steel) and its high yield strength.

A slider mechanism is added to the chassis to provide additional z-axis load endurance. This mechanism will travel with the z-axis linear motion actuator. This mechanism was added after performing simulation (to lower z-axis deflection under maximum loads).

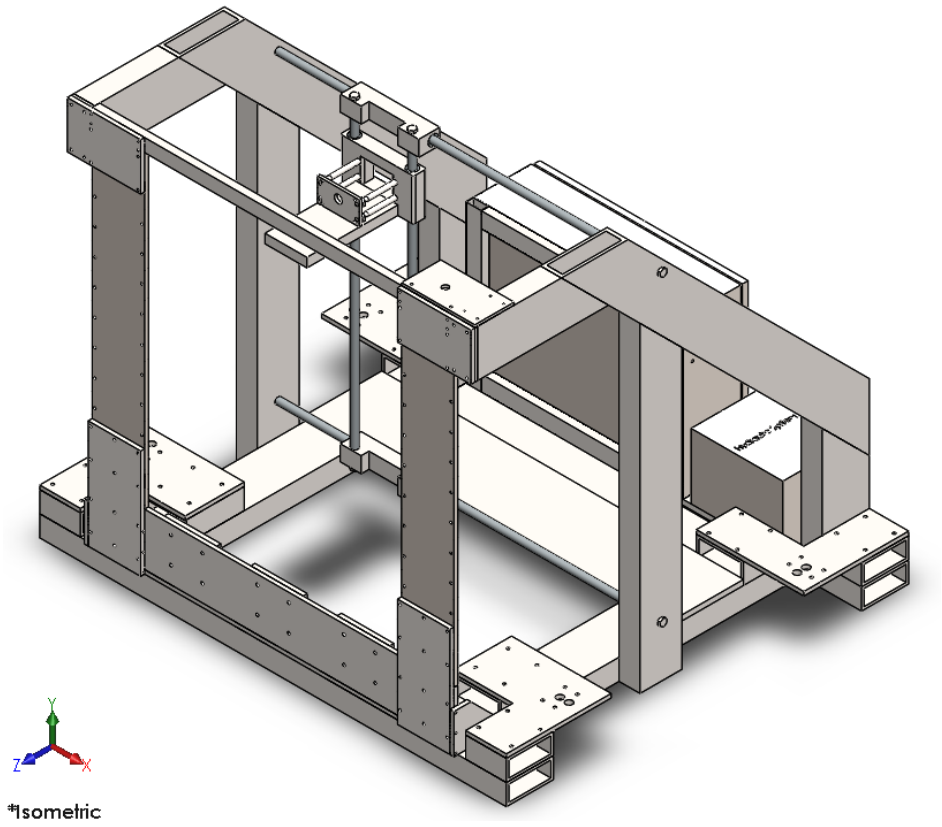


**Figure 3-5: Frame (chassis)**

**Module 4: Damping and Mobility System**

Figure 3-6 shows the damping and mobility systems of the machine. Leveler feet are used to provide damping by utilizing rubber-like material improving the desired output motion accuracy. On the other hand, these leveler feet possess high friction so that no slipping will occur during the machine operation. As for mobility, wheels are used to move the machine to the desired position. These wheels are attached to hydraulic cylinders that push them down when the machine needs to be moved, and raises them when the machine needs to be settled. These hydraulic cylinders are attached to a hydraulic system comprising of a reservoir, a pump, a selector (directional valve), and a pressure gauge.

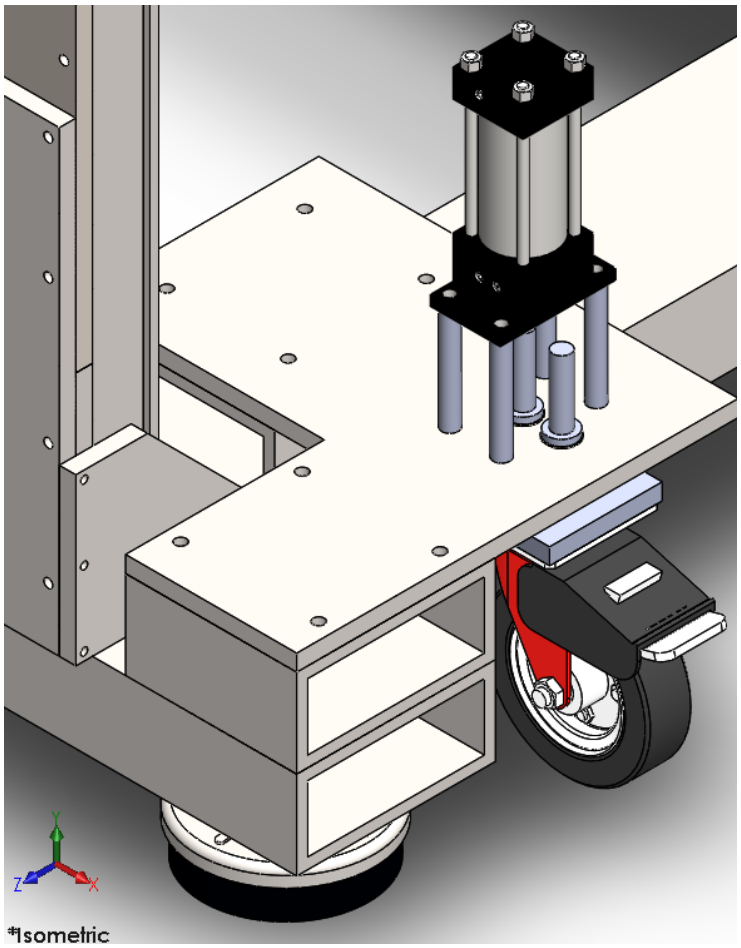


**Figure 3-6: Damping and Mobility System (Wheels and Raising Mechanism)**

**Machine Assembly**

Figure 3-7 shows the fully assembled FSWM. The spindle is mounted on the z-axis linear actuator (in the travel assembly), and the travel assembly is mounted on the frame. BAHR company[38] mechanical actuators are used in this design as well as Delta servo motors[39]. The frame contains the mobility wheels, the hydraulic cylinders, the hydraulic and electric cabinets, and the leveler feet.

The bill of materials of the assembled machine and the standard dimensions are listed in APPENDIX C in detail.

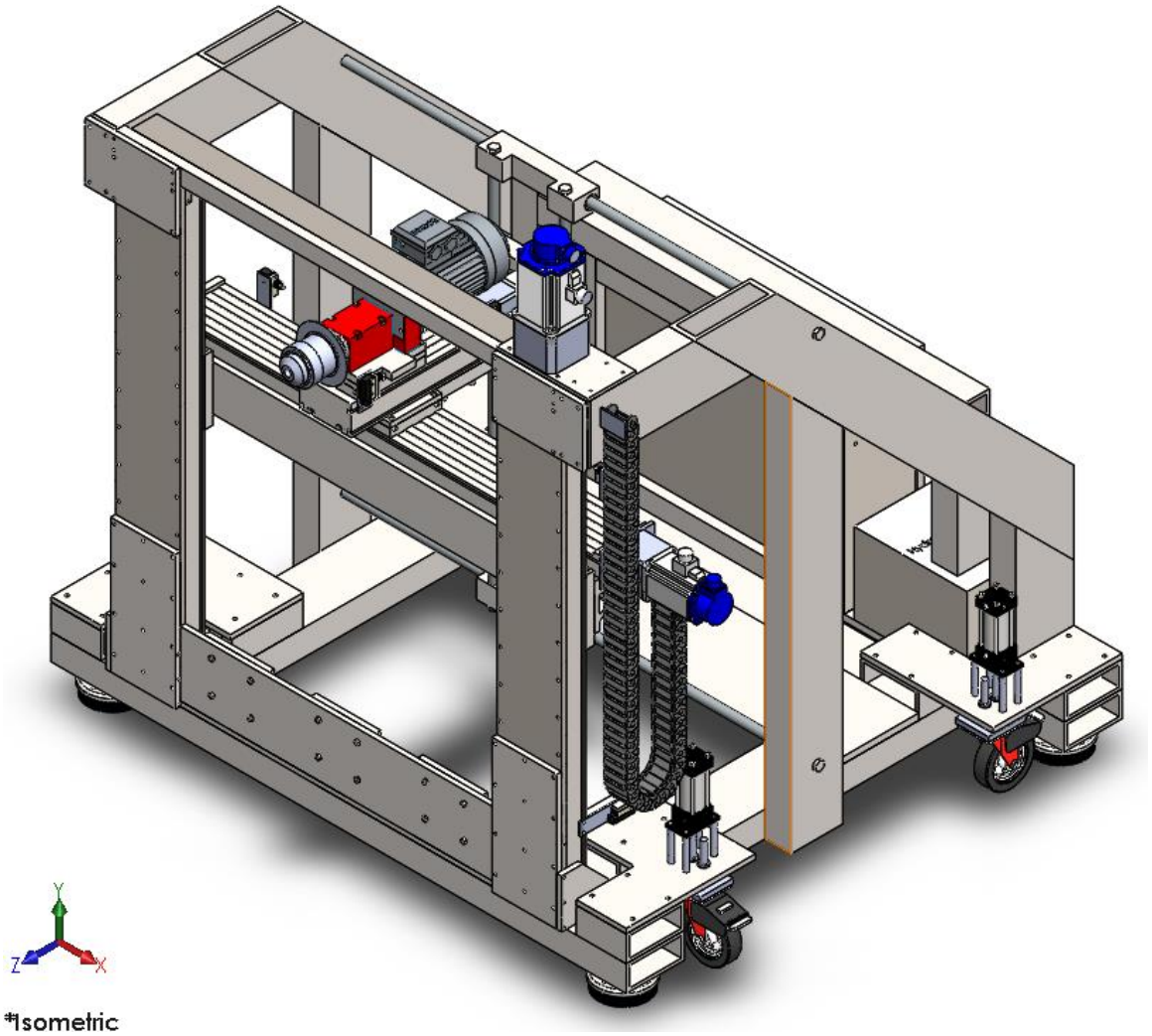


**Figure 3-7 Overall FSWM**

In this chapter, the design parameters and the machine components were discussed. The design provided in Figure 3-7 was assembled after visualizing the components that are suitable with the design parameters. The machine composes of static and dynamic components. The dynamic components of the machine should be studied to relate their output motion with the power input. This will be carried out on the linear actuators in Chapter 4.

# SYSTEMS AND CONTROL STRATEGY

The control strategy is essential to find the required forces and torques needed to provide the translational motion of the machine bridge. Given the required power, each motor can produce torque and speed translating the spindle to the requested position in a specified time interval. The motors should work in an orderly sequence according to the weld joint path. For example, to weld a horizontal joint, the z-axis linear module servo motor should work first to plunge the tool to the required depth, then the x-axis linear module servo motor will push the tool to travel in a horizontal path. An automated software is used to provide the proper inputs to the servo motors and their working sequence to fulfil the motion requirement.

## 4.1 Motion Control Modeling

In this work, one of the main objectives is to relate the input forces to the resulting motion. As stated before, in addition to the spindle rotating motion, the tool travels in the x, y, and z-directions. Each motion will require a certain input torque from each motor to resist the welding reaction forces.

It is simpler to model each module separately where each model will give an EOM relating the power input with the output motion. The EOMs will provide a direct relation between the power input and the motion for all the modules in the x, y, and z-directions. These equations can be used to find machine parameters, helping select the proper motor torque. Figure 4-1 shows an exploded view of a single linear actuator. The numbered balloons represent the components of the module as follows:

1- Module casing

2- Bearing

3- Power screw

4- Coupling

5- Motor support extension

6- Motor mounting

7- Servo motor

8- Power nut

9- Carriage

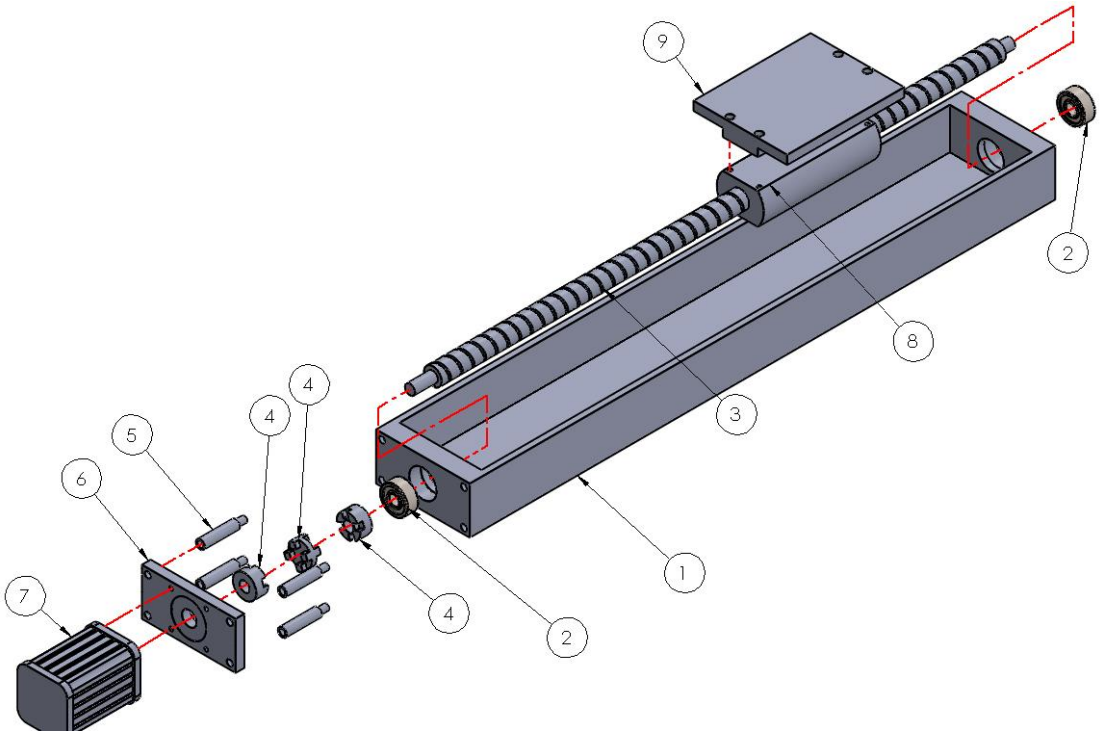


**Figure 4-1: Linear Actuator (Exploded View)**

Figure 4-2 shows a FBD of the ball screw driven linear module. This FBD concentrates on the carriage used to derive the equation of motion of this particular module.

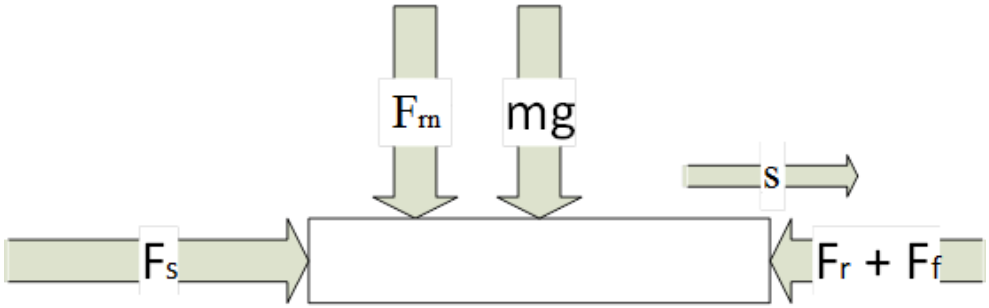


**Figure 4-2: Linear Actuator Carriage FBD**

where:

$F_s$: Force provided by the screw (motor) [ N ]

$F_r$: Reaction force the carriage exhibits from welding [ N ]

$F_f$: Equivalent friction force opposing the motion [ N ]

$F_{rn}$: Vertical force due to welding traverse motion [ N ]

$mg$: Weight of the part on top of the carriage taken into consideration [ N ]

$s$: Direction of the motion of the carriage [ m ]

In the FBD above, there are four forces. The first one is the one generated from the motor to drive the carriage $F_s$. An additional subscript is added to this force based on the actuator direction ($F_{sx}$, $F_{sy}$, or $F_{sz}$). The rest of the forces opposes the driving force either as a reaction to welding penetration and traverse motion $F_r$ or due to friction force $F_f$. They are also subscripted based on the actuator direction (e.g. $F_{rx}$, $F_{fx}$ … etc.).

Deriving the EOM is performed by using Lagrange approach. To find the kinetic and potential energy, a relation between the rotation and translation motion must be identified. Rotational screw motion can be related to the carriage linear motion by:

$$x(t) = \left\{\frac{l}{2\pi}\right\}\theta_x(t) \tag{4-1}$$

where $l$ is the lead of the screw in [m], $\theta_x(t)$ is rotational angle in [rad], and $x(t)$ is the linear displacement in [m].

By differentiating the above equation with respect to time, we will obtain the following equation describing the speed of the carriage,

$$\dot{x}(t) = \left\{\frac{l}{2\pi}\right\} \dot{\theta}_x(t) \tag{4-2}$$

Finding the Kinetic Energy of the linear drive module,

$$T = \frac{1}{2} J_x \dot{\theta}_x{}^2 + \frac{1}{2} m_x \dot{x}^2 \tag{4-3}$$

where $J_x$ is the mass moment of inertia of the screw in [kg.m$^2$] and $m_x$ is the mass carried by the x-axis module in [kg].

Substituting $\dot{\theta}_x$ from equation (4-2) into equation (4-3),

$$T = \frac{1}{2} J_x \left\{\frac{2\pi}{l}\right\}^2 \dot{x}^2 + \frac{1}{2} m_x \dot{x}^2 \tag{4-4}$$

By taking $\dot{x}$ as a common factor:

$$T = \frac{1}{2} \left\{\frac{\pi^2}{l^2} J_x + m_x\right\} \dot{x}^2 \tag{4-5}$$

Noting that,

$$m_x = m_{z-module} + m_z \tag{4-6}$$

where $m_{z-module}$ is the mass of the z-axis linear module in [kg] and $m_z$ is the mass carried by the z-axis module in [kg] which in this case is the spindle and the tool.

As shown in the kinetic energy equation (4-5), there are only two inertias in the system which are the mass carried by the carriage (including the carriage mass) and the screw's mass moment of inertia.

Figure 4-3 shows the stiffness and viscous damping found in the linear module's internal components. of the coupling and ball bearings respectively. $k_{x1}$ and $k_{x2}$ are the stiffnesses of the ball screw and the coupling respectively. They are placed in series. $C_{x1}$ and $C_{x2}$ are the viscous damping the ball bearings impose on the system. They are considered to operate in parallel form.

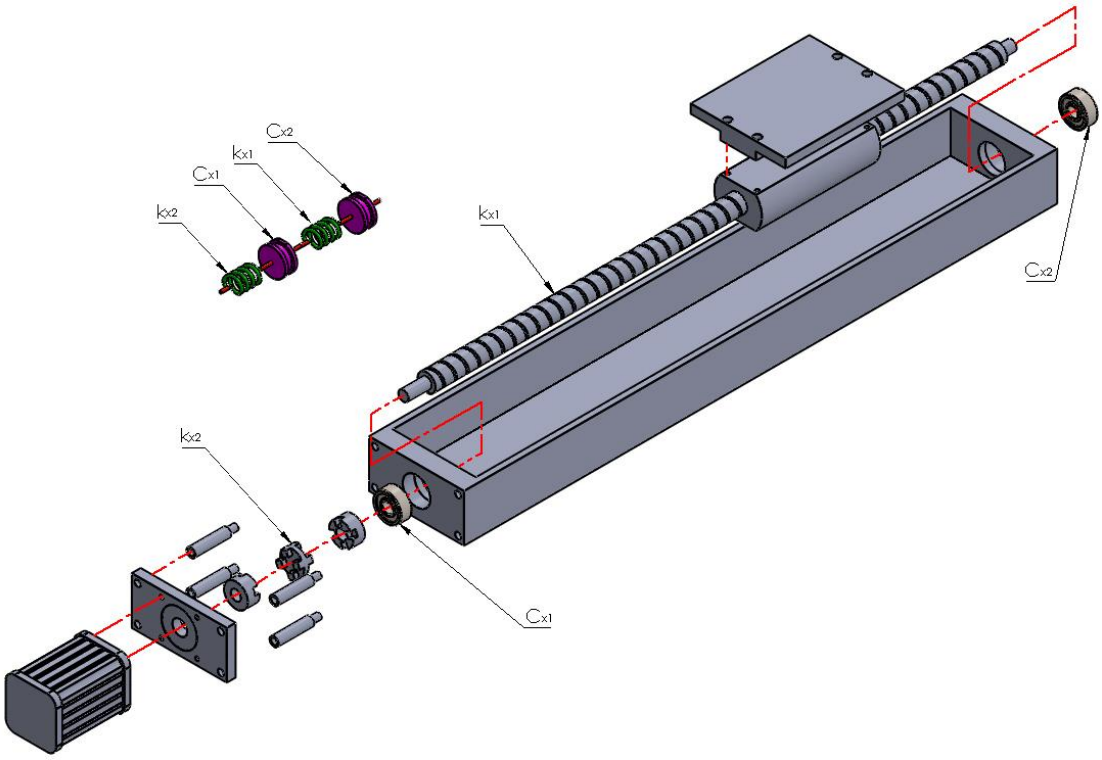


**Figure 4-3: Location of Stiffness and Damping**

Finding the strain energy,

$$V = \frac{1}{2}\left\{\frac{k_{x1}k_{x2}}{k_{x1}+k_{x2}}\right\}\theta_x{}^2 \tag{4-7}$$

Substituting $\theta_x$ from equation (4-1),

$$V = \frac{1}{2}\left\{\frac{k_{x1}k_{x2}}{k_{x1}+k_{x2}}\right\}\left(\frac{4\pi^2}{l^2}\right)x^2 \tag{4-8}$$

where $k_{x1}$ and $k_{x2}$ are the stiffnesses of the screw and the coupling, respectively, in [N/m].

For a torsional rod the stiffness can be calculated as follows[40]:

$$k = \frac{\pi G}{32 l_s} d^4 \tag{4-9}$$

where $G$ is the shear modulus in [Pa], $l_s$: is the length of the rod in [m], and $d$ is the diameter of the rod in [m].

Beside the stiffness of the screw and coupling, the spring-like forces in the system are considered negligible due to the high rigidity of the machine.

Finding the dissipation energy,

$$D = \frac{1}{2}\{C_{x1} + C_{x2}\}\dot{\theta}_x{}^2 \tag{4-10}$$

Substituting $\dot{\theta}_x$ from equation (4-2),

$$D = \frac{1}{2}\{C_{x1} + C_{x2}\}\left(\frac{4\pi^2}{l^2}\right)\dot{x}^2 \tag{4-11}$$

The dissipation energy is a result of the bearing viscous damping ($C_{x1}$ and $C_{x2}$) opposing the rotational motion.

To identify the generalized forces, the virtual work done by the carriage must be found. To find the virtual work, the forces and their directions of action must be identified. It is simply shown that all forces act on a single axis.

The generalized forces are,

$$Q_x = F_{sx} - F_{fx} - F_{rx} \tag{4-12}$$

where $F_{sx}$ is the force provided by the screw (motor) in [N], $F_{rx}$ is the reaction force the carriage exhibits from welding in [N], and $F_{fx}$ is the dry friction force opposing the motion in [N].

The input force $F_{sx}$ is provided by the rotation of the motor. The motor initially provides torque and rotational speed to the screw, thus moving the carriage in a linear motion by the nut coupled to it. The input force can be related to the torque by the following equation (losses are neglected):

$$P = Fv = T\omega \tag{4-13}$$

where $P$ is power in [watts], $v$: is linear velocity of the carriage in [m/s], $F$: is force imposed onto the carriage in [N], $T$: is torque provided by the ball screw in [N.m], and $\omega$ is angular velocity of the ball screw in [rad/s].

$$T = \frac{Fv}{\omega} = \frac{F\dot{x}}{\dot{\theta}} \tag{4-14}$$

$$T = \frac{F\left(\frac{l\dot{\theta}}{2\pi}\right)}{\dot{\theta}} \tag{4-15}$$

$$T = \frac{Fl}{2\pi} \tag{4-16}$$

The friction force in equation (4-12) results from dry friction imposed by the rollers on the sliding guide. This friction can be represented as coulomb's damping as shown below [41]:

$$F_{fx} = \mu_x N_1 sign(\dot{x}) \tag{4-17}$$

$$N_1 = m_x g + F_{rny} \tag{4-18}$$

where $\mu_x$ is the coefficient of friction between the rollers and the guide and $N_1$ is the normal force acting on the carriage.The reaction forces ($F_{rx}$,$F_{rny}$) can be either constant force, sinusoidal force, pulse, or impulse force, or even a combination for two or more types. This force can be selected from the previous experimentation results [32-33] found while welding tubes to tube-sheet. Referring to Figure 4-2 the friction force can be assumed as:

$$F_{rx} = A_0 cos\omega t \tag{4-19}$$

where $A_0$ is the amplitude of the reaction force and $\omega$ is its frequency.

The Lagrangian is defined as:

$$L = T - V \tag{4-20}$$

$$L = \frac{1}{2}\left\{\frac{\pi^2}{l^2}J_x + m_x\right\}\dot{x}^2 - \frac{1}{2}\left(\frac{4\pi^2}{l^2}\right)\left\{\frac{k_{x1}k_{x2}}{k_{x1}+k_{x2}}\right\}x^2 \tag{4-21}$$

Using Lagrange equation to derive the equations of motion

$$\frac{d}{dt}\left(\frac{\partial L}{\partial \dot{q}_j}\right) + \frac{\partial D}{\partial \dot{q}_j} - \frac{\partial L}{\partial q_j} = \sum Q_j \tag{4-22}$$

Where:

$$\frac{\partial L}{\partial \dot{x}} = \left\{\frac{4\pi^2}{l^2}J_x + m_x\right\}\dot{x} \tag{4-23}$$

$$\frac{d}{dt}\left(\frac{\partial L}{\partial \dot{x}}\right) = \left\{\frac{4\pi^2}{l^2}J_x + m_x\right\}\ddot{x} \tag{4-24}$$

$$\frac{\partial D}{\partial \dot{x}} = \left(\frac{4\pi^2}{l}\right)\{C_{x1} + C_{x2}\}\dot{x} \tag{4-25}$$

$$\frac{\partial L}{\partial x} = -\left(\frac{4\pi^2)}{l}\right)\left\{\frac{k_{x1}k_{x2}}{k_{x1}+k_{x2}}\right\}x \tag{4-26}$$

The equation of motion for the linear screw driven module is given by:

$$\left\{\frac{4\pi^2}{l^2}J_x + m_x\right\}\ddot{x} + \left(\frac{4\pi^2}{l}\right)\{C_{x1} + C_{x2}\}\dot{x} + \left(\frac{4\pi^2)}{l}\right)\left\{\frac{k_{x1}k_{x2}}{k_{x1}+k_{x2}}\right\}x +$$

$$\mu_x N_1 sign(\dot{x}) = F_x - F_{rx} \tag{4-27}$$

Using the same procedure, we can find the equations of motion for the linear actuators in the y and z-directions.

$$\left\{\frac{8\pi^2}{l^2}J_y\right\}\ddot{y} + \left(\frac{8\pi^2}{l}\right)\{C_{y1} + C_{y2}\}\dot{y} + \left(\frac{8\pi^2}{l}\right)\left\{\frac{k_{y1}k_{y2}}{k_{y1}+k_{y2}}\right\}y + \mu_y N_2 sign(\dot{y}) =$$

$$F_y + m_y g - F_{ry} \tag{4-28}$$

where:

$$m_y = m_{x-module} + m_x \tag{4-29}$$

$$N_2 = F_{rz} \tag{4-30}$$

$$\left\{\frac{4\pi^2}{l^2}J_z + m_z\right\}\ddot{z} + \left(\frac{4\pi^2}{l}\right)\{C_{z1} + C_{z2}\}\dot{z} + \left(\frac{4\pi^2}{l}\right)\left\{\frac{k_{z1}k_{z2}}{k_{z1}+k_{z2}}\right\}z +$$

$$\mu_z N_3 sign(\dot{z}) = F_z - F_{rz} \tag{4-31}$$

where:

$$m_z = m_{spindle} + m_{tool} \tag{4-32}$$

$$N_3 = m_z g + F_{ry} \tag{4-33}$$

## 4.2 Electrical System

The electrical system is essential for operating the machine. The machine needs to start, stop, and run using electrical components. The electrical components needed for machine operation are:

1- Relays and/or contactors

2- Switches and pushbuttons

3- Limit switches

4- Wires and wire support chain

5- Servo motors

6- Spindle motor

7- Motor drives

The relays and/or contactors are used to provide or cut off electricity to the motor drives, control system, and variable frequency drive (VFD). They are triggered by the push buttons including start, stop, and emergency push buttons. They can also be triggered by the control system or through the guided user interface (GUI).

The servo motors are provided with power through the motor drives. The required power will be based on the control system. The limit switches, shown in Figure 4-4 are used as a safety measure for the linear actuators to make sure that the carriage will never collide with either end of the module.

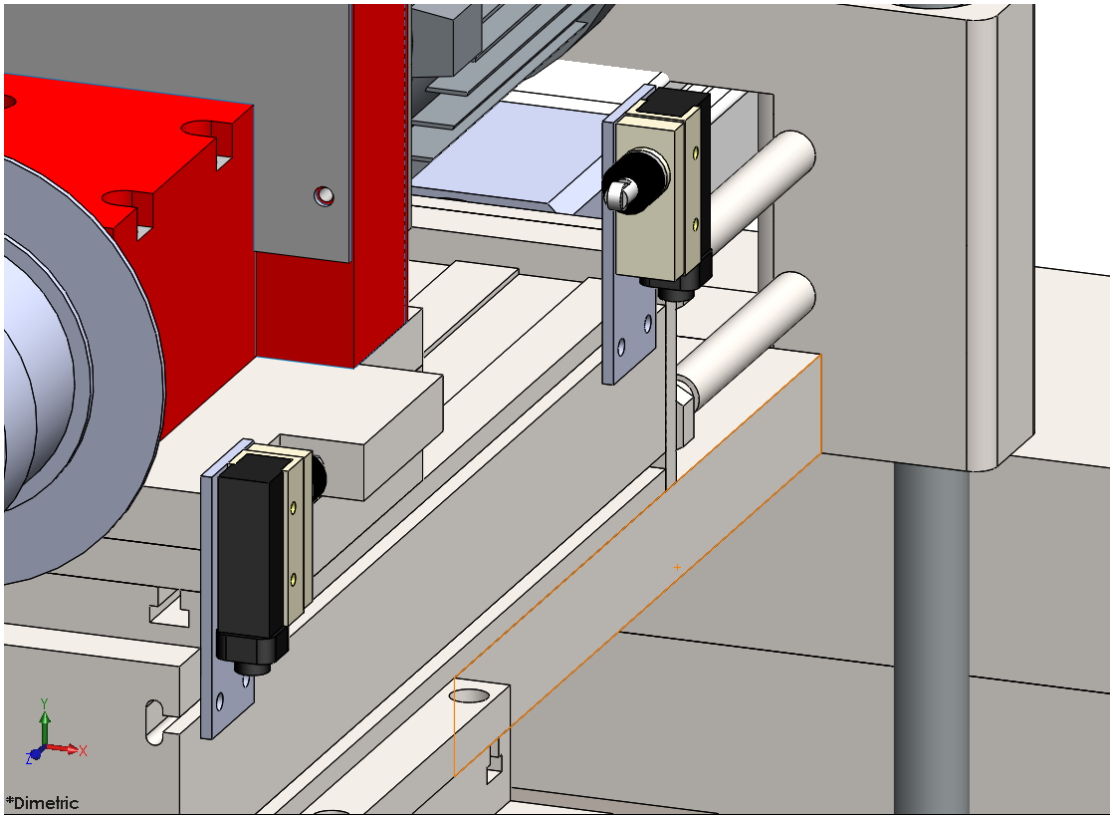


**Figure 4-4: Limit Switch Position on z-axis Linear Actuator**

## 4.3 Computer Numerical Control (CNC)

Computer numerical control is widely used in many machines and applications. Lathe and milling machines in general operate using this control method. CNC is considered as a mean of Computer Aided Manufacturing (CAM). CAM software is used to analyze the joint location and geometry of a model to generate a path, providing the CNC program a set of coordinates, which will eventually be used to move the tool.

Computer Aided Design(CAD) is widely used to model different components with different geometries. SOLIDWORKS software is used to 3-D model a component and/or components. Provided the tube pattern and size, the CAD model is exported to the CAM software which can then calculate the tool path, rotational speeds, and travel speeds.

CNC is used as a solution for high speed, high precision machines. It is considered greatly advantageous providing stable machine motion and high production rate. It is also user friendly with easy tuning and adjusting.

Delta, a South Korean company [39], provides good industrial automation solutions. One of the solutions it offers is shown in Figure 4-5. The solution consists of three servo motors used for the three axes motion, their controllers, a VFD, and a GUI. This control system will be run by a software that reads G-code, which can be obtained by the CAM software.


**Figure 4-5: Delta CNC Solution[42]**

## 4.4 Hydraulic System

Portability is one of the important features of this machine. This is done by moving the machine via four heavy duty wheels. A hydraulic system is needed to carry the FSWM on its wheels. The machine can rise over the leveler feet height till the leveler feet have no contact with the floor. The wheels and the raising mechanism can be seen in Figure 3-6.

The hydraulic system needs a set of components to operate. These components are needed for efficient and safe operation of the system. These components comprise:

1- Double acting hydraulic cylinders

2- Directional valves (4-way 3-position), solenoid operated

3- Check valves

4- Pressure relief valves

5- Hydraulic pipe lines

6- Pressure gauges

7- Gear pump

8- Oil reservoir

9- Oil filters

A simple on-off system can be utilized for the mobility system since the only dynamic function present is lifting and lowering the machine. It is important to consider the pump size and the cylinder bores to be able to lift the weight of the machine. Pressure gauges are important to monitor the hydraulic system. This system can also be used when the machine is welding to cool off the spindle.

# PROCEDURE FOR STRUCTURAL ANALYSIS

The main requirement in a FSWM is to maintain contact pressure in the form of axial force and to provide adequate welding torque necessary to stir material [43]. This means that the FSWM must provide the required force and torque to obtain sound weld. While these forces and torques are provided, the machine behavior must be analyzed to minimize the probability of damage or breakdown.

Four types of analyses are conducted on the FSWM to ensure the robustness and stability of the FSWM.

- static analysis
- fatigue analysis
- frequency analysis
- dynamic analysis

## 5.1 Static Analysis

Static analysis is of paramount importance to make sure that the machine is mechanically robust. This analysis will provide the stresses, strains, and displacements of the machine components given the required input forces and torques. The involved stresses are calculated based on the shape of the structure and the load applied at specific points or areas. Stress analysis is performed using SOLIDWORKS FEM software considering distortion energy failure criteria by calculating Von Mises stresses. This criterion is used to predict yielding of the parts under static loading conditions. In terms of principal stresses $\sigma_1$ , $\sigma_2$, $\sigma_3$, the Von Mises is expressed as:

$$\sigma' = \{[(\sigma_1 - \sigma_2)^2 + (\sigma_2 - \sigma_3)^2 + (\sigma_1 - \sigma_3)^2]/2\}^{1/2} \quad (5\text{-}1)$$

SOLIDWORKS simulation uses the displacement formulation of the finite element method to calculate component displacements, strains, and stresses under internal and external loads. The geometry under analysis is discretized using tetrahedral (3D), triangular (2D), and beam elements, and solved by either a direct sparse or iterative solver. SOLIDWORKS Simulation can use either an h or p adaptive element type, providing a great advantage to designers and engineers as the adaptive method ensures that the solution has converged.

**Geometric Model**

Analysis is run based on the fine mesh as shown in Figure 5-1. The meshing process divides the machine's physical components to smaller elements with tetrahedron shapes over which a set of equations are solved. Meshing is curvature based where the mesh will become fine near holes, pockets, fillets, chamfers, and on shafts. The mesh sizing becomes coarse at non-critical locations where the geometry is less complicated. Sizing was chosen based on convergence for each analysis, providing accurate readings.

The element used throughout SOLIDWORKS' FEA is h adaptive type. This type is used to obtain more accurate information by increasing the number of elements that is by refining the mesh used in the model. For example, if a part is modeled with coarse mesh, the h adaptive type FEA will keep refining the mesh element sizes to reach the required accuracy. This is the reason why meshing is finer near the complex contours in the machine. The machine consists of 2,286,488 elements whilst meshing is performed for 98% target accuracy.

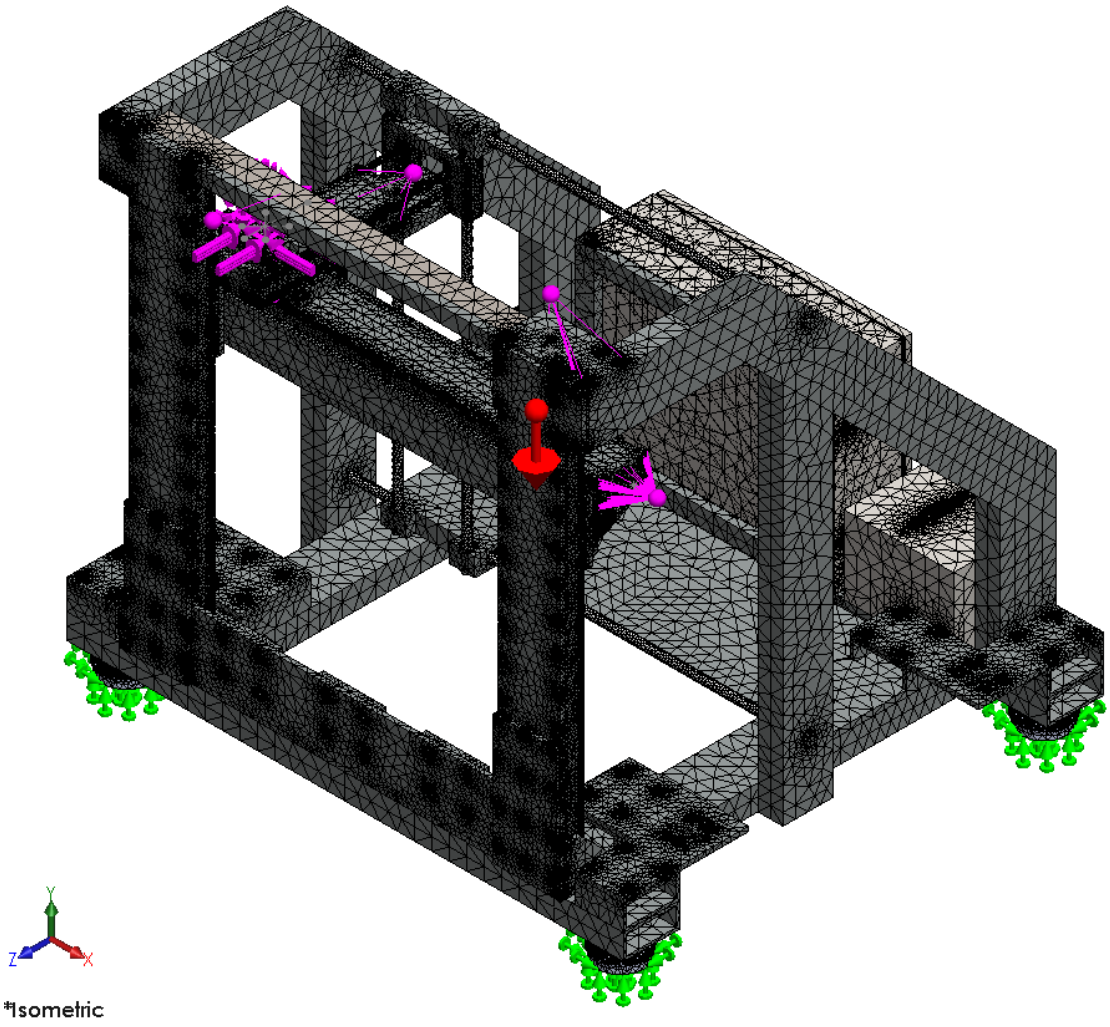


**Figure 5-1: Machine Meshing**

## Boundary Conditions

While performing the static analysis, the machine must be constrained. Boundary conditions were assumed to be on the bottom surfaces of the leveler feet where sufficient amount of weight opposes the machines ability to slip as shown in Figure 5-2. Loads will be composed of radial, axial, and torsional constant loads that are situated in the bolt holes of the spindle base as shown in Figures 5-3 and 5-4. Values of the maximum loads obtained by the previous experimental data in Table 3-1 are

considered where the applied loads will have slightly greater values than those provided in Table 3-1 to ensure machine robustness.

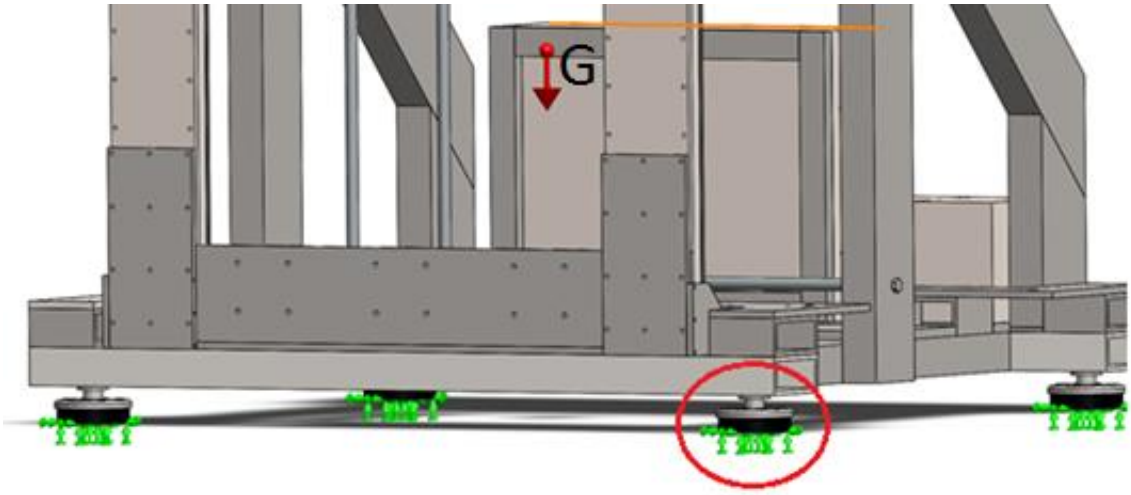


**Figure 5-2: Machine Boundary Conditions and Center of Gravity (G)**

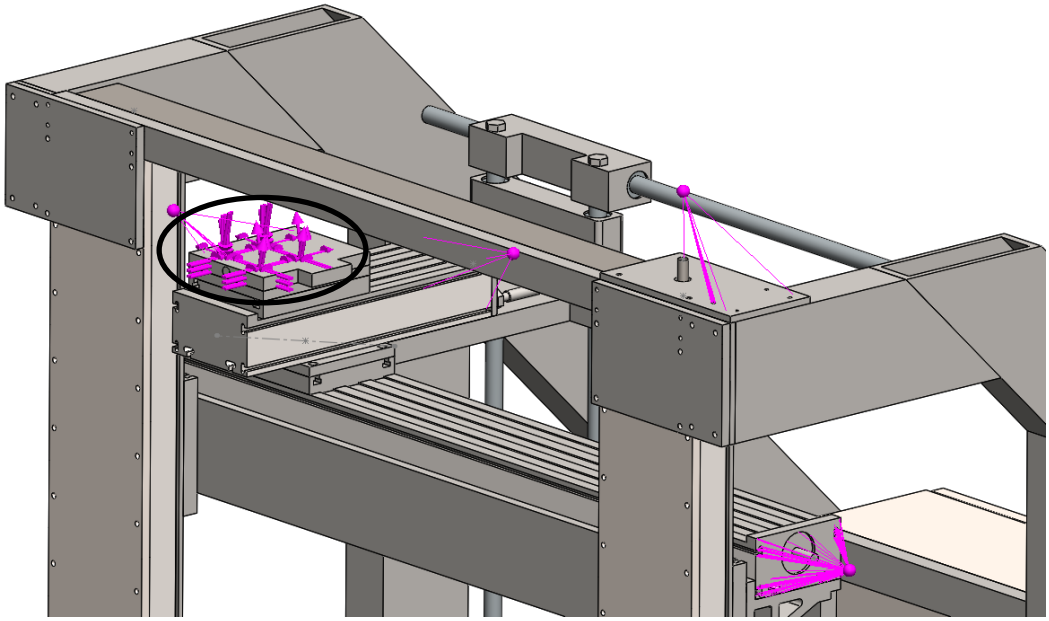

**Figure 5-3: Location of the Forces/Torque**

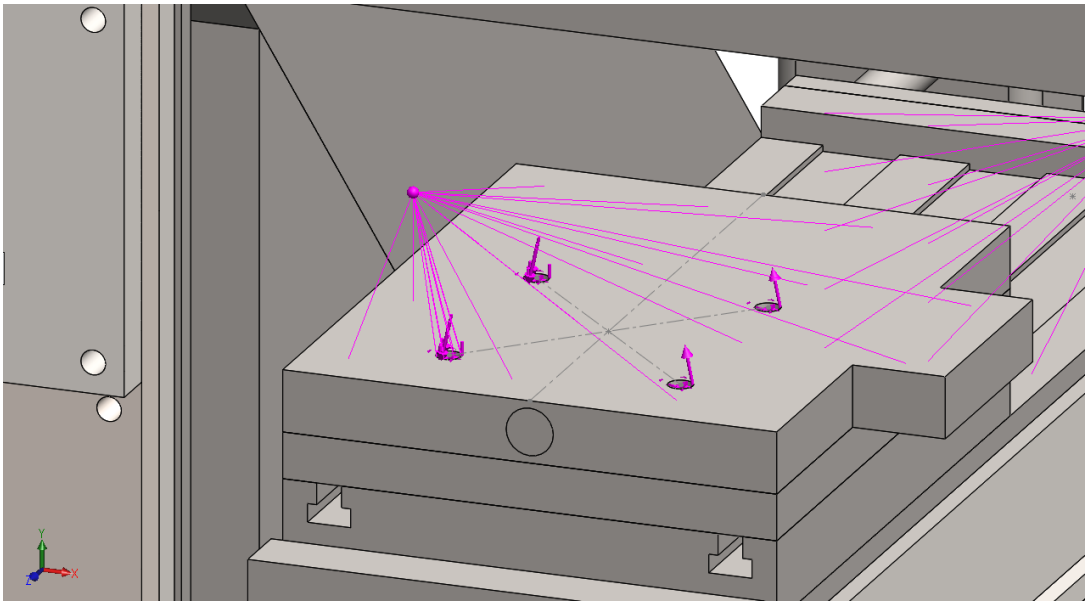

**Figure 5-4: Location of the Forces/Torque (Magnified)**

## Material Properties

For the machine to work in the safe side, the highest Von Mises stresses must be relatively lower than the material yielding strength. The high material yield strength increases the rigidity of the machine and its mechanical robustness. The material considered for these parts is plain carbon steel (equivalent to AISI 1018), which is most appropriate due to its high stiffness, strength, workability, and low cost. Plain carbon steel properties and their values used in the analysis are shown in Table 5-1 [44].

**Table 5-1: Plain Carbon Steel Properties Used in SOLIDWORKS**

| Property | Value | Unit |
|---|---|---|
| Modulus of Elasticity | 210 | GPa |
| Poisson's Ratio | 0.28 | |
| Shear Modulus of Rigidity | 79 | GPa |
| Mass Density | 7800 | $kg/m^3$ |
| Tensile Strength | 400 | MPa |
| Yield Strength | 220 | MPa |
| Thermal Expansion Coefficient | $1.3 \times 10^{-5}$ | K |
| Thermal Conductivity | 43 | $W/(m.K)$ |
| Specific Heat | 440 | $J/(kg.K)$ |

**Spindle Positions and Processes for Analysis**

Four static analyses studies will be performed. The difference among them is the position of the spindle head and the process of operation (plunging or traversing). The two positions selected for the analysis are the top left and the center which will be shown in more detail in chapter 6. In each position, there will be two types of operations, the first is plunging where there is a force in the z-axis direction and a moment around the same axis, and the second is traversing where there are three forces in the x, y, and z-directions and a moment around the z-axis. These positions and operation processes will also be used in the forthcoming. The forces and torque used are summarized in Table 5-2. These values will also be plugged in for the fatigue and dynamic analyses.

**Table 5-2: Load Values Used in Static, Fatigue, and Dynamic Analyses**

| **Process** | Force/Torque | Direction |
|---|---|---|
| **Plunging** | $F_x = 0$ N<br>$F_y = 0$ N<br>$F_z = 2000$ N<br>$T_z = 45$ N. m | x-direction<br>y-direction<br>z-direction<br>about z-axis |
| **Traversing** | $F_x = 1200$ N<br>$F_y = 1200$ N<br>$F_z = 600$ N<br>$T_z = 25$ N. m | x-direction<br>y-direction<br>z-direction<br>about z-axis |

## 5.2 Fatigue Analysis

Fatigue is the failure of a material caused by repeatedly applied loads. In this study, the stresses (results) that are provided from static analysis are used to find the machine cyclic life in the fatigue analysis. The fatigue life of the machine structure is based on the S-N curve provided for plain carbon steel shown in Figure 5-5. This log-log curve is based on ASME carbon steel curves, where it is derived from the material's elastic modulus.

Fatigue analysis is performed with the same loads used in the static analysis for both plunge and traverse processes in both top left and center spindle positions. These loads will be applied in fully reversed cycles on the machine. The analysis will provide the damage that will occur by the number of cycles as well as the total life of the machine and the load factor needed for the machine to breakdown. This will provide the information needed to predict the time the machine needs to reach failure while working with the assumed maximum loads (found in Table 5-2).

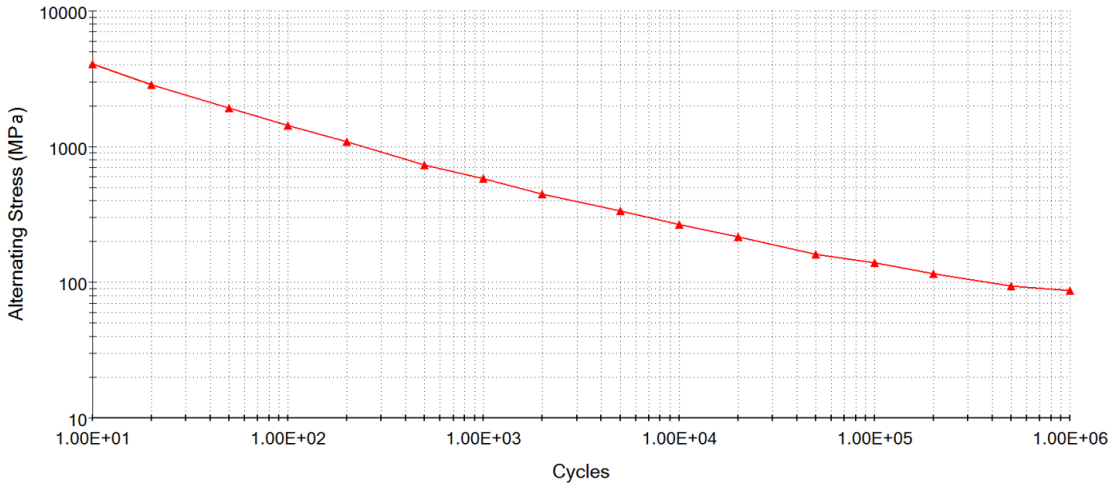


**Figure 5-5: S-N Curve (Log-Log) for Plain Carbon Steel (AISI 1018) Used in SOLIDWORKS[44]**

## 5.3 Frequency Analysis

Frequency analysis is important to know machine resonance frequencies and make sure that the modules will work in a safe frequency range with stable response. This is accomplished by finding the lowest resonant frequencies of the machine and their mode shapes. Working in the range below these frequencies is predicted to avoid cutting machine working lifetime that will eventually lead to breakdown. Using SOLIDWORKS' FEA, the first five resonant frequencies are obtained for both positions used for the machine (top left and center positions). These values are discussed in chapter 6.

Machine frequencies can also be obtained from the machine model by deriving its equations of motions. This can be done by modeling the screws tightening the components and mechanisms as springs (stiffness) and dampers. Each screw can be considered as a three-dimensional node that can translate in any of the three axes directions as shown in Figure 5-6. The screw locations are shown in Figures 5-7 – 5-8,

where each node is given a letter-number symbolizing its location (e.g. A1, A2, …). In addition to that, each part has a letter symbolizing it (A, B, C, and D).

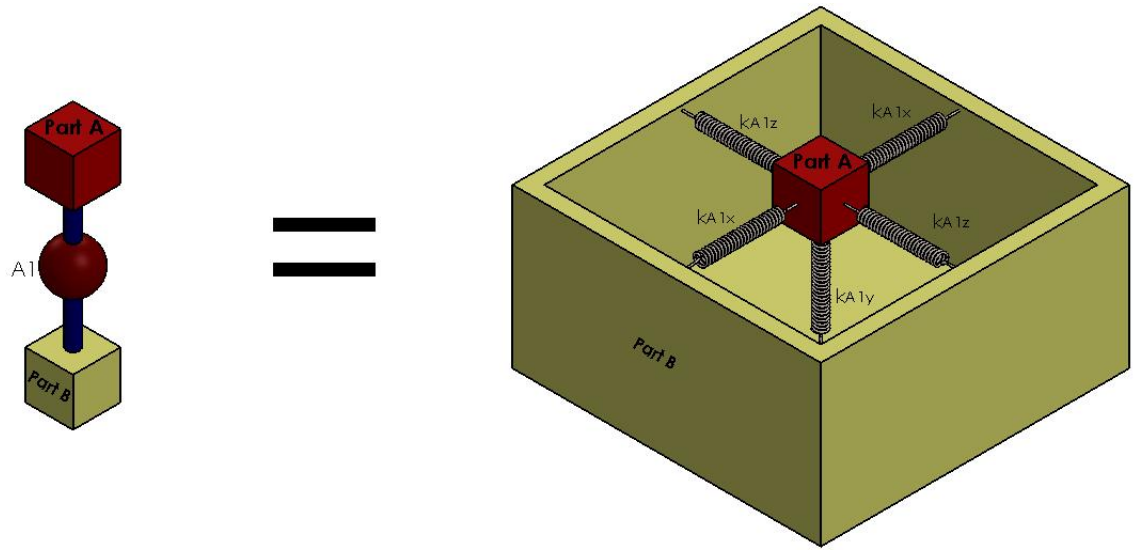


**Figure 5-6: Screw Node**

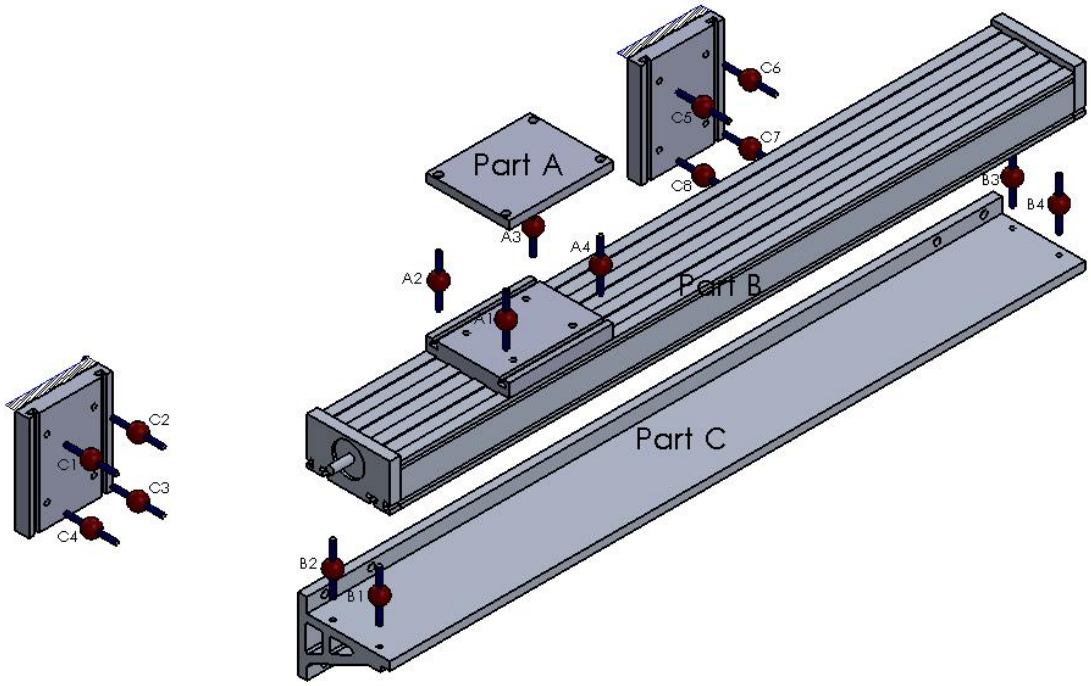


**Figure 5-7: Node Locations Magnified**

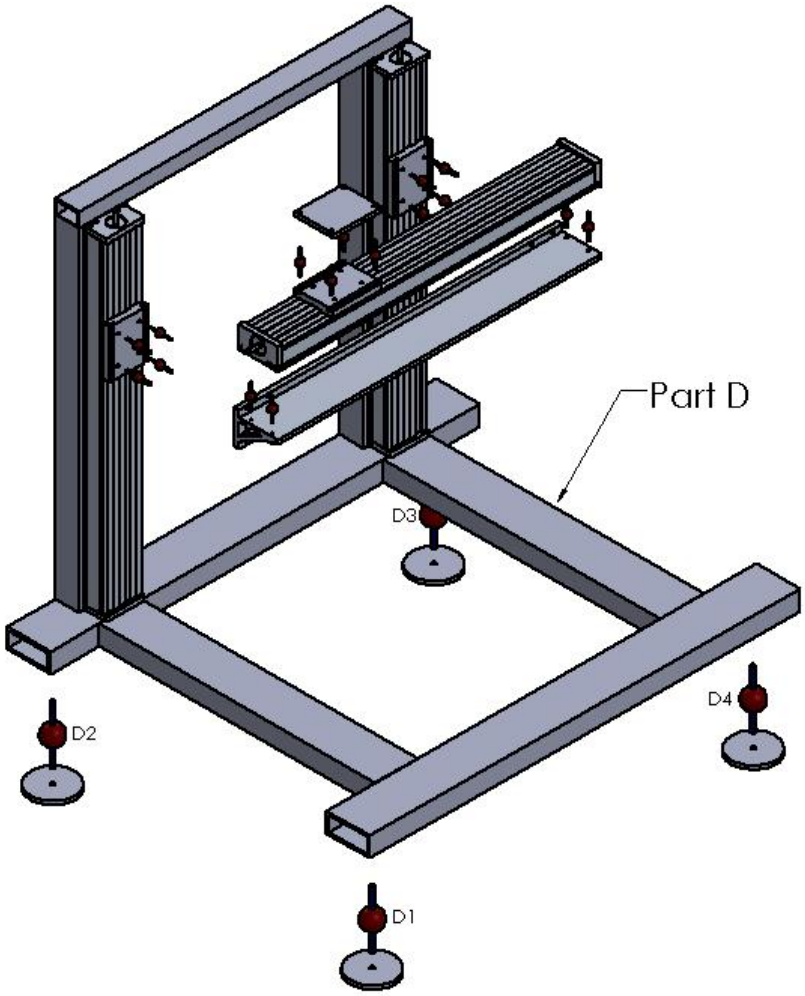


**Figure 5-8: Node Locations Full Machine**

**Generalized Coordinates**

The generalized coordinates that account for each part of the machine will be defined and accounted for in the formulation of the dynamic model to specify the motion of each part. The generalized coordinates are shown in Figures 5-9 – 5-10.

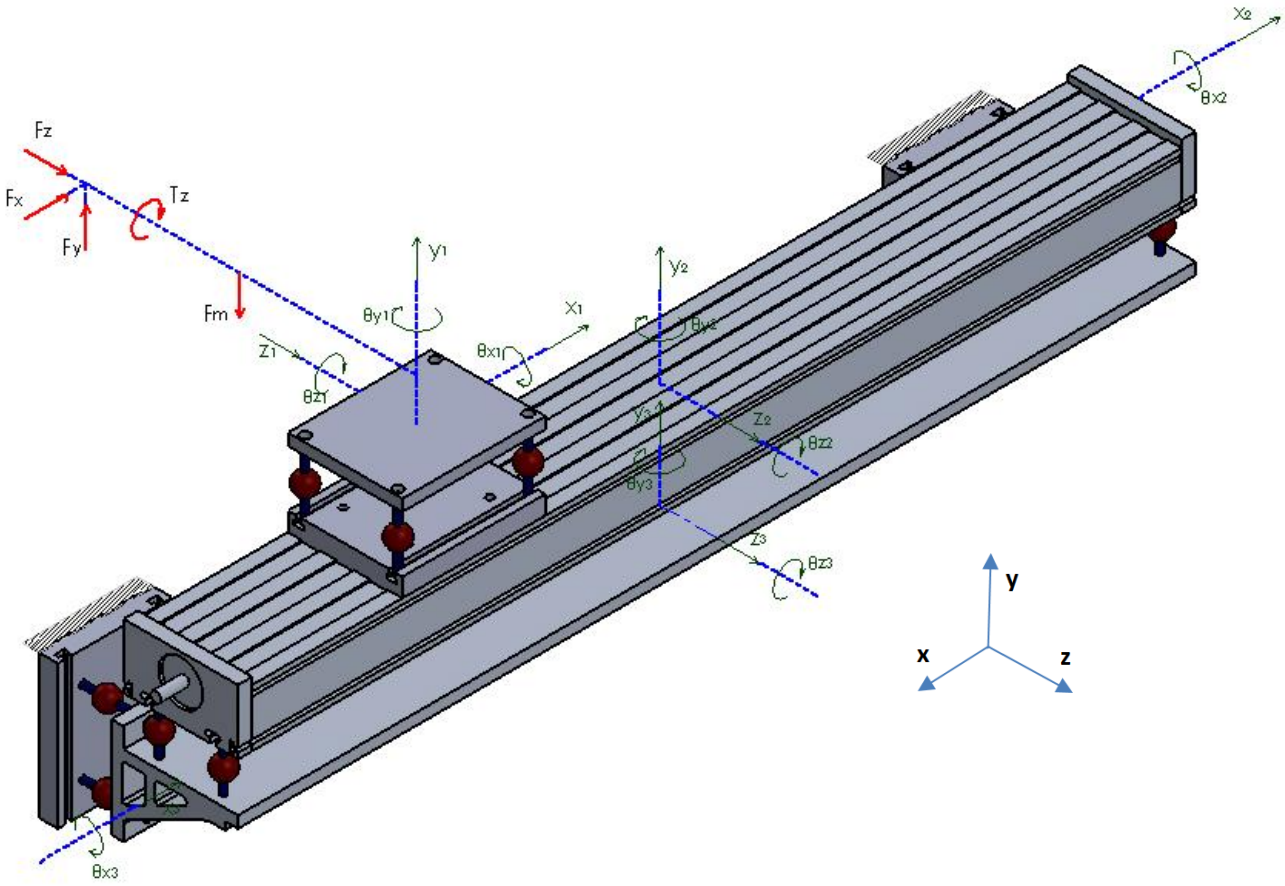


**Figure 5-9: Generalized Coordinates of the Machine Structure**

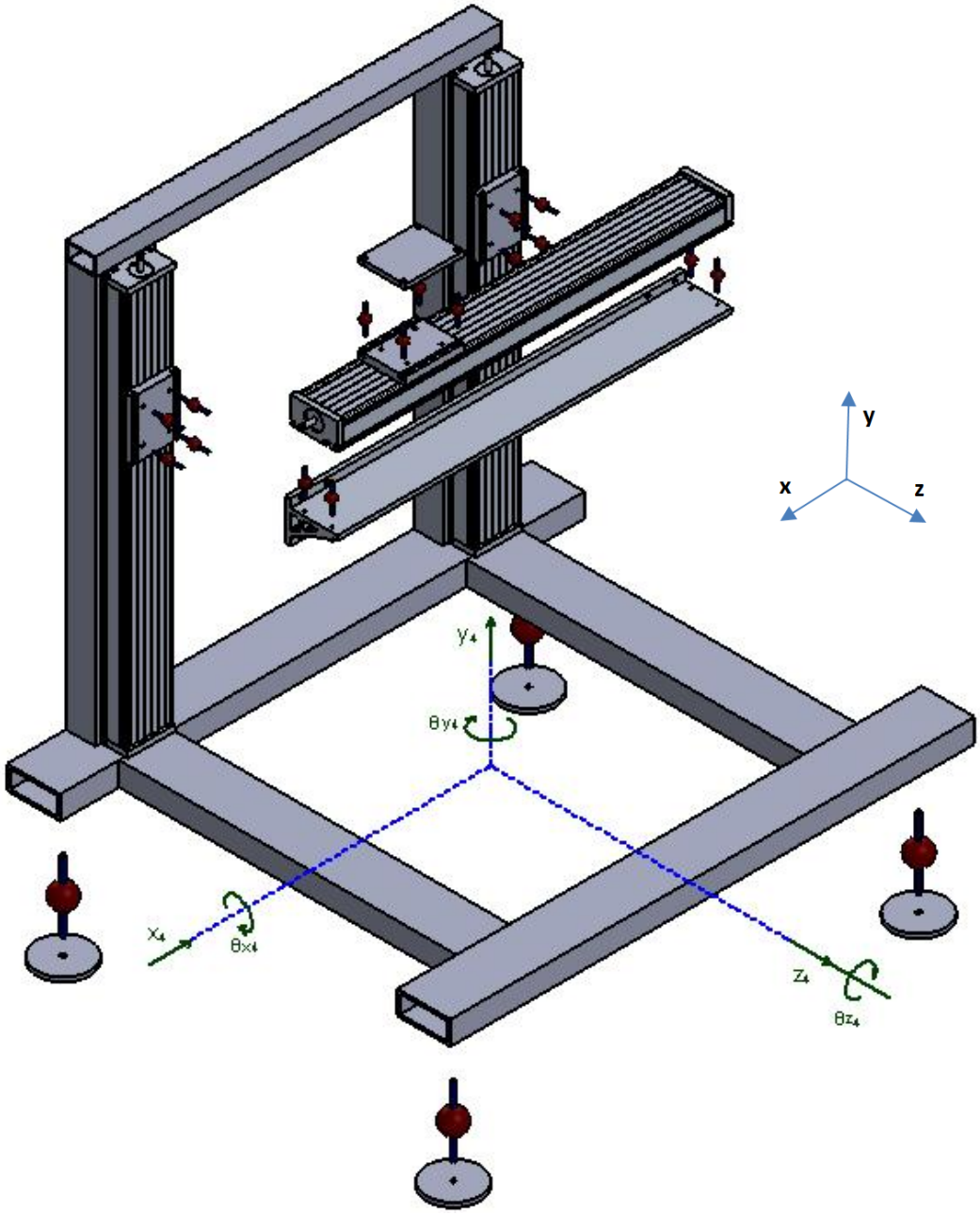


**Figure 5-10: Generalized Coordinates of the Machine Structure Continued**

Generalized coordinates describing the motion of the machine are defined together with the generalized prescribed force/moment. Generalized coordinates describing the motion of each part (as shown in Figures 5-9 and 5-10) are defined in Table 5-3. Each part has six generalized coordinates, describing three linear motions (in x, y, and z-directions) and three angular motions ($\theta_x, \theta_y, \theta_z$). Equations of motions

of the proposed dynamic model will be derived using Lagrange equations in terms of the generalized coordinates.

**Table 5-3: Generalized Coordinates of Parts A, B, C, and D**

| Motion | Part A | Part B | Part C | Part D |
|---|---|---|---|---|
| Translation in *x*-direction | $x_1$ | $x_2$ | $x_3$ | $x_4$ |
| Translation in *y*-direction | $y_1$ | $y_2$ | $y_3$ | $y_4$ |
| Translation in *z*-direction | $z_1$ | $z_2$ | $z_3$ | $z_4$ |
| Rotation about *x*-axis | $q_{x1}$ | $q_{x2}$ | $q_{x3}$ | $q_{x4}$ |
| Rotation about *y*-axis | $q_{y1}$ | $q_{y2}$ | $q_{y3}$ | $q_{y4}$ |
| Rotation about *z*-axis | $q_{z1}$ | $q_{z2}$ | $q_{z3}$ | $q_{z4}$ |

**System Elements**

Inertia and mass properties are defined for each part of the proposed machine in Table 5-4. The stiffness and damping elements of each node are presented in Table 5-5.

**Table 5-4: Mass and Inertia Properties of Parts A, B, C, and D**

| Property | Part A | Part B | Part C | Part D |
|---|---|---|---|---|
| Mass | $M_A$ | $M_B$ | $M_C$ | $M_D$ |
| Mass moment of inertia about *x*-axis | $I_{xA}$ | $I_{xB}$ | $I_{xC}$ | $I_{xD}$ |
| Mass moment of inertia about *y*-axis | $I_{yA}$ | $I_{yB}$ | $I_{yC}$ | $I_{yD}$ |
| Mass moment of inertia about *z*-axis | $I_{zA}$ | $I_{zB}$ | $I_{zC}$ | $I_{zD}$ |

**Table 5-5: Spring and Damping Elements for Each Node**

| Node | Spring Elements | Damping Elements |
|---|---|---|
| A1 | $k_{A1\ (x,y,z)}$ | $C_{A1\ (x,y,z)}$ |
| A2 | $k_{A2\ (x,y,z)}$ | $C_{A2\ (x,y,z)}$ |
| A3 | $k_{A3\ (x,y,z)}$ | $C_{A3\ (x,y,z)}$ |
| A4 | $k_{A4\ (x,y,z)}$ | $C_{A4\ (x,y,z)}$ |
| B1 | $k_{B1\ (x,y,z)}$ | $C_{B1\ (x,y,z)}$ |
| B2 | $k_{B2\ (x,y,z)}$ | $C_{B2\ (x,y,z)}$ |
| B3 | $k_{B3\ (x,y,z)}$ | $C_{B3\ (x,y,z)}$ |
| B4 | $k_{B4\ (x,y,z)}$ | $C_{B4\ (x,y,z)}$ |
| C1 | $k_{C1\ (x,y,z)}$ | $C_{C1\ (x,y,z)}$ |
| C2 | $k_{C2\ (x,y,z)}$ | $C_{C2\ (x,y,z)}$ |
| C3 | $k_{C3\ (x,y,z)}$ | $C_{C3\ (x,y,z)}$ |

| | | |
|---|---|---|
| C4 | $k_{C4\ (x,y,z)}$ | $C_{C4\ (x,y,z)}$ |
| C5 | $k_{C5\ (x,y,z)}$ | $C_{C5\ (x,y,z)}$ |
| C6 | $k_{C6\ (x,y,z)}$ | $C_{C6\ (x,y,z)}$ |
| C7 | $k_{C7\ (x,y,z)}$ | $C_{C7\ (x,y,z)}$ |
| C8 | $k_{C8\ (x,y,z)}$ | $C_{C8\ (x,y,z)}$ |
| D1 | $k_{D1\ (x,y,z)}$ | $C_{D1\ (x,y,z)}$ |
| D2 | $k_{D2\ (x,y,z)}$ | $C_{D2\ (x,y,z)}$ |
| D3 | $k_{D3\ (x,y,z)}$ | $C_{D3\ (x,y,z)}$ |
| D4 | $k_{D4\ (x,y,z)}$ | $C_{D4\ (x,y,z)}$ |

**Generalized Forces and Moments**

Generalized forces and moments will be identified and defined according to the input force/moment imposed on the machine.

**Table 5-6: Generalized Forces/Torque Imposed on the Machine**

| Direction of Force/Torque | Force/Torque |
|---|---|
| Along x-direction | $F_X = f_{X0} sin\omega_X t$ |
| Along y-direction | $F_Y = f_{Y0} sin\omega_Y t$ |
| Along z-direction | $F_Z = f_{Z0} sin\omega_Z t$ |
| About z-axis | $T_0 = T_{Z0} sin\omega_{Z0} t$ |
| Along y-direction | $F_S = m_{spindle} * g$ (weight of the spindle) |

**Lagrange Approach**

Equations of motion of the entire system are derived in terms of generalized coordinates using Lagrangian formulation. This is done by writing the potential, kinetic, and dissipation energies of the system as well as the imposed external forces/moments in the system. The equations of motion will be derived using the following Lagrange's Equation

$$\frac{d}{dt}\left(\frac{\partial L}{\partial \dot{q}_j}\right) + \frac{\partial D}{\partial \dot{q}_j} - \frac{\partial L}{\partial q_j} = \sum Q_j \tag{5-2}$$

where $L$ is the Lagrangian. The expression for the Lagrangian is given by

$$L = T - V \tag{5-3}$$

Where $T$ is the kinetic energy, $V$ is the potential energy, $D$ is the dissipation energy, and $Q_j$ are the generalized forces/moments.

The equation of motion will be written in vector-matrix form as

$$\left[\mathbf{M}\right]_{24\times 24}\{\ddot{\mathbf{q}}\}_{24\times 1} + \left[\mathbf{C}\right]_{24\times 24}\{\dot{\mathbf{q}}\}_{24\times 1} + \left[\mathbf{K}\right]_{24\times 24}\{\mathbf{q}\}_{24\times 1} = \{\mathbf{Q}\}_{24\times 1} \tag{5-4}$$

where $\left[\mathbf{M}\right]$ is the inertia matrix, $\left[\mathbf{C}\right]$ is the damping matrix and $\left[\mathbf{K}\right]$ is the stiffness matrix of the entire system and $\left[\mathbf{Q}\right]$ represents the vector of generalized forces/moments. In the above, the vector $\{\mathbf{q}\}$ represents the displacement vector in terms of generalized coordinates.

The kinetic energy is given by:

$$T = \frac{1}{2}M_A\left(\dot{x}_1{}^2 + \dot{y}_1{}^2 + \dot{z}_1{}^2\right) + \frac{1}{2}M_B\left(\dot{x}_2{}^2 + \dot{y}_2{}^2 + \dot{z}_2{}^2\right) +$$
$$\frac{1}{2}M_C\left(\dot{x}_3{}^2 + \dot{y}_3{}^2 + \dot{z}_3{}^2\right) + \frac{1}{2}M_D\left(\dot{x}_4{}^2 + \dot{y}_4{}^2 + \dot{z}_4{}^2\right) + \frac{1}{2}I_{xA}\dot{\theta}_{x1}{}^2 + \frac{1}{2}I_{xB}\dot{\theta}_{x2}{}^2 +$$
$$\frac{1}{2}I_{xC}\dot{\theta}_{x3}{}^2 + \frac{1}{2}I_{xD}\dot{\theta}_{x4}{}^2 + \frac{1}{2}I_{yA}\dot{\theta}_{y1}{}^2 + \frac{1}{2}I_{yB}\dot{\theta}_{y2}{}^2 + \frac{1}{2}I_{yC}\dot{\theta}_{y3}{}^2 + \frac{1}{2}I_{yD}\dot{\theta}_{y4}{}^2 +$$
$$\frac{1}{2}I_{zA}\dot{\theta}_{z1}{}^2 + \frac{1}{2}I_{zB}\dot{\theta}_{z2}{}^2 + \frac{1}{2}I_{zC}\dot{\theta}_{z3}{}^2 + \frac{1}{2}I_{zD}\dot{\theta}_{z4}{}^2 \tag{5-5}$$

The strain energy is given by:

$$V = \frac{1}{2}k_{A1x}\left(x_1 - \frac{L_{z4}}{2}\theta_{y1} - x_2 + \frac{L_{z4}}{2}\theta_{y2}\right)^2 + \frac{1}{2}k_{A2x}\left(x_1 + \frac{L_{z4}}{2}\theta_{y1} - x_2 - \frac{L_{z4}}{2}\theta_{y2}\right)^2 +$$
$$\frac{1}{2}k_{A3x}\left(x_1 + \frac{L_{z4}}{2}\theta_{y1} - x_2 - \frac{L_{z4}}{2}\theta_{y2}\right)^2 + \frac{1}{2}k_{A4x}\left(x_1 - \frac{L_{z4}}{2}\theta_{y1} - x_2 + \frac{L_{z4}}{2}\theta_{y2}\right)^2 +$$
$$\frac{1}{2}k_{B1x}\left(x_2 - \frac{L_{z6}}{2}\theta_{y2} - x_3 + \frac{L_{z6}}{2}\theta_{y3}\right)^2 + \frac{1}{2}k_{B2x}\left(x_2 + \frac{L_{z6}}{2}\theta_{y2} - x_3 - \frac{L_{z6}}{2}\theta_{y3}\right)^2 +$$
$$\frac{1}{2}k_{B3x}\left(x_2 + \frac{L_{z6}}{2}\theta_{y2} - x_3 - \frac{L_{z6}}{2}\theta_{y3}\right)^2 + \frac{1}{2}k_{B4x}\left(x_2 - \frac{L_{z6}}{2}\theta_{y2} - x_3 + \frac{L_{z6}}{2}\theta_{y3}\right)^2 +$$
$$\frac{1}{2}k_{C1x}\left(x_3 + L_{z7}\theta_{y3} + \frac{L_{y7}}{2}\theta_{z3} - x_4 - L_{z9}\theta_{y4} - L_{y12}\theta_{z4}\right)^2 + \frac{1}{2}k_{C2x}\left(x_3 + L_{z7}\theta_{y3} +\right.$$

$$\frac{L_{y7}}{2}\theta_{z3} - x_4 - L_{z9}\theta_{y4} - L_{y12}\theta_{z4}\Big)^2 + \frac{1}{2}k_{C3x}\Big(x_3 + L_{z7}\theta_{y3} - \frac{L_{y7}}{2}\theta_{z3} - x_4 - L_{z9}\theta_{y4} -$$

$$L_{y11}\theta_{z4}\Big)^2 + \frac{1}{2}k_{C4x}\Big(x_3 + L_{z7}\theta_{y3} - \frac{L_{y7}}{2}\theta_{z3} - x_4 - L_{z9}\theta_{y4} - L_{y11}\theta_{z4}\Big)^2 +$$

$$\frac{1}{2}k_{C5x}\Big(x_3 + L_{z7}\theta_{y3} + \frac{L_{y7}}{2}\theta_{z3} - x_4 - L_{z9}\theta_{y4} - L_{y12}\theta_{z4}\Big)^2 + \frac{1}{2}k_{C6x}\Big(x_3 + L_{z7}\theta_{y3} +$$

$$\frac{L_{y7}}{2}\theta_{z3} - x_4 - L_{z9}\theta_{y4} - L_{y12}\theta_{z4}\Big)^2 + \frac{1}{2}k_{C7x}\Big(x_3 + L_{z7}\theta_{y3} - \frac{L_{y7}}{2}\theta_{z3} - x_4 - L_{z9}\theta_{y4} -$$

$$L_{y11}\theta_{z4}\Big)^2 + \frac{1}{2}k_{C8x}\Big(x_3 + L_{z7}\theta_{y3} - \frac{L_{y7}}{2}\theta_{z3} - x_4 - L_{z9}\theta_{y4} - L_{y11}\theta_{z4}\Big)^2 +$$

$$\frac{1}{2}k_{D1x}\Big(x_4 - \frac{L_{z10}}{2}\theta_{y4}\Big)^2 + \frac{1}{2}k_{D2x}\Big(x_4 + \frac{L_{z10}}{2}\theta_{y4}\Big)^2 + \frac{1}{2}k_{D3x}\Big(x_4 + \frac{L_{z10}}{2}\theta_{y4}\Big)^2 +$$

$$\frac{1}{2}k_{D4x}\Big(x_4 - \frac{L_{z10}}{2}\theta_{y4}\Big)^2 + \frac{1}{2}k_{A1y}\Big(y_1 - \frac{L_{z4}}{2}\theta_{x1} + \frac{L_{x2}}{2}\theta_{z1} - y_2 + \frac{L_{z4}}{2}\theta_{x2} -$$

$$\Big(L_{x3} + \frac{L_{x2}}{2}\Big)\theta_{z2}\Big)^2 + \frac{1}{2}k_{A2y}\Big(y_1 + \frac{L_{z4}}{2}\theta_{x1} + \frac{L_{x2}}{2}\theta_{z1} - y_2 - \frac{L_{z4}}{2}\theta_{x2} - \Big(L_{x3} +$$

$$\frac{L_{x2}}{2}\Big)\theta_{z2}\Big)^2 + \frac{1}{2}k_{A3y}\Big(y_1 + \frac{L_{z4}}{2}\theta_{x1} - \frac{L_{x2}}{2}\theta_{z1} - y_2 - \frac{L_{z4}}{2}\theta_{x2} - \Big(L_{x3} - \frac{L_{x2}}{2}\Big)\theta_{z2}\Big)^2 +$$

$$\frac{1}{2}k_{A4y}\Big(y_1 - \frac{L_{z4}}{2}\theta_{x1} - \frac{L_{x2}}{2}\theta_{z1} - y_2 + \frac{L_{z4}}{2}\theta_{x2} - \Big(L_{x3} - \frac{L_{x2}}{2}\Big)\theta_{z2}\Big)^2 + \frac{1}{2}k_{B1y}\Big(y_2 -$$

$$\frac{L_{z6}}{2}\theta_{x2} + \frac{L_{x4}}{2}\theta_{z2} - y_3 + \frac{L_{z6}}{2}\theta_{x3} - \frac{L_{x4}}{2}\theta_{z3}\Big)^2 + \frac{1}{2}k_{B2y}\Big(y_2 + \frac{L_{z6}}{2}\theta_{x2} + \frac{L_{x4}}{2}\theta_{z2} - y_3 -$$

$$\frac{L_{z6}}{2}\theta_{x3} - \frac{L_{x4}}{2}\theta_{z3}\Big)^2 + \frac{1}{2}k_{B3y}\Big(y_2 + \frac{L_{z6}}{2}\theta_{x2} - \frac{L_{x4}}{2}\theta_{z2} - y_3 - \frac{L_{z6}}{2}\theta_{x3} + \frac{L_{x4}}{2}\theta_{z3}\Big)^2 +$$

$$\frac{1}{2}k_{B4y}\Big(y_2 - \frac{L_{z6}}{2}\theta_{x2} - \frac{L_{x4}}{2}\theta_{z2} - y_3 + \frac{L_{z6}}{2}\theta_{x3} + \frac{L_{x4}}{2}\theta_{z3}\Big)^2 + \frac{1}{2}\big(k_{C1y} + k_{C4y}\big)\Big(y_3 +$$

$$L_{z7}\theta_{x3} + \frac{L_{x6}}{2}\theta_{z3} - y_4 - L_{z9}\theta_{x4} - L_{x8}\theta_{z4}\Big)^2 + \frac{1}{2}\big(k_{C2y} + k_{C3y}\big)\Big(y_3 + L_{z7}\theta_{x3} +$$

$$\frac{L_{x5}}{2}\theta_{z3} - y_4 - L_{z9}\theta_{x4} - L_{x9}\theta_{z4}\Big)^2 + \frac{1}{2}\big(k_{C5y} + k_{C8y}\big)\Big(y_3 + L_{z7}\theta_{x3} - \frac{L_{x5}}{2}\theta_{z3} - y_4 -$$

$$L_{z9}\theta_{x4} + L_{x9}\theta_{z4}\Big)^2 + \frac{1}{2}\big(k_{C6y} + k_{C7y}\big)\Big(y_3 + L_{z7}\theta_{x3} - \frac{L_{x6}}{2}\theta_{z3} - y_4 - L_{z9}\theta_{x4} +$$

$$L_{x8}\theta_{z4}\Big)^2 + \frac{1}{2}k_{D1y}\Big(y_4 - \frac{L_{z10}}{2}\theta_{x4} + \frac{L_{x7}}{2}\theta_{z4}\Big)^2 + \frac{1}{2}k_{D2y}\Big(y_4 + \frac{L_{z10}}{2}\theta_{x4} + \frac{L_{x7}}{2}\theta_{z4}\Big)^2 +$$

$$\frac{1}{2}k_{D3y}\Big(y_4 + \frac{L_{z10}}{2}\theta_{x4} - \frac{L_{x7}}{2}\theta_{z4}\Big)^2 + \frac{1}{2}k_{D4y}\Big(y_4 - \frac{L_{z10}}{2}\theta_{x4} - \frac{L_{x7}}{2}\theta_{z4}\Big)^2 + \frac{1}{2}(k_{A1z} +$$

$$k_{A2z})\left(z_1-\left(\frac{L_{y2}}{2}+\frac{L_{y3}}{2}\right)\theta_{x1}-\frac{L_{x2}}{2}\theta_{y1}-z_2+\left(L_{x3}+\frac{L_{x2}}{2}\right)\theta_{y2}-L_{y8}\theta_{x2}\right)^2+\frac{1}{2}(k_{A3z}+$$

$$k_{A4z})\left(z_1-\left(\frac{L_{y2}}{2}+\frac{L_{y3}}{2}\right)\theta_{x1}+\frac{L_{x2}}{2}\theta_{y1}-z_2+\left(L_{x3}-\frac{L_{x2}}{2}\right)\theta_{y2}-L_{y8}\theta_{x2}\right)^2+\frac{1}{2}(k_{B1z}+$$

$$k_{B2z})\left(z_2-L_{y9}\theta_{x2}-\frac{L_{x4}}{2}\theta_{y2}-z_3-L_{y10}\theta_{x3}+\frac{L_{x4}}{2}\theta_{y3}\right)^2+\frac{1}{2}(k_{B3z}+$$

$$k_{B4z})\left(z_2-L_{y9}\theta_{x2}+\frac{L_{x4}}{2}\theta_{y2}-z_3-L_{y10}\theta_{x3}-\frac{L_{x4}}{2}\theta_{y3}\right)^2+\frac{1}{2}k_{C1z}\left(z_3+\frac{L_{y7}}{2}\theta_{x3}-\right.$$

$$\left.\frac{L_{x6}}{2}\theta_{y3}-z_4-L_{y12}\theta_{x4}+L_{x8}\theta_{y4}\right)^2+\frac{1}{2}k_{C2z}\left(z_3+\frac{L_{y7}}{2}\theta_{x3}-\frac{L_{x5}}{2}\theta_{y3}-z_4-\right.$$

$$\left.L_{y12}\theta_{x4}+L_{x9}\theta_{y4}\right)^2+\frac{1}{2}k_{C3z}\left(z_3-\frac{L_{y7}}{2}\theta_{x3}-\frac{L_{x5}}{2}\theta_{y3}-z_4-L_{y11}\theta_{x4}+L_{x9}\theta_{y4}\right)^2+$$

$$\frac{1}{2}k_{C4z}\left(z_3-\frac{L_{y7}}{2}\theta_{x3}-\frac{L_{x6}}{2}\theta_{y3}-z_4-L_{y11}\theta_{x4}+L_{x8}\theta_{y4}\right)^2+\frac{1}{2}k_{C5z}\left(z_3+\frac{L_{y7}}{2}\theta_{x3}+\right.$$

$$\left.\frac{L_{x5}}{2}\theta_{y3}-z_4-L_{y12}\theta_{x4}-L_{x9}\theta_{y4}\right)^2+\frac{1}{2}k_{C6z}\left(z_3+\frac{L_{y7}}{2}\theta_{x3}+\frac{L_{x6}}{2}\theta_{y3}-z_4-\right.$$

$$\left.L_{y12}\theta_{x4}-L_{x8}\theta_{y4}\right)^2+\frac{1}{2}k_{C7z}\left(z_3-\frac{L_{y7}}{2}\theta_{x3}+\frac{L_{x6}}{2}\theta_{y3}-z_4-L_{y11}\theta_{x4}-L_{x8}\theta_{y4}\right)^2+$$

$$\frac{1}{2}k_{C8z}\left(z_3-\frac{L_{y7}}{2}\theta_{x3}+\frac{L_{x5}}{2}\theta_{y3}-z_4-L_{y11}\theta_{x4}-L_{x9}\theta_{y4}\right)^2+\frac{1}{2}k_{D1z}\left(z_4-\frac{L_{x7}}{2}\theta_{y4}\right)^2+$$

$$\frac{1}{2}k_{D2z}\left(z_4-\frac{L_{x7}}{2}\theta_{y4}\right)^2+\frac{1}{2}k_{D3z}\left(z_4+\frac{L_{x7}}{2}\theta_{y4}\right)^2+\frac{1}{2}k_{D4z}\left(z_4+\frac{L_{x7}}{2}\theta_{y4}\right)^2$$

(5-6)

The dissipation energy is given by:

$$D=\frac{1}{2}C_{A1x}\left(\dot{x}_1-\frac{L_{z4}}{2}\dot{\theta}_{y1}-\dot{x}_2+\frac{L_{z4}}{2}\dot{\theta}_{y2}\right)^2+\frac{1}{2}C_{A2x}\left(\dot{x}_1+\frac{L_{z4}}{2}\dot{\theta}_{y1}-\dot{x}_2-\frac{L_{z4}}{2}\dot{\theta}_{y2}\right)^2+$$

$$\frac{1}{2}C_{A3x}\left(\dot{x}_1+\frac{L_{z4}}{2}\dot{\theta}_{y1}-\dot{x}_2-\frac{L_{z4}}{2}\dot{\theta}_{y2}\right)^2+\frac{1}{2}C_{A4x}\left(\dot{x}_1-\frac{L_{z4}}{2}\dot{\theta}_{y1}-\dot{x}_2+\frac{L_{z4}}{2}\dot{\theta}_{y2}\right)^2+$$

$$\frac{1}{2}C_{B1x}\left(\dot{x}_2-\frac{L_{z6}}{2}\dot{\theta}_{y2}-\dot{x}_3+\frac{L_{z6}}{2}\dot{\theta}_{y3}\right)^2+\frac{1}{2}C_{B2x}\left(\dot{x}_2+\frac{L_{z6}}{2}\dot{\theta}_{y2}-\dot{x}_3-\frac{L_{z6}}{2}\dot{\theta}_{y3}\right)^2+$$

$$\frac{1}{2}C_{B3x}\left(\dot{x}_2+\frac{L_{z6}}{2}\dot{\theta}_{y2}-\dot{x}_3-\frac{L_{z6}}{2}\dot{\theta}_{y3}\right)^2+\frac{1}{2}C_{B4x}\left(\dot{x}_2-\frac{L_{z6}}{2}\dot{\theta}_{y2}-\dot{x}_3+\frac{L_{z6}}{2}\dot{\theta}_{y3}\right)^2+$$

$$\frac{1}{2}C_{C1x}\left(\dot{x}_3+L_{z7}\dot{\theta}_{y3}+\frac{L_{y7}}{2}\dot{\theta}_{z3}-\dot{x}_4-L_{z9}\dot{\theta}_{y4}-L_{y12}\dot{\theta}_{z4}\right)^2+\frac{1}{2}C_{C2x}\left(\dot{x}_3+L_{z7}\dot{\theta}_{y3}+\right.$$

$$\frac{L_{y7}}{2}\dot{\theta}_{z3} - \dot{x}_4 - L_{z9}\dot{\theta}_{y4} - L_{y12}\dot{\theta}_{z4}\Big)^2 + \frac{1}{2}C_{C3x}\Big(\dot{x}_3 + L_{z7}\dot{\theta}_{y3} - \frac{L_{y7}}{2}\dot{\theta}_{z3} - \dot{x}_4 - L_{z9}\dot{\theta}_{y4} -$$

$$L_{y11}\dot{\theta}_{z4}\Big)^2 + \frac{1}{2}C_{C4x}\Big(\dot{x}_3 + L_{z7}\dot{\theta}_{y3} - \frac{L_{y7}}{2}\dot{\theta}_{z3} - \dot{x}_4 - L_{z9}\dot{\theta}_{y4} - L_{y11}\dot{\theta}_{z4}\Big)^2 +$$

$$\frac{1}{2}C_{C5x}\Big(\dot{x}_3 + L_{z7}\dot{\theta}_{y3} + \frac{L_{y7}}{2}\dot{\theta}_{z3} - \dot{x}_4 - L_{z9}\dot{\theta}_{y4} - L_{y12}\dot{\theta}_{z4}\Big)^2 + \frac{1}{2}C_{C6x}\Big(\dot{x}_3 + L_{z7}\dot{\theta}_{y3} +$$

$$\frac{L_{y7}}{2}\dot{\theta}_{z3} - \dot{x}_4 - L_{z9}\dot{\theta}_{y4} - L_{y12}\dot{\theta}_{z4}\Big)^2 + \frac{1}{2}C_{C7x}\Big(\dot{x}_3 + L_{z7}\dot{\theta}_{y3} - \frac{L_{y7}}{2}\dot{\theta}_{z3} - \dot{x}_4 - L_{z9}\dot{\theta}_{y4} -$$

$$L_{y11}\dot{\theta}_{z4}\Big)^2 + \frac{1}{2}C_{C8x}\Big(\dot{x}_3 + L_{z7}\dot{\theta}_{y3} - \frac{L_{y7}}{2}\dot{\theta}_{z3} - \dot{x}_4 - L_{z9}\dot{\theta}_{y4} - L_{y11}\dot{\theta}_{z4}\Big)^2 +$$

$$\frac{1}{2}C_{D1x}\Big(\dot{x}_4 - \frac{L_{z10}}{2}\dot{\theta}_{y4}\Big)^2 + \frac{1}{2}C_{D2x}\Big(\dot{x}_4 + \frac{L_{z10}}{2}\dot{\theta}_{y4}\Big)^2 + \frac{1}{2}C_{D3x}\Big(\dot{x}_4 + \frac{L_{z10}}{2}\dot{\theta}_{y4}\Big)^2 +$$

$$\frac{1}{2}C_{D4x}\Big(\dot{x}_4 - \frac{L_{z10}}{2}\dot{\theta}_{y4}\Big)^2 + \frac{1}{2}C_{A1y}\Big(\dot{y}_1 - \frac{L_{z4}}{2}\dot{\theta}_{x1} + \frac{L_{x2}}{2}\dot{\theta}_{z1} - \dot{y}_2 + \frac{L_{z4}}{2}\dot{\theta}_{x2} -$$

$$\Big(L_{x3} + \frac{L_{x2}}{2}\Big)\dot{\theta}_{z2}\Big)^2 + \frac{1}{2}C_{A2y}\Big(\dot{y}_1 + \frac{L_{z4}}{2}\dot{\theta}_{x1} + \frac{L_{x2}}{2}\dot{\theta}_{z1} - \dot{y}_2 - \frac{L_{z4}}{2}\dot{\theta}_{x2} - \Big(L_{x3} +$$

$$\frac{L_{x2}}{2}\Big)\dot{\theta}_{z2}\Big)^2 + \frac{1}{2}C_{A3y}\Big(\dot{y}_1 + \frac{L_{z4}}{2}\dot{\theta}_{x1} - \frac{L_{x2}}{2}\dot{\theta}_{z1} - \dot{y}_2 - \frac{L_{z4}}{2}\dot{\theta}_{x2} - \Big(L_{x3} - \frac{L_{x2}}{2}\Big)\dot{\theta}_{z2}\Big)^2 +$$

$$\frac{1}{2}C_{A4y}\Big(\dot{y}_1 - \frac{L_{z4}}{2}\dot{\theta}_{x1} - \frac{L_{x2}}{2}\dot{\theta}_{z1} - \dot{y}_2 + \frac{L_{z4}}{2}\dot{\theta}_{x2} - \Big(L_{x3} - \frac{L_{x2}}{2}\Big)\dot{\theta}_{z2}\Big)^2 + \frac{1}{2}C_{B1y}\Big(\dot{y}_2 -$$

$$\frac{L_{z6}}{2}\dot{\theta}_{x2} + \frac{L_{x4}}{2}\dot{\theta}_{z2} - \dot{y}_3 + \frac{L_{z6}}{2}\dot{\theta}_{x3} - \frac{L_{x4}}{2}\dot{\theta}_{z3}\Big)^2 + \frac{1}{2}C_{B2y}\Big(\dot{y}_2 + \frac{L_{z6}}{2}\dot{\theta}_{x2} + \frac{L_{x4}}{2}\dot{\theta}_{z2} - \dot{y}_3 -$$

$$\frac{L_{z6}}{2}\dot{\theta}_{x3} - \frac{L_{x4}}{2}\dot{\theta}_{z3}\Big)^2 + \frac{1}{2}C_{B3y}\Big(\dot{y}_2 + \frac{L_{z6}}{2}\dot{\theta}_{x2} - \frac{L_{x4}}{2}\dot{\theta}_{z2} - \dot{y}_3 - \frac{L_{z6}}{2}\dot{\theta}_{x3} + \frac{L_{x4}}{2}\dot{\theta}_{z3}\Big)^2 +$$

$$\frac{1}{2}C_{B4y}\Big(\dot{y}_2 - \frac{L_{z6}}{2}\dot{\theta}_{x2} - \frac{L_{x4}}{2}\dot{\theta}_{z2} - \dot{y}_3 + \frac{L_{z6}}{2}\dot{\theta}_{x3} + \frac{L_{x4}}{2}\dot{\theta}_{z3}\Big)^2 + \frac{1}{2}(C_{C1y} + C_{C4y})\Big(\dot{y}_3 +$$

$$L_{z7}\dot{\theta}_{x3} + \frac{L_{x6}}{2}\dot{\theta}_{z3} - \dot{y}_4 - L_{z9}\dot{\theta}_{x4} - L_{x8}\dot{\theta}_{z4}\Big)^2 + \frac{1}{2}(C_{C2y} + C_{C3y})\Big(\dot{y}_3 + L_{z7}\dot{\theta}_{x3} +$$

$$\frac{L_{x5}}{2}\dot{\theta}_{z3} - \dot{y}_4 - L_{z9}\dot{\theta}_{x4} - L_{x9}\dot{\theta}_{z4}\Big)^2 + \frac{1}{2}(C_{C5y} + C_{C8y})\Big(\dot{y}_3 + L_{z7}\dot{\theta}_{x3} - \frac{L_{x5}}{2}\dot{\theta}_{z3} - \dot{y}_4 -$$

$$L_{z9}\dot{\theta}_{x4} + L_{x9}\dot{\theta}_{z4}\Big)^2 + \frac{1}{2}(C_{C6y} + C_{C7y})\Big(\dot{y}_3 + L_{z7}\dot{\theta}_{x3} - \frac{L_{x6}}{2}\dot{\theta}_{z3} - \dot{y}_4 - L_{z9}\dot{\theta}_{x4} +$$

$$L_{x8}\dot{\theta}_{z4}\Big)^2 + \frac{1}{2}C_{D1y}\Big(\dot{y}_4 - \frac{L_{z10}}{2}\dot{\theta}_{x4} + \frac{L_{x7}}{2}\dot{\theta}_{z4}\Big)^2 + \frac{1}{2}C_{D2y}\Big(\dot{y}_4 + \frac{L_{z10}}{2}\dot{\theta}_{x4} + \frac{L_{x7}}{2}\dot{\theta}_{z4}\Big)^2 +$$

$$\frac{1}{2}C_{D3y}\Big(\dot{y}_4 + \frac{L_{z10}}{2}\dot{\theta}_{x4} - \frac{L_{x7}}{2}\dot{\theta}_{z4}\Big)^2 + \frac{1}{2}C_{D4y}\Big(\dot{y}_4 - \frac{L_{z10}}{2}\dot{\theta}_{x4} - \frac{L_{x7}}{2}\dot{\theta}_{z4}\Big)^2 + \frac{1}{2}(C_{A1z} +$$

$$C_{A2z})\left(\dot{z}_1-\left(\frac{L_{y2}}{2}+\frac{L_{y3}}{2}\right)\dot{\theta}_{x1}-\frac{L_{x2}}{2}\dot{\theta}_{y1}-\dot{z}_2+\left(L_{x3}+\frac{L_{x2}}{2}\right)\dot{\theta}_{y2}-L_{y8}\dot{\theta}_{x2}\right)^2+\frac{1}{2}(C_{A3z}+$$

$$C_{A4z})\left(\dot{z}_1-\left(\frac{L_{y2}}{2}+\frac{L_{y3}}{2}\right)\dot{\theta}_{x1}+\frac{L_{x2}}{2}\dot{\theta}_{y1}-\dot{z}_2+\left(L_{x3}-\frac{L_{x2}}{2}\right)\dot{\theta}_{y2}-L_{y8}\dot{\theta}_{x2}\right)^2+\frac{1}{2}(C_{B1z}+$$

$$C_{B2z})\left(\dot{z}_2-L_{y9}\dot{\theta}_{x2}-\frac{L_{x4}}{2}\dot{\theta}_{y2}-\dot{z}_3-L_{y10}\dot{\theta}_{x3}+\frac{L_{x4}}{2}\dot{\theta}_{y3}\right)^2+\frac{1}{2}(C_{B3z}+$$

$$C_{B4z})\left(\dot{z}_2-L_{y9}\dot{\theta}_{x2}+\frac{L_{x4}}{2}\dot{\theta}_{y2}-\dot{z}_3-L_{y10}\dot{\theta}_{x3}-\frac{L_{x4}}{2}\dot{\theta}_{y3}\right)^2+\frac{1}{2}C_{C1z}\left(\dot{z}_3+\frac{L_{y7}}{2}\dot{\theta}_{x3}-\right.$$

$$\left.\frac{L_{x6}}{2}\dot{\theta}_{y3}-\dot{z}_4-L_{y12}\dot{\theta}_{x4}+L_{x8}\dot{\theta}_{y4}\right)^2+\frac{1}{2}C_{C2z}\left(\dot{z}_3+\frac{L_{y7}}{2}\dot{\theta}_{x3}-\frac{L_{x5}}{2}\dot{\theta}_{y3}-\dot{z}_4-\right.$$

$$\left.L_{y12}\dot{\theta}_{x4}+L_{x9}\dot{\theta}_{y4}\right)^2+\frac{1}{2}C_{C3z}\left(\dot{z}_3-\frac{L_{y7}}{2}\dot{\theta}_{x3}-\frac{L_{x5}}{2}\dot{\theta}_{y3}-\dot{z}_4-L_{y11}\dot{\theta}_{x4}+L_{x9}\dot{\theta}_{y4}\right)^2+$$

$$\frac{1}{2}C_{C4z}\left(\dot{z}_3-\frac{L_{y7}}{2}\dot{\theta}_{x3}-\frac{L_{x6}}{2}\dot{\theta}_{y3}-\dot{z}_4-L_{y11}\dot{\theta}_{x4}+L_{x8}\dot{\theta}_{y4}\right)^2+\frac{1}{2}C_{C5z}\left(\dot{z}_3+\frac{L_{y7}}{2}\dot{\theta}_{x3}+\right.$$

$$\left.\frac{L_{x5}}{2}\dot{\theta}_{y3}-\dot{z}_4-L_{y12}\dot{\theta}_{x4}-L_{x9}\dot{\theta}_{y4}\right)^2+\frac{1}{2}C_{C6z}\left(\dot{z}_3+\frac{L_{y7}}{2}\dot{\theta}_{x3}+\frac{L_{x6}}{2}\dot{\theta}_{y3}-\dot{z}_4-\right.$$

$$\left.L_{y12}\dot{\theta}_{x4}-L_{x8}\dot{\theta}_{y4}\right)^2+\frac{1}{2}C_{C7z}\left(\dot{z}_3-\frac{L_{y7}}{2}\dot{\theta}_{x3}+\frac{L_{x6}}{2}\dot{\theta}_{y3}-\dot{z}_4-L_{y11}\dot{\theta}_{x4}-L_{x8}\dot{\theta}_{y4}\right)^2+$$

$$\frac{1}{2}C_{C8z}\left(\dot{z}_3-\frac{L_{y7}}{2}\dot{\theta}_{x3}+\frac{L_{x5}}{2}\dot{\theta}_{y3}-\dot{z}_4-L_{y11}\dot{\theta}_{x4}-L_{x9}\dot{\theta}_{y4}\right)^2+\frac{1}{2}C_{D1z}\left(\dot{z}_4-\frac{L_{x7}}{2}\dot{\theta}_{y4}\right)^2+$$

$$\frac{1}{2}C_{D2z}\left(\dot{z}_4-\frac{L_{x7}}{2}\dot{\theta}_{y4}\right)^2+\frac{1}{2}C_{D3z}\left(\dot{z}_4+\frac{L_{x7}}{2}\dot{\theta}_{y4}\right)^2+\frac{1}{2}C_{D4z}\left(\dot{z}_4+\frac{L_{x7}}{2}\dot{\theta}_{y4}\right)^2 \qquad (5\text{-}7)$$

After deriving the kinetic, strain, and dissipation energy expressions, and performing the appropriate differentiation according to Lagrange's equation, the following matrix form will hold the equations of motion of the system. There are twenty-four EOMs.

$$\begin{bmatrix} M_{0101} & \cdots & M_{0124} \\ \vdots & \ddots & \vdots \\ M_{2401} & \cdots & M_{2424} \end{bmatrix}\begin{bmatrix} \ddot{q}_1 \\ \vdots \\ \ddot{q}_{24} \end{bmatrix}+\begin{bmatrix} C_{0101} & \cdots & C_{0124} \\ \vdots & \ddots & \vdots \\ C_{2401} & \cdots & C_{2424} \end{bmatrix}\begin{bmatrix} \dot{q}_1 \\ \vdots \\ \dot{q}_{24} \end{bmatrix}+\begin{bmatrix} k_{0101} & \cdots & k_{0124} \\ \vdots & \ddots & \vdots \\ k_{2401} & \cdots & k_{2424} \end{bmatrix}\begin{bmatrix} q_1 \\ \vdots \\ q_{24} \end{bmatrix}$$
$$=\begin{bmatrix} Q_1 \\ \vdots \\ Q_{24} \end{bmatrix}$$

where:

$$[q] = \begin{bmatrix} x_1 \\ \vdots \\ x_4 \\ y_1 \\ \vdots \\ y_4 \\ z_1 \\ \vdots \\ z_4 \\ \theta_{x1} \\ \vdots \\ \theta_{x4} \\ \theta_{y1} \\ \vdots \\ \theta_{y4} \\ \theta_{z1} \\ \vdots \\ \theta_{z4} \end{bmatrix}$$

The non-zero elements of the mass, stiffness, and damping matrices are given in Appendix A.

Each EOM can be structured into a mathematical model of inputs, outputs, and state variables known as state space representation. State space representation provides a compact way to model and analyze systems with multiple inputs and outputs. The general state space representation of the system equations of motion will be written in vector-matrix form as

$$\{\dot{\mathbf{r}}\}_{48\times 1} = [\mathbf{A}]_{48\times 48}\{\mathbf{r}\}_{48\times 1} + [\mathbf{B}]_{48\times 48}\{\mathbf{u}\}_{48\times 1} \tag{5-8}$$

$$\{\mathbf{y(t)}\}_{48\times 1} = [\bar{\mathbf{C}}]_{48\times 48}\{\mathbf{r}\}_{48\times 1} + [\bar{\mathbf{D}}]_{48\times 48}\{\mathbf{u}\}_{48\times 1} \tag{5-9}$$

where $[\mathbf{A}]$ is the state matrix, $[\mathbf{B}]$ is the input matrix and $[\bar{\mathbf{C}}]$ is the output matrix, and $[\bar{\mathbf{D}}]$ is the feedforward matrix. In the above, the vector $\{\mathbf{r}\}$ represents the state vector, $\{\mathbf{y(t)}\}$ represents the output vector, and $\{\mathbf{u}\}$ is the input vector.

The size of the matrices with their symbols are shown below. The $\bar{D}$ matrix is considered zero since there is no feed forward in this system.

$$\begin{bmatrix} \dot{r}_1 \\ \vdots \\ \dot{r}_{48} \end{bmatrix} = \begin{bmatrix} A_{0101} & \cdots & A_{0148} \\ \vdots & \ddots & \vdots \\ A_{4801} & \cdots & A_{4848} \end{bmatrix} \begin{bmatrix} r_1 \\ \vdots \\ r_{48} \end{bmatrix} + \begin{bmatrix} B_{0101} & \cdots & B_{0148} \\ \vdots & \ddots & \vdots \\ B_{4801} & \cdots & B_{4848} \end{bmatrix} \begin{bmatrix} u_1 \\ \vdots \\ u_{48} \end{bmatrix}$$

$$\begin{bmatrix} y_1 \\ \vdots \\ y_{48} \end{bmatrix} = \begin{bmatrix} \bar{C}_{0101} & \cdots & \bar{C}_{0148} \\ \vdots & \ddots & \vdots \\ \bar{C}_{4801} & \cdots & \bar{C}_{4848} \end{bmatrix} \begin{bmatrix} r_1 \\ \vdots \\ r_{48} \end{bmatrix} + [0] \begin{bmatrix} u_1 \\ \vdots \\ u_{48} \end{bmatrix}$$

Where $r_{ij}$ are the state variables given by:

$r_1 = x_1$
$r_2 = \dot{x}_1$
$r_3 = x_2$
$r_4 = \dot{x}_2$
$r_5 = x_3$
$r_6 = \dot{x}_3$
$r_7 = x_4$
$r_8 = \dot{x}_4$
$r_9 = y_1$
$r_{10} = \dot{y}_1$
$r_{11} = y_2$
$r_{12} = \dot{y}_2$
$r_{13} = y_3$
$r_{14} = \dot{y}_3$
$r_{15} = y_4$
$r_{16} = \dot{y}_4$
$r_{17} = z_1$
$r_{18} = \dot{z}_1$
$r_{19} = z_2$
$r_{20} = \dot{z}_2$
$r_{21} = z_3$
$r_{22} = \dot{z}_3$
$r_{23} = z_4$
$r_{24} = \dot{z}_4$
$r_{25} = \theta_{x1}$
$r_{26} = \dot{\theta}_{x1}$
$r_{27} = \theta_{x2}$
$r_{28} = \dot{\theta}_{x2}$
$r_{29} = \theta_{x3}$
$r_{30} = \dot{\theta}_{x3}$
$r_{31} = \theta_{x4}$
$r_{32} = \dot{\theta}_{x4}$
$r_{33} = \theta_{y1}$
$r_{34} = \dot{\theta}_{y1}$
$r_{35} = \theta_{y2}$
$r_{36} = \dot{\theta}_{y2}$
$r_{37} = \theta_{y3}$
$r_{38} = \dot{\theta}_{y3}$
$r_{39} = \theta_{y4}$
$r_{40} = \dot{\theta}_{y4}$
$r_{41} = \theta_{z1}$
$r_{42} = \dot{\theta}_{z1}$
$r_{43} = \theta_{z2}$
$r_{44} = \dot{\theta}_{z2}$
$r_{45} = \theta_{z3}$
$r_{46} = \dot{\theta}_{z3}$
$r_{47} = \theta_{z4}$
$r_{48} = \dot{\theta}_{z4}$

The expressions of the A, B, and C matrices are given in Appendix B.

## 5.4 Dynamic Analysis

Dynamic analysis is conducted to predict the machine behavior while enduring cyclic loads. By using natural frequencies that are determined in the frequency analysis of the machine, and plugging the magnitude and frequency of the loads, it is possible to predict the motion at any point on the machine. This is done using SOLIDWORKS' Dynamic Analysis. Two types of dynamic analyses are performed on the machine. The first is Harmonic analysis where the Amplitude-Frequency plot is acquired. The second is time based history analysis giving the time history plot.

In these dynamic analyses, the loads used are the maximum needed for the welding application for both processes (plunging and traversing) as shown in Table 5-3. The frequencies of the applied loads are varying between 3.33 Hz and 20 Hz. The displacement of point A shown in Figure 5-10 (in the circle) will be studied with variation in time. This point is located at the center of the four bolt holes that the spindle will be attached on. This will give an idea of the behavior of the spindle base, and its stability.

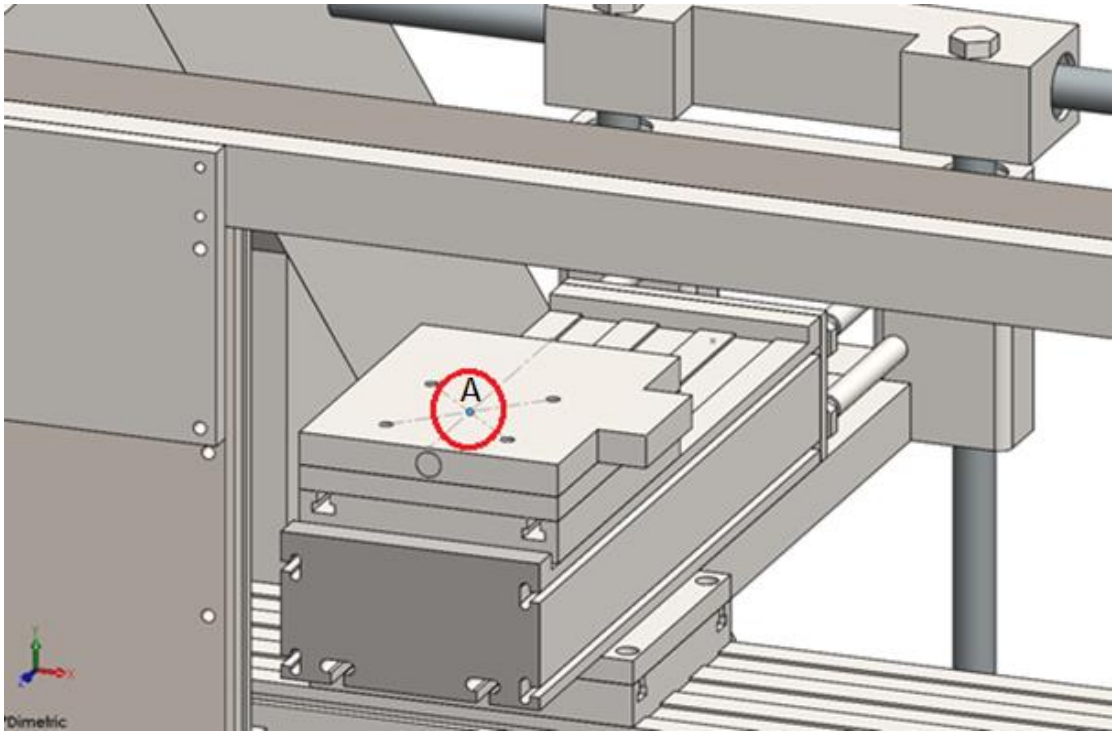


**Figure 5-11: Point Used for Motion Study**

# RESULTS AND DISCUSSION

According to Crandall [45], engineering problems can be classified into three categories:

- Equilibrium problems
- Eigenvalue problems
- Propagation problems

Equilibrium problems are characterized by mechanical deformation due to repetitive loading. Their solution could be in the form of stress or deformation state under a given load.

Eigenvalue problems are considered extensions of equilibrium problems in that their solutions are dictated by the same equilibrium states. Their solutions are characterized by a unique set of system configurations such as resonance.

Propagation problems are to predict the subsequent stresses or deformation states under a time varying load.

Four types of analyses are performed in this work. These are stress, strain, frequency, and dynamic analysis. These analyses are conducted for two different locations of the spindle; namely, the top left position and the center position of the work frame. In these positions, the spindle will be running in either plunging or traversing process. The plunging process is characterized by the motion of the spindle in the z-direction. The traversing process is characterized by the traveling motion of the spindle in the x, and y direction during welding.

## 6.1 Static Analysis

Static analysis is crucial to the study under investigation as it ensures that the machine can withstand the maximum forces depicted in Table 3-1. Results arising from this analysis include the stress and deformation of the machine as a result of the applied loads in the different directions. The main goal is to obtain a maximum stress that should be lower than the yielding strength of the material. Figures 6-1 – 6-16 are generated by SOLIDWORKS. They include a model of the machine with colors that change based on the endured stresses or deformation and a corresponding bar to the right showing the magnitude with the associated colors. The red color is the maximum positive stress/deformation, while the blue one indicates either the lowest positive value, or the maximum negative value.

### 6.1.1 Static Analysis when the Spindle is at Top Left Position of the Machine Frame

Studies in this section were conducted while the spindle is operating in the top left position of the machine. Analysis is performed in this position for both the plunging and traverse processes.

**A- Plunging process when the spindle is at top left position of the machine frame**

During plunging, it is assumed that the tool will only move in the z-direction while the tool is rotating about z-axis to penetrate the workpiece. In these studies, the reaction force in the z-direction and the torque around the z-axis will have a value above the maximum shown it Table 3-1, to ensure that the machine will produce high precision

welds even when exceeding maximum design parameter values. Load value used in this analysis are 2000 N and 45 N.m., respectively. These values are higher than those reported in [31-32].

### 1- Stresses (Top left, Plunging)

Figure 6-1 displays the von Mises stresses that the machine endures when the spindle is located at the top left position and plunging. Stress values are indicated by the corresponding bar to the right of the figure. The machine deflections are exaggerated in the figure for clarification.

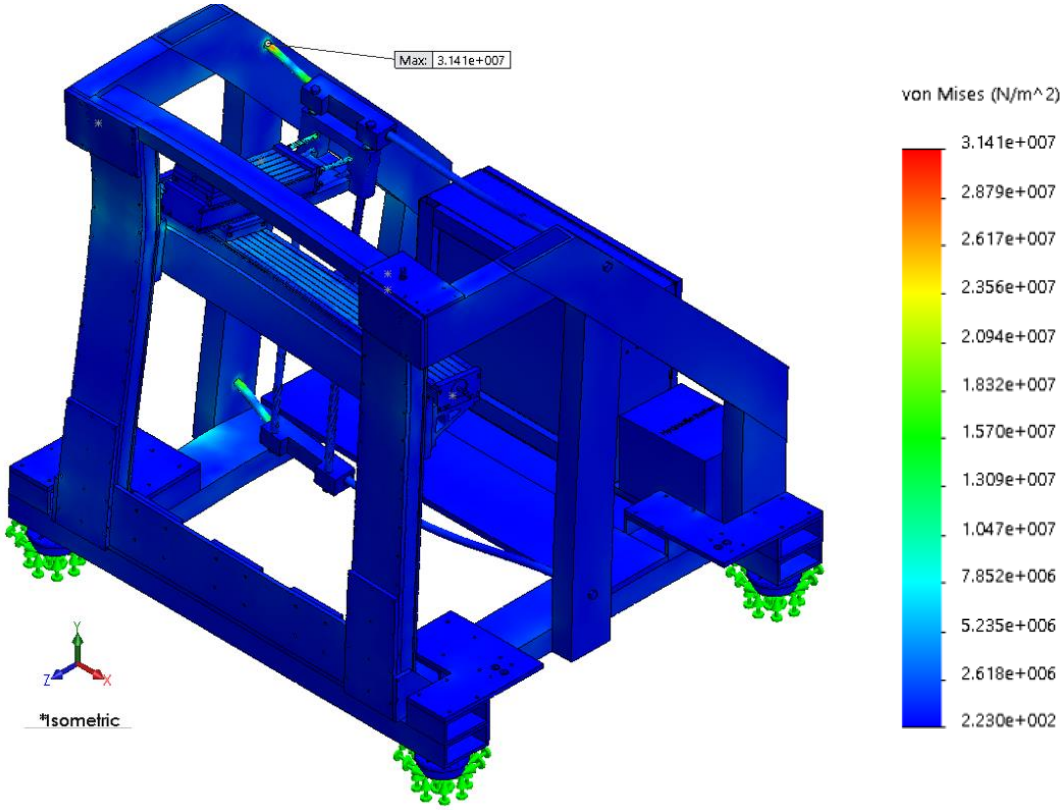


**Figure 6-1: Von Mises Stresses (Top Left Position-Plunging)**

In Figure 6-1, low von Mises stress values (indicated by the blue color) range between 223 Pa and 7.852 MPa. Highly stressed areas (in green, yellow, and red) range

between 10.47 MPa and 31.41 MPa. The frame upper left side and the backbone shaft of the machine are shown to endure higher forces.

The maximum von Mises stress value is 31.41 MPa. That is mainly bending stress on the top shaft of the backbone. This stress is considered small compared to the yielding strength of the material 220.59 MPa (shown in Table 5-1). This indicates that the highest applied plunging forces will not damage the machine.

### 2- Deformation (Top left, Plunging)

Figures 6-2, 6-3, and 6-4 show the deformations of the structure of the machine in the x, y, and z-directions, respectively, due to plunging. In these figures, the overall displacement is compared to the grey shaded nondeformed shape of the machine for which the color changes of the deformed machine indicates displacement size.

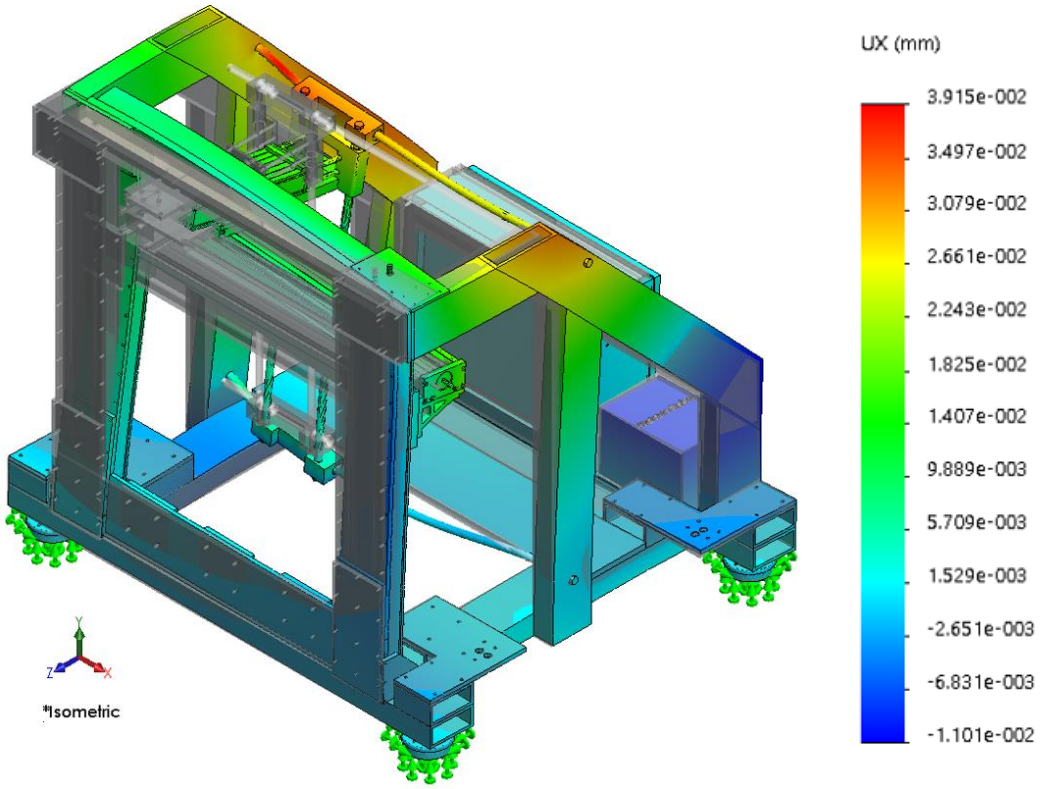


**Figure 6-2: Deformation of the machine in x-direction (Top left-Plunging)**

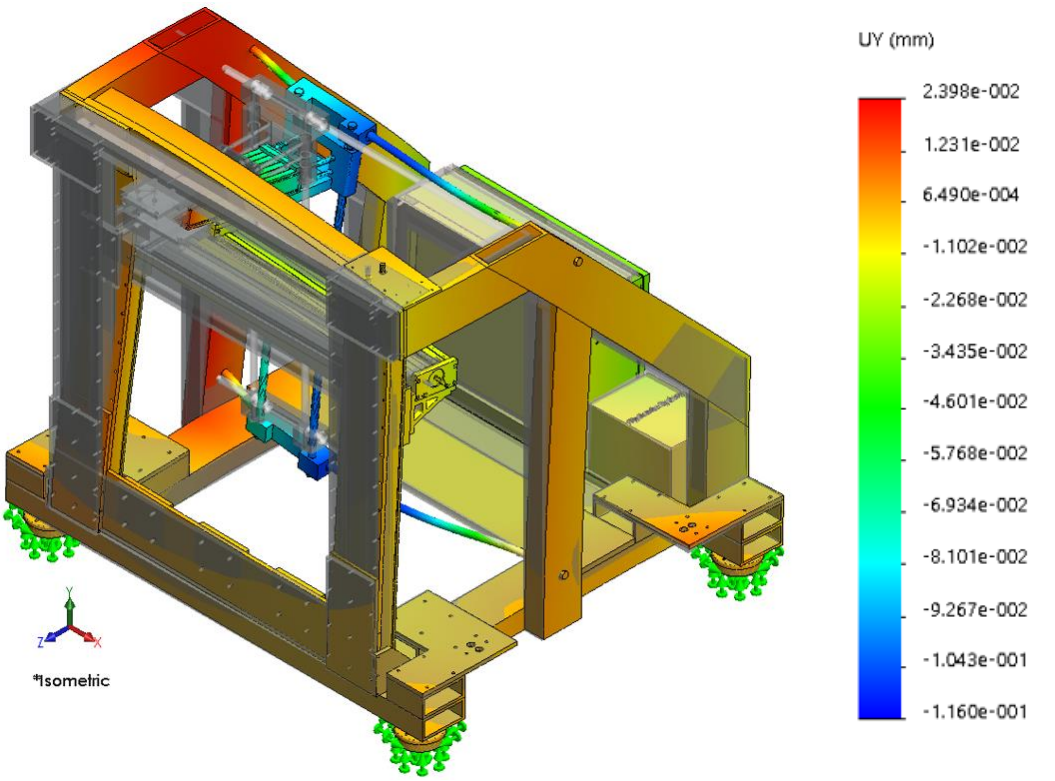


**Figure 6-3: Deformation of the machine in y-direction (Top left-Plunging)**

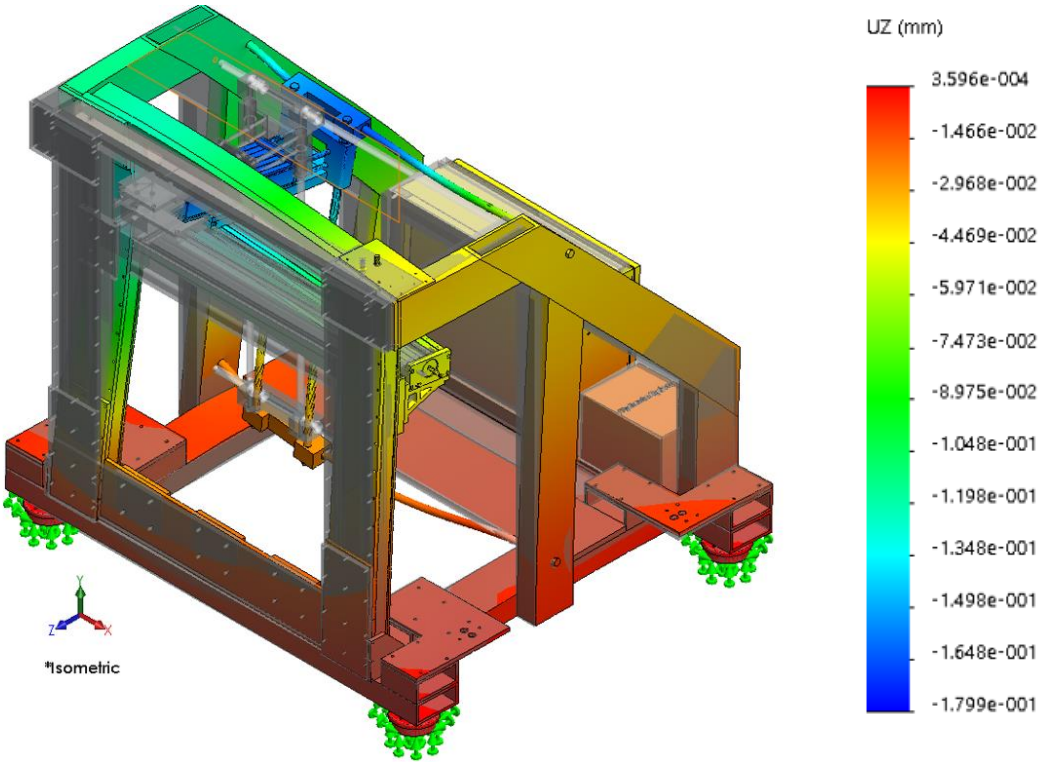


**Figure 6-4: Deformation of the machine in z-direction (Top left-Plunging)**

The maximum displacement is 0.039 mm and is shown by the red color in Figure 6-2. The displacement of the z-axis linear actuator (where the spindle is mounted) is nearly 0.02 mm.

The maximum displacement in the y-direction (Figure 6-3) is 0.116 mm shown in the blue color (with negative value). The displacement in the z-direction (Figure 6-4) is considered the highest, in comparison with displacements in x and y directions, because the main force in this case is the penetrating force in the z-direction. The maximum displacement the machine endures in the z-direction is 0.1799 mm.

**B- Traversing process when the spindle is at top left position of the machine frame**

Traversing means that the machine will travel in the x-y plane while maintaining the z-axis pressure on the rotating tool. In this case there are forces in the x, y, and z-directions, in addition to the torque around the z-axis resulting from tool rotation. In this case, $F_x$ and $F_y$ will each be 1200 N, $F_z$ will be 600 N, and the torque in z-axis is 25 N.m. These forces were selected to be larger than those in Table 3-1 to increase the safety factor of the machine.

**1- Stresses (Top left, Traversing)**

Von Mises stresses investigated in this part are those of the top left position due to traverse force.

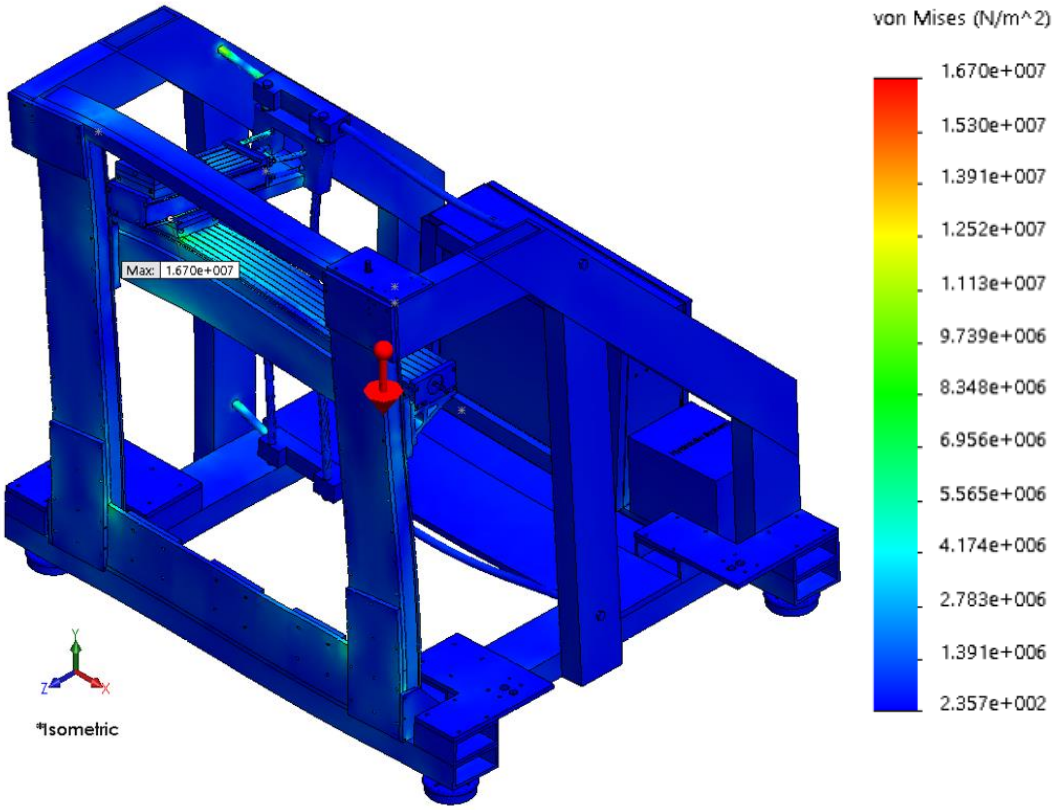


**Figure 6-5: Von Mises Stresses (Top Left Position-Traversing)**

As shown in Figure 6-5, the maximum von Mises stress the machine endures (shown in red) is 16.7 MPa. This stress is occuring near the spindle carriage. Since the working stress is much lower than the yielding strength (220.59 MPa), then the machine will work in safe conditions under the specified traverse loads.

### 2- Deformation (Top left, Traversing)

Figures 6-6 – 6-8 show the deformations of the machine structure in the x, y, and z-directions, respectively, due to applied traverse loads at the top left position of the structure. In these figures, the blue color indicates the maximum negative displacement, under static traverse loads (-0.07597, -0.09559, -0.04957, mm for x, y, and z-directions,

respectively), which are higher than the maximum positive displacements shown in red ($5.585\times10^{-3}$, $23.95\times10^{-3}$, $0.4355\times10^{-3}$, mm for x, y, and z-directions, respectively).

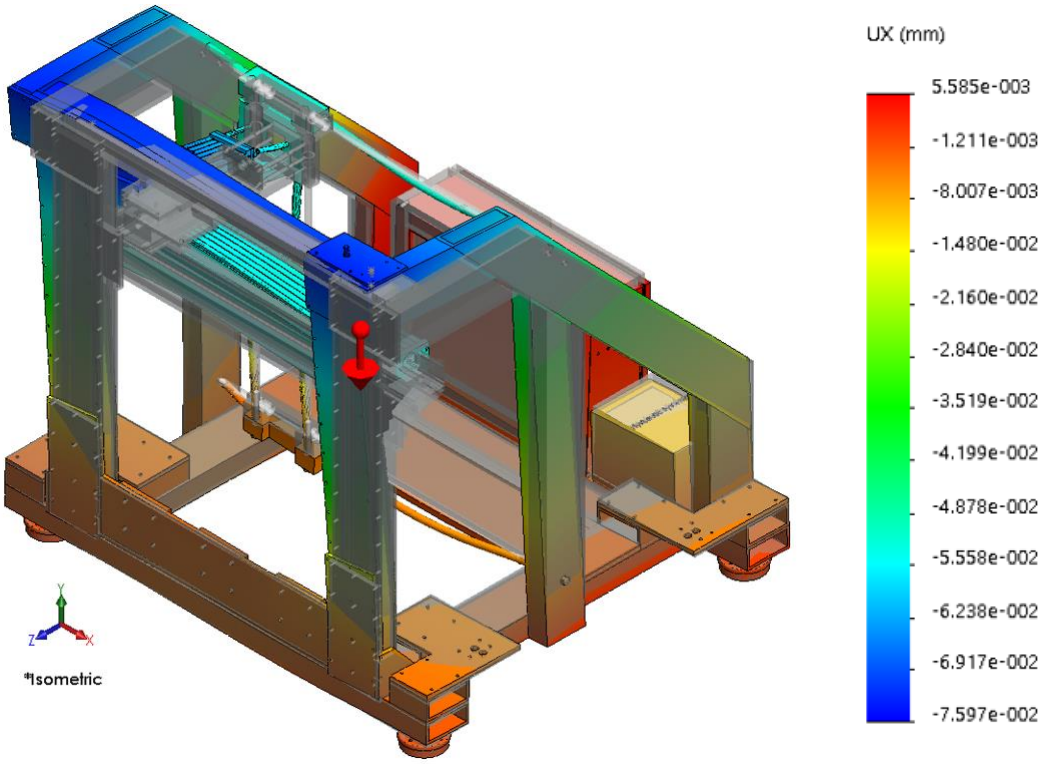


**Figure 6-6: Deformation of the machine in x-direction (Top left-Traversing)**

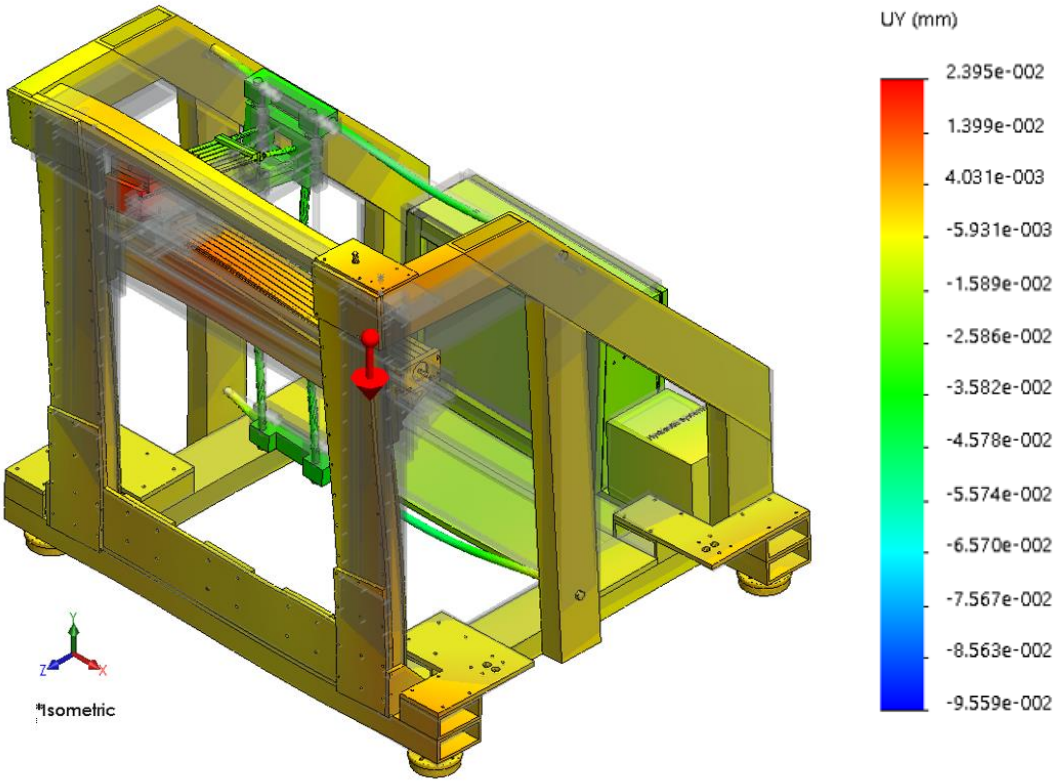


**Figure 6-7: Deformation of the machine in y-direction (Top left-Traversing)**

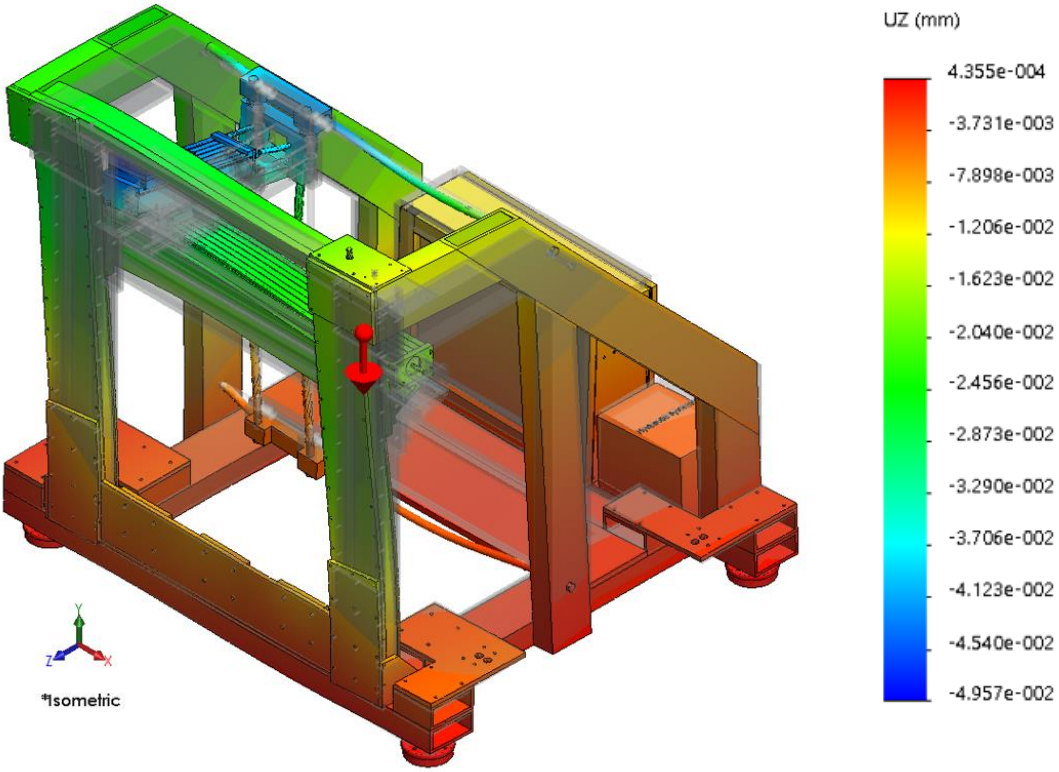


**Figure 6-8: Deformation of the machine in z-direction (Top left-Traversing)**

It can be noticed from Figure 6-7 that the maximum structural deformation of the machine is 0.096 mm. In Figure 6-6, the top side of the machine frame has the highest deformation. If a severe case of x-axis force might be endured, the displacement of the frame can be improved (decreased) by adding x-axis fixtures as shown in Figure C-2 (in APPENDIX C). These fixtures may be of rectangular profiles that are connected making a triangular shape in the x-y plane similar to shape that is already used in the machine in the y-z plane. This can be done at the expense of the machine overall dimension and weight.

### 6.1.2 Static Analysis when the Spindle is at Center Position of the Machine Frame

The following analysis is performed with the spindle operating in the center position of the machine frame as shown in Figures 6-9 - 6-16. The analysis was also conducted on the machine while enduring plunging and traversing loads separately.

**A- Plunging process when the spindle is at center position of the machine frame**

In this part, the z-direction reaction force ($F_z$) and the torque around the z-direction are 2000 N and 45 N.m. respectively. Resulting stress and deformation values are displayed in the following figures.

**1- Stresses (Top left, Plunging)**

In this part, the von Mises stresses are evaluated throughout the machine while enduring plunging forces.

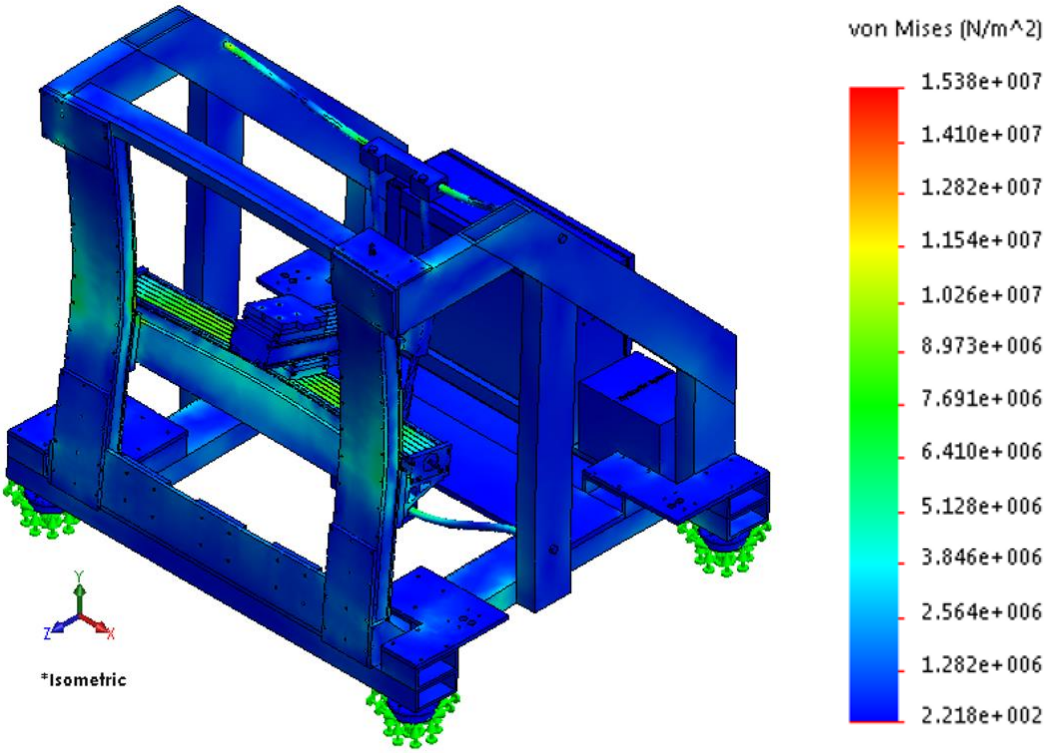


**Figure 6-9: Von Mises Stresses (Center Position-Plunging)**

Figure 6-9 shows the von Mises stresses that the machine experiences due to plunging force ($F_z = 2000\ N, T_z = 45\ N.m$ ). The range for exhibited stresses in this condition is mostly between 221 Pa and 11 MPa. The highest stressed areas are the x-axis mechanical actuator, the frame center, and the backbone x-axis shafts (especially the bottom one). These parts can be distinguished by the green color that is covering them.

The maximum von Mises stress that occurs while the spindle is situated in the center position is 15.38 MPa. This value is considered small compared to the yield strength of the material under investigation. Therefore, the machine can withstand the specified loads without any static failure.

## 2- Deformation (Top left, Plunging)

Figures 6-10 – 6-12 show the deformations of the machine structure in the x, y, and z-directions, respectively. The spindle in this case is located at the center position facing plunging forces.

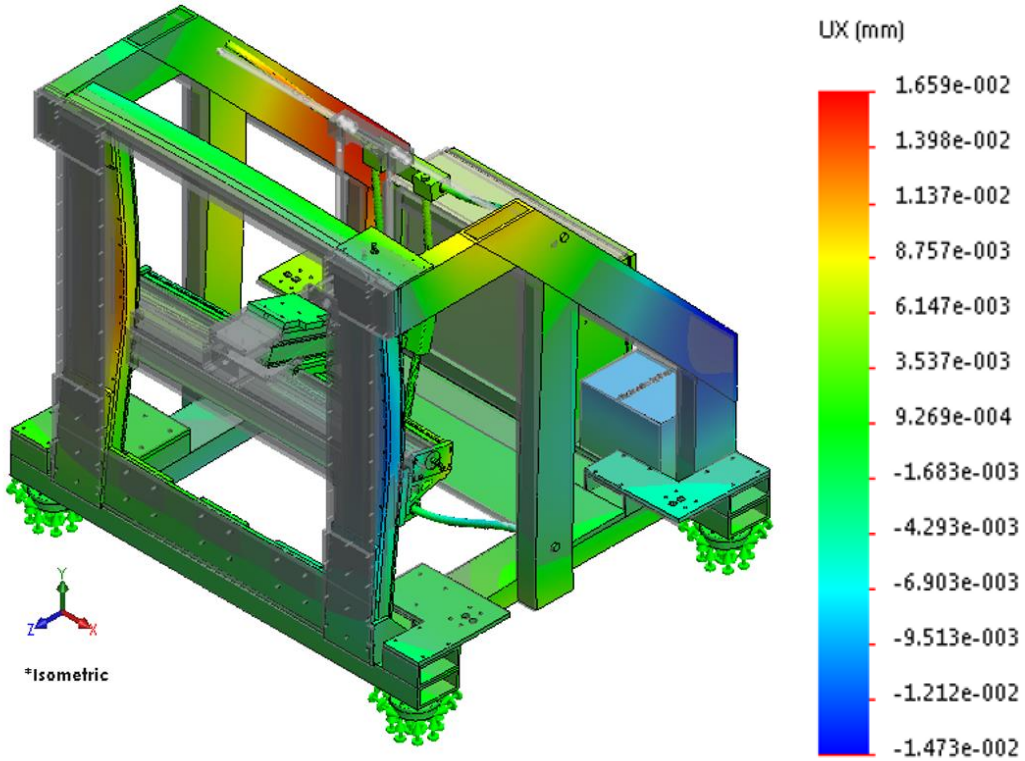


**Figure 6-10: Deformation of the machine in x-direction (Center-Plunging)**

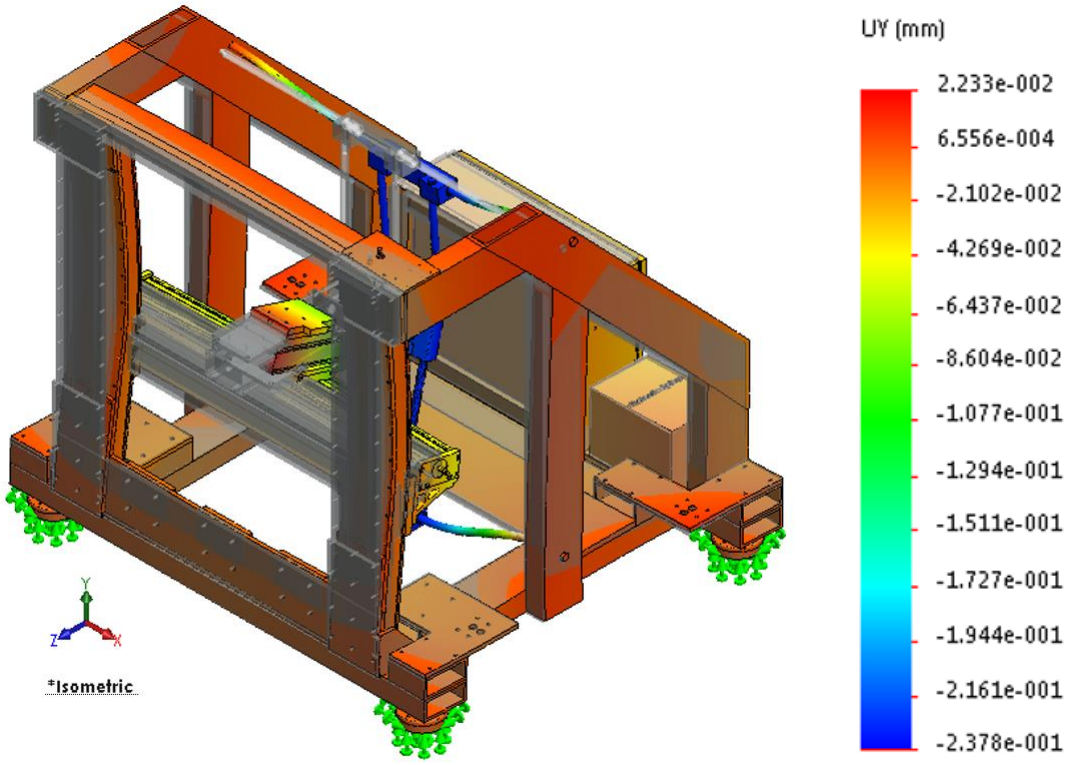


**Figure 6-11: Deformation of the machine in y-direction (Center-Plunging)**

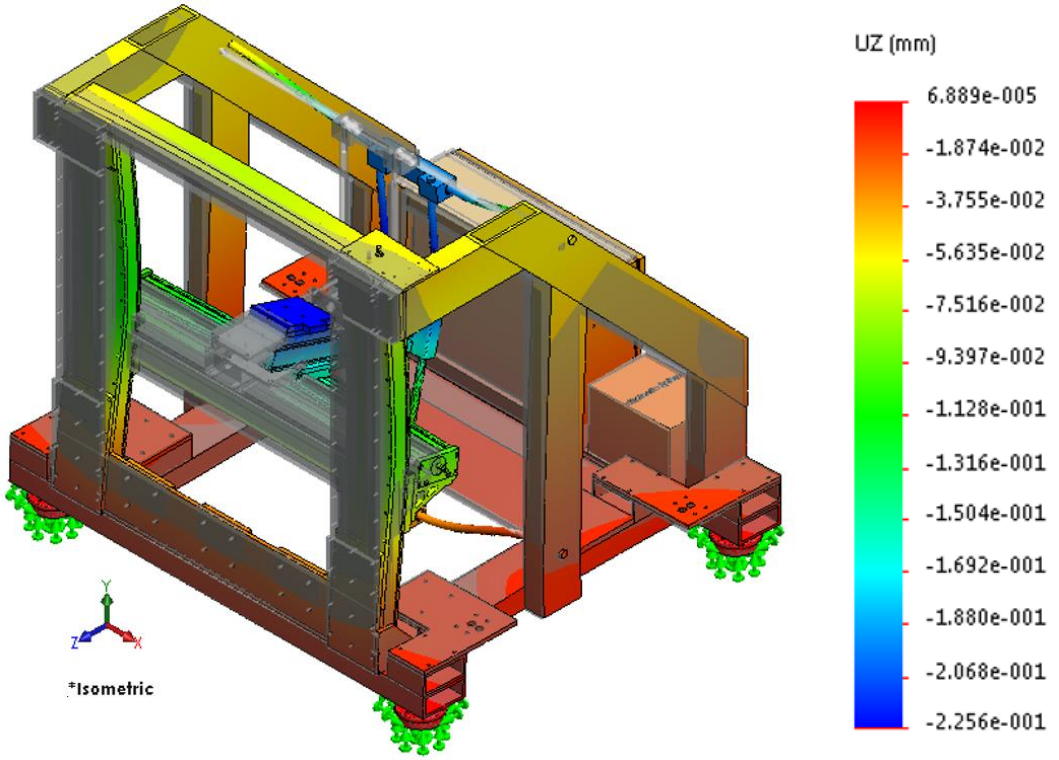


**Figure 6-12: Deformation of the machine in z-direction (Center-Plunging)**

The displacement in the y-direction shown in Figure 6-11 has the highest maximum deformation compared to previous cases (Figures 6-2 – 6-10). It is located at the back side of the z-axis linear actuator and at the backbone. This can be considered advantageous since this area is far from the spindle location, which is deformed nearly 0.05 mm in the y-direction.

Figure 6-12 shows the highest deformation (-0.2256 mm) compared to all the previous deformation figures. Angular deflection was also examined around the x-axis linear actuator and was found to be 0.007 degrees. Displacement can be minimized by using thicker backbone shafts and/or larger linear actuators.

**B- Traversing process when the spindle is at center position of the machine frame**

The following studies are conducted while the machine is at the center position of the machine frame and enduring traverse loads. The used traverse loads have the same values as those used in the previous traverse study on the top left position. Stress and deformation results are displayed below.

**1- Stresses (Top left, Traversing)**

The von Mises stress plot for the machine while working in traversing process while the spindle is at the center of the machine frame is displayed in Figure 6-13.

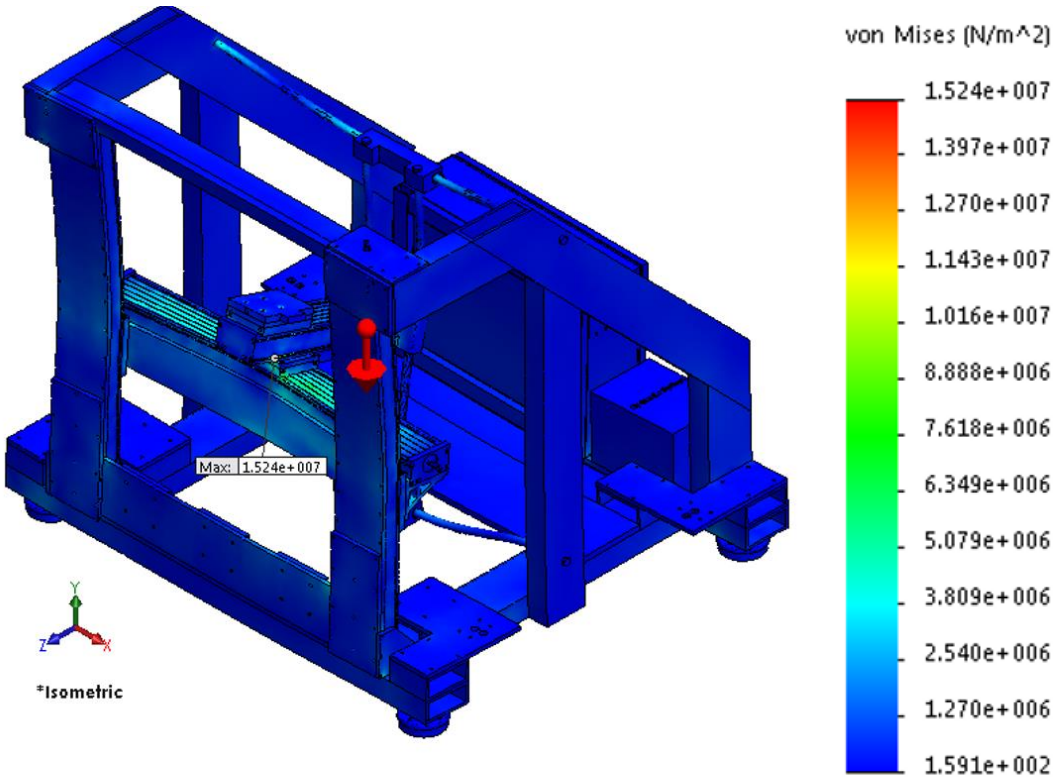


**Figure 6-13: Von Mises Stresses (Center Position-Traversing)**

The maximum von Mises stress the machine endures in this position under traversing loads is 15.24 MPa as shown in Figure 6-13.

### 2- Deformation (Top left, Traversing)

Figures 6-14 – 6-16 represent the deformations in the x, y, and z-directions, respectively, for the FSWM where the spindle is at the center position of the machine frame and traversing along the workpiece.

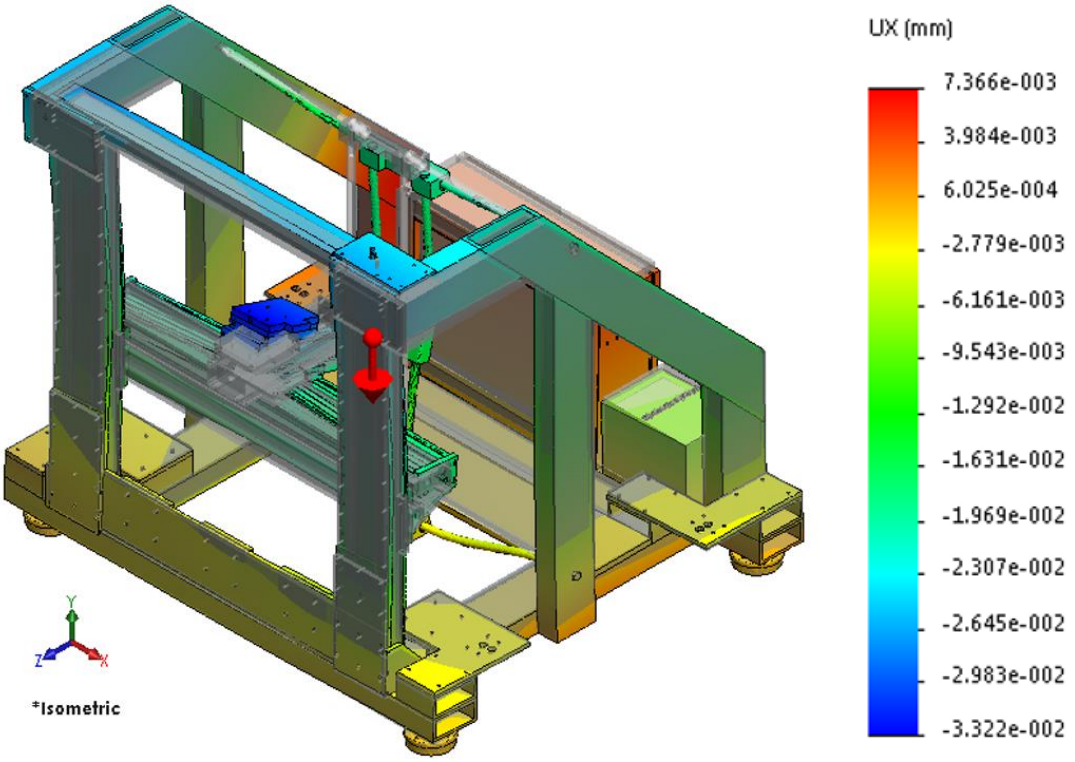


**Figure 6-14: Deformation of the machine in x-direction (Center-Traversing)**

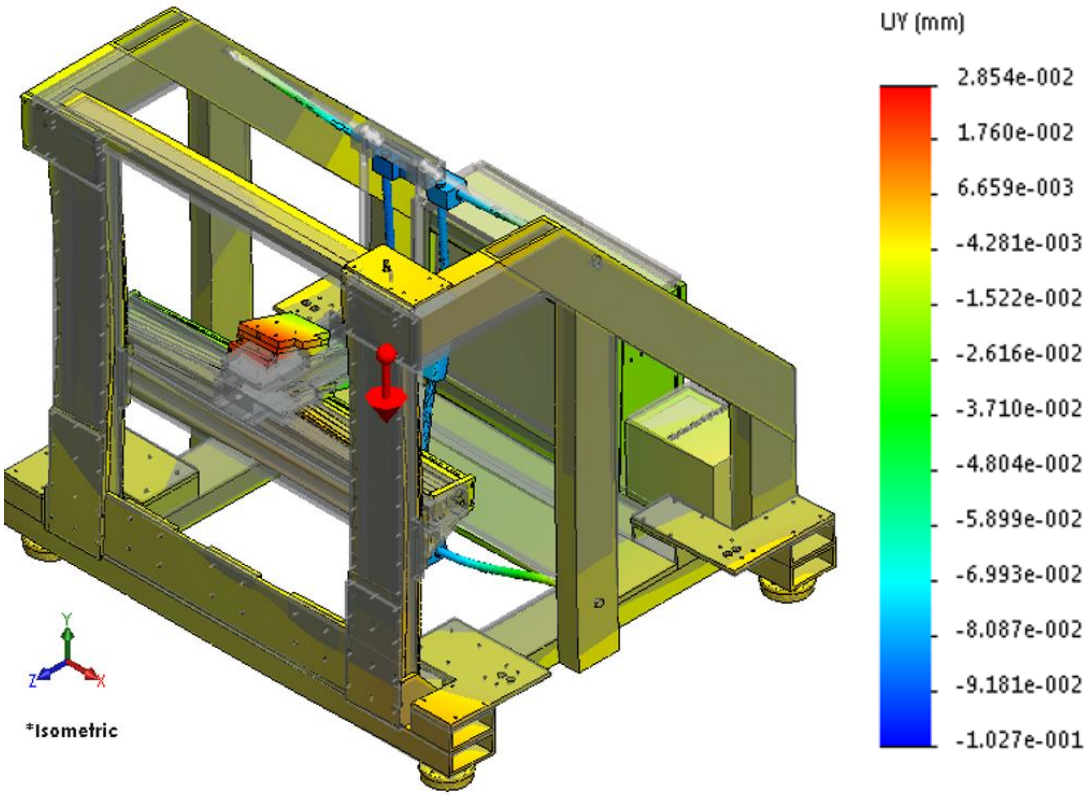


**Figure 6-15: Deformation of the machine in y-direction (Center-Traversing)**

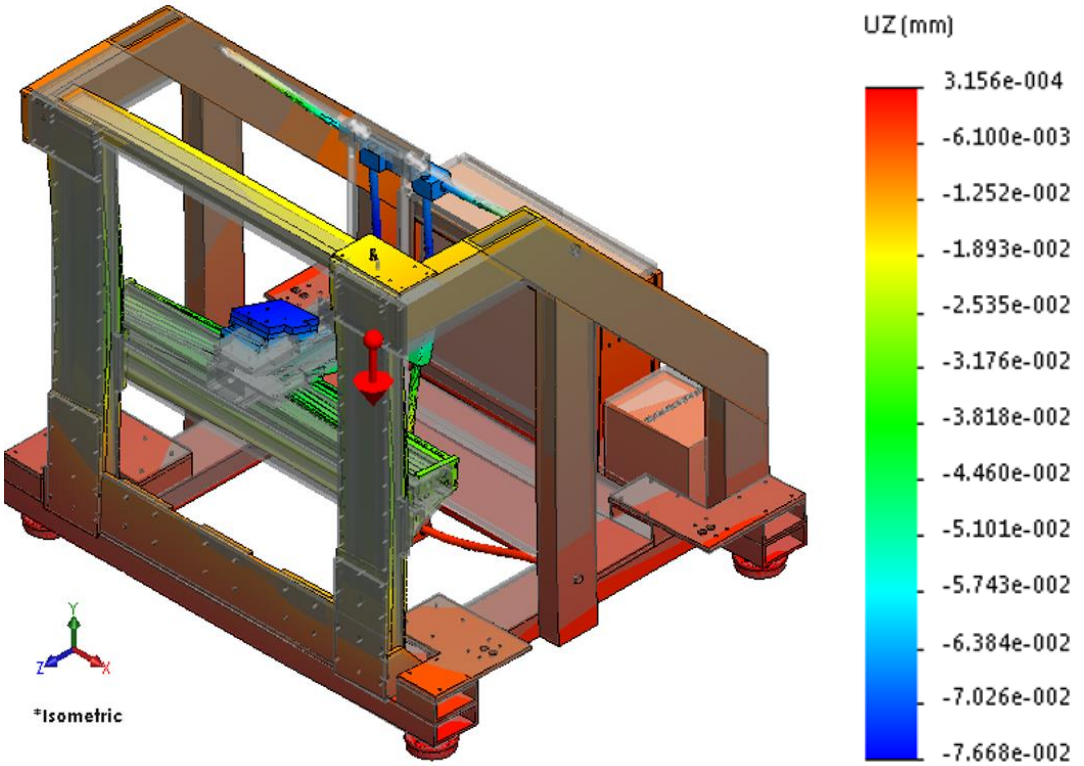


**Figure 6-16: Deformation of the machine in z-direction (Center-Traversing)**

As observed in Figures 6-14 – 6-16, the deformation of the machine structure at the spindle location in all directions does not exceed 0.11 mm. The maximum deformation observed in this situation is at the back of the z-axis linear actuator, which is 0.1027 mm in the y-direction (Figure 6-15). Displacement due to traversing loads are much smaller than those of plunging loads.

## 6.2 Fatigue Analysis

Fatigue analysis is performed for both spindle positions (top-left and center) and processes (plunging and traversing) and results in infinite life for the proposed machine. In this study, the same loads used in static analysis were utilized as cyclic loads. When performing the static analysis, it was observed that the applied stresses on the machine structure as a result of the applied loads were much lower than the endurance limit ($S_e = 87.246$ MPa) of the material. Thus, by looking at the S-N curve in Figure 5-4, the stresses are far from those needed to define the machine life, indicating that the machine life is infinite.

It should be noted that the machine stiffness is very high, so that machine structure deformations due to applied loads are very low. This is required for high precision welding.

## 6.3 Frequency Analysis

The goal of this study is to make sure the machine spindle can operate at required rotational speeds below the fundamental frequency of the machine structure. Frequency analysis is performed to find the resonant frequencies, and the mode shapes. The resonant frequencies and corresponding mode shapes were analyzed for both the top left and center positions.

### 6.3.1 Frequency Analysis when the Spindle is at Top Left Position of the Machine Frame

Throughout this analysis, the mesh was fine controlled to obtain high accuracy. The first ten frequencies were obtained. These frequencies are listed in Table 6-1.

**Table 6-1: Resonant Frequencies (Top Left)**

| Mode No. | Frequency | |
|---|---|---|
| | [Rad/sec] | [Hertz] |
| 1 | 360.02 | 57.298 |
| 2 | 370.47 | 58.963 |
| 3 | 380.45 | 60.551 |
| 4 | 381.34 | 60.692 |
| 5 | 385.4 | 61.338 |
| 6 | 389.56 | 62 |
| 7 | 402.64 | 64.083 |
| 8 | 409.72 | 65.209 |
| 9 | 583.83 | 92.919 |
| 10 | 608.61 | 96.863 |

As shown in the Table 6-1, the fundamental frequency is 57.298 Hz. The higher frequencies have close values to each other till we reach the eighth mode. The ninth mode jumps to 92.919 Hz, that makes a difference of 27.71 Hz between it and eighth mode. As shown in Figures 6-17 – 6-18, components that are susceptible to have high deformations at these frequencies are the internal screws of the linear actuators, which have the highest resultant amplitude shown in green and red colors. Note that the resultant amplitude is dimensionless and is only a mean for comparison. The first eight modes all resonate due to bending of the same internal screws. This can be avoided by choosing linear actuators with higher internal screw stiffness. If this is achieved, the resonant frequencies would be shifted to a higher frequency range that is far from operating frequency range.

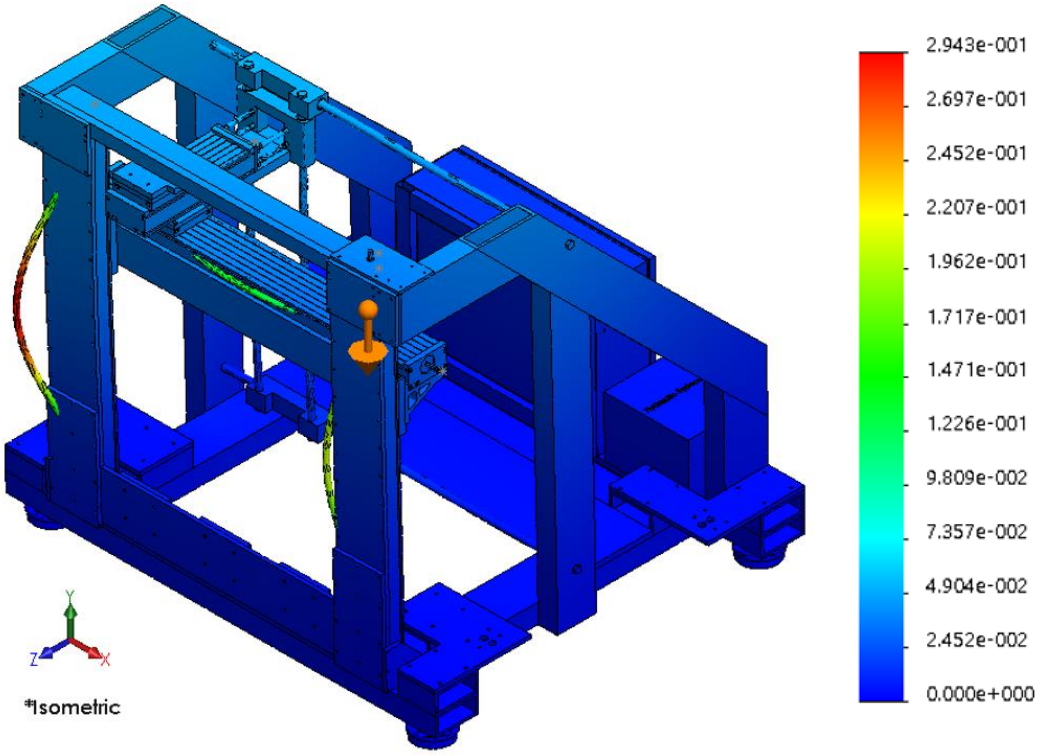


**Figure 6-17: First mode shape of the machine structure corresponding to fundamental frequency of 57.298 Hz (Top left)**

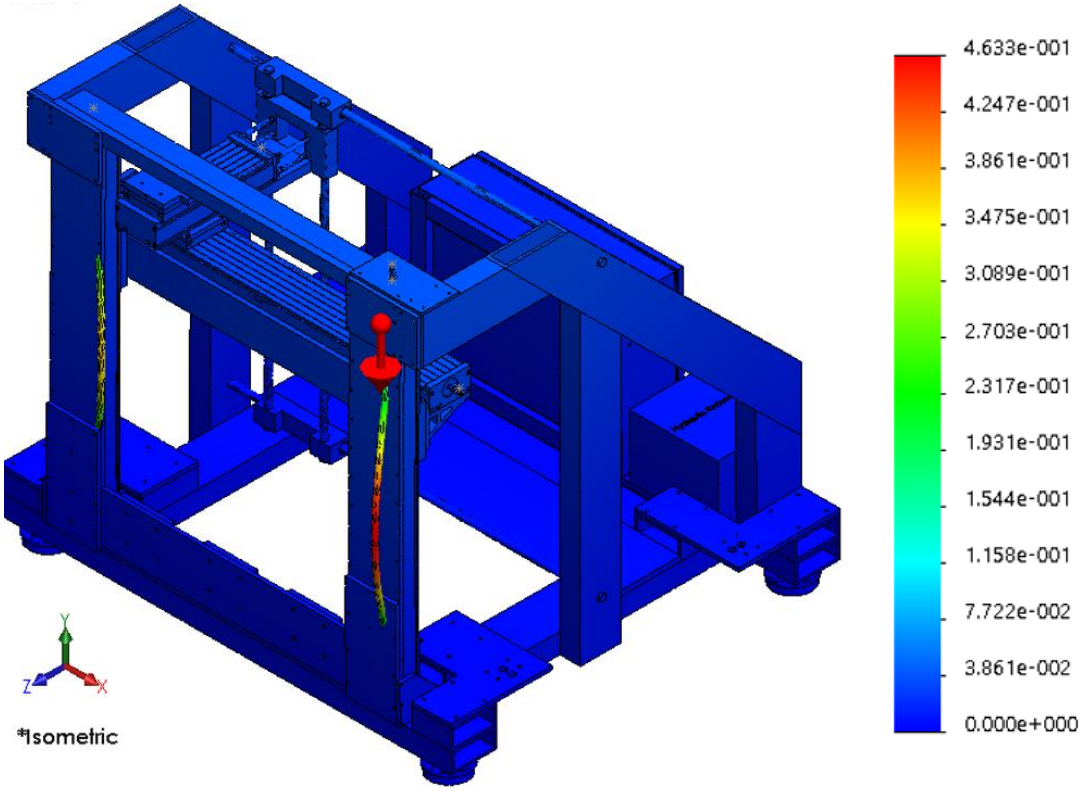


**Figure 6-18: Second mode shape of the machine structure corresponding to a frequency of 58.963 Hz (Top left)**

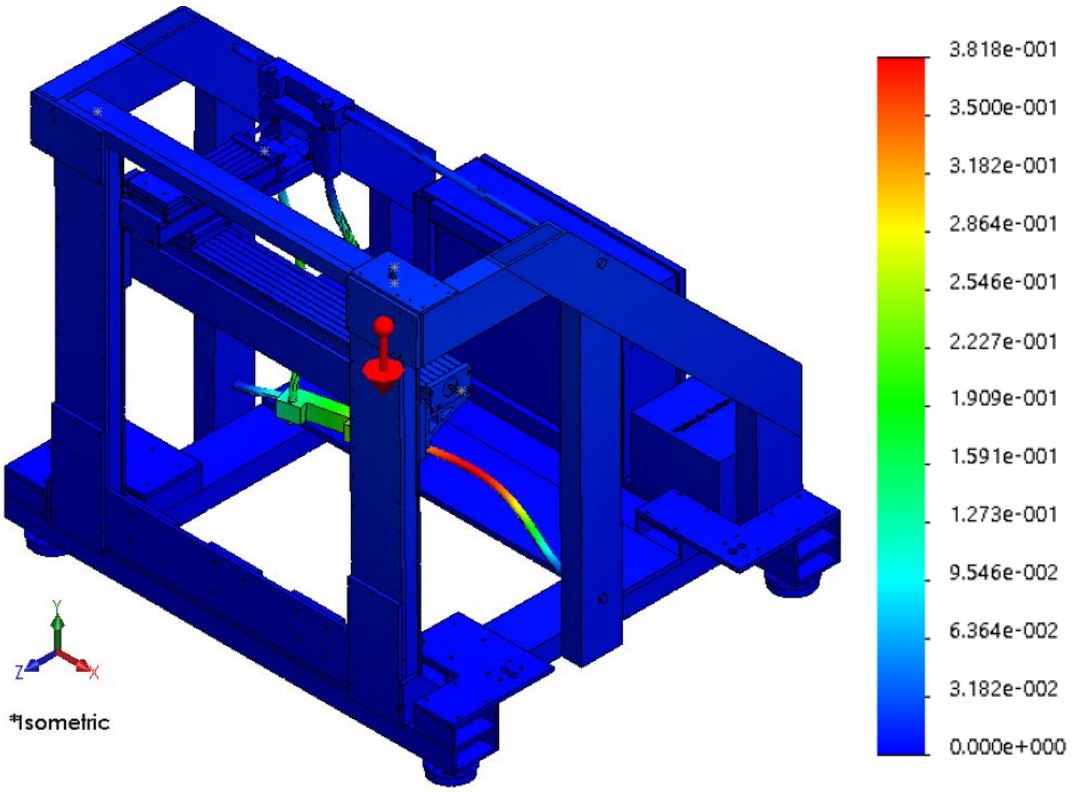


**Figure 6-19: Ninth mode shape of the machine structure corresponding to a frequency of 92.919 Hz (Top left)**

### 6.3.2 Frequency Analysis when the Spindle is at Center Position of the Machine Frame

In this section, the spindle is located at the center of the machine frame. The operating frequency range of the FSWM for this particular position must be lower than 49.02 Hz, which is the fundamental resonant frequency the machine encounters according to the frequency depicted in Table 6-2. The first lowest ten resonant frequencies of the FSWM when the spindle is at center position are listed in Table 6-2.

**Table 6-2: Resonant Frequencies (Center)**

| Mode No. | Frequency | |
|---|---|---|
| | [Rad/sec] | [Hertz] |
| 1 | 308.03 | 49.024 |
| 2 | 357.52 | 56.9 |
| 3 | 375.94 | 59.832 |
| 4 | 385.13 | 61.295 |
| 5 | 388.22 | 61.788 |
| 6 | 395.97 | 63.02 |
| 7 | 402.54 | 64.067 |
| 8 | 406.05 | 64.625 |
| 9 | 411.65 | 65.517 |
| 10 | 447.73 | 71.258 |

As shown in the Table 6-2, the first mode is 49.024 Hz. These frequencies are lower than those previously obtained for the upper left spindle position. This is because the spindle is located at the center of the backbone shafts in the x and y-axes directions. Moreover, the spindle is located at the center of the screws of the x and y-axes linear actuators. Stiffness has lowest value at the center of shafts when both sides are of the shaft are fixed, thus resulting in bending. All ten mode shapes depict that the backbone shafts and/or the linear modules internal screws are prone to bending and are the lead cause for the lowest studied resonant frequencies. When higher operating frequencies are required to run the machine at higher speeds, resonant frequency values can be raised by increasing the stiffnesses of the shafts and internal ball screws.

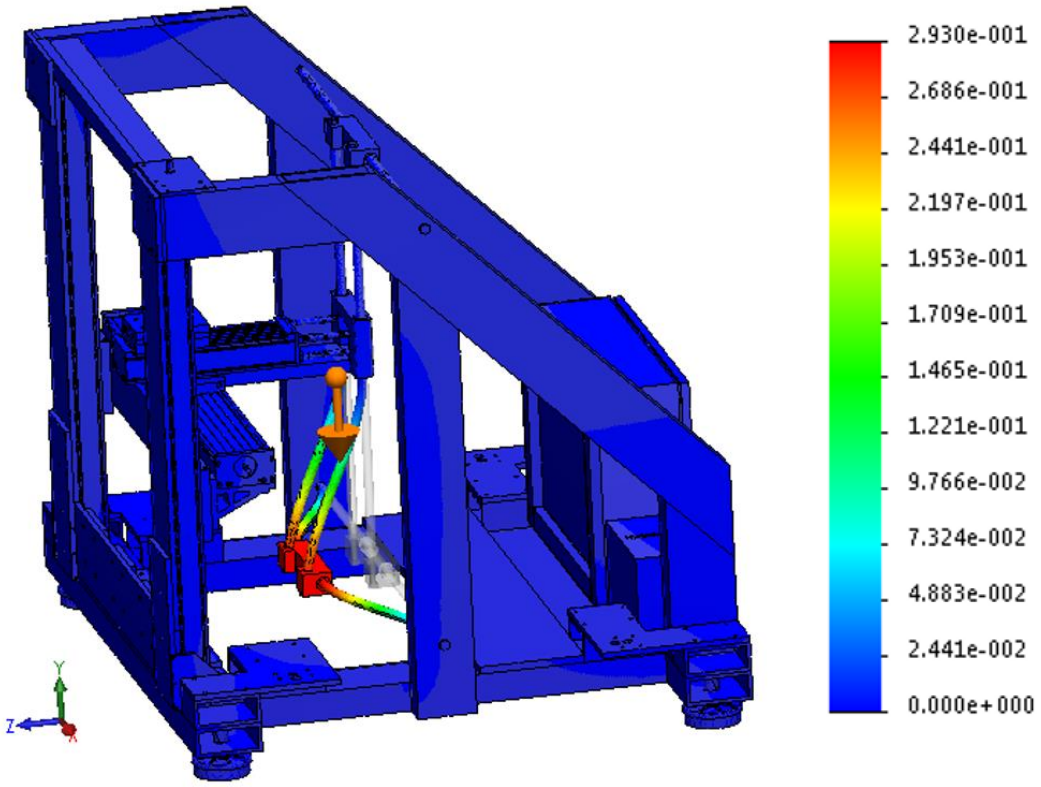


**Figure 6-20: First mode shape of the machine structure corresponding to fundamental frequency of 49.024Hz (Center)**

Figure 6-20 – 6-21 display deformation of the machine structure at the first and second mode, respectively. To shift the first resonant frequency to a higher value, the lower shaft of the backbone needs to have higher stiffness. In the second mode till the tenth mode, the components affected from resonance are the backbone shafts, and the screws of the x and y-axes linear actuators as shown in Figure 6-21.

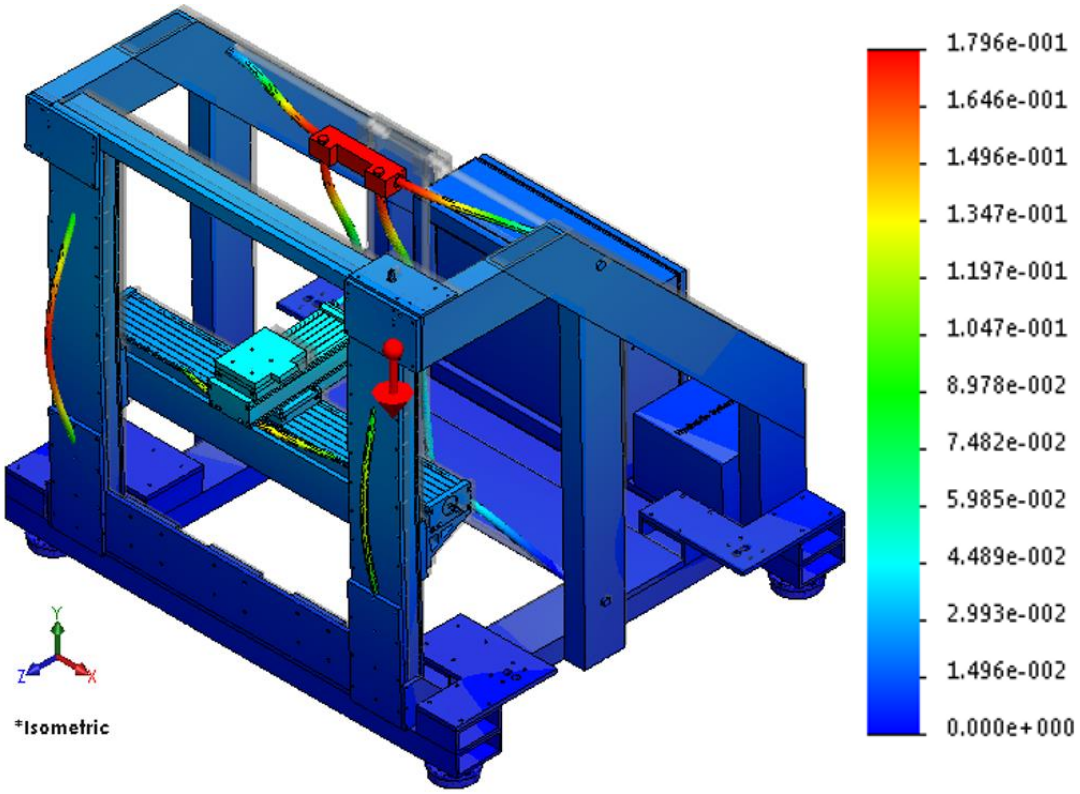


**Figure 6-21: Second mode shape of the machine structure corresponding to a frequency of 56.9Hz (Center)**

## 6.4 Dynamic Analysis

Dynamic analysis is important when the applied load is not constant, inducing unstable modes of vibration to the machine's structure, thus, shortening the machine's life or leading to an unexpected failure.

Dynamic Analysis is performed to investigate the motion of the machine at different frequencies and locations using SOLIDWORKS Software. The machine dynamic analysis will be conducted for both top left and center positions with both plunge and traverse processes for each position. Both the frequency-response and the time-response plots will be investigated and shown in what follows.

### 6.4.1 Machine Structure Response when the Spindle is at Top Left Position of the Machine Frame

In this section, dynamic analysis will be conducted while the spindle is located at the top left spindle position of the machine frame for both plunge and traverse processes. Applied loads at specified frequencies are fed to the software. The time range and sampling frequency are also specified.

**A- Plunging while spindle is in top left position**

The applied loads used while plunging is the reaction force $F_z = 2000$ N and a torque around the z-direction of 45 N.m, respectively. Loads are applied at the spindle bolt locations as shown in Figure 5-3 – 5-4. Motion of the point shown in Figure 5-10 will be analyzed. This point was selected because it is located at the center of the spindle mounting bolts on the spindle base.

Figure 6-22 shows the frequency-amplitude plot where amplitude is the maximum machine displacement under the applied loads. SOLIDWORKS generates this plot by increasing the forced frequency (starting from zero) and recording the machine's maximum amplitudes (displacement). The fundamental frequency is at nearly 57 Hz. From Figure 6-22 it is noticed that for a frequency lower than 50 Hz, the amplitude of vibration remains within 0.25 mm for the loading conditions mentioned above.

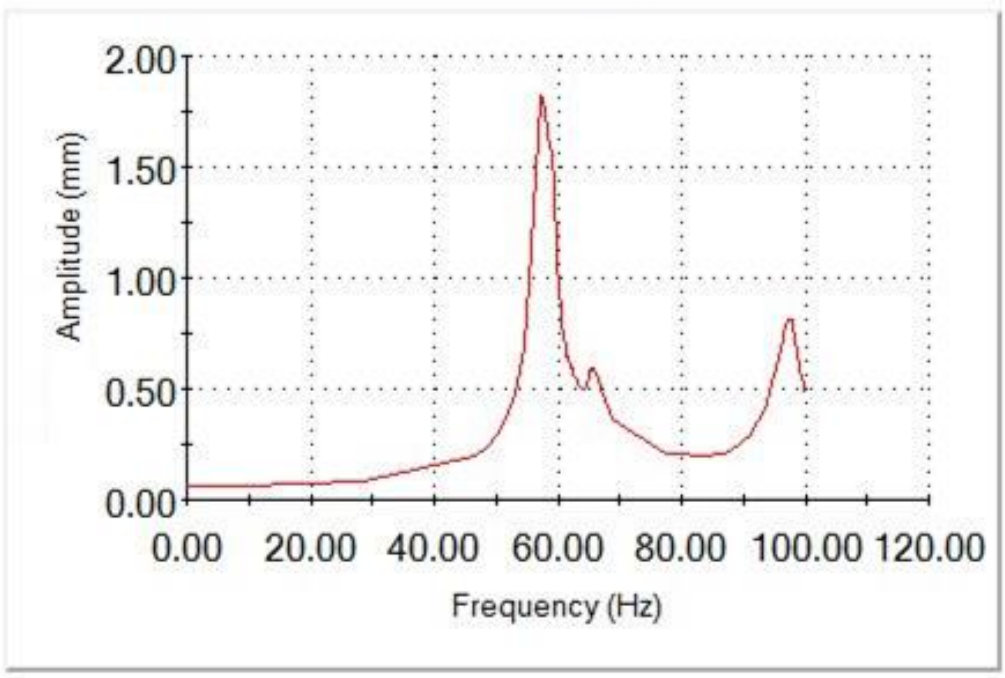


**Figure 6-22: Frequency-Amplitude Plot (Top Left-Plunging)**

The motion of the spindle base is analyzed for two forced frequencies, 3.33 Hz and 20 Hz. These frequencies were chosen because most metals are welded at speeds between 200 rpm to 1200 rpm [28]. The time response in x, y, and z-directions of the point shown in Figure 5-11 will be studied due to plunging,

**1- Motion of the spindle due to plunging at a frequency of 3.33Hz**

Figures 6-23 – 6-25 display the motion of the spindle base in the x, y, and z-axes directions at 3.33 Hz under the effect of plunging loads $F_z = 2000\sin(6.67\pi t)$ N, $T_z = 45\sin(6.67\pi t)$ N.m. The time range taken for these studies is 2 seconds and the sampling frequency is 50 Hz. The highest amplitude displacement is in the z-direction with a value of 0.15 mm as shown in Figure 6-25.

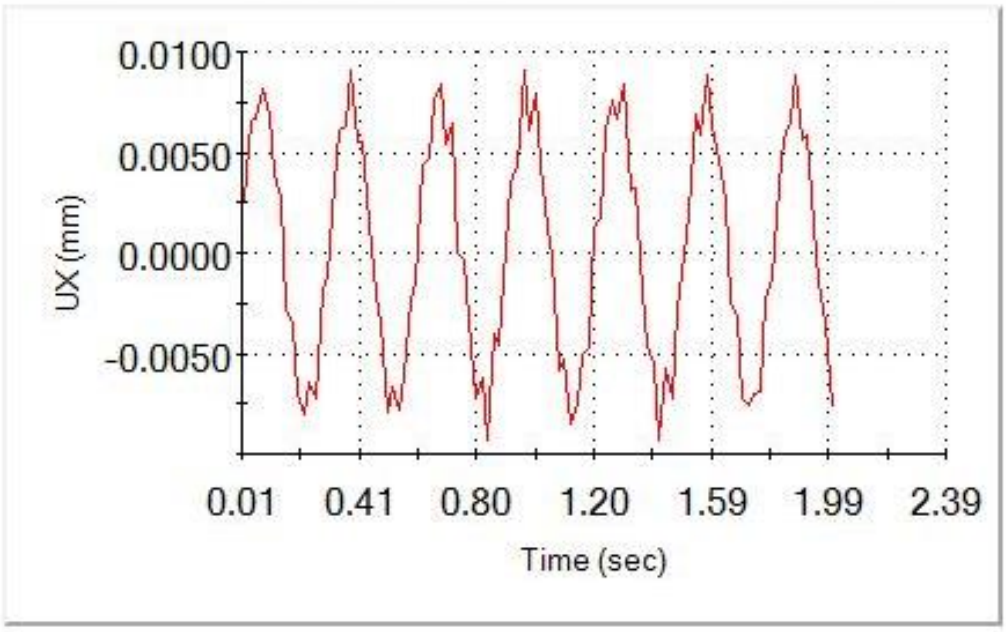


**Figure 6-23: Motion of the spindle in x-direction, 3.33 Hz (Top Left- Plunging)**

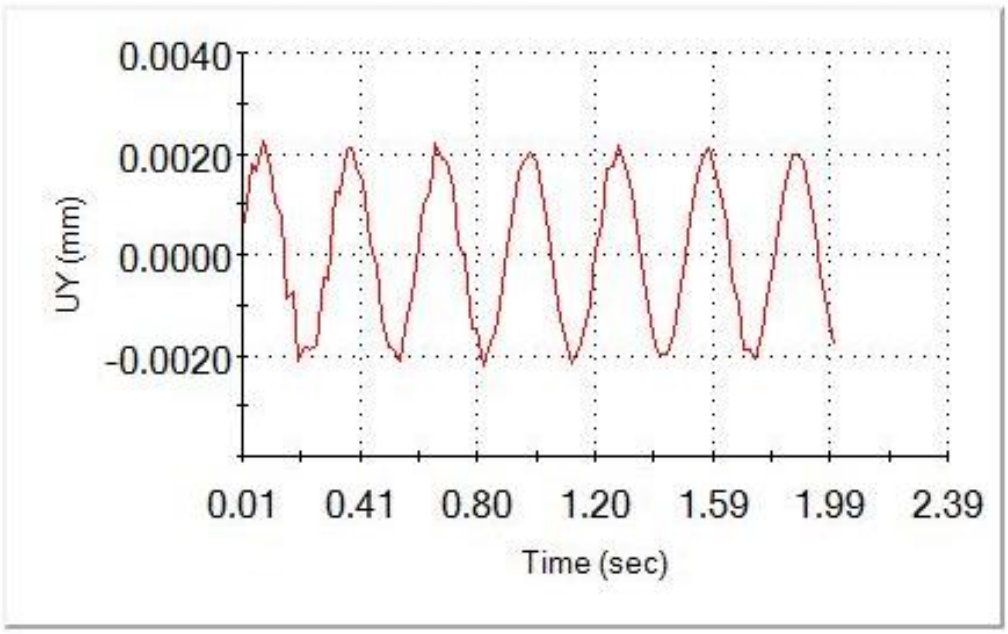


**Figure 6-24: Motion of the spindle in y-direction, 3.33 Hz (Top Left- Plunging)**

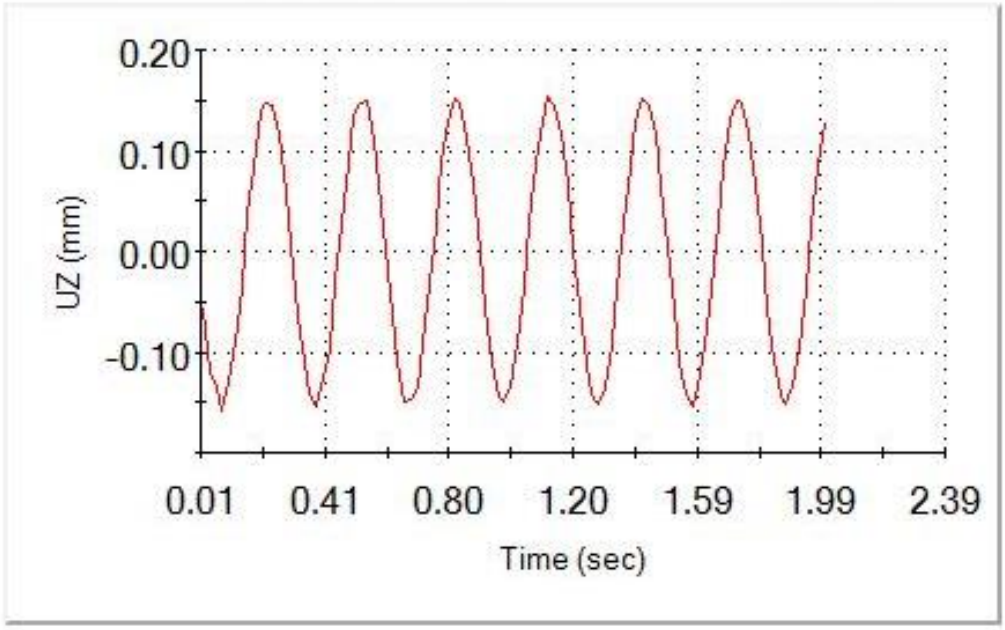


**Figure 6-25: Motion of the spindle in z-direction, 3.33 Hz (Top Left- Plunging)**

**2- Motion of the spindle due to plunging at a frequency of 20 Hz**

Figures 6-26 – 6-28 represent the motion of the spindle base in the x, y, and z-directions, respectively, for 20 Hz maximum plunging loads ($F_z = 2000 \sin(40\pi t)$ N, $T_z = 45 \sin(40\pi t)$ N.m. For all three plots, the time range is taken to be 1s, while the sampling frequency is 140 Hz, where aliasing error is less than 5% according to the following equation [37].

$$\text{Max Error (\%)} = 100 * (1 - \cos(\frac{\pi}{N})) \quad (6\text{-}1)$$

where *N* is the number of samples per cycle.

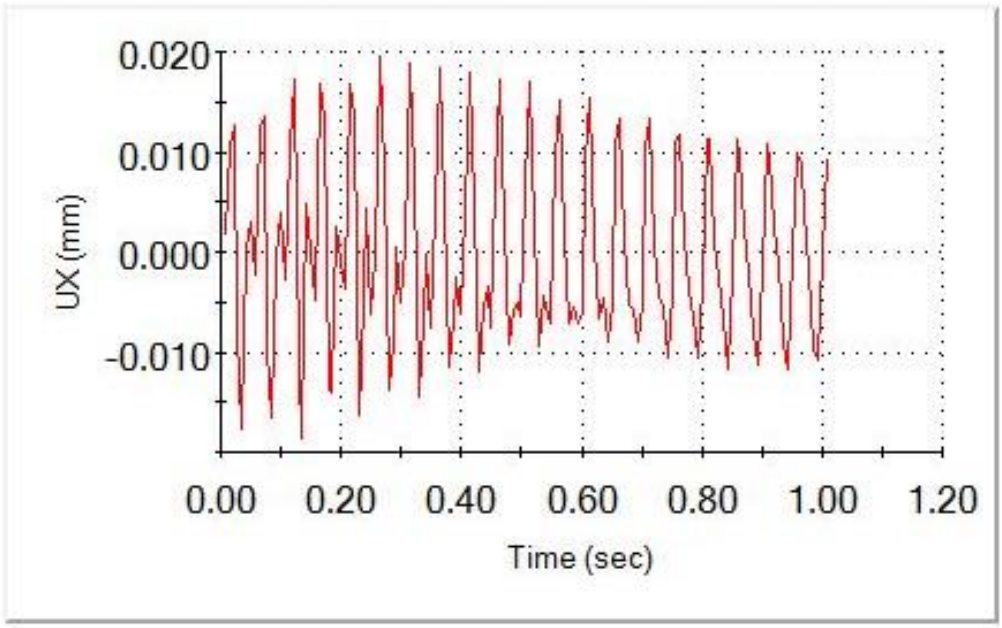


**Figure 6-26: Motion of the spindle in x-direction, 20 Hz (Top Left- Plunging)**

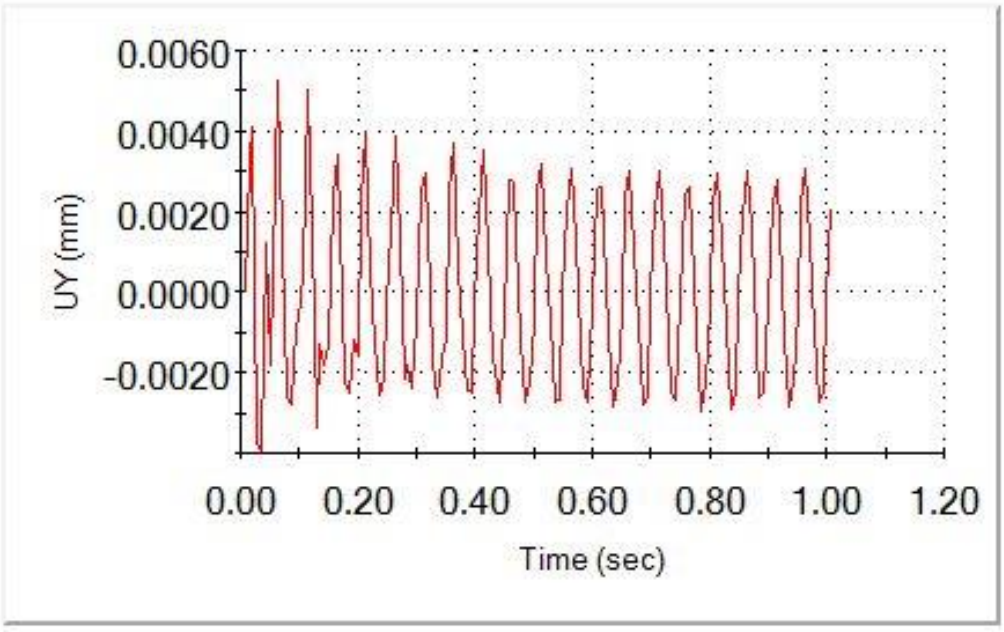


**Figure 6-27: Motion of the spindle in y-direction, 20 Hz (Top Left- Plunging)**

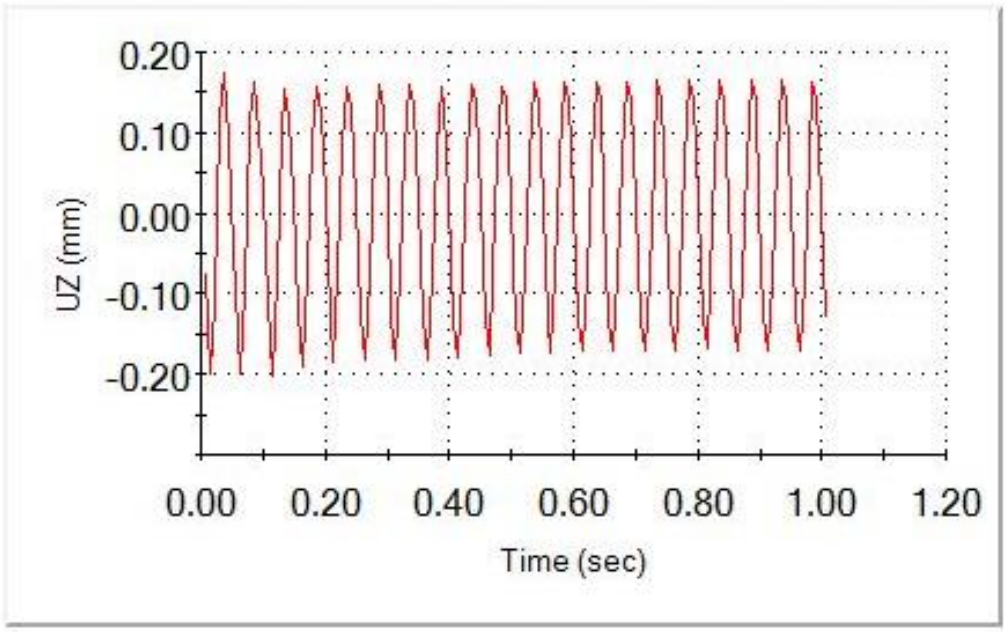


**Figure 6-28: Motion of the spindle in z-direction, 20 Hz (Top Left- Plunging)**

Motions in the x and y direction are small compared to the motion in the z-direction. Motion in the z-direction has a steady state displacement of nearly 0.15 mm.

**B- Traversing while spindle is in top left position**

The traverse forces are given by:

$$F_x = F_y = 1200\sin(6.67\pi t) \text{ N},$$

$$F_z = 600\sin(6.67\pi t) \text{ N}$$

While the torque is given by:

$$T_z = 25\sin(6.67\pi t) \text{ N.m}$$

Motion to be studied is concerned with the point shown in Figure 5-10 that is located at the center of the spindle mounting bolts on the spindle base.

Figure 6-29 displays the frequency-amplitude plot where amplitude is displacement. The fundamental frequency is nearly 58 Hz. It is noticed that for a frequency lower than 50 Hz, the amplitude of vibration remains within 0.25 mm for the

loading conditions mentioned above. It should be noted that the amplitude is overall displacement, regardless of the direction.

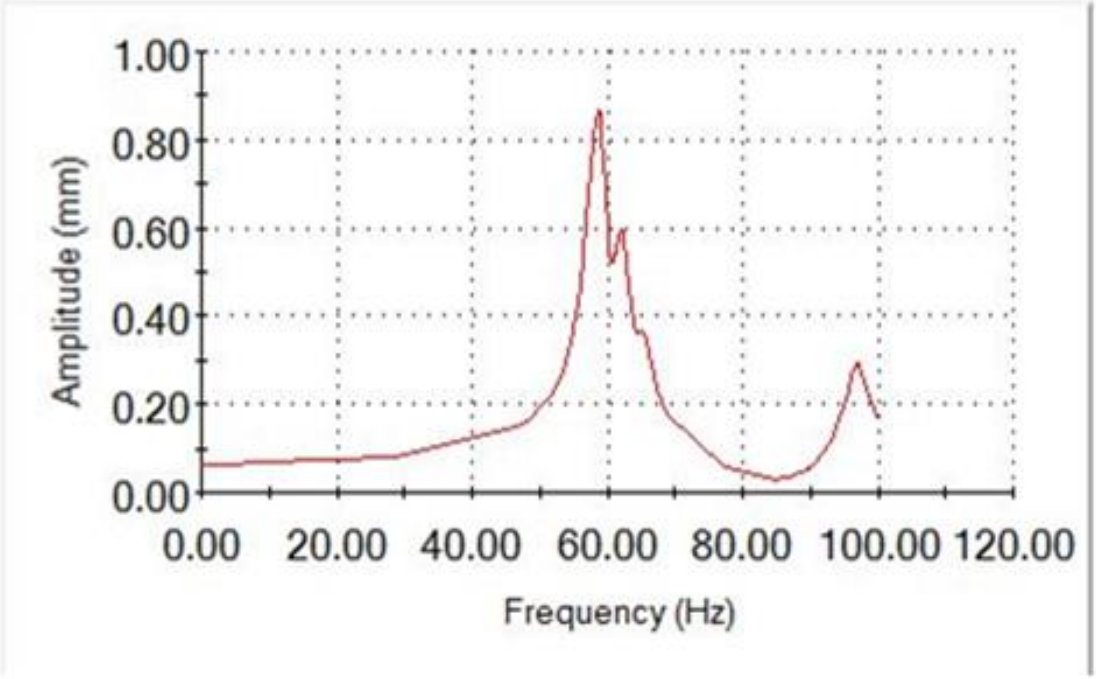


**Figure 6-29: Frequency-Amplitude Plot (Top Left-Traversing)**

The time-displacement plots for the traversing process will be shown next at forced frequencies of 3.33 Hz and 20 Hz, respectively.

**1- Motion of the spindle due to traversing at a frequency of 3.33 Hz**

Figures 6-30 – 6-32 represent the motion of the spindle base in the x, y, and z-directions, respectively, for 3.33 Hz maximum traversing loads.

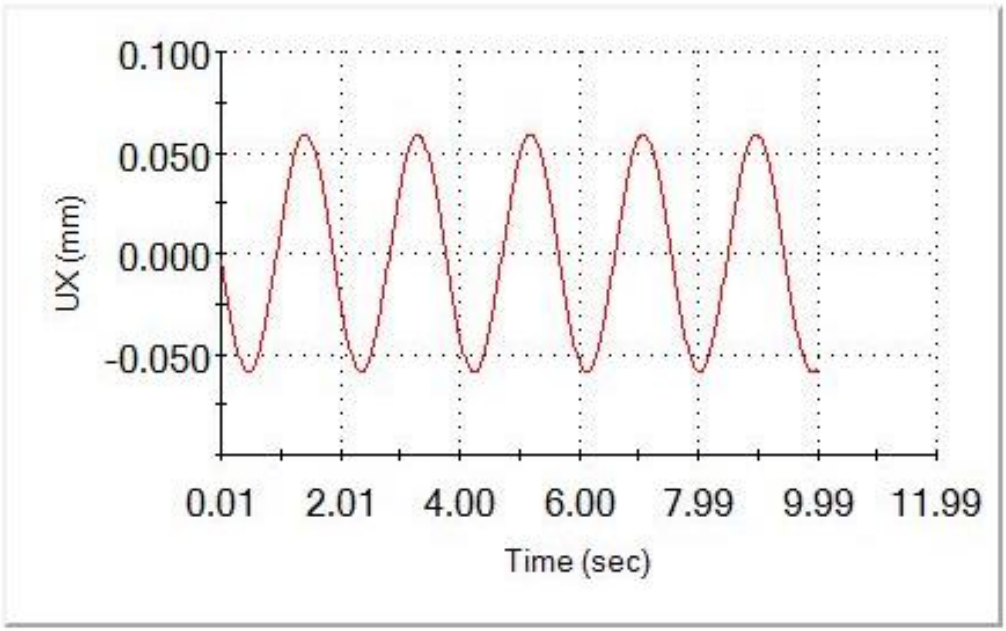


**Figure 6-30: Motion of the spindle in x-direction, 3.33 Hz (Top Left-Traversing)**

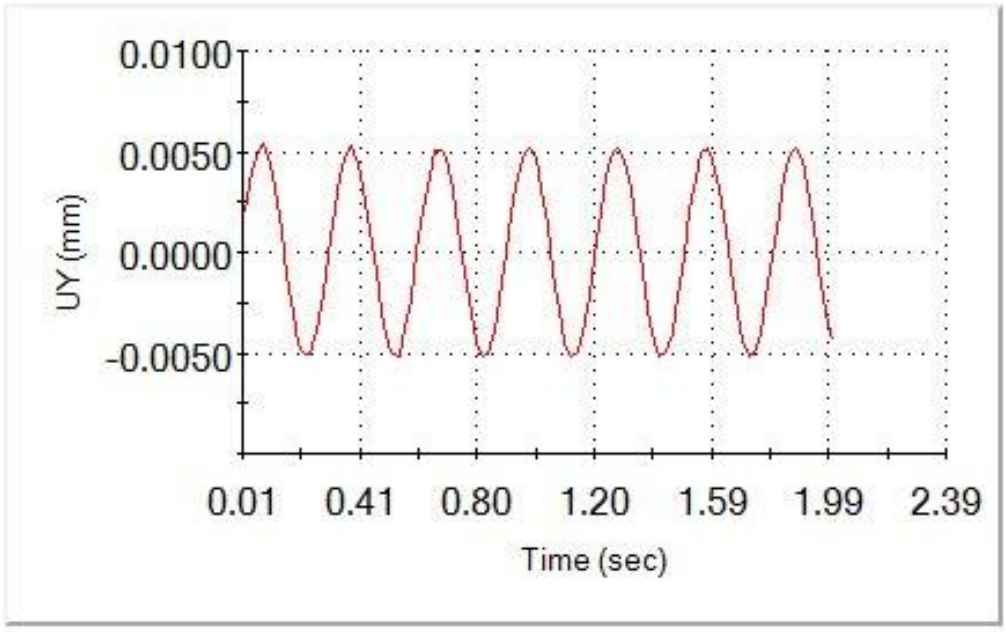


**Figure 6-31: Motion of the spindle in y-direction, 3.33 Hz (Top Left-Traversing)**

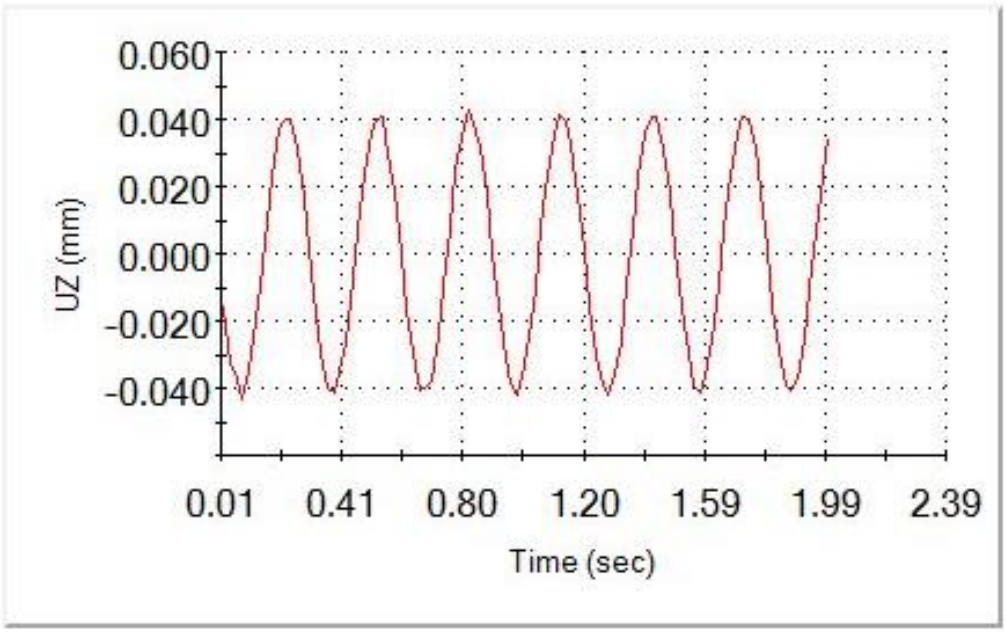


**Figure 6-32: Motion of the spindle in z-direction, 3.33 Hz (Top Left-Traversing)**

It can be noticed from Figures 6-30 – 6-35 that the maximum amplitude at both 3.33 Hz and 20 Hz forced frequencies is observed in the x-axis direction with an amplitude of 0.065 mm.

**2- Motion of the spindle due to traversing at a frequency of 20 Hz**

Figures 6-33 – 6-35 represent the motion of the spindle base in the x, y, and z-directions, respectively, for 20 Hz maximum traversing loads.

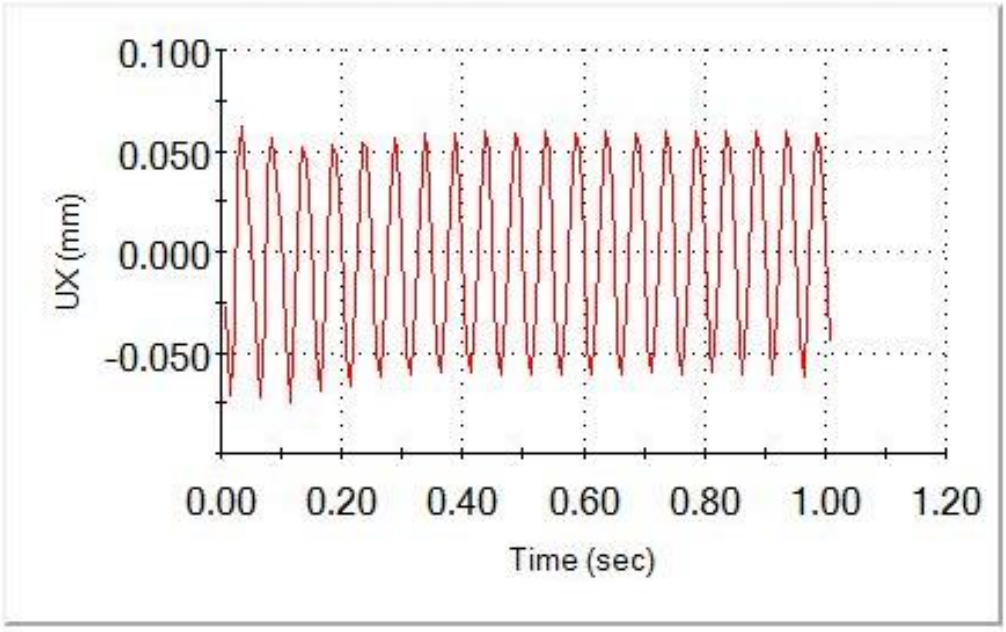


**Figure 6-33: Motion of the spindle in x-direction, 20 Hz (Top Left-Traversing)**

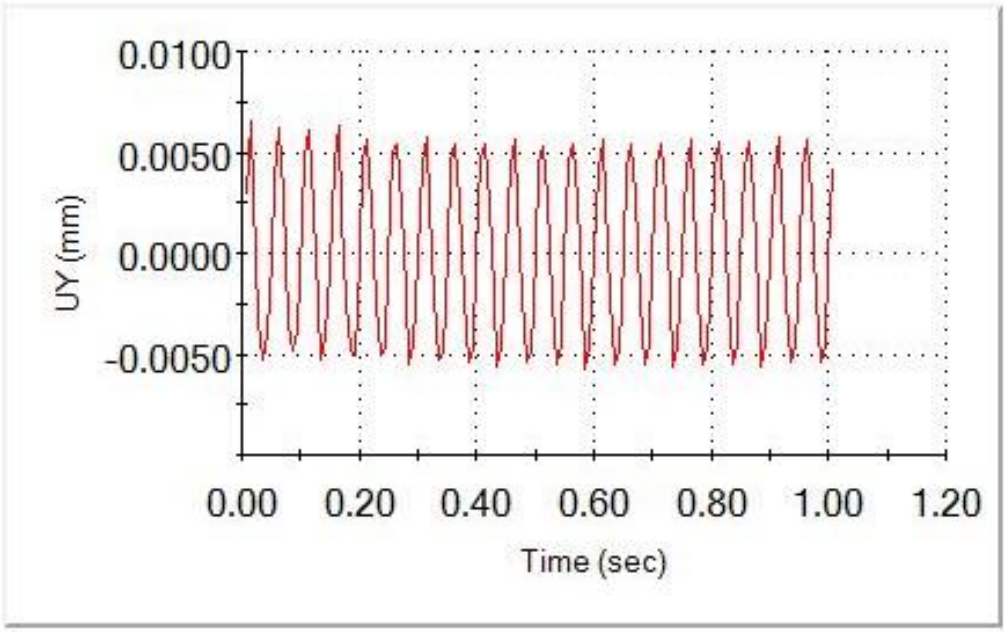


**Figure 6-34: Motion of the spindle in y-direction, 20 Hz (Top Left-Traversing)**

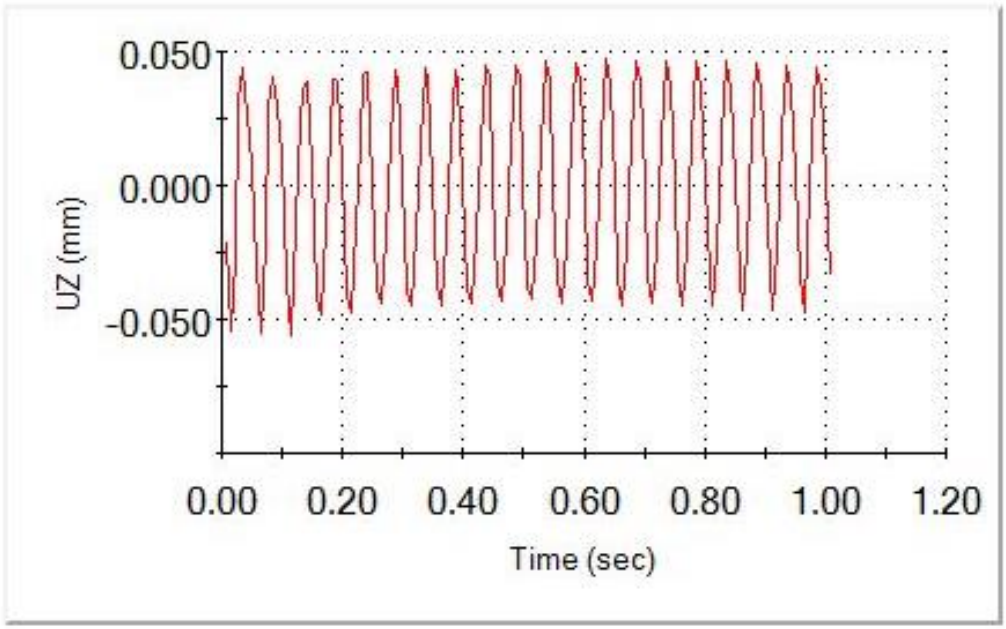


**Figure 6-35: Motion of the spindle in z-direction, 20 Hz (Top Left-Traversing)**

### 6.4.2 Machine Structure Response when the Spindle is at Center Position of the Machine Frame

In this section, dynamic analysis will be conducted in the center spindle position for both plunge and traverse processes.

#### A- Plunging while spindle is in center position

The spindle base is analyzed when it is located at the center of the machine frame during plunging process. The plunging forces have the same values as those used in the previous studies. Figures 6-36 - 6-41 represent amplitude variations with time at forced frequency of 3.33 Hz and 20 Hz.

### 1- Motion of the spindle due to plunging at a frequency of 3.33 Hz

The values of the plunging loads are $F_z = 2000\sin(6.67\pi t)$ N, $T_z = 45\sin(6.67\pi t)$ N.m. The duration of each study is 2 seconds and the sampling frequency is 50 Hz. It can be noticed that in Figures 6-36 - 6-38 the maximum displacement was in the z-direction with a magnitude of 0.18 mm.

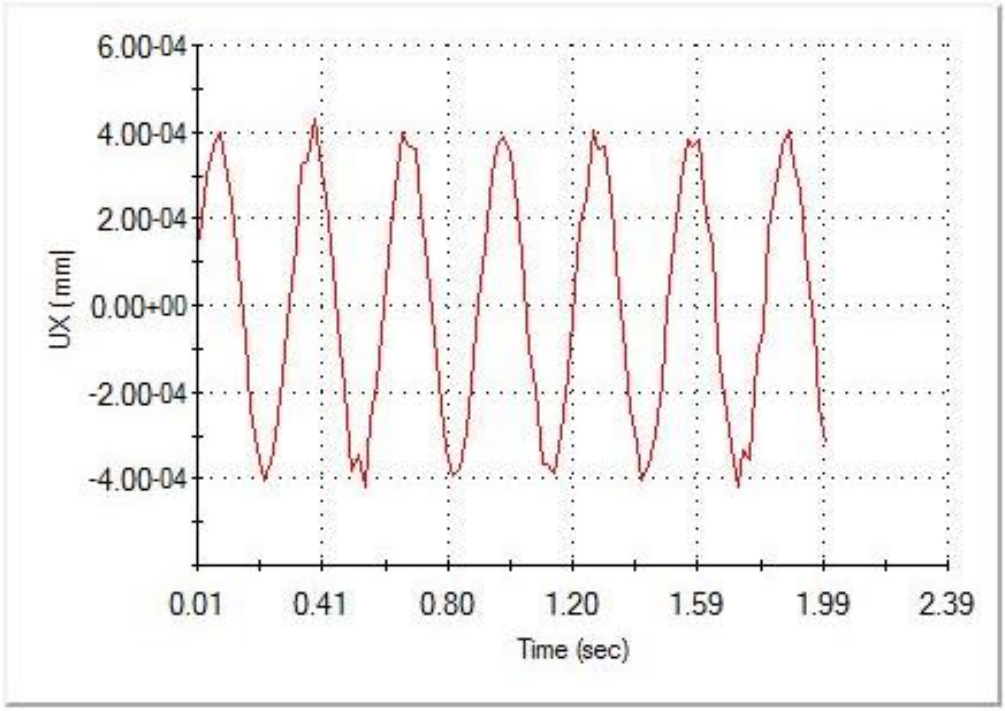


**Figure 6-36: Motion of the spindle in x-direction, 3.33 Hz (Center- Plunging)**

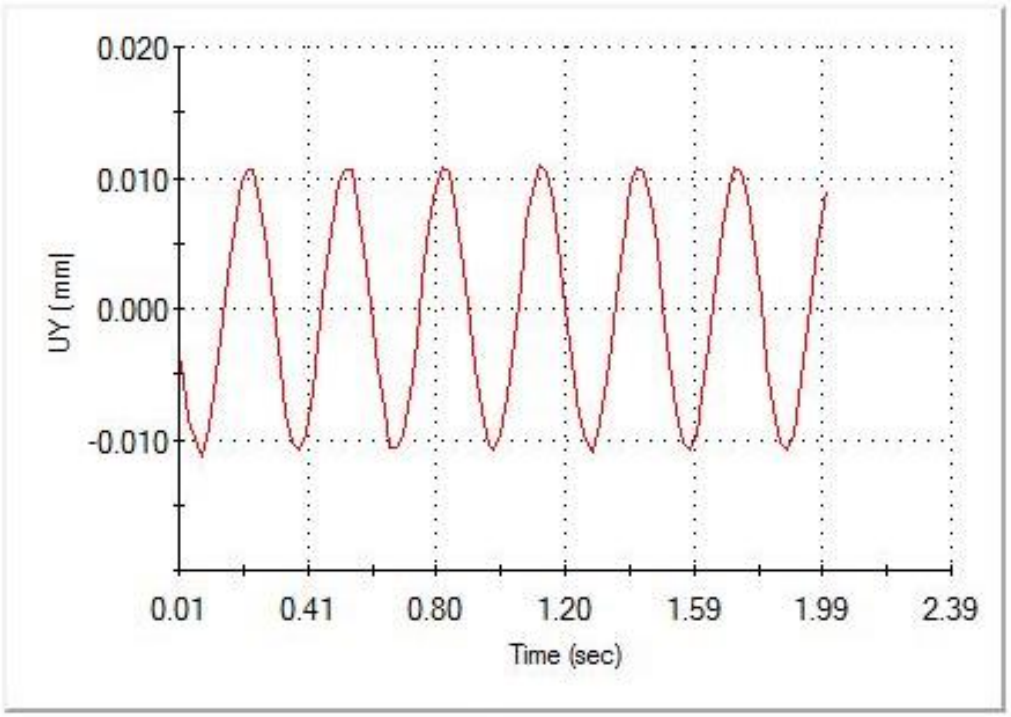


**Figure 6-37: Motion of the spindle in y-direction, 3.33 Hz (Center- Plunging)**

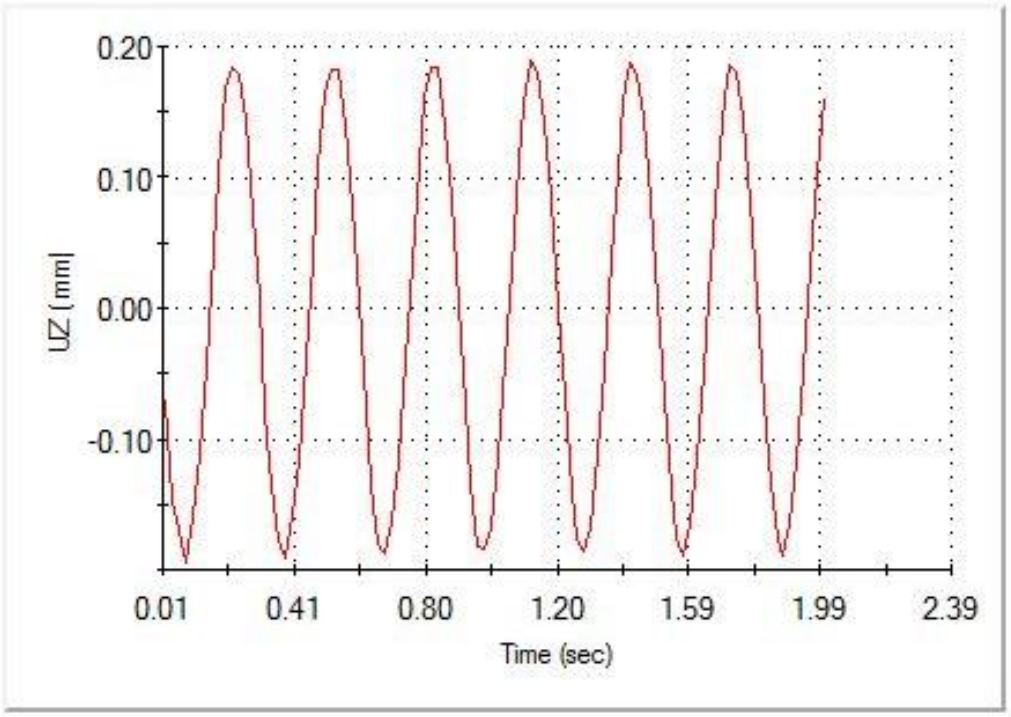


**Figure 6-38: Motion of the spindle in z-direction, 3.33 Hz (Center-Plunging)**

### 2- Motion of the spindle due to plunging at a frequency of 20 Hz

In Figures 6-39 – 6- 41 the time range is taken to be 1s, while the sampling frequency is 140 Hz. The same plunging forces are used as the previous study. The maximum displacement is 0.22 mm in the z-direction. This value is slightly larger than that found while operating at 3.33 Hz (0.18 mm).

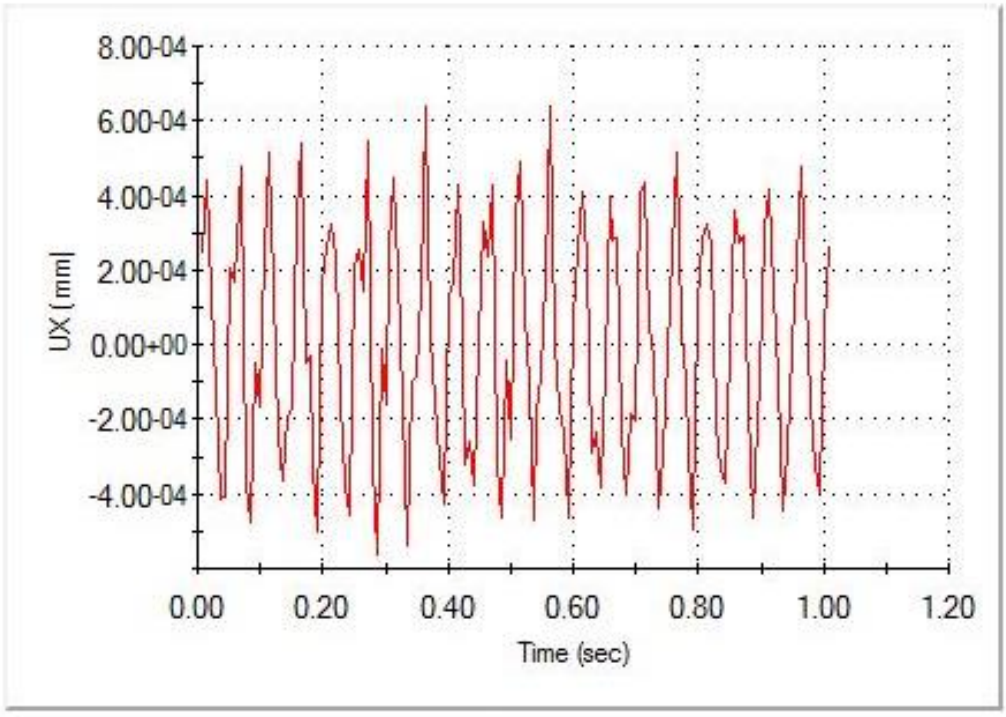


**Figure 6-39: Motion of the spindle in x-direction, 20 Hz (Center- Plunging)**

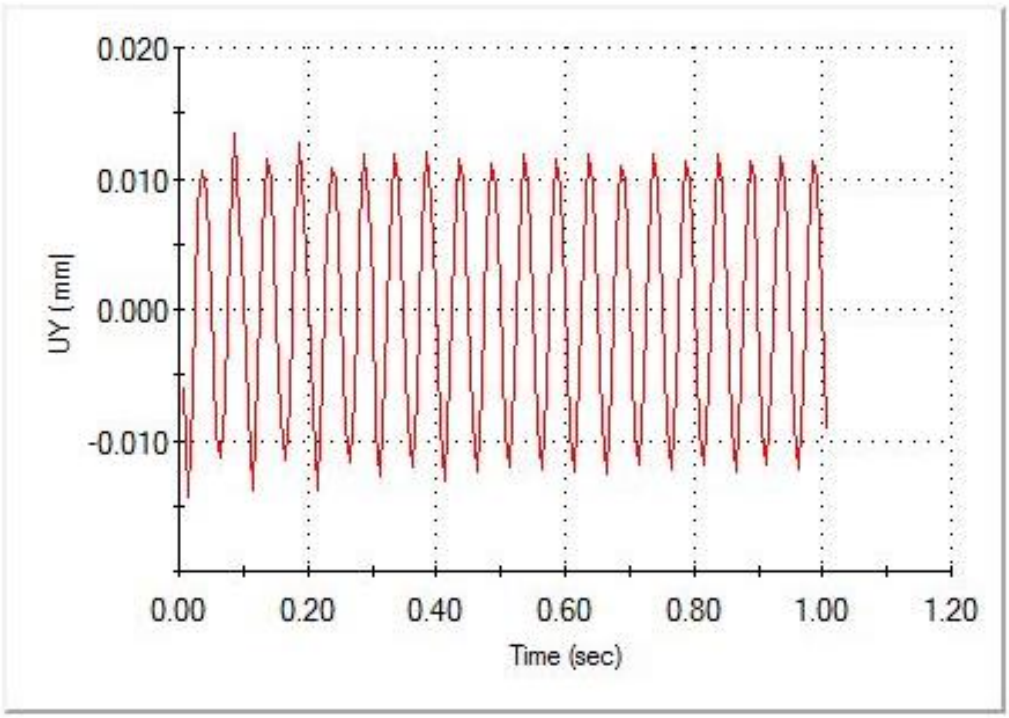


**Figure 6-40: Motion of the spindle in y-direction, 20 Hz (Center- Plunging)**

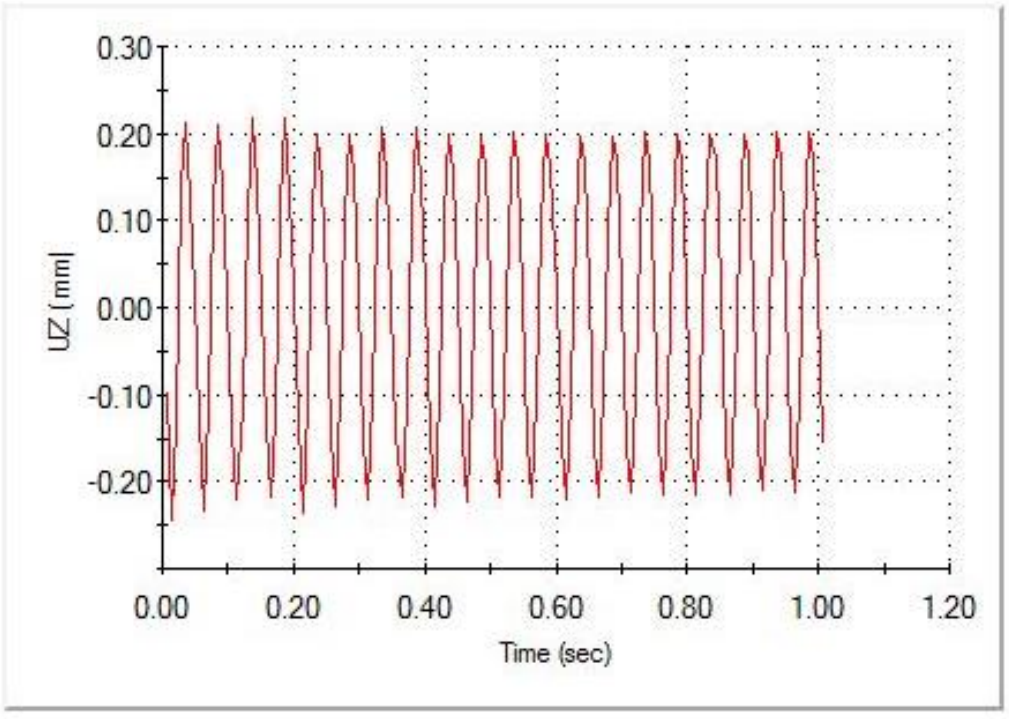


**Figure 6-41: Motion of the spindle in z-direction, 20 Hz (Center- Plunging)**

**B- Traversing while spindle is in center position**

The motion of the spindle base is studied when it is located at the center of the machine frame and traversing. The traversing forces are the same as the ones used before. Figures 6-42 - 6-44 are the displacements of the spindle base at 3.33 Hz forced frequency while Figures 6-45 – 6-47 are the displacements at 20 Hz forced frequency.

**1- Motion of the spindle due to traversing at a frequency of 3.33 Hz**

Figures 6-42 – 6-44 represent the motion of the spindle base in the x, y, and z-directions, respectively, for 3.33 Hz maximum traversing loads.

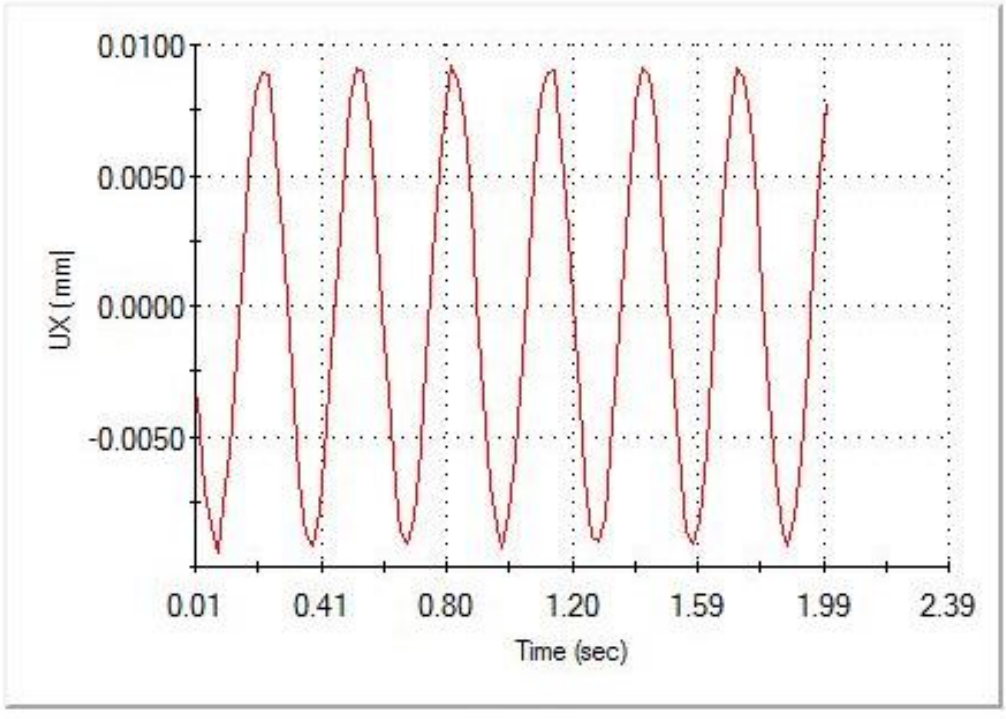


**Figure 6-42: Motion of the spindle in x-direction, 3.33 Hz (Center- Traversing)**

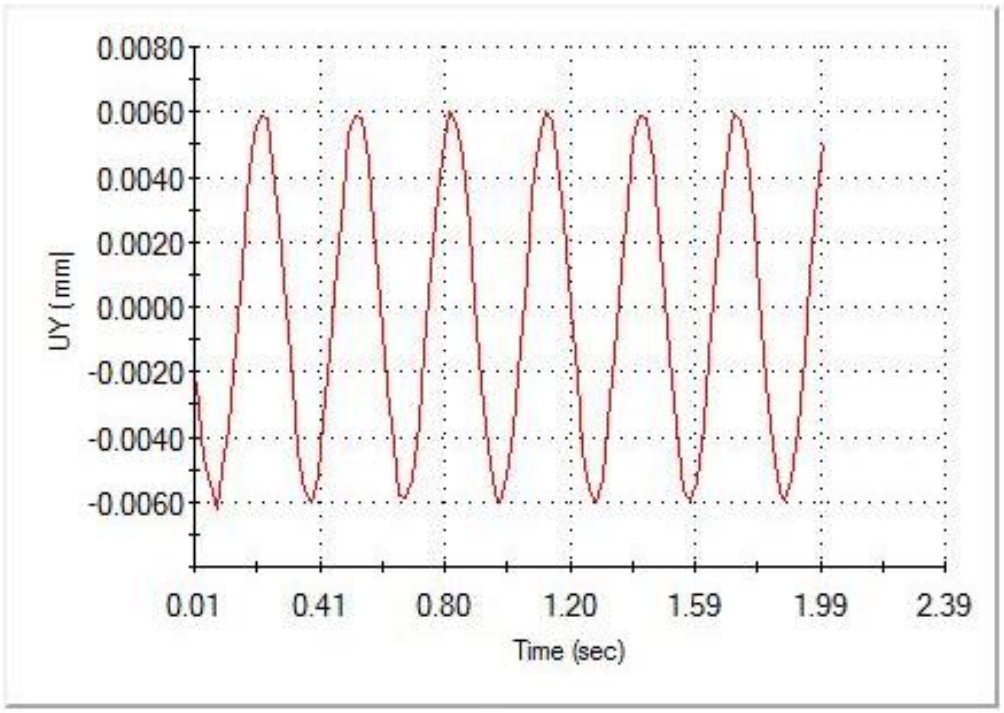


**Figure 6-43: Motion of the spindle in y-direction, 3.33 Hz (Center- Traversing)**

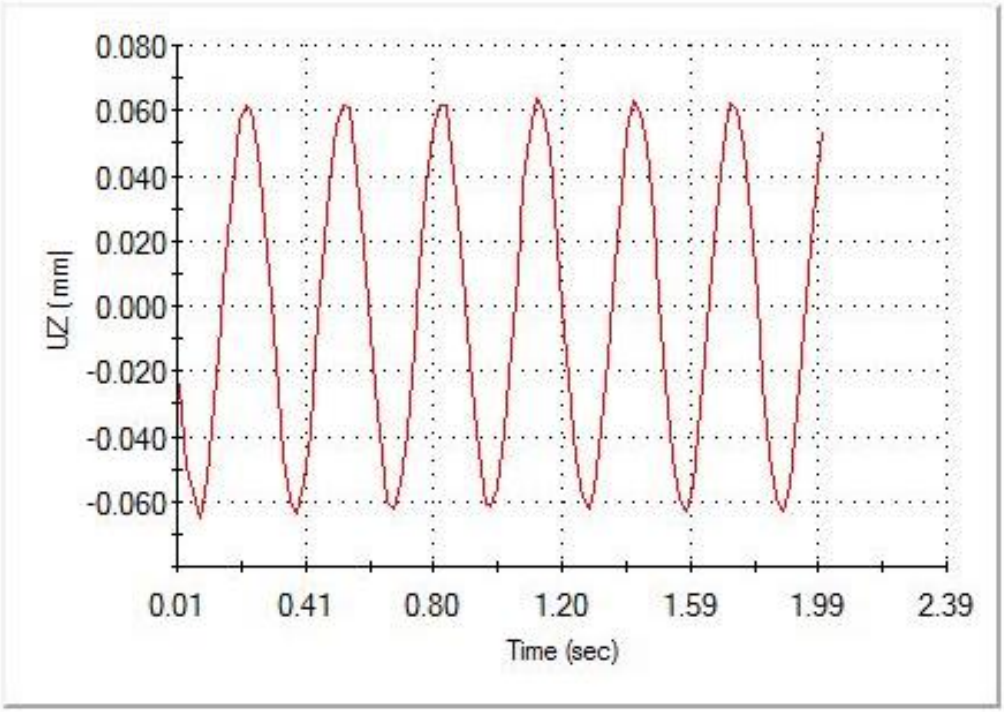


**Figure 6-44: Motion of the spindle in z-direction, 3.33 Hz (Center- Traversing)**

**2- Motion of the spindle due to traversing at a frequency of 20 Hz**

Figures 6-45 – 6-47 represent the motion of the spindle base in the x, y, and z-directions, respectively, for 20 Hz maximum traversing loads.

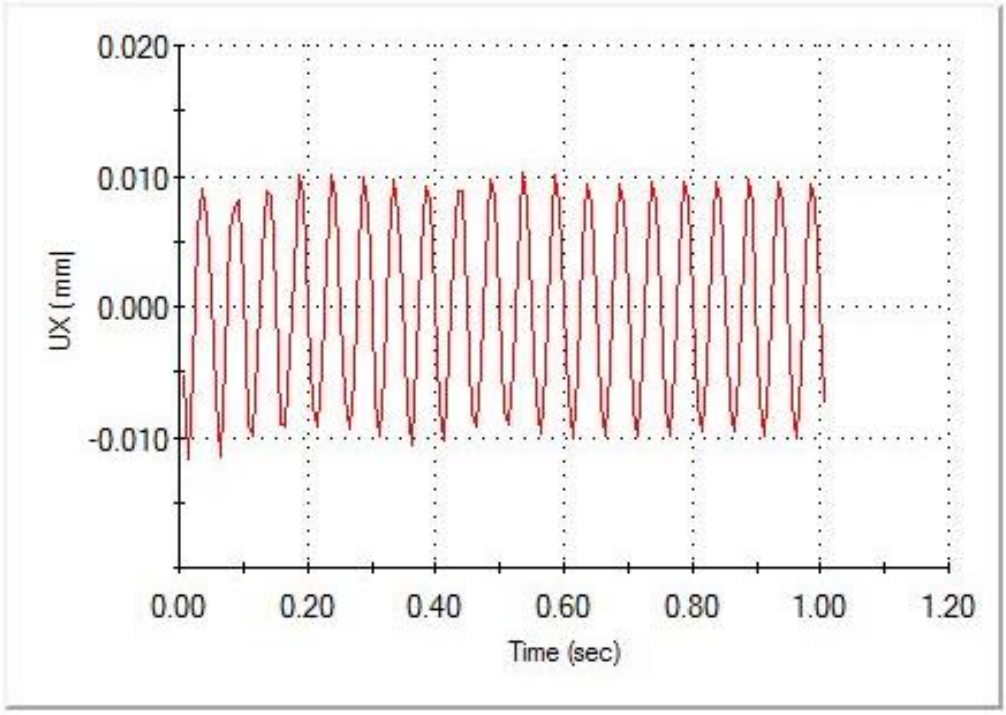


**Figure 6-45: Motion of the spindle in x-direction, 20 Hz (Center- Traversing)**

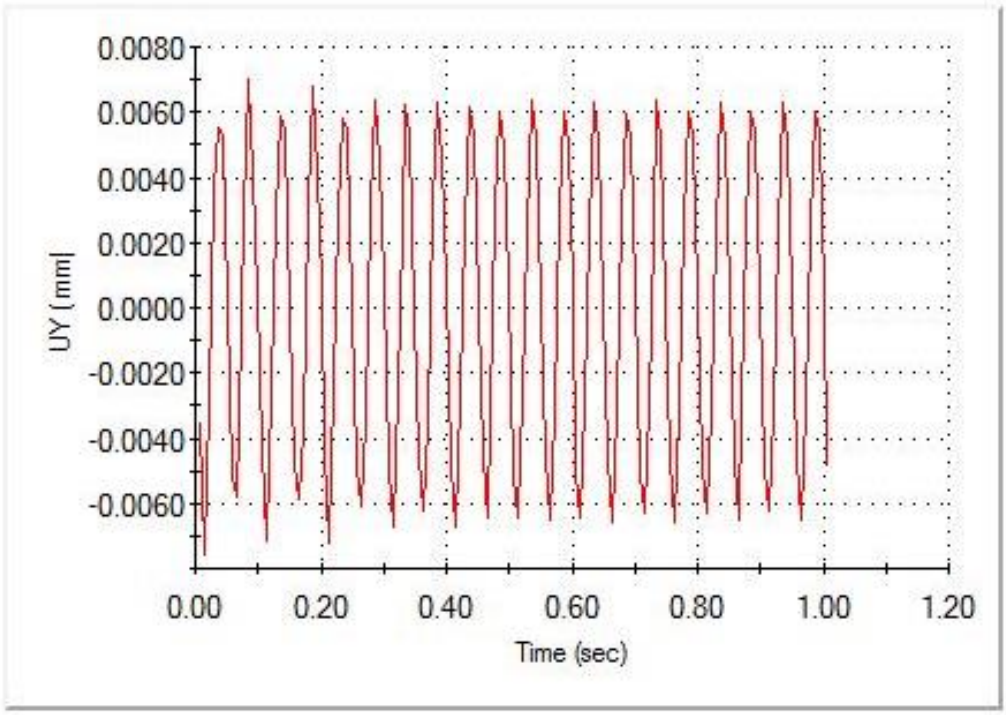


**Figure 6-46: Motion of the spindle in y-direction, 20 Hz (Center- Traversing)**

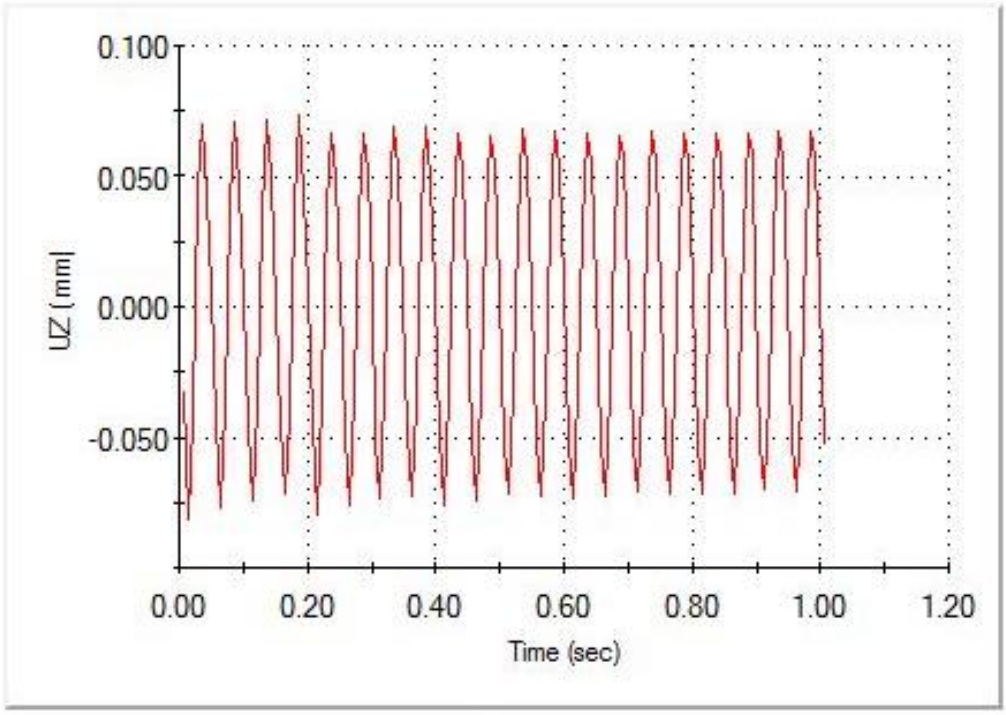


**Figure 6-47: Motion of the spindle in z-direction, 20 Hz (Center- Traversing)**

## 6.5 Other Case Studies

The behavior of the machine is examined at high loads and/or near resonant frequencies. The static studies are displayed first then the dynamic (time history based) studies are shown.

### 6.5.1 Static Cases

For each case of what follows, the operation process and the subjected loads are specified

**Static Case 1:**

This study is performed while the spindle is located at the top left position and plunging. The loads are similar to those selected previously in this chapter, and the varied load is bolded as shown below:

$F_x = 0$ N
$F_y = 0$ N
$\mathbf{F_z = 3000\ N}$
$T_z = 45$ N. m

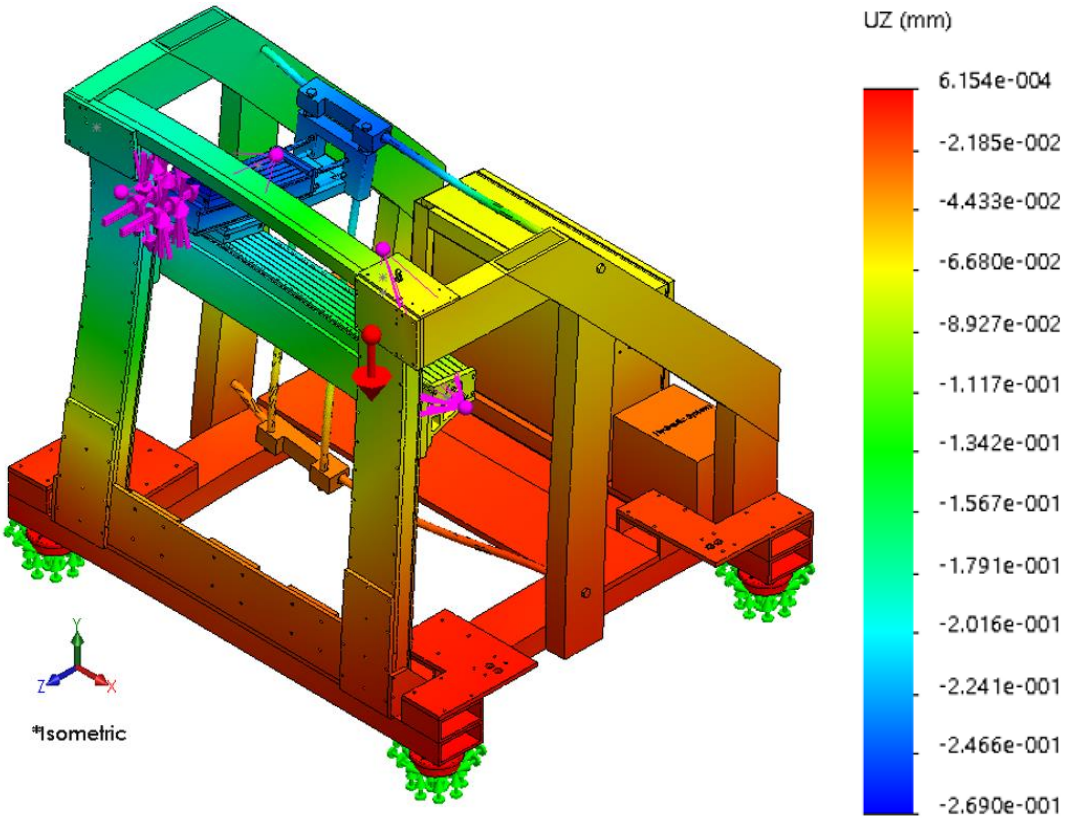


**Figure 6-48: Displacement in z-direction for Static Case 1 (Top left-Plunging)**

The value of the z-axis plunging force ($F_z$) in this case was increased. The purpose is to prove the machine's endurance and rigidity. The maximum displacement is -0.269 mm in the z-direction as shown in Figure 6-48.

**Static Case 2:**

This study is performed while the spindle is located at the top left of the machine frame and plunging. The load that is varied compared to the previous case is bolded as shown below:

$F_x = 0$ N

$F_y = 0$ N

$F_z = 3000$ N

$\mathbf{T_z = 60\ N.m}$

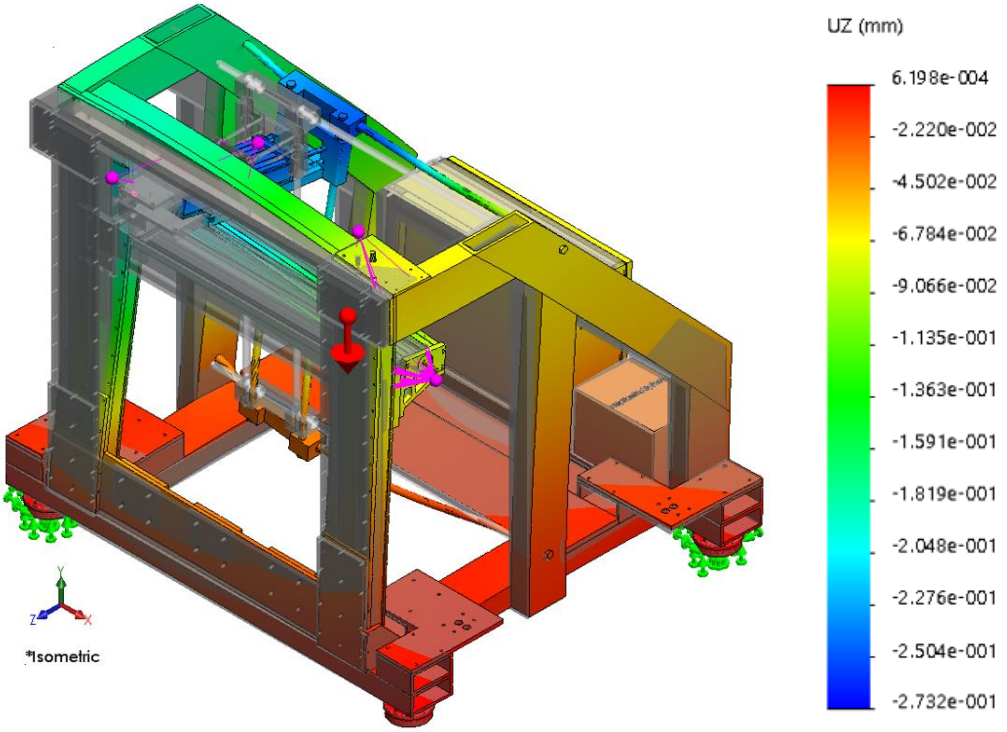


**Figure 6-49: Displacement in z-direction for Static Case 2 (Top left-Plunging)**

The difference between this case and the previous one, is the variance of the torque about the z-axis ($T_z$). The z-direction displacement can be seen in Figure 6-49. The maximum deflection of the machine in this case (-0.273 mm) and previous one (-0.269 mm) have little difference, showing that the machine is highly rigid. This small difference also indicates that ($T_z$) slightly affects the z-direction deformation.

**Static Case 3:**

This study is performed while the spindle is located at the center of the machine frame and plunging. The loads are similar to those selected previously in this chapter, and the varied load is bolded as shown below:

$F_x = 0$ N

$F_y = 0$ N

$F_z = 2000$ N

$\mathbf{T_z = 60\ N.m}$

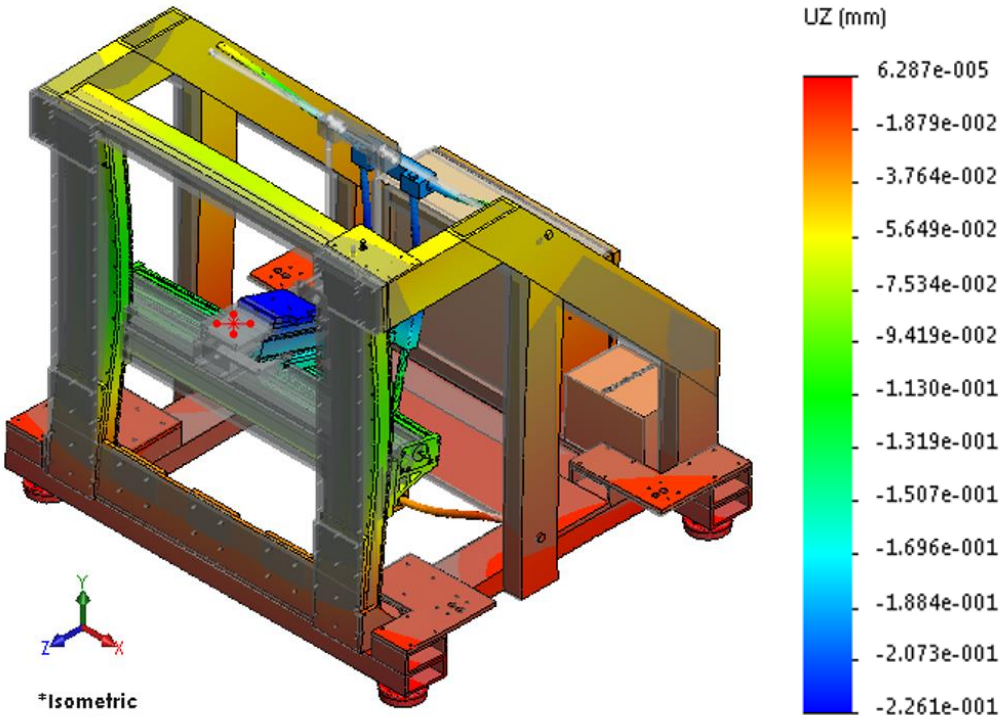


**Figure 6-50: Displacement in z-direction for Static Case 3 (Center-Plunging)**

This case is performed to see the impact of a high z-axis torque ($T_z$) when no other load values are changed. The deformation depicted in Figure 6-50 shows that the maximum displacement is -0.2261 mm in the z-direction.

### 6.5.2 Dynamic Cases

For each case of what follows, the spindle position, the operation process, the subjected loads, forced frequency as well as sampling frequency are specified.

**Dynamic Case 1:**

In this case, the spindle is located at the top left position of the frame and plunging

$$F_x = F_y = 0 \text{ N}$$

$$F_z = 2000 \sin(2\pi f t) \text{ N},$$

and

$$T_z = 45 \sin(2\pi f t) \text{ N.m})$$

The applied loads are similar to those specified previously in this chapter. The difference is that the forced frequency is 75 Hz, and the sampling frequency is 300 Hz.

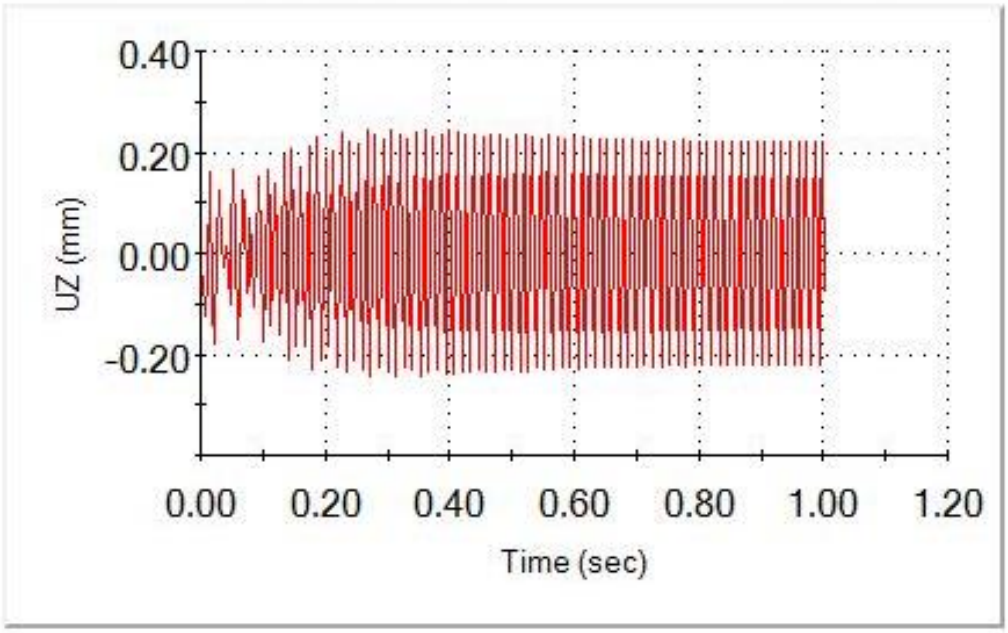


**Figure 6-51: Motion of the spindle in z-direction for Dynamic Case 1**

At this frequency, the motion of the spindle base in the z-direction became nearly 0.22 mm from reference point as shown in Figure 6-51.

**Dynamic Case 2:**

In this case, the spindle is located at the center of the frame and plunging

$$F_x = F_y = 0 \text{ N}$$

$$F_z = 2000 \sin(2\pi f t) \text{ N},$$

and

$$T_z = 45 \sin(2\pi f t) \text{ N.m})$$

The applied loads are similar to those specified previously in this chapter. The difference is that the forced frequency is 49 Hz, and the sampling frequency is 140 Hz.

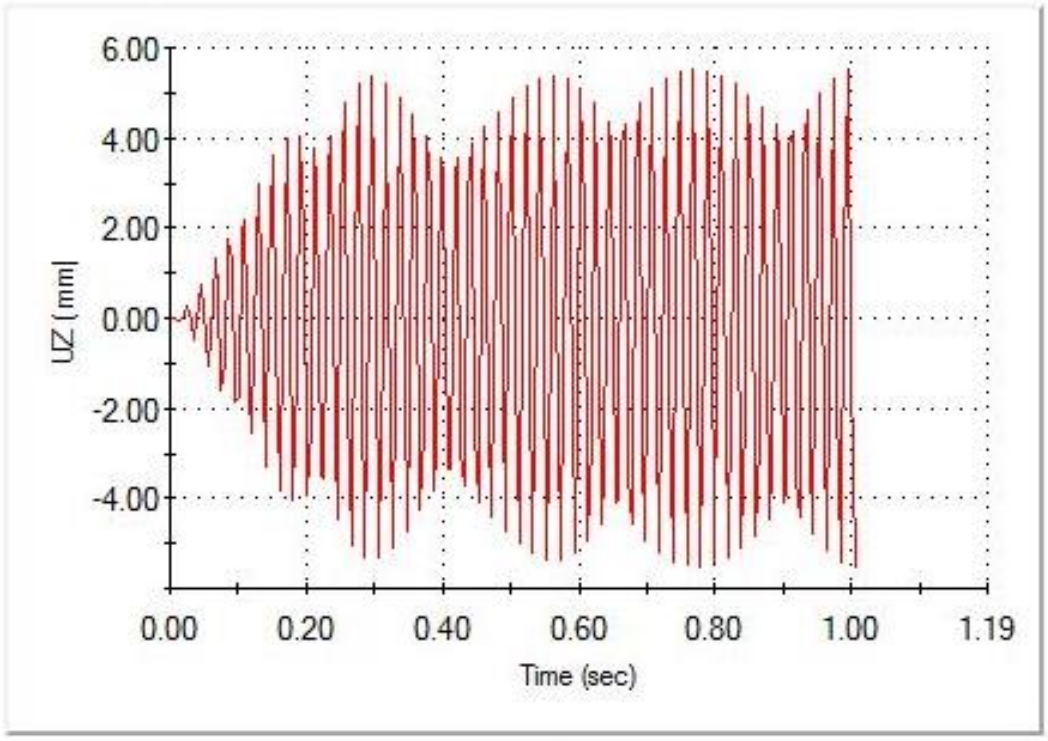


**Figure 6-52: Motion in z-direction for Dynamic Case 2**

The applied forced frequency is near the fundamental frequency of the machine when the spindle is in center position. The motion in the z-direction (shown in Figure 6-52) becomes large (5 mm), exceeding permanent deformation limit (1.75 mm for critical locations, deduced from Figure 6-22) while exhibiting resonance phenomenon, in a short period (0.07 s).

**Dynamic Case 3:**

The spindle is located at the center of the frame and plunging

$$F_x = F_y = 0 \text{ N}$$

$$F_z = 2000 \sin(2\pi f t) \text{ N},$$

and

$$T_z = 45 \sin(2\pi f t) \text{ N.m})$$

The applied loads are the same ones specified previously in this chapter. The difference between this case and the previous one lies in the applied load frequency (50 Hz) and the sampling frequency (140 Hz).

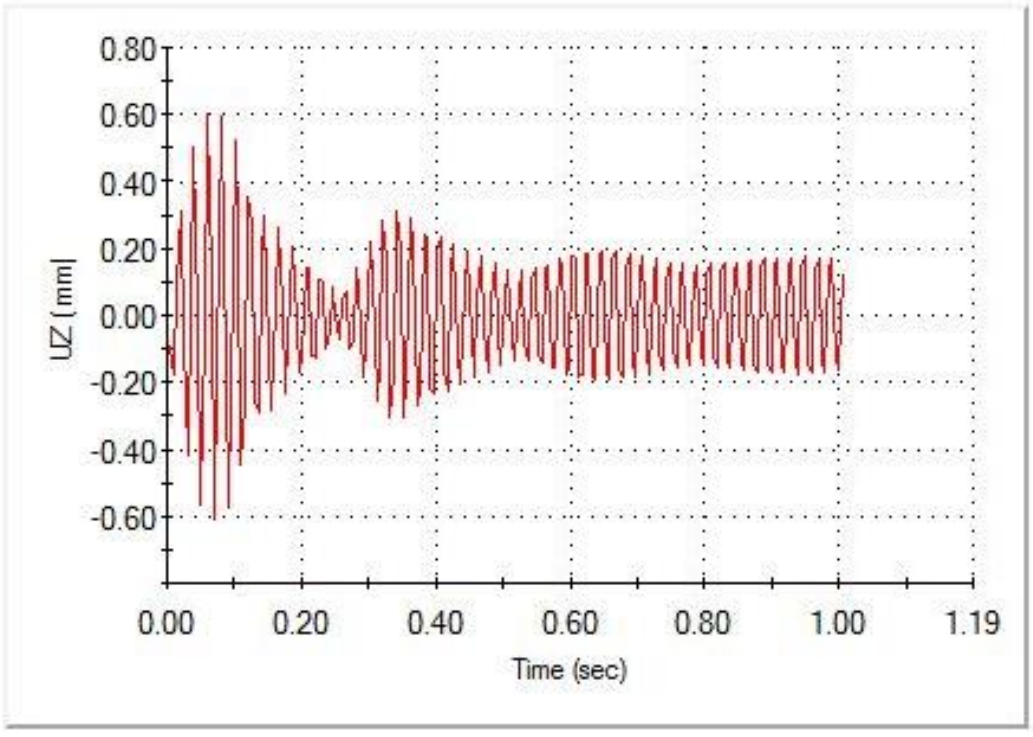


**Figure 6-53: Motion in z-direction for Dynamic Case 3**

At Forced frequency of 50Hz, the motion of the spindle base in the z-direction (as shown in figure 6-53) becomes large at nearly 0.07 second, with the presence of beat phenomenon. Then after 0.8 second the motion becomes more stable.

## 6.6 Validation

In this section, a comparison between SOLIDWORKS FEA with the mathematical model's equations of motion is performed to validate both frequency and dynamic analyses. The equations of motion are simulated using MATLAB software.

Due to problems in troubleshooting a large system's MATLAB code, a simplified model was used as an alternative. Simplification was performed by combining the parts A, B, and C (from Figure 5-6) as a single lumped mass. Part D (shown in Figure 5-7) is considered a fixed part. The nodes used between the lumped mass and the fixed part D are the C nodes. All other nodes are canceled.

The generalized coordinates used for the motion of the mass lump are $x_3$, $y_3$, $z_3$, $q_{x3}$, $q_{y3}$, and $q_{z3}$ (from Figure 5-8). The equations of motion are found in APPENDIX D. The spindle is considered to be located at the center of the machine frame.

The natural frequencies of the machine frame obtained from SOLIDWORKS FEA is compared with those from MATLAB in Table 6-3. Noting that all resonant frequencies are due to bending.

**Table 6-3: Comparing Frequencies from SOLIDWORKS and MATLAB**

| Frequency (Hz) SOLIWORKS | Frequency (Hz) MATLAB | % error |
|---|---|---|
| 49.024 | 45.2188 | 7.76% |
| 210.04 | 205.6476 | 2.13% |
| 219.21 | 208.4091 | 5.18% |
| 347.73 | 356.7736 | 2.53% |
| 361.73 | 358.8240 | 0.81% |
| 372.56 | 363.8796 | 2.3% |

The dynamic motion of the machine structure is compared at three points for both MATLAB and SOLIWORKS models. These points are shown in Figures 6-54 – 6-55, where the first point is the reference of the generalized coordinates in the mathematical model. The analyses performed using both software have the same parameter values (e.g. stiffnesses, dimensions, etc.). The spindle is considered traversing with $F_x = F_y = 1200\sin(2\pi ft)$ N, $F_z = 600\sin(2\pi ft)$ N, and $T_z = 25\sin(2\pi ft)$ N. m. Notice that $f$ is taken at 3.33 and 20 Hz.

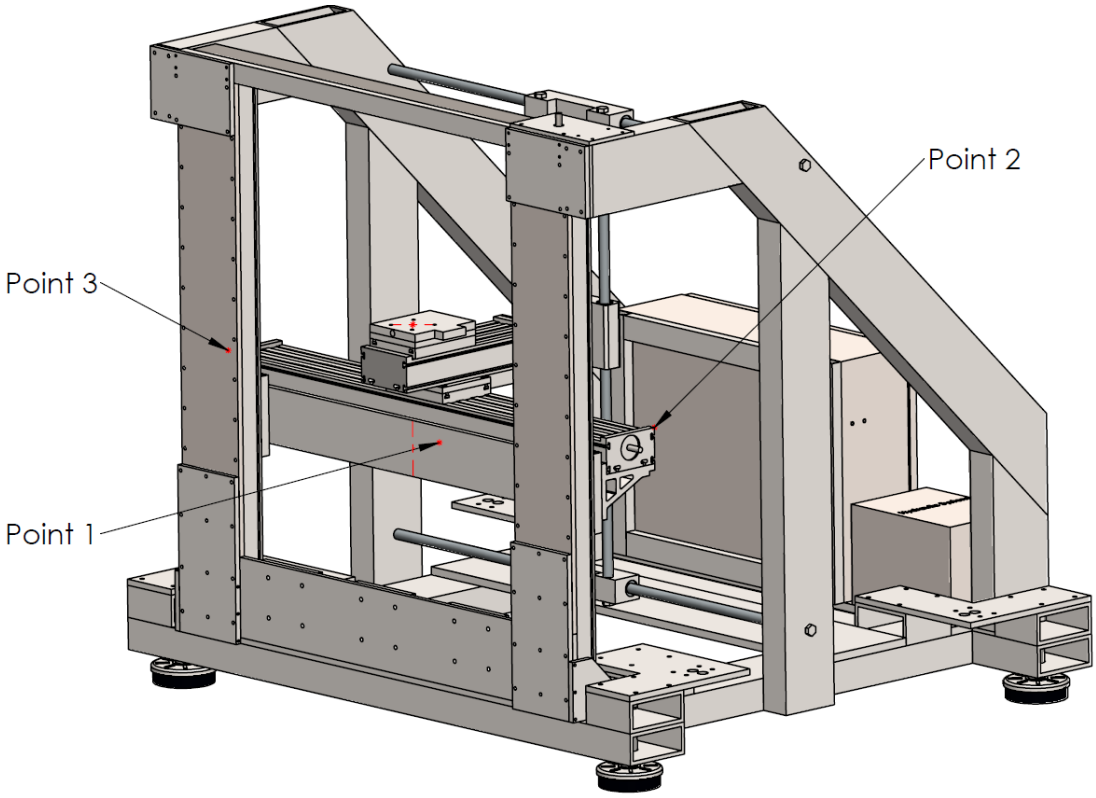


**Figure 6-54: Points for Comparison in Machine Structure (View-1)**

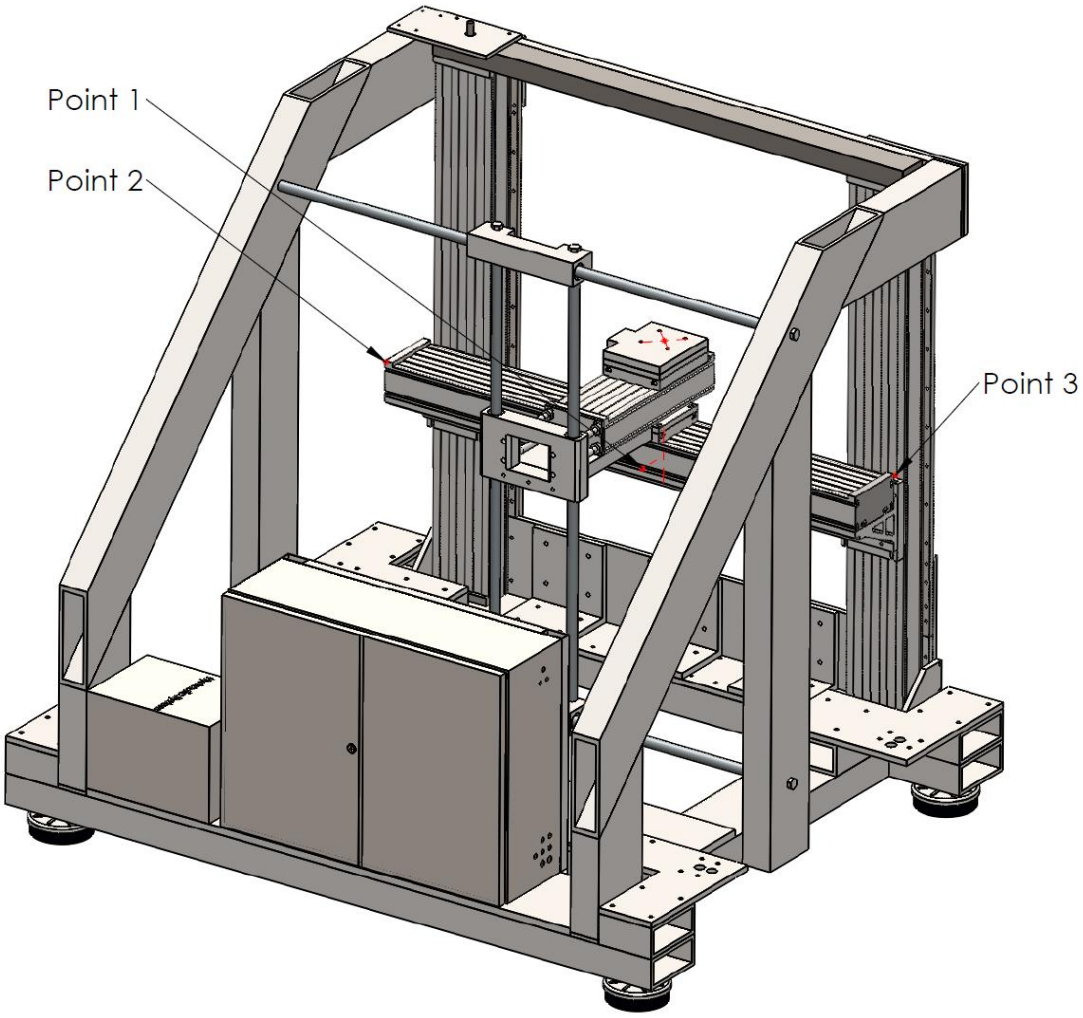


**Figure 6-55: Points for Comparison in Machine Structure (View-2)**

### 1- Motion at point 1 while spindle is traversing at a frequency of 3.33 Hz

Figure 6-56 – 6-58 show the deflection of the machine frame using SOLIDWORKS and MATLAB, where the motion is taken at point 1, in the x, y, and z-directions respectively. At this point, the plotted data obtained from both software have close values. SOLIDWORKS simulation uses 2,286,488 elements, which gives a much more detailed result than the MATLAB lumped mass model, leading to the differences shown in the mentioned figures.

The time range taken for these studies is 2 seconds and the sampling frequency is 50 Hz. The highest amplitude displacement is in the z-direction with a value of 0.028 mm as shown in Figure 6-58.

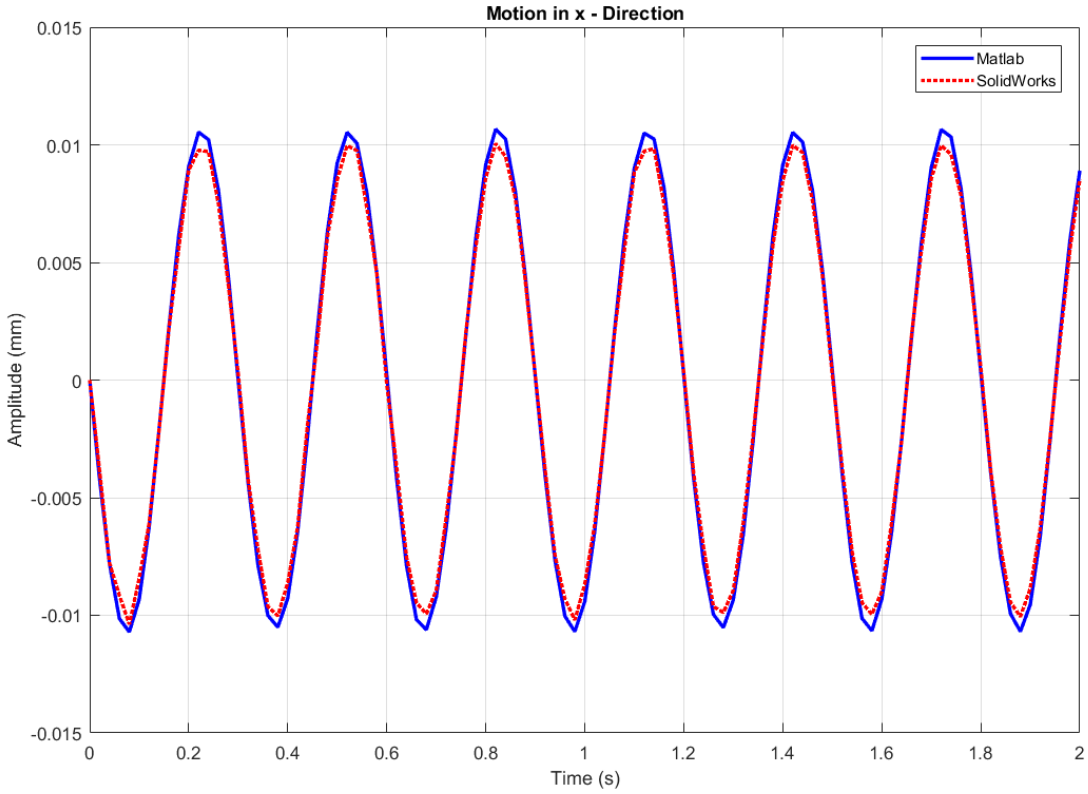


**Figure 6-56: Motion of point 1 in x-direction, 3.33 Hz (Center- Traversing)**

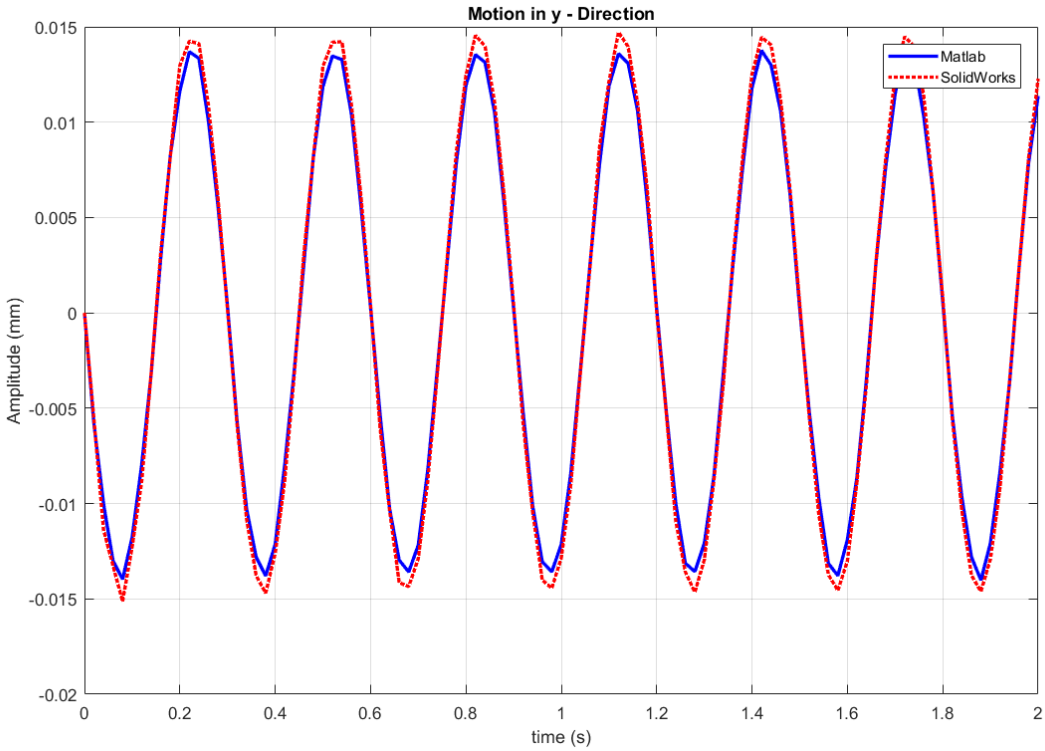


**Figure 6-57: Motion of point 1 in y-direction, 3.33 Hz (Center- Traversing)**

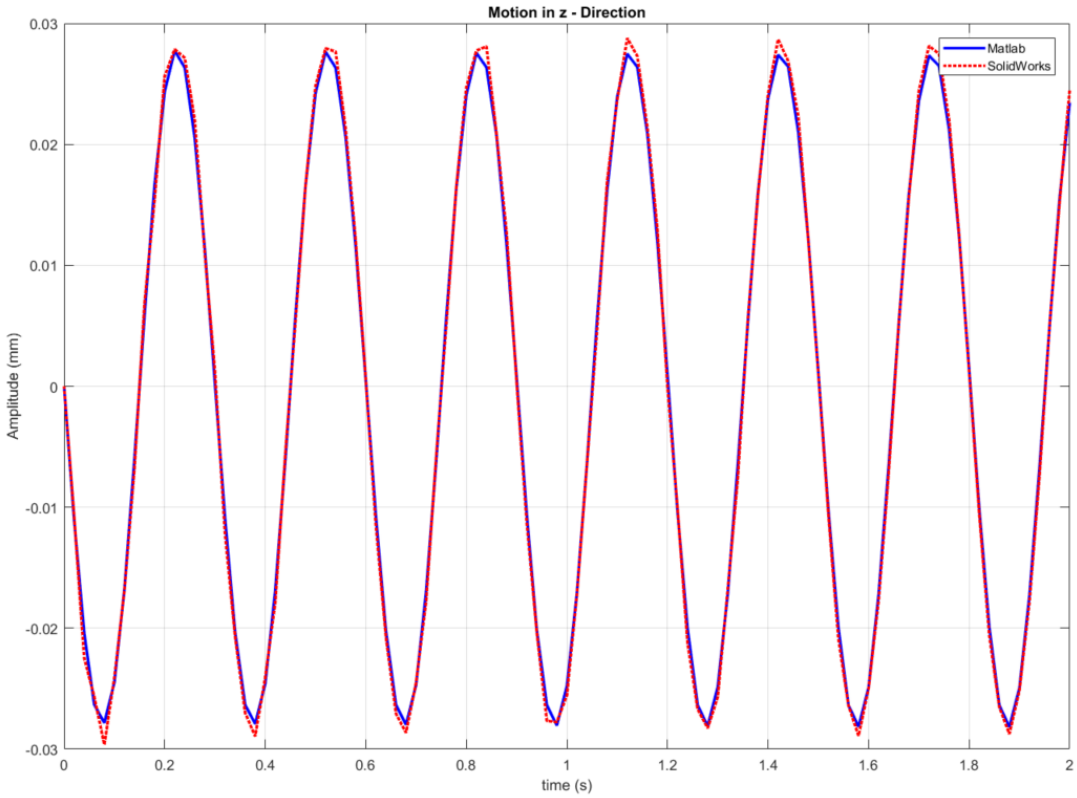


**Figure 6-58: Motion of point 1 in z-direction, 3.33 Hz (Center- Traversing)**

**2- Motion at point 1 while spindle is traversing at a frequency of 20Hz**

Figures 6-59 – 6-61 represent the motion of point 1 in the x, y, and z-directions, respectively, for 20 Hz traversing loads. The time range is taken to be 1s, while the sampling frequency is 140 Hz. The higher differences shown in Figures 6-60 and 6-61 peaks values, can be linked to the material bending in the y and z-directions that SOLIDWORKS accounts for unlike the MATLAB model.

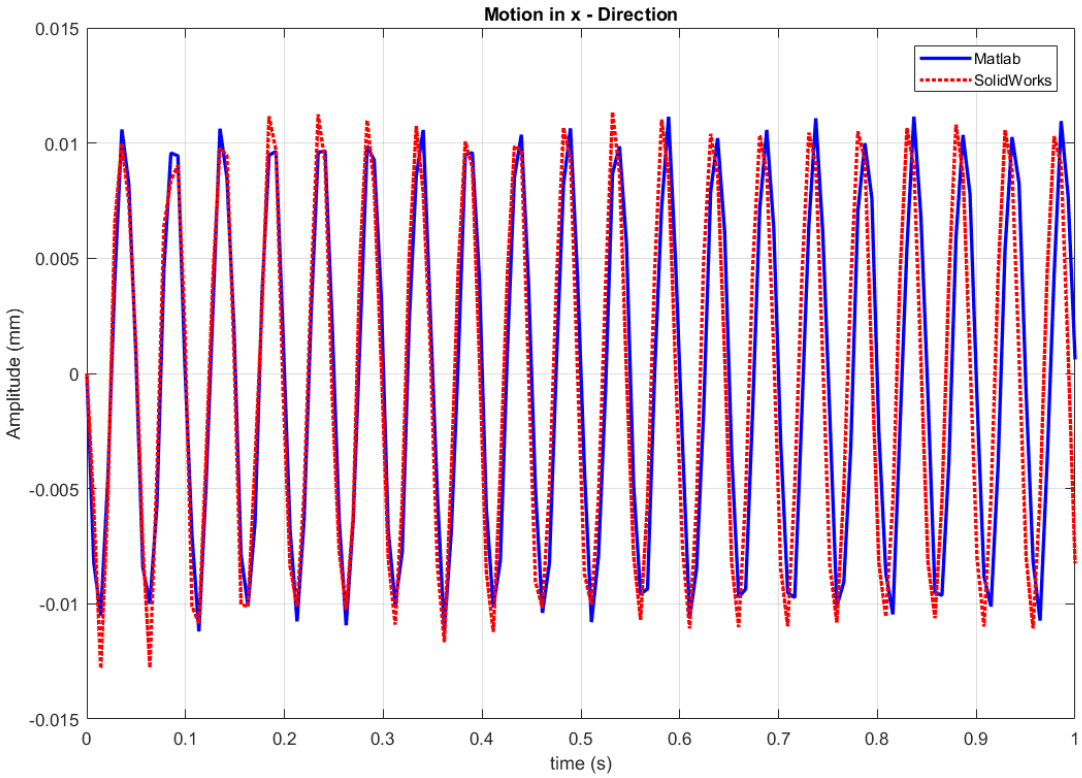


**Figure 6-59: Motion of point 1 in x-direction, 20 Hz (Center- Traversing)**

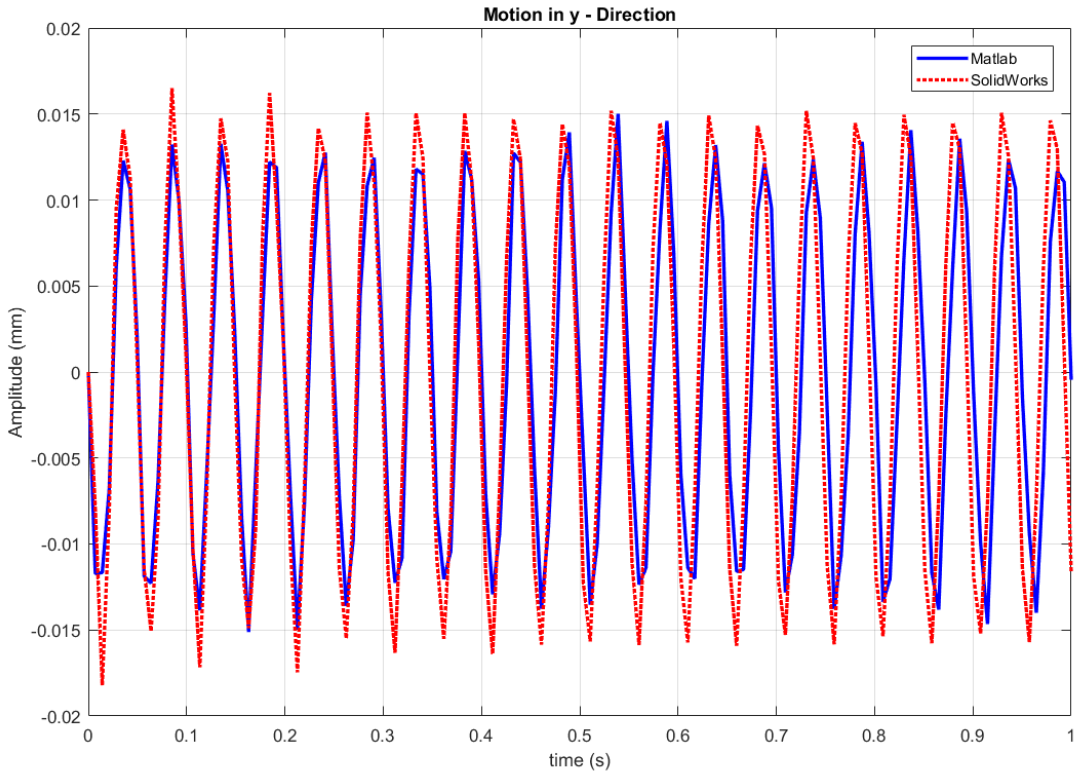


**Figure 6-60: Motion of point 1 in y-direction, 20 Hz (Center- Traversing)**

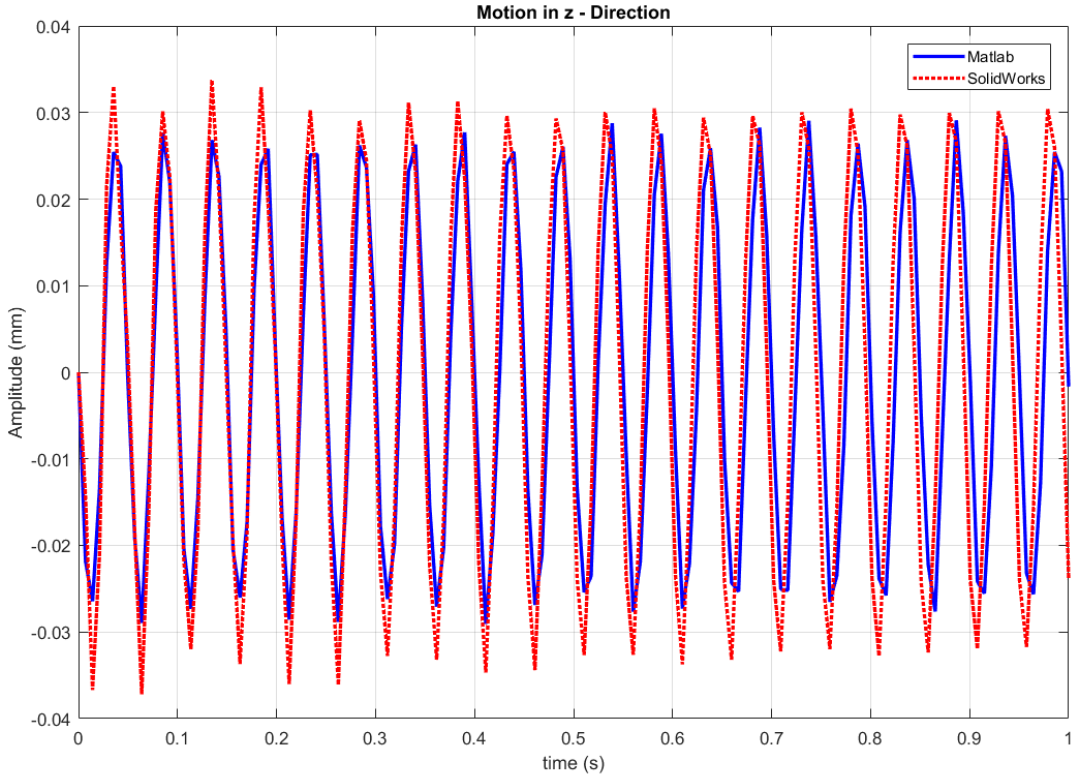


**Figure 6-61: Motion of point 1 in z-direction, 20 Hz (Center- Traversing)**

### 3- Motion at point 2 while spindle is traversing at a frequency of 3.33Hz

Figure 6-62 – 6-64 show the deflection of the machine frame at point 2, in the x, y, and z-directions respectively. The time range taken for these studies is 2 seconds and the sampling frequency is 50 Hz. The highest amplitude displacement is in the z-direction with a value of 0.027 mm (from MATLAB) as shown in Figure 6-64.

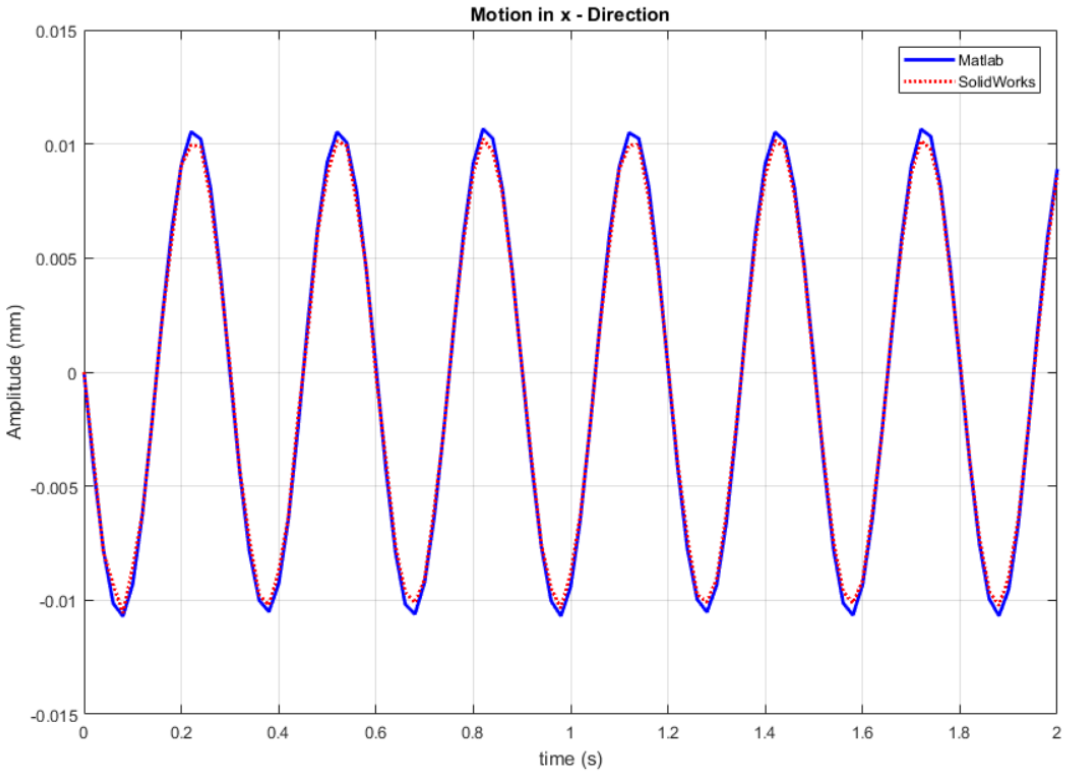


**Figure 6-62: Motion of point 2 in x-direction, 3.33 Hz (Center- Traversing)**

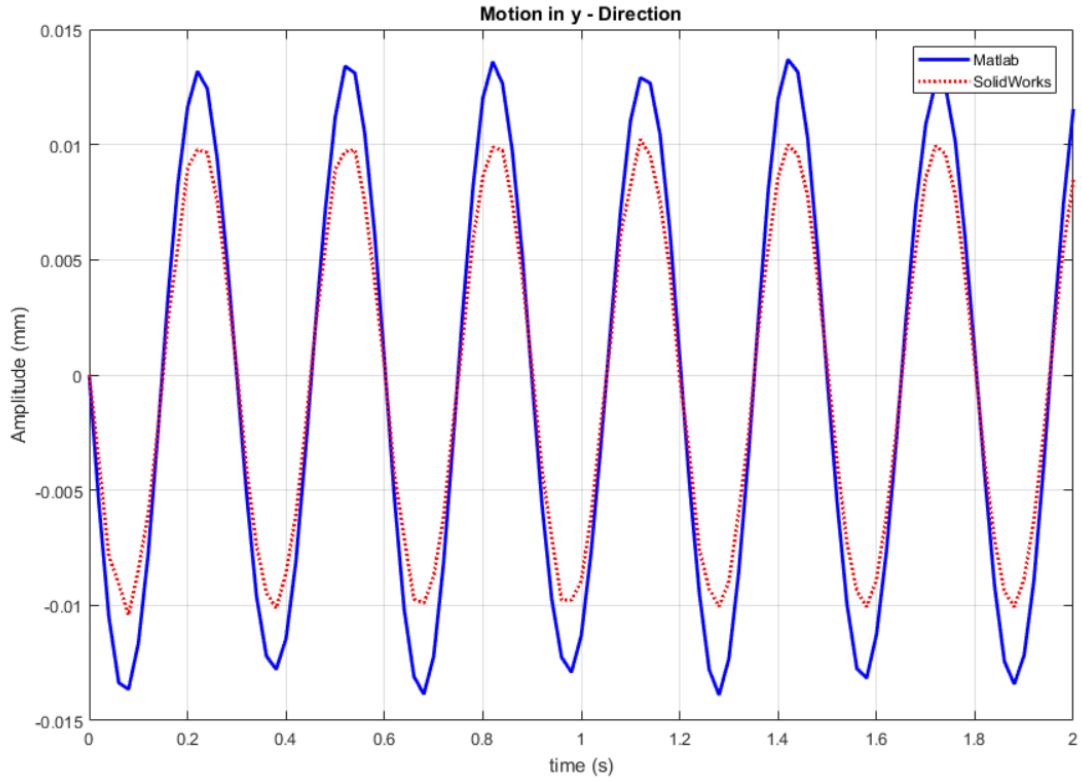


**Figure 6-63: Motion of point 2 in y-direction, 3.33 Hz (Center- Traversing)**

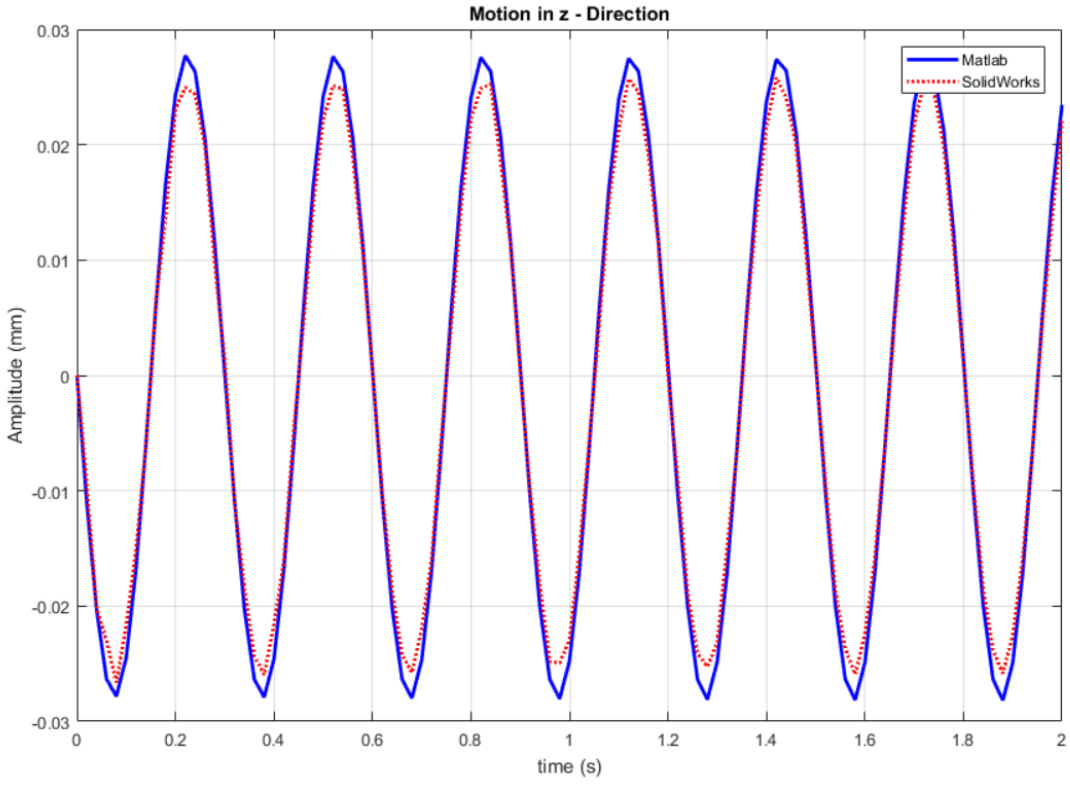


**Figure 6-64: Motion of point 2 in z-direction, 3.33 Hz (Center- Traversing)**

**4- Motion at point 2 while spindle is traversing at a frequency of 20Hz**

The motion of point 2 in the x, y, and z-directions are presented in Figures 6-65 – 6-67, respectively, for 20 Hz traversing loads. The time range is taken to be 1s, while the sampling frequency is 140 Hz.

By comparing z-directional motion for point 2 at 3.33 HZ and 20 Hz (Figures 6-64 and 6-67), the transient state amplitude increased slightly more at 20 Hz than at 3.33 Hz.

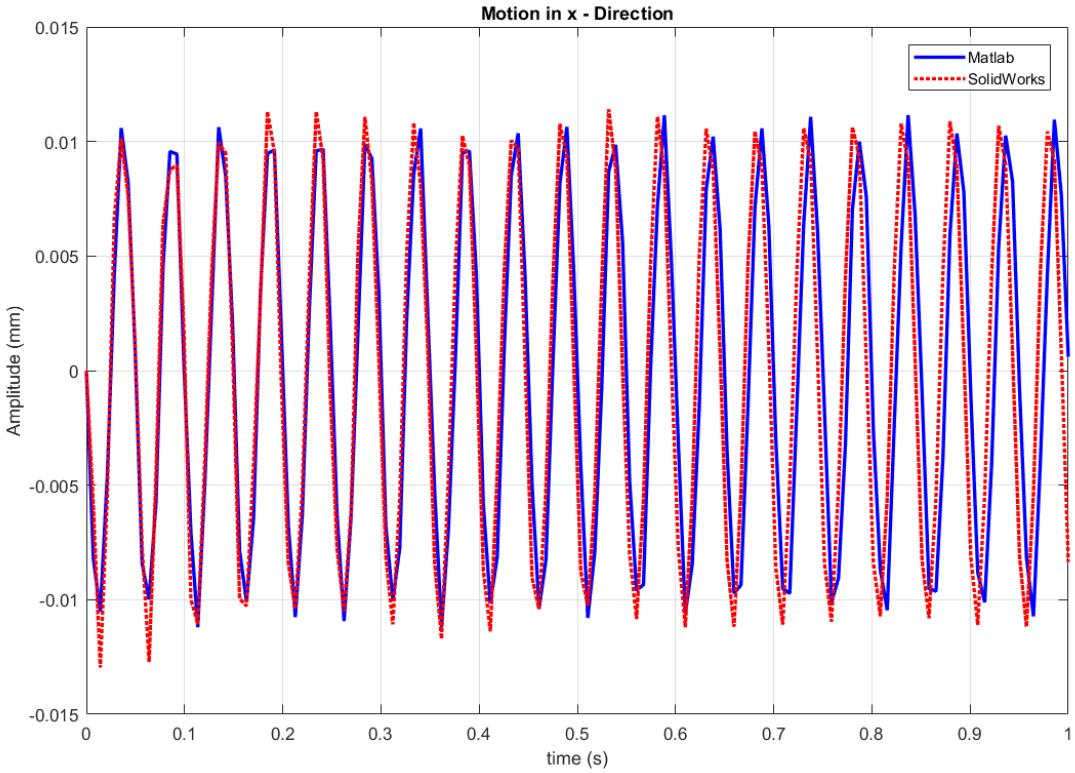


**Figure 6-65: Motion of point 2 in x-direction, 20Hz (Center- Traversing)**

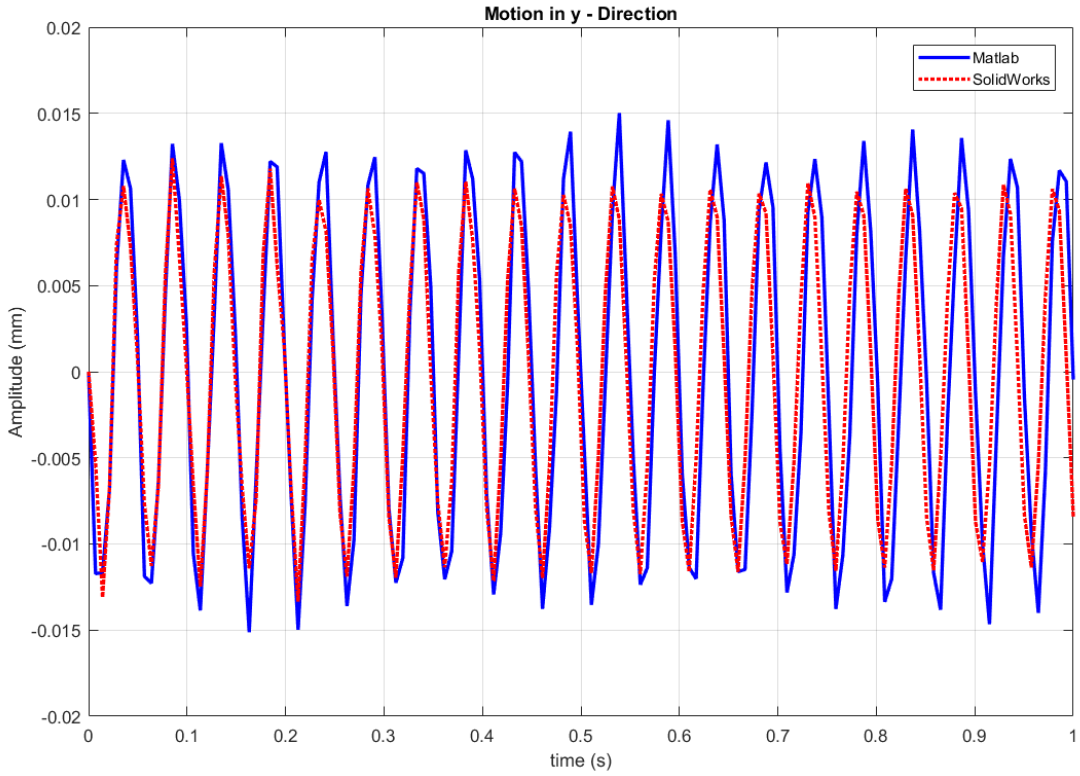


**Figure 6-66: Motion of point 2 in y-direction, 20Hz (Center- Traversing)**

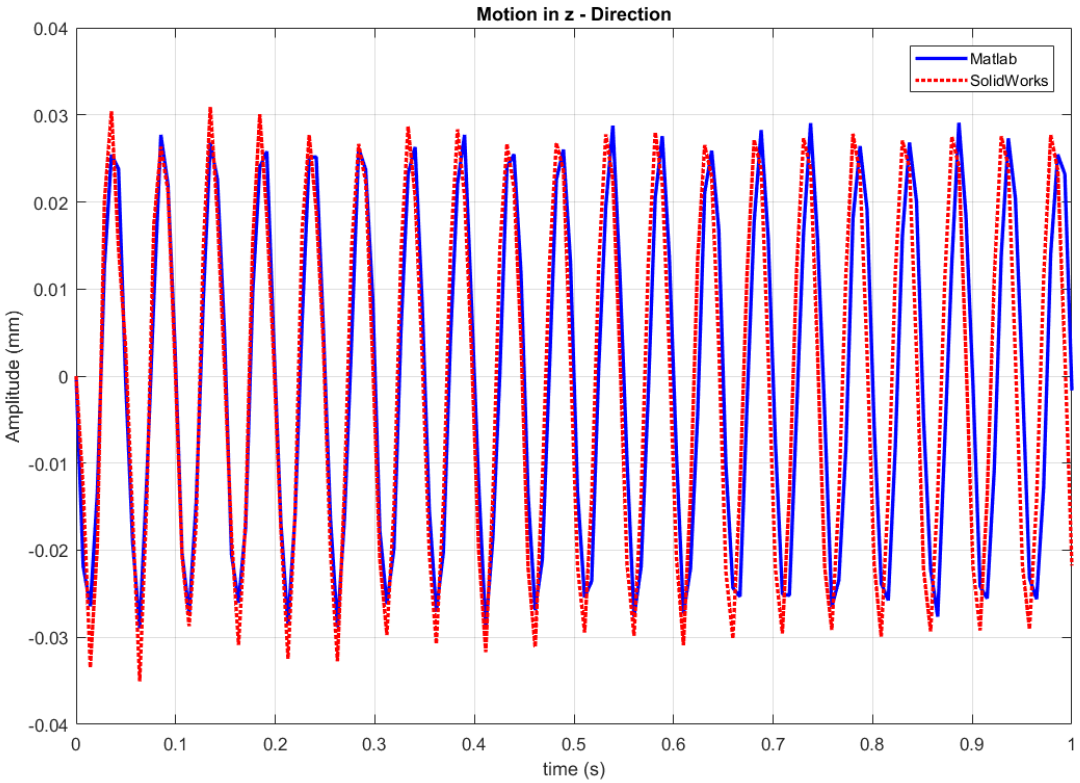


**Figure 6-67: Motion of point 2 in z-direction, 20Hz (Center- Traversing)**

**5- Motion at point 3 while spindle is traversing at a frequency of 3.33Hz**

Figure 6-68 – 6-70 show the deflection of the machine frame at point 3, due to traverse loads, in the x, y, and z-directions respectively. The time range taken for these studies is 2 seconds and the sampling frequency is 50 Hz.

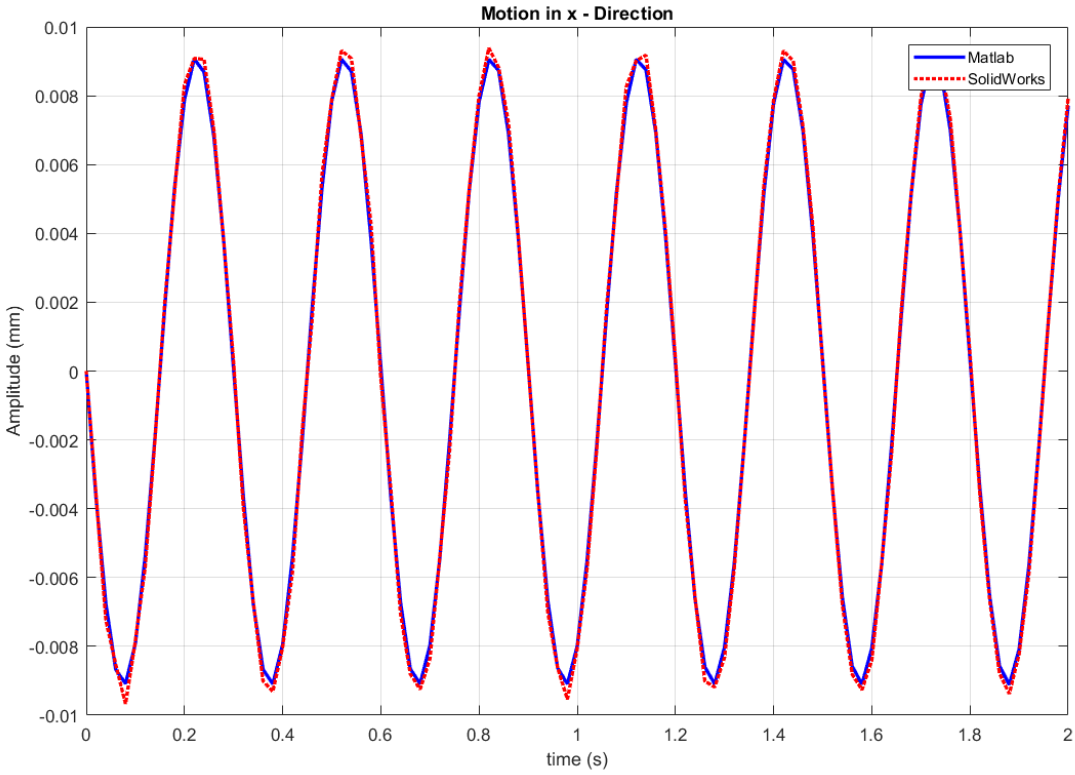


**Figure 6-68: Motion of point 3 in x-direction, 3.33Hz (Center- Traversing)**

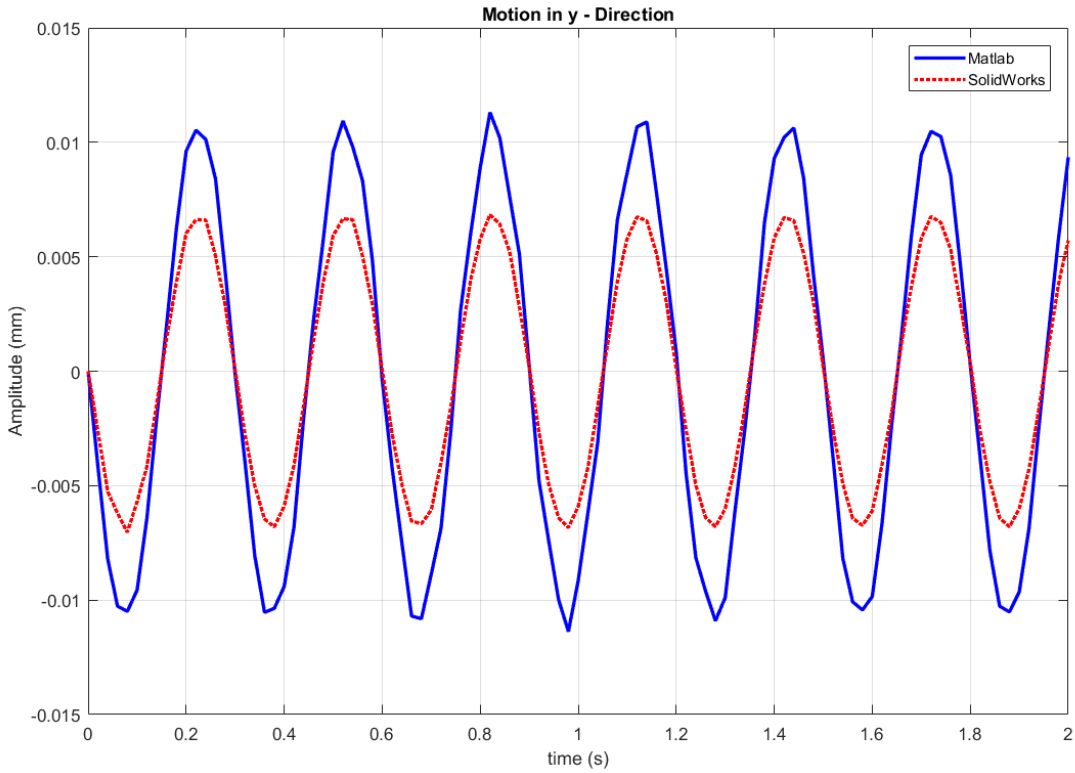


**Figure 6-69: Motion of point 3 in y-direction, 3.33Hz (Center- Traversing)**

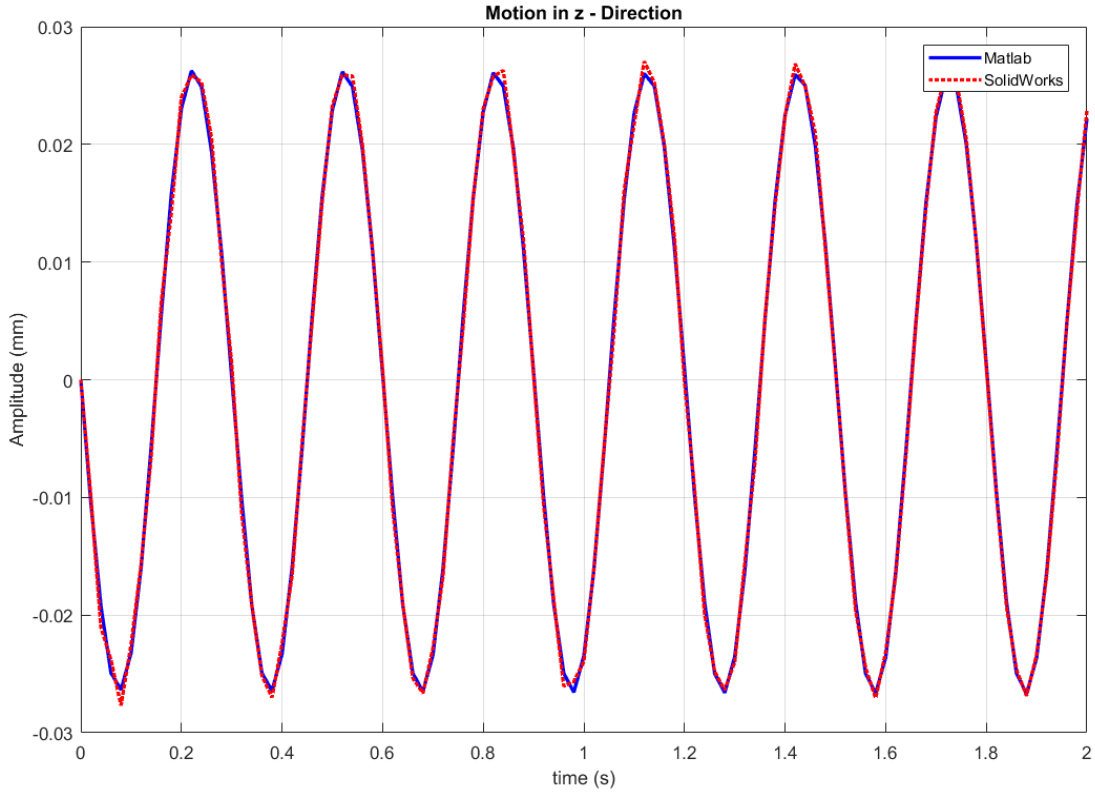


**Figure 6-70: Motion of point 3 in z-direction, 3.33Hz (Center- Traversing)**

**6- Motion at point 3 while spindle is traversing at a frequency of 20Hz**

Presented in Figures 6-65 – 6-67 is the motion of point 3 in the x, y, and z-directions are, respectively, for 20 Hz with applied traverse loads. The time range is taken to be 1s, while the sampling frequency is 140 Hz.

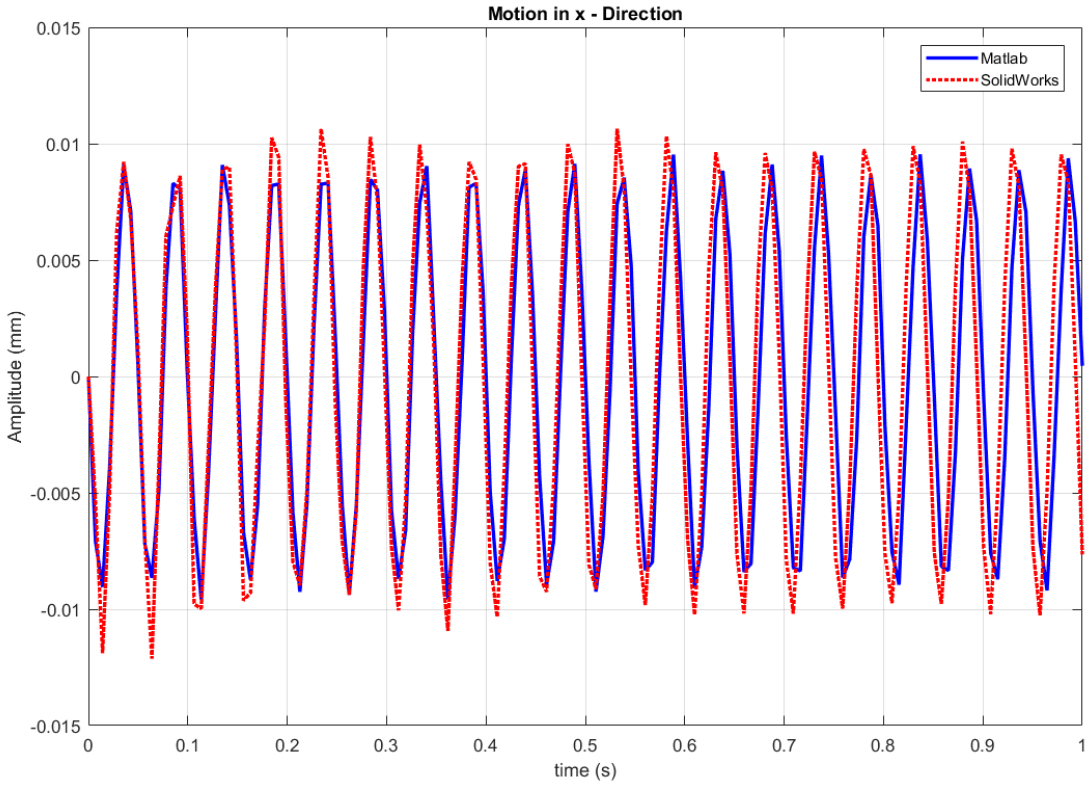


**Figure 6-71: Motion of point 3 in x-direction, 20Hz (Center- Traversing)**

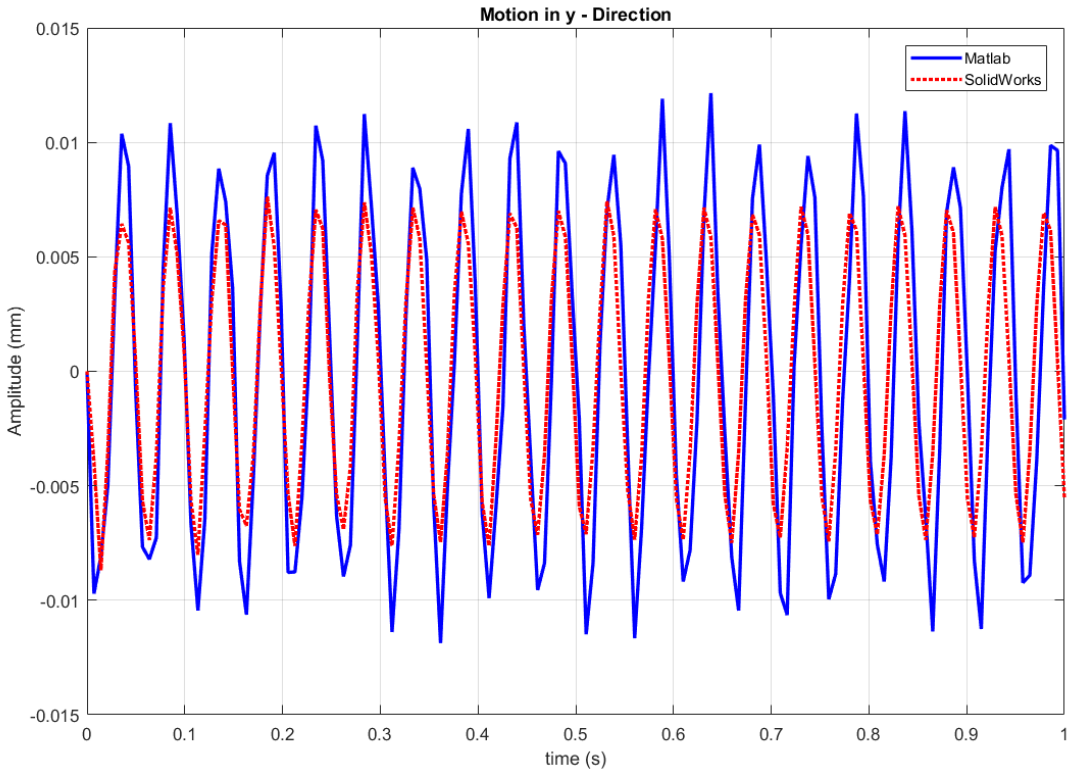


**Figure 6-72: Motion of point 3 in y-direction, 20Hz (Center- Traversing)**

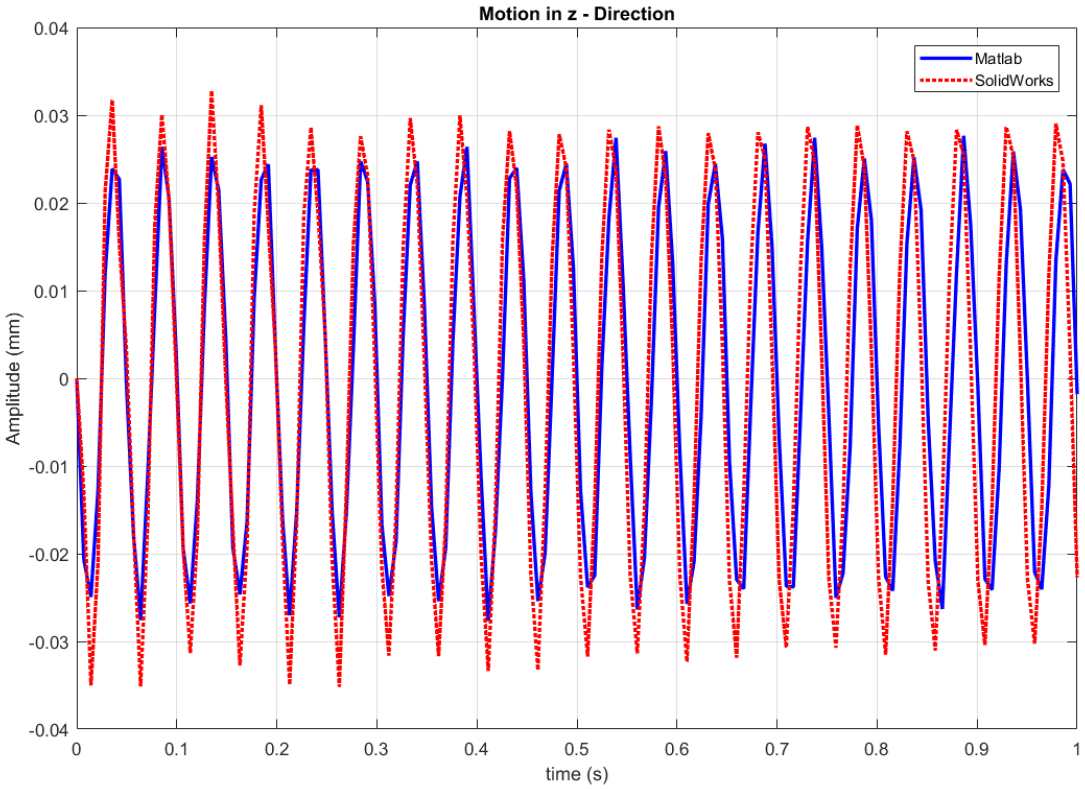


**Figure 6-73: Motion of point 3 in z-direction, 20Hz (Center- Traversing)**

# CONCLUSION

A Friction Stir Welding Machine (FSWM) suitable for welding tubes to tube-sheets is designed based on the functional requirement, working parameters, and required robustness. This design was developed by first selecting the proper components that fulfill the required functions. Then performing static and dynamic simulations to ensure that these components are fit to perform their functions with high welding precision (small displacement). The backbone mechanism was later added to lower the static displacement of the spindle in the z-direction for higher spindle precision. This helped decrease the spindle deformation in z-direction when located at the top left position of the machine frame by nearly 20% (from 0.25 mm to 0.18 mm) of its original value while enduring plunging loads.

Four types of analysis studies were conducted. The first one is the static analysis, showing small deformations for both center and top left position. The stress analysis showed that the machine endures von Mises stresses much lower than the yielding strength of the components. The maximum displacement was found at the center position during plunging. Deflection of the structure was more pronounced under plunging loads in the z-direction. Since plunging is a quick process that converts to traversing in matter of seconds, the maximum deformations will only last for a short time.

Fatigue analysis displayed that the machine has infinite life under full cyclic loads with values fed from static analysis. Since the considered von Mises stresses are far from the yielding strength, the machine will operate safely under fully inverted cyclic loads.

The resonant frequencies and corresponding mode shapes were shown through the frequency analysis. It was noticed that when the spindle is located at the center of the machine frame, it will resonate at a lower frequency compared to when located at the top left position. It can be noted that the machine will start resonating at nearly 47 Hz, at that position. The screws and the backbone mechanism are susceptible to bending and are the main reason of the lowest resonance frequencies. Raising the stiffness of the screws and backbone shafts can shift the minimum resonant frequency but at the expense of its weight.

Dynamic analysis was last conducted to examine the dynamic response of the machine in relation with imposed loads. The frequency-amplitude plots showed that it is advisable to work at a frequency less than 40 Hz; the overall displacement in this case while working in the preferred range was seen to be below 0.23 mm, thus avoiding high cyclic amplitude (displacement) of the different parts of the machine structure. As for the time-amplitude plots, it was clear that the highest amplitudes were at the plunging process in the z-direction, for both spindle positions (top left and center of the machine frame). Two frequencies were accounted for, namely; 3.33 Hz and 20 Hz since most metals are welded at speeds between 200-1200 rpm. Furthermore, operating at 20 Hz had slightly higher transient amplitudes than the 3.33 Hz, due to overshoot.

Motion at three different points on the machine structure was analyzed in the x, y, and z-directions using both MATLAB and SOLIDWORKS' FEA at 3.33 Hz and 20 Hz forced frequencies using traverse loading. The displacements agreed very well for most cases. It was realized that the output response is the closest at the reference point of the generalized coordinates, and at lower frequencies.

In conclusion, the overall results from both static and dynamic analysis show that the machine has high stiffness and that the spindle will be precise if operated at

loads below the maximum (for plunging and traversing) and at a frequency less than 40 Hz. The most severe case in these studies, which happens while the spindle tool is plunging, is of considerably low value and can even be further lowered by enhancing the backbone mechanism. However, enhancement is not necessary because the plunging process is a quick process that turns to traverse process in a matter of seconds. The operating frequencies of the machine ensures that any metal can be welded, since the range provide rotational speeds higher than needed.

Further recommendations for future work:

- Construction of FSWM prototype using the proposed parts and material
- Comparing the linear modules equations of motion provided in control strategy (chapter 4), with experimental testing
- Provide a detailed electrical and hydraulic schematic for the FSWM
- Motion of the prototype's spindle should be compared to that provided from SOLIDWORKS and MATLAB
- Adding a mechanism to the design enabling the tool to move in a fourth axis for providing tilt angles
- Studying the ability to add a calibration tool to position the machine correctly with the workpiece

# APPENDIX A

# ELEMENT VALUES OF MASS, DAMPING, AND STIFFNESS

The non-zero elements of the mass are:

$$M_{0101} = M_A \qquad M_{1313} = I_{xA}$$
$$M_{0202} = M_B \qquad M_{1414} = I_{xB}$$
$$M_{0303} = M_C \qquad M_{1515} = I_{xC}$$
$$M_{0404} = M_D \qquad M_{1616} = I_{xD}$$
$$M_{0505} = M_A \qquad M_{1717} = I_{yA}$$
$$M_{0606} = M_B \qquad M_{1818} = I_{yB}$$
$$M_{0707} = M_C \qquad M_{1919} = I_{yC}$$
$$M_{0808} = M_D \qquad M_{2020} = I_{yD}$$
$$M_{0909} = M_A \qquad M_{2121} = I_{zA}$$
$$M_{1010} = M_B \qquad M_{2222} = I_{zB}$$
$$M_{1111} = M_C \qquad M_{2323} = I_{zC}$$
$$M_{1212} = M_D \qquad M_{2424} = I_{zD}$$

The non-zero elements of the dissipation matrix are:

$$C_{0101} = (C_{A1x} + C_{A2x} + C_{A3x} + C_{A4x})$$
$$C_{0201} = -(C_{A1x} + C_{A2x} + C_{A3x} + C_{A4x})$$
$$C_{0202} = (C_{A1x} + C_{A2x} + C_{A3x} + C_{A4x} + C_{B1x} + C_{B2x} + C_{B3x} + C_{B4x})$$
$$C_{0302} = -(C_{B1x} + C_{B2x} + C_{B3x} + C_{B4x})$$
$$C_{0303} = (C_{B1x} + C_{B2x} + C_{B3x} + C_{B4x} + C_{C1x} + C_{C2x} + C_{C3x} + C_{C4x} + C_{C5x} + C_{C6x} + C_{C7x} + C_{C8x})$$
$$C_{0403} = -(C_{C1x} + C_{C2x} + C_{C3x} + C_{C4x} + C_{C5x} + C_{C6x} + C_{C7x} + C_{C8x})$$
$$C_{0404} = (C_{C1x} + C_{C2x} + C_{C3x} + C_{C4x} + C_{C5x} + C_{C6x} + C_{C7x} + C_{C8x} + C_{D1x} + C_{D2x} + C_{D3x} + C_{D4x})$$
$$C_{0505} = (C_{A1y} + C_{A2y} + C_{A3y} + C_{A4y})$$
$$C_{0605} = -(C_{A1y} + C_{A2y} + C_{A3y} + C_{A4y})$$
$$C_{0606} = (C_{A1y} + C_{A2y} + C_{A3y} + C_{A4y} + C_{B1y} + C_{B2y} + C_{B3y} + C_{B4y})$$

$$C_{0706} = -(C_{B1y} + C_{B2y} + C_{B3y} + C_{B4y})$$

$$C_{0707} = (C_{B1y} + C_{B2y} + C_{B3y} + C_{B4y} + C_{C1y} + C_{C2y} + C_{C3y} + C_{C4y} + C_{C5y} + C_{C6y} + C_{C7y} + C_{C8y})$$

$$C_{0807} = -(C_{C1y} + C_{C2y} + C_{C3y} + C_{C4y} + C_{C5y} + C_{C6y} + C_{C7y} + C_{C8y})$$

$$C_{0808} = (C_{C1y} + C_{C2y} + C_{C3y} + C_{C4y} + C_{C5y} + C_{C6y} + C_{C7y} + C_{C8y} + C_{D1y} + C_{D2y} + C_{D3y} + C_{D4y})$$

$$C_{0909} = (C_{A1z} + C_{A2z} + C_{A3z} + C_{A4z})$$

$$C_{1009} = -(C_{A1z} + C_{A2z} + C_{A3z} + C_{A4z})$$

$$C_{1010} = (C_{A1z} + C_{A2z} + C_{A3z} + C_{A4z} + C_{B1z} + C_{B2z} + C_{B3z} + C_{B4z})$$

$$C_{1110} = -(C_{B1z} + C_{B2z} + C_{B3z} + C_{B4z})$$

$$C_{1111} = (C_{B1z} + C_{B2z} + C_{B3z} + C_{B4z} + C_{C1z} + C_{C2z} + C_{C3z} + C_{C4z} + C_{C5z} + C_{C6z} + C_{C7z} + C_{C8z})$$

$$C_{1211} = -(C_{C1z} + C_{C2z} + C_{C3z} + C_{C4z} + C_{C5z} + C_{C6z} + C_{C7z} + C_{C8z})$$

$$C_{1212} = (C_{C1z} + C_{C2z} + C_{C3z} + C_{C4z} + C_{C5z} + C_{C6z} + C_{C7z} + C_{C8z} + C_{D1z} + C_{D2z} + C_{D3z} + C_{D4z})$$

$$C_{1305} = \frac{1}{2} L_{z4} \left(-C_{A1y} + C_{A2y} + C_{A3y} - C_{A4y}\right)$$

$$C_{1306} = \frac{1}{2} L_{z4} (C_{A1y} - C_{A2y} - C_{A3y} + C_{A4y})$$

$$C_{1309} = -(\frac{1}{2} L_{y2} + \frac{1}{2} L_{y3})(C_{A1z} + C_{A2z} + C_{A3z} + C_{A4z})$$

$$C_{1310} = (\frac{1}{2} L_{y2} + \frac{1}{2} L_{y3})(C_{A1z} + C_{A2z} + C_{A3z} + C_{A4z})$$

$$C_{1313} = \frac{1}{4} L_{z4}^2 (C_{A1y} + C_{A2y} + C_{A3y} + C_{A4y}) + (\frac{1}{2} L_{y2} + \frac{1}{2} L_{y3})^2 (C_{A1z} + C_{A2z} + C_{A3z} + C_{A4z})$$

$$C_{1405} = \frac{1}{2} L_{z4} (C_{A1y} - C_{A2y} - C_{A3y} + C_{A4y})$$

$$C_{1406} = \frac{1}{2} L_{z4} (-C_{A1y} + C_{A2y} + C_{A3y} - C_{A4y}) + \frac{1}{2} L_{z6} (-C_{B1y} + C_{B2y} + C_{B3y} - C_{B4y})$$

$$C_{1407} = \frac{1}{2} L_{z6} (-C_{B1y} + C_{B2y} + C_{B3y} - C_{B4y})$$

$$C_{1409} = -L_{y8} (C_{A1z} + C_{A2z} + C_{A3z} + C_{A4z})$$

$$C_{1410} = L_{y8} (C_{A1z} + C_{A2z} + C_{A3z} + C_{A4z}) - L_{y9} (C_{B1z} + C_{B2z} + C_{B3z} + C_{B4z})$$

$$C_{1411} = L_{y9} (C_{B1z} + C_{B2z} + C_{B3z} + C_{B4z})$$

$$C_{1413} = \frac{1}{4} L_{z4}^2 (-C_{A1y} - C_{A2y} - C_{A3y} - C_{A4y}) + (\frac{1}{2} L_{y2} L_{y8})(C_{A1z} + C_{A2z} + C_{A3z} + C_{A4z})$$

$$+(\frac{1}{2} L_{y3} L_{y8})(C_{A1z} + C_{A2z} + C_{A3z} + C_{A4z})$$

$$C_{1414} = \frac{1}{4} L_{z4}^2 (C_{A1y} + C_{A2y} + C_{A3y} + C_{A4y}) + \frac{1}{4} L_{z6}^2 (C_{B1y} + C_{B2y} + C_{B3y} + C_{B4y})$$

$$+L_{y8}^2 (C_{A1z} + C_{A2z} + C_{A3z} + C_{A4z}) + L_{y9}^2 (C_{B1z} + C_{B2z} + C_{B3z} + C_{B4z})$$

$$C_{1510} = -(C_{B1z} + C_{B2z} + C_{B3z} + C_{B4z})$$

$$C_{1511} = (C_{B1z} + C_{B2z} + C_{B3z} + C_{B4z} + C_{C1z} + C_{C2z} + C_{C3z} + C_{C4z} + C_{C5z} + C_{C6z} + C_{C7z} + C_{C8z})$$

$$C_{1512} = -(C_{C1z} + C_{C2z} + C_{C3z} + C_{C4z} + C_{C5z} + C_{C6z} + C_{C7z} + C_{C8z})$$

$$C_{1514} = L_{y9}(C_{B1z} + C_{B2z} + C_{B3z} + C_{B4z})$$

$$C_{1515} = \frac{1}{2}L_{y7}(C_{C1z} + C_{C2z} - C_{C3z} - C_{C4z} + C_{C5z} + C_{C6z} - C_{C7z} - C_{C8z}) + L_{y10}(C_{B1z} + C_{B2z} + C_{B3z} + C_{B4z})$$

$$C_{1607} = -L_{z9}(C_{C1y} + C_{C2y} + C_{C3y} + C_{C4y} + C_{C5y} + C_{C6y} + C_{C7y} + C_{C8y})$$

$$C_{1608} = L_{z9}(C_{C1y} + C_{C2y} + C_{C3y} + C_{C4y} + C_{C5y} + C_{C6y} + C_{C7y} + C_{C8y}) - \frac{1}{2}L_{z10}(C_{D1y} - C_{D2y} - C_{D3y} + C_{D4y})$$

$$C_{1611} = -L_{y11}(C_{C3z} + C_{C4z} + C_{C7z} + C_{C8z}) - L_{y12}(C_{C1z} + C_{C2z} + C_{C5z} + C_{C6z})$$

$$C_{1612} = L_{y11}(C_{C3z} + C_{C4z} + C_{C7z} + C_{C8z}) + L_{y12}(C_{C1z} + C_{C2z} + C_{C5z} + C_{C6z})$$

$$C_{1615} = -L_{z9}L_{z7}(C_{C1y} + C_{C2y} + C_{C3y} + C_{C4y} + C_{C5y} + C_{C6y} + C_{C7y} + C_{C8y}) + \frac{1}{2}L_{y7}L_{y11}(C_{C3z} + C_{C4z} + C_{C7z} + C_{C8z})$$

$$-\frac{1}{2}L_{y7}L_{y12}(C_{C1z} + C_{C2z} + C_{C5z} + C_{C6z})$$

$$C_{1616} = L_{y11}^2(C_{C3z} + C_{C4z} + C_{C7z} + C_{C8z}) + L_{y12}^2(C_{C1z} + C_{C2z} + C_{C5z} + C_{C6z}) + \frac{1}{4}L_{z10}^2(C_{D1y} + C_{D2y} + C_{D3y} + C_{D4y})$$

$$+L_{z9}^2(C_{C1y} + C_{C2y} + C_{C3y} + C_{C4y} + C_{C5y} + C_{C6y} + C_{C7y} + C_{C8y})$$

$$C_{1701} = \frac{1}{2}L_{z4}(-C_{A1x} + C_{A2x} + C_{A3x} - C_{A4x})$$

$$C_{1702} = \frac{1}{2}L_{z4}(C_{A1x} - C_{A2x} - C_{A3x} + C_{A4x})$$

$$C_{1709} = \frac{1}{2}L_{x2}(-C_{A1z} - C_{A2z} + C_{A3z} + C_{A4z})$$

$$C_{1710} = -\frac{1}{2}L_{x2}(-C_{A1z} - C_{A2z} + C_{A3z} + C_{A4z})$$

$$C_{1713} = \frac{1}{2}L_{x2}(\frac{1}{2}L_{y2} + \frac{1}{2}L_{y3})(C_{A1z} + C_{A2z} - C_{A3z} - C_{A4z})$$

$$C_{1714} = \frac{1}{2}L_{x2}L_{y8}(C_{A1z} + C_{A2z} - C_{A3z} - C_{A4z})$$

$$C_{1717} = \frac{1}{4}L_{x2}^2(C_{A1z} + C_{A2z} + C_{A3z} + C_{A4z}) + \frac{1}{4}L_{z4}^2(C_{A1x} + C_{A2x} + C_{A3x} + C_{A4x})$$

$$C_{1801} = \frac{1}{2}L_{z4}(C_{A1x} - C_{A2x} - C_{A3x} + C_{A4x})$$

$$C_{1802} = -\frac{1}{2}L_{z4}(C_{A1x} - C_{A2x} - C_{A3x} + C_{A4x}) - \frac{1}{2}L_{z6}(C_{B1x} - C_{B2x} - C_{B3x} + C_{B4x})$$

$$C_{1803} = \frac{1}{2}L_{z6}(C_{B1x} - C_{B2x} - C_{B3x} + C_{B4x})$$

$$C_{1809} = \frac{1}{2}L_{x2}(C_{A1z} + C_{A2z} - C_{A3z} - C_{A4z}) + L_{x3}(C_{A1z} + C_{A2z} + C_{A3z} + C_{A4z})$$

$$C_{1810} = \frac{1}{2}L_{x2}(-C_{A1z} - C_{A2z} + C_{A3z} + C_{A4z}) - L_{x3}(C_{A1z} + C_{A2z} + C_{A3z} + C_{A4z}) - \frac{1}{2}L_{x4}(C_{B1z} + C_{B2z} - C_{B3z} - C_{B4z})$$

$$C_{1811} = \frac{1}{2}L_{x4}(C_{B1z} + C_{B2z} - C_{B3z} - C_{B4z})$$

$$C_{1813} = -\frac{1}{2}(L_{x3}L_{y2} + L_{x3}L_{y3})(C_{A1z} + C_{A2z} + C_{A3z} + C_{A4z}) - \frac{1}{4}(L_{x2}L_{y2} + L_{x2}L_{y3})(C_{A1z} + C_{A2z} - C_{A3z} - C_{A4z})$$

$$C_{1814} = -\frac{1}{2}L_{x2}L_{y8}(C_{A1z} + C_{A2z} - C_{A3z} - C_{A4z}) - L_{x3}L_{y8}(C_{A1z} + C_{A2z} + C_{A3z} + C_{A4z}) - \frac{1}{2}L_{x4}L_{y9}(-C_{B1z} - C_{B2z} + C_{B3z} + C_{B4z})$$

$$C_{1815} = \frac{1}{2}L_{x4}L_{y10}(C_{B1z} + C_{B2z} - C_{B3z} - C_{B4z})$$

$$C_{1817} = -\frac{1}{4}L_{z4}^2(C_{A1x} + C_{A2x} + C_{A3x} + C_{A4x}) - \frac{1}{4}L_{x2}^2(C_{A1z} + C_{A2z} + C_{A3z} + C_{A4z}) - \frac{1}{2}L_{x2}L_{x3}(C_{A1z} + C_{A2z} - C_{A3z} - C_{A4z})$$

$$C_{1818} = \frac{1}{4}L_{z4}^2(C_{A1x} + C_{A2x} + C_{A3x} + C_{A4x}) + \frac{1}{4}L_{x2}^2(C_{A1z} + C_{A2z} + C_{A3z} + C_{A4z}) + L_{x3}^2(C_{A1z} + C_{A2z} + C_{A3z} + C_{A4z})$$

$$+L_{x2}L_{x3}(C_{A1z} + C_{A2z} - C_{A3z} - C_{A4z}) + \frac{1}{4}L_{z6}^2(C_{B1x} + C_{B2x} + C_{B3x} + C_{B4x}) + \frac{1}{4}L_{x4}^2(C_{B1z} + C_{B2z} + C_{B3z} + C_{B4z})$$

$$C_{1902} = \frac{1}{2}L_{z6}(C_{B1x} - C_{B2x} - C_{B3x} + C_{B4x})$$

$$C_{1903} = \frac{1}{2}L_{z6}(-C_{B1x} + C_{B2x} + C_{B3x} - C_{B4x}) + L_{z7}(C_{C1x} + C_{C2x} + C_{C3x} + C_{C4x} + C_{C5x} + C_{C6x} + C_{C7x} + C_{C8x})$$

$$C_{1904} = -L_{z7}(C_{C1x} + C_{C2x} + C_{C3x} + C_{C4x} + C_{C5x} + C_{C6x} + C_{C7x} + C_{C8x})$$

$$C_{1910} = \frac{1}{2}L_{x4}(C_{B1z} + C_{B2z} - C_{B3z} - C_{B4z})$$

$$C_{1911} = -\frac{1}{2}L_{x4}(C_{B1z} + C_{B2z} - C_{B3z} - C_{B4z}) - \frac{1}{2}L_{x6}(C_{C1z} + C_{C4z} - C_{C6z} - C_{C7z}) - \frac{1}{2}L_{x5}(C_{C2z} + C_{C3z} - C_{C5z} - C_{C8z})$$

$$C_{1912} = \frac{1}{2}L_{x6}(C_{C1z} + C_{C4z} - C_{C6z} - C_{C7z}) + \frac{1}{2}L_{x5}(C_{C2z} + C_{C3z} - C_{C5z} - C_{C8z})$$

$$C_{1914} = \frac{1}{2}L_{x4}L_{y9}(-C_{B1z} - C_{B2z} + C_{B3z} + C_{B4z})$$

$$C_{1915} = -\frac{1}{2}L_{x4}L_{y10}(C_{B1z} + C_{B2z} - C_{B3z} - C_{B4z}) - \frac{1}{4}L_{x6}L_{y7}(C_{C1z} - C_{C4z} - C_{C6z} + C_{C7z}) - \frac{1}{4}L_{x5}L_{y7}(C_{C2z} - C_{C3z} - C_{C5z} + C_{C8z})$$

$$C_{1916} = \frac{1}{2}L_{x6}L_{y12}(C_{C1z} - C_{C6z}) + \frac{1}{2}L_{x5}L_{y12}(C_{C2z} - C_{C5z}) + \frac{1}{2}L_{x5}L_{y11}(C_{C3z} - C_{C8z}) + \frac{1}{2}L_{x6}L_{y11}(C_{C4z} - C_{C7z})$$

$$C_{1918} = -\frac{1}{4}L_{z6}^2(C_{B1x} + C_{B2x} + C_{B3x} + C_{B4x}) - \frac{1}{4}L_{x4}^2(C_{B1z} + C_{B2z} + C_{B3z} + C_{B4z})$$

$$C_{1919} = \frac{1}{4}L_{z6}^2(C_{B1x} + C_{B2x} + C_{B3x} + C_{B4x}) + \frac{1}{4}L_{x4}^2(C_{B1z} + C_{B2z} + C_{B3z} + C_{B4z}) + \frac{1}{4}L_{x6}^2(C_{C1z} + C_{C4z} + C_{C6z} + C_{C7z})$$

$$+\frac{1}{4}L_{x5}^2(C_{C2z} + C_{C3z} + C_{C5z} + C_{C8z}) + L_{z7}^2(C_{C1x} + C_{C2x} + C_{C3x} + C_{C4x} + C_{C5x} + C_{C6x} + C_{C7x} + C_{C8x})$$

$$C_{2003} = -L_{z9}(C_{C1x} + C_{C2x} + C_{C3x} + C_{C4x} + C_{C5x} + C_{C6x} + C_{C7x} + C_{C8x})$$

$$C_{2004} = L_{z9}(C_{C1x} + C_{C2x} + C_{C3x} + C_{C4x} + C_{C5x} + C_{C6x} + C_{C7x} + C_{C8x}) + \frac{1}{2}L_{z10}(-C_{D1x} + C_{D2x} + C_{D3x} - C_{D4x})$$

$$C_{2011} = L_{x8}(C_{C1z} + C_{C4z} - C_{C6z} - C_{C7z}) + L_{x9}(C_{C2z} + C_{C3z} - C_{C5z} - C_{C8z})$$

$$C_{2012} = -L_{x8}(C_{C1z} + C_{C4z} - C_{C6z} - C_{C7z}) - L_{x9}(C_{C2z} + C_{C3z} - C_{C5z} - C_{C8z}) - \frac{1}{2}L_{x7}(C_{D1z} + C_{D2z} - C_{D3z} - C_{D4z})$$

$$C_{2015} = \frac{1}{2}L_{x8}L_{y7}(C_{C1z} - C_{C4z} - C_{C6z} + C_{C7z}) + \frac{1}{2}L_{x9}L_{y7}(C_{C2z} - C_{C3z} - C_{C5z} + C_{C8z})$$

$$C_{2016} = -L_{x8}L_{y12}(C_{C1z} - C_{C6z}) - L_{x9}L_{y11}(C_{C3z} - C_{C8z}) - L_{x8}L_{y11}(C_{C4z} - C_{C7z}) - L_{x9}L_{y12}(C_{C2z} - C_{C5z})$$

$$C_{2019} = -L_{z9}L_{z7}(C_{C1x} + C_{C2x} + C_{C3x} + C_{C4x} + C_{C5x} + C_{C6x} + C_{C7x} + C_{C8x})$$

$$-\frac{1}{2}L_{x6}L_{x8}(C_{C1z} + C_{C4z} + C_{C6z} + C_{C7z}) - \frac{1}{2}L_{x5}L_{x9}(C_{C2z} + C_{C3z} + C_{C5z} + C_{C8z})$$

$$C_{2020} = L_{x8}^2(C_{C1z} + C_{C4z} + C_{C6z} + C_{C7z}) + L_{x9}^2(C_{C2z} + C_{C3z} + C_{C5z} + C_{C8z})$$

$$+L_{z9}^2(C_{C1x} + C_{C2x} + C_{C3x} + C_{C4x} + C_{C5x} + C_{C6x} + C_{C7x} + C_{C8x})$$

$$+\frac{1}{4}L_{z10}^2(C_{D1x} + C_{D2x} + C_{D3x} + C_{D4x}) + \frac{1}{4}L_{x7}^2(C_{D1z} + C_{D2z} + C_{D3z} + C_{D4z})$$

$$C_{2105} = \frac{1}{2} L_{x2}(C_{A1y} + C_{A2y} - C_{A3y} - C_{A4y})$$

$$C_{2106} = -\frac{1}{2} L_{x2}(C_{A1y} + C_{A2y} - C_{A3y} - C_{A4y})$$

$$C_{2113} = -\frac{1}{4} L_{x2} L_{z4}(C_{A1y} - C_{A2y} + C_{A3y} - C_{A4y})$$

$$C_{2114} = \frac{1}{4} L_{x2} L_{z4}(C_{A1y} - C_{A2y} + C_{A3y} - C_{A4y})$$

$$C_{2121} = \frac{1}{4} L_{x2}^2(C_{A1y} + C_{A2y} + C_{A3y} + C_{A4y})$$

$$C_{2205} = -\frac{1}{2} L_{x2}(C_{A1y} + C_{A2y} - C_{A3y} - C_{A4y}) - L_{x3}(C_{A1y} + C_{A2y} + C_{A3y} + C_{A4y})$$

$$C_{2206} = \frac{1}{2} L_{x2}(C_{A1y} + C_{A2y} - C_{A3y} - C_{A4y}) + L_{x3}(C_{A1y} + C_{A2y} + C_{A3y} + C_{A4y}) + \frac{1}{2} L_{x4}(C_{B1y} + C_{B2y} - C_{B3y} - C_{B4y})$$

$$C_{2207} = -\frac{1}{2} L_{x4}(C_{B1y} + C_{B2y} - C_{B3y} - C_{B4y})$$

$$C_{2213} = \frac{1}{4} L_{x2} L_{z4}(C_{A1y} - C_{A2y} + C_{A3y} - C_{A4y}) + \frac{1}{2} L_{x3} L_{z4}(C_{A1y} - C_{A2y} - C_{A3y} + C_{A4y})$$

$$C_{2214} = -\frac{1}{4} L_{z6} L_{x4}(C_{B1y} - C_{B2y} + C_{B3y} - C_{B4y}) - \frac{1}{4} L_{x2} L_{z4}(C_{A1y} - C_{A2y} + C_{A3y} - C_{A4y}) - \frac{1}{2} L_{x3} L_{z4}(C_{A1y} - C_{A2y} - C_{A3y} + C_{A4y})$$

$$C_{2215} = \frac{1}{4} L_{z6} L_{x4}(C_{B1y} - C_{B2y} + C_{B3y} - C_{B4y})$$

$$C_{2221} = -\frac{1}{4} L_{x2}^2(C_{A1y} + C_{A2y} + C_{A3y} + C_{A4y}) - \frac{1}{2} L_{x2} L_{x3}(C_{A1y} + C_{A2y} - C_{A3y} - C_{A4y})$$

$$C_{2222} = \frac{1}{4} L_{x2}^2(C_{A1y} + C_{A2y} + C_{A3y} + C_{A4y}) + L_{x3}^2(C_{A1y} + C_{A2y} + C_{A3y} + C_{A4y}) + L_{x2} L_{x3}(C_{A1y} + C_{A2y} - C_{A3y} - C_{A4y})$$
$$+ \frac{1}{4} L_{x4}^2(C_{B1z} + C_{B2z} + C_{B3z} + C_{B4z})$$

$$C_{2303} = \frac{1}{2} L_{y7}(C_{C1x} + C_{C2x} - C_{C3x} - C_{C4x} + C_{C5x} + C_{C6x} - C_{C7x} - C_{C8x})$$

$$C_{2304} = -\frac{1}{2} L_{y7}(C_{C1x} + C_{C2x} - C_{C3x} - C_{C4x} + C_{C5x} + C_{C6x} - C_{C7x} - C_{C8x})$$

$$C_{2306} = \frac{1}{2} L_{x4}(-C_{B1y} - C_{B2y} + C_{B3y} + C_{B4y})$$

$$C_{2307} = -\frac{1}{2} L_{x4}(-C_{B1y} - C_{B2y} + C_{B3y} + C_{B4y}) - \frac{1}{2} L_{x5}(-C_{C2y} - C_{C3y} + C_{C5y} + C_{C8y}) - \frac{1}{2} L_{x6}(-C_{C1y} - C_{C4y} + C_{C6y} + C_{C7y})$$

$$C_{2308} = \frac{1}{2} L_{x5}(-C_{C2y} - C_{C3y} + C_{C5y} + C_{C8y}) + \frac{1}{2} L_{x6}(-C_{C1y} - C_{C4y} + C_{C6y} + C_{C7y})$$

$$C_{2314} = \frac{1}{4} L_{z6} L_{x4}(C_{B1y} - C_{B2y} + C_{B3y} - C_{B4y})$$

$$C_{2315} = -\frac{1}{4} L_{z6} L_{x4}(C_{B1y} - C_{B2y} + C_{B3y} - C_{B4y}) - \frac{1}{2} L_{x6} L_{y7}(-C_{C1y} - C_{C4y} + C_{C6y} + C_{C7y}) - \frac{1}{2} L_{x5} L_{y7}(-C_{C2y} - C_{C3y} + C_{C5y} + C_{C8y})$$

$$C_{2316} = \frac{1}{2} L_{x6} L_{z9}(-C_{C1y} - C_{C4y} + C_{C6y} + C_{C7y}) + \frac{1}{2} L_{x5} L_{z9}(-C_{C2y} - C_{C3y} + C_{C5y} + C_{C8y})$$

$$C_{2319} = -\frac{1}{2} L_{y7} L_{z7}(-C_{C1x} - C_{C2x} + C_{C3x} + C_{C4x} - C_{C5x} - C_{C6x} + C_{C7x} + C_{C8x})$$

$$C_{2320} = \frac{1}{2} L_{y7} L_{z9}(-C_{C1x} - C_{C2x} + C_{C3x} + C_{C4x} - C_{C5x} - C_{C6x} + C_{C7x} + C_{C8x})$$

$$C_{2322} = -\frac{1}{4} L_{x4}^2(C_{B1y} + C_{B2y} + C_{B3y} + C_{B4y})$$

$$C_{2323} = \frac{1}{4}L_{x4}^2(C_{B1y} + C_{B2y} + C_{B3y} + C_{B4y}) + \frac{1}{4}L_{x5}^2(C_{C2y} + C_{C3y} + C_{C5y} + C_{C8y}) + \frac{1}{4}L_{x6}^2(C_{C1y} + C_{C4y} + C_{C6y} + C_{C7y})$$
$$+\frac{1}{4}L_{y7}^2(C_{C1x} + C_{C2x} + C_{C3x} + C_{C4x} + C_{C5x} + C_{C6x} + C_{C7x} + C_{C8x})$$
$$C_{2403} = -L_{y11}(C_{C3x} + C_{C4x} + C_{C7x} + C_{C8x}) - L_{y12}(C_{C1x} + C_{C2x} + C_{C5x} + C_{C6x})$$
$$C_{2404} = L_{y11}(C_{C3x} + C_{C4x} + C_{C7x} + C_{C8x}) + L_{y12}(C_{C1x} + C_{C2x} + C_{C5x} + C_{C6x})$$
$$C_{2407} = L_{x8}(-C_{C1y} - C_{C4y} + C_{C6y} + C_{C7y}) + L_{x9}(-C_{C2y} - C_{C3y} + C_{C5y} + C_{C8y})$$
$$C_{2408} = \frac{1}{2}L_{x7}(C_{D1y} + C_{D2y} - C_{D3y} - C_{D4y}) - L_{x8}(-C_{C1y} - C_{C4y} + C_{C6y} + C_{C7y}) - L_{x9}(-C_{C2y} - C_{C3y} + C_{C5y} + C_{C8y})$$
$$C_{2415} = L_{x8}L_{z7}(-C_{C1y} - C_{C4y} + C_{C6y} + C_{C7y}) + L_{x9}L_{z7}(-C_{C2y} - C_{C3y} + C_{C5y} + C_{C8y})$$
$$C_{2416} = -\frac{1}{4}L_{x7}L_{z10}(C_{D1y} - C_{D2y} + C_{D3y} - C_{D4y}) - L_{x8}L_{z9}(-C_{C1y} - C_{C4y} + C_{C6y} + C_{C7y}) - L_{x9}L_{z9}(-C_{C2y} - C_{C3y} + C_{C5y} + C_{C8y})$$
$$C_{2419} = -L_{y11}L_{z7}(C_{C3x} + C_{C4x} + C_{C7x} + C_{C8x}) - L_{y12}L_{z7}(C_{C1x} + C_{C2x} + C_{C5x} + C_{C6x})$$
$$C_{2420} = L_{y11}L_{z9}(C_{C3x} + C_{C4x} + C_{C7x} + C_{C8x}) + L_{y12}L_{z9}(C_{C1x} + C_{C2x} + C_{C5x} + C_{C6x})$$
$$C_{2423} = -\frac{1}{2}L_{x6}L_{x8}(C_{C1y} + C_{C4y} + C_{C6y} + C_{C7y}) - \frac{1}{2}L_{x5}L_{x9}(C_{C2y} + C_{C3y} + C_{C5y} + C_{C8y}) - \frac{1}{2}L_{y12}L_{y7}(C_{C1x} + C_{C2x} + C_{C5x} + C_{C6x})$$
$$+\frac{1}{2}L_{y11}L_{y7}(C_{C3x} + C_{C4x} + C_{C7x} + C_{C8x})$$
$$C_{2424} = L_{x8}^2(C_{C1y} + C_{C4y} + C_{C6y} + C_{C7y}) + L_{x9}^2(C_{C2y} + C_{C3y} + C_{C5y} + C_{C8y}) + L_{y11}^2(C_{C3x} + C_{C4x} + C_{C7x} + C_{C8x})$$
$$+L_{y12}^2(C_{C1x} + C_{C2x} + C_{C5x} + C_{C6x}) + \frac{1}{4}L_{x7}^2(C_{D1y} + C_{D2y} + C_{D3y} + C_{D4y})$$

The non-zeros elements of the lower part of the stiffness matrix are:

$$k_{0101} = (k_{A1x} + k_{A2x} + k_{A3x} + k_{A4x})$$
$$k_{0201} = -(k_{A1x} + k_{A2x} + k_{A3x} + k_{A4x})$$
$$k_{0202} = (k_{A1x} + k_{A2x} + k_{A3x} + k_{A4x} + k_{B1x} + k_{B2x} + k_{B3x} + k_{B4x})$$
$$k_{0302} = -(k_{B1x} + k_{B2x} + k_{B3x} + k_{B4x})$$
$$k_{0303} = (k_{B1x} + k_{B2x} + k_{B3x} + k_{B4x} + k_{C1x} + k_{C2x} + k_{C3x} + k_{C4x} + k_{C5x} + k_{C6x} + k_{C7x} + k_{C8x})$$
$$k_{0403} = -(k_{C1x} + k_{C2x} + k_{C3x} + k_{C4x} + k_{C5x} + k_{C6x} + k_{C7x} + k_{C8x})$$
$$k_{0404} = (k_{C1x} + k_{C2x} + k_{C3x} + k_{C4x} + k_{C5x} + k_{C6x} + k_{C7x} + k_{C8x} + k_{D1x} + k_{D2x} + k_{D3x} + k_{D4x})$$
$$k_{0505} = (k_{A1y} + k_{A2y} + k_{A3y} + k_{A4y})$$
$$k_{0605} = -(k_{A1y} + k_{A2y} + k_{A3y} + k_{A4y})$$
$$k_{0606} = (k_{A1y} + k_{A2y} + k_{A3y} + k_{A4y} + k_{B1y} + k_{B2y} + k_{B3y} + k_{B4y})$$
$$k_{0706} = -(k_{B1y} + k_{B2y} + k_{B3y} + k_{B4y})$$
$$k_{0707} = (k_{B1y} + k_{B2y} + k_{B3y} + k_{B4y} + k_{C1y} + k_{C2y} + k_{C3y} + k_{C4y} + k_{C5y} + k_{C6y} + k_{C7y} + k_{C8y})$$
$$k_{0807} = -(k_{C1y} + k_{C2y} + k_{C3y} + k_{C4y} + k_{C5y} + k_{C6y} + k_{C7y} + k_{C8y})$$
$$k_{0808} = (k_{C1y} + k_{C2y} + k_{C3y} + k_{C4y} + k_{C5y} + k_{C6y} + k_{C7y} + k_{C8y} + k_{D1y} + k_{D2y} + k_{D3y} + k_{D4y})$$
$$k_{0909} = (k_{A1z} + k_{A2z} + k_{A3z} + k_{A4z})$$
$$k_{1009} = -(k_{A1z} + k_{A2z} + k_{A3z} + k_{A4z})$$
$$k_{1010} = (k_{A1z} + k_{A2z} + k_{A3z} + k_{A4z} + k_{B1z} + k_{B2z} + k_{B3z} + k_{B4z})$$
$$k_{1110} = -(k_{B1z} + k_{B2z} + k_{B3z} + k_{B4z})$$
$$k_{1111} = (k_{B1z} + k_{B2z} + k_{B3z} + k_{B4z} + k_{C1z} + k_{C2z} + k_{C3z} + k_{C4z} + k_{C5z} + k_{C6z} + k_{C7z} + k_{C8z})$$
$$k_{1211} = -(k_{C1z} + k_{C2z} + k_{C3z} + k_{C4z} + k_{C5z} + k_{C6z} + k_{C7z} + k_{C8z})$$
$$k_{1212} = (k_{C1z} + k_{C2z} + k_{C3z} + k_{C4z} + k_{C5z} + k_{C6z} + k_{C7z} + k_{C8z} + k_{D1z} + k_{D2z} + k_{D3z} + k_{D4z})$$
$$k_{1305} = \frac{1}{2} L_{z4} \left(-k_{A1y} + k_{A2y} + k_{A3y} - k_{A4y}\right)$$
$$k_{1306} = \frac{1}{2} L_{z4} (k_{A1y} - k_{A2y} - k_{A3y} + k_{A4y})$$
$$k_{1309} = -(\frac{1}{2} L_{y2} + \frac{1}{2} L_{y3})(k_{A1z} + k_{A2z} + k_{A3z} + k_{A4z})$$
$$k_{1310} = (\frac{1}{2} L_{y2} + \frac{1}{2} L_{y3})(k_{A1z} + k_{A2z} + k_{A3z} + k_{A4z})$$
$$k_{1313} = \frac{1}{4} L_{z4}^2 (k_{A1y} + k_{A2y} + k_{A3y} + k_{A4y}) + (\frac{1}{2} L_{y2} + \frac{1}{2} L_{y3})^2 (k_{A1z} + k_{A2z} + k_{A3z} + k_{A4z})$$
$$k_{1405} = \frac{1}{2} L_{z4} (k_{A1y} - k_{A2y} - k_{A3y} + k_{A4y})$$
$$k_{1406} = \frac{1}{2} L_{z4} (-k_{A1y} + k_{A2y} + k_{A3y} - k_{A4y}) + \frac{1}{2} L_{z6} (-k_{B1y} + k_{B2y} + k_{B3y} - k_{B4y})$$

$$k_{1407} = \frac{1}{2} L_{z6}(-k_{B1y} + k_{B2y} + k_{B3y} - k_{B4y})$$

$$k_{1409} = -L_{y8}(k_{A1z} + k_{A2z} + k_{A3z} + k_{A4z})$$

$$k_{1410} = L_{y8}(k_{A1z} + k_{A2z} + k_{A3z} + k_{A4z}) - L_{y9}(k_{B1z} + k_{B2z} + k_{B3z} + k_{B4z})$$

$$k_{1411} = L_{y9}(k_{B1z} + k_{B2z} + k_{B3z} + k_{B4z})$$

$$k_{1413} = \frac{1}{4} L_{z4}^2(-k_{A1y} - k_{A2y} - k_{A3y} - k_{A4y}) + (\frac{1}{2} L_{y2} L_{y8})(k_{A1z} + k_{A2z} + k_{A3z} + k_{A4z}) + (\frac{1}{2} L_{y3} L_{y8})(k_{A1z} + k_{A2z} + k_{A3z} + k_{A4z})$$

$$k_{1414} = \frac{1}{4} L_{z4}^2(k_{A1y} + k_{A2y} + k_{A3y} + k_{A4y}) + \frac{1}{4} L_{z6}^2(k_{B1y} + k_{B2y} + k_{B3y} + k_{B4y}) + L_{y8}^2(k_{A1z} + k_{A2z} + k_{A3z} + k_{A4z})$$
$$+ L_{y9}^2(k_{B1z} + k_{B2z} + k_{B3z} + k_{B4z})$$

$$k_{1510} = -(k_{B1z} + k_{B2z} + k_{B3z} + k_{B4z})$$

$$k_{1511} = (k_{B1z} + k_{B2z} + k_{B3z} + k_{B4z} + k_{C1z} + k_{C2z} + k_{C3z} + k_{C4z} + k_{C5z} + k_{C6z} + k_{C7z} + k_{C8z})$$

$$k_{1512} = -(k_{C1z} + k_{C2z} + k_{C3z} + k_{C4z} + k_{C5z} + k_{C6z} + k_{C7z} + k_{C8z})$$

$$k_{1514} = L_{y9}(k_{B1z} + k_{B2z} + k_{B3z} + k_{B4z})$$

$$k_{1515} = \frac{1}{2} L_{y7}(k_{C1z} + k_{C2z} - k_{C3z} - k_{C4z} + k_{C5z} + k_{C6z} - k_{C7z} - k_{C8z}) + L_{y10}(k_{B1z} + k_{B2z} + k_{B3z} + k_{B4z})$$

$$k_{1607} = -L_{z9}(k_{C1y} + k_{C2y} + k_{C3y} + k_{C4y} + k_{C5y} + k_{C6y} + k_{C7y} + k_{C8y})$$

$$k_{1608} = L_{z9}(k_{C1y} + k_{C2y} + k_{C3y} + k_{C4y} + k_{C5y} + k_{C6y} + k_{C7y} + k_{C8y}) - \frac{1}{2} L_{z10}(k_{D1y} - k_{D2y} - k_{D3y} + k_{D4y})$$

$$k_{1611} = -L_{y11}(k_{C3z} + k_{C4z} + k_{C7z} + k_{C8z}) - L_{y12}(k_{C1z} + k_{C2z} + k_{C5z} + k_{C6z})$$

$$k_{1612} = L_{y11}(k_{C3z} + k_{C4z} + k_{C7z} + k_{C8z}) + L_{y12}(k_{C1z} + k_{C2z} + k_{C5z} + k_{C6z})$$

$$k_{1615} = -L_{z9} L_{z7}(k_{C1y} + k_{C2y} + k_{C3y} + k_{C4y} + k_{C5y} + k_{C6y} + k_{C7y} + k_{C8y}) + \frac{1}{2} L_{y7} L_{y11}(k_{C3z} + k_{C4z} + k_{C7z} + k_{C8z})$$
$$- \frac{1}{2} L_{y7} L_{y12}(k_{C1z} + k_{C2z} + k_{C5z} + k_{C6z})$$

$$k_{1616} = L_{y11}^2(k_{C3z} + k_{C4z} + k_{C7z} + k_{C8z}) + L_{y12}^2(k_{C1z} + k_{C2z} + k_{C5z} + k_{C6z}) + \frac{1}{4} L_{z10}^2(k_{D1y} + k_{D2y} + k_{D3y} + k_{D4y})$$
$$+ L_{z9}^2(k_{C1y} + k_{C2y} + k_{C3y} + k_{C4y} + k_{C5y} + k_{C6y} + k_{C7y} + k_{C8y})$$

$$k_{1701} = \frac{1}{2} L_{z4}(-k_{A1x} + k_{A2x} + k_{A3x} - k_{A4x})$$

$$k_{1702} = \frac{1}{2} L_{z4}(k_{A1x} - k_{A2x} - k_{A3x} + k_{A4x})$$

$$k_{1709} = \frac{1}{2} L_{x2}(-k_{A1z} - k_{A2z} + k_{A3z} + k_{A4z})$$

$$k_{1710} = -\frac{1}{2} L_{x2}(-k_{A1z} - k_{A2z} + k_{A3z} + k_{A4z})$$

$$k_{1713} = \frac{1}{2} L_{x2}(\frac{1}{2} L_{y2} + \frac{1}{2} L_{y3})(k_{A1z} + k_{A2z} - k_{A3z} - k_{A4z})$$

$$k_{1714} = \frac{1}{2} L_{x2} L_{y8} (k_{A1z} + k_{A2z} - k_{A3z} - k_{A4z})$$

$$k_{1717} = \frac{1}{4} L_{x2}^2 (k_{A1z} + k_{A2z} + k_{A3z} + k_{A4z}) + \frac{1}{4} L_{z4}^2 (k_{A1x} + k_{A2x} + k_{A3x} + k_{A4x})$$

$$k_{1801} = \frac{1}{2} L_{z4} (k_{A1x} - k_{A2x} - k_{A3x} + k_{A4x})$$

$$k_{1802} = -\frac{1}{2} L_{z4} (k_{A1x} - k_{A2x} - k_{A3x} + k_{A4x}) - \frac{1}{2} L_{z6} (k_{B1x} - k_{B2x} - k_{B3x} + k_{B4x})$$

$$k_{1803} = \frac{1}{2} L_{z6} (k_{B1x} - k_{B2x} - k_{B3x} + k_{B4x})$$

$$k_{1809} = \frac{1}{2} L_{x2} (k_{A1z} + k_{A2z} - k_{A3z} - k_{A4z}) + L_{x3} (k_{A1z} + k_{A2z} + k_{A3z} + k_{A4z})$$

$$k_{1810} = \frac{1}{2} L_{x2} (-k_{A1z} - k_{A2z} + k_{A3z} + k_{A4z}) - L_{x3} (k_{A1z} + k_{A2z} + k_{A3z} + k_{A4z}) - \frac{1}{2} L_{x4} (k_{B1z} + k_{B2z} - k_{B3z} - k_{B4z})$$

$$k_{1811} = \frac{1}{2} L_{x4} (k_{B1z} + k_{B2z} - k_{B3z} - k_{B4z})$$

$$k_{1813} = -\frac{1}{2} (L_{x3} L_{y2} + L_{x3} L_{y3}) (k_{A1z} + k_{A2z} + k_{A3z} + k_{A4z}) - \frac{1}{4} (L_{x2} L_{y2} + L_{x2} L_{y3}) (k_{A1z} + k_{A2z} - k_{A3z} - k_{A4z})$$

$$k_{1814} = -\frac{1}{2} L_{x2} L_{y8} (k_{A1z} + k_{A2z} - k_{A3z} - k_{A4z}) - L_{x3} L_{y8} (k_{A1z} + k_{A2z} + k_{A3z} + k_{A4z}) - \frac{1}{2} L_{x4} L_{y9} (-k_{B1z} - k_{B2z} + k_{B3z} + k_{B4z})$$

$$k_{1815} = \frac{1}{2} L_{x4} L_{y10} (k_{B1z} + k_{B2z} - k_{B3z} - k_{B4z})$$

$$k_{1817} = -\frac{1}{4} L_{z4}^2 (k_{A1x} + k_{A2x} + k_{A3x} + k_{A4x}) - \frac{1}{4} L_{x2}^2 (k_{A1z} + k_{A2z} + k_{A3z} + k_{A4z}) - \frac{1}{2} L_{x2} L_{x3} (k_{A1z} + k_{A2z} - k_{A3z} - k_{A4z})$$

$$k_{1818} = \frac{1}{4} L_{z4}^2 (k_{A1x} + k_{A2x} + k_{A3x} + k_{A4x}) + \frac{1}{4} L_{x2}^2 (k_{A1z} + k_{A2z} + k_{A3z} + k_{A4z}) + L_{x3}^2 (k_{A1z} + k_{A2z} + k_{A3z} + k_{A4z})$$

$$+ L_{x2} L_{x3} (k_{A1z} + k_{A2z} - k_{A3z} - k_{A4z}) + \frac{1}{4} L_{z6}^2 (k_{B1x} + k_{B2x} + k_{B3x} + k_{B4x}) + \frac{1}{4} L_{x4}^2 (k_{B1z} + k_{B2z} + k_{B3z} + k_{B4z})$$

$$k_{1902} = \frac{1}{2} L_{z6} (k_{B1x} - k_{B2x} - k_{B3x} + k_{B4x})$$

$$k_{1903} = \frac{1}{2} L_{z6} (-k_{B1x} + k_{B2x} + k_{B3x} - k_{B4x}) + L_{z7} (k_{C1x} + k_{C2x} + k_{C3x} + k_{C4x} + k_{C5x} + k_{C6x} + k_{C7x} + k_{C8x})$$

$$k_{1904} = -L_{z7} (k_{C1x} + k_{C2x} + k_{C3x} + k_{C4x} + k_{C5x} + k_{C6x} + k_{C7x} + k_{C8x})$$

$$k_{1910} = \frac{1}{2} L_{x4} (k_{B1z} + k_{B2z} - k_{B3z} - k_{B4z})$$

$$k_{1911} = -\frac{1}{2} L_{x4} (k_{B1z} + k_{B2z} - k_{B3z} - k_{B4z}) - \frac{1}{2} L_{x6} (k_{C1z} + k_{C4z} - k_{C6z} - k_{C7z}) - \frac{1}{2} L_{x5} (k_{C2z} + k_{C3z} - k_{C5z} - k_{C8z})$$

$$k_{1912} = \frac{1}{2} L_{x6} (k_{C1z} + k_{C4z} - k_{C6z} - k_{C7z}) + \frac{1}{2} L_{x5} (k_{C2z} + k_{C3z} - k_{C5z} - k_{C8z})$$

$$k_{1914} = \frac{1}{2} L_{x4} L_{y9} (-k_{B1z} - k_{B2z} + k_{B3z} + k_{B4z})$$

$$k_{1915} = -\frac{1}{2} L_{x4} L_{y10} (k_{B1z} + k_{B2z} - k_{B3z} - k_{B4z}) - \frac{1}{4} L_{x6} L_{y7} (k_{C1z} - k_{C4z} - k_{C6z} + k_{C7z}) - \frac{1}{4} L_{x5} L_{y7} (k_{C2z} - k_{C3z} - k_{C5z} + k_{C8z})$$

$$k_{1916} = \frac{1}{2} L_{x6} L_{y12} (k_{C1z} - k_{C6z}) + \frac{1}{2} L_{x5} L_{y12} (k_{C2z} - k_{C5z}) + \frac{1}{2} L_{x5} L_{y11} (k_{C3z} - k_{C8z}) + \frac{1}{2} L_{x6} L_{y11} (k_{C4z} - k_{C7z})$$

$$k_{1918} = -\frac{1}{4} L_{z6}^2 (k_{B1x} + k_{B2x} + k_{B3x} + k_{B4x}) - \frac{1}{4} L_{x4}^2 (k_{B1z} + k_{B2z} + k_{B3z} + k_{B4z})$$

$$k_{1919} = \frac{1}{4}L_{z6}^2(k_{B1x} + k_{B2x} + k_{B3x} + k_{B4x}) + \frac{1}{4}L_{x4}^2(k_{B1z} + k_{B2z} + k_{B3z} + k_{B4z}) + \frac{1}{4}L_{x6}^2(k_{C1z} + k_{C4z} + k_{C6z} + k_{C7z})$$

$$+\frac{1}{4}L_{x5}^2(k_{C2z} + k_{C3z} + k_{C5z} + k_{C8z}) + L_{z7}^2(k_{C1x} + k_{C2x} + k_{C3x} + k_{C4x} + k_{C5x} + k_{C6x} + k_{C7x} + k_{C8x})$$

$$k_{2003} = -L_{z9}(k_{C1x} + k_{C2x} + k_{C3x} + k_{C4x} + k_{C5x} + k_{C6x} + k_{C7x} + k_{C8x})$$

$$k_{2004} = L_{z9}(k_{C1x} + k_{C2x} + k_{C3x} + k_{C4x} + k_{C5x} + k_{C6x} + k_{C7x} + k_{C8x}) + \frac{1}{2}L_{z10}(-k_{D1x} + k_{D2x} + k_{D3x} - k_{D4x})$$

$$k_{2011} = L_{x8}(k_{C1z} + k_{C4z} - k_{C6z} - k_{C7z}) + L_{x9}(k_{C2z} + k_{C3z} - k_{C5z} - k_{C8z})$$

$$k_{2012} = -L_{x8}(k_{C1z} + k_{C4z} - k_{C6z} - k_{C7z}) - L_{x9}(k_{C2z} + k_{C3z} - k_{C5z} - k_{C8z}) - \frac{1}{2}L_{x7}(k_{D1z} + k_{D2z} - k_{D3z} - k_{D4z})$$

$$k_{2015} = \frac{1}{2}L_{x8}L_{y7}(k_{C1z} - k_{C4z} - k_{C6z} + k_{C7z}) + \frac{1}{2}L_{x9}L_{y7}(k_{C2z} - k_{C3z} - k_{C5z} + k_{C8z})$$

$$k_{2016} = -L_{x8}L_{y12}(k_{C1z} - k_{C6z}) - L_{x9}L_{y11}(k_{C3z} - k_{C8z}) - L_{x8}L_{y11}(k_{C4z} - k_{C7z}) - L_{x9}L_{y12}(k_{C2z} - k_{C5z})$$

$$k_{2019} = -L_{z9}L_{z7}(k_{C1x} + k_{C2x} + k_{C3x} + k_{C4x} + k_{C5x} + k_{C6x} + k_{C7x} + k_{C8x}) - \frac{1}{2}L_{x6}L_{x8}(k_{C1z} + k_{C4z} + k_{C6z} + k_{C7z})$$

$$-\frac{1}{2}L_{x5}L_{x9}(k_{C2z} + k_{C3z} + k_{C5z} + k_{C8z})$$

$$k_{2020} = L_{x8}^2(k_{C1z} + k_{C4z} + k_{C6z} + k_{C7z}) + L_{x9}^2(k_{C2z} + k_{C3z} + k_{C5z} + k_{C8z}) + L_{z9}^2(k_{C1x} + k_{C2x} + k_{C3x} + k_{C4x} + k_{C5x} + k_{C6x} + k_{C7x} + k_{C8x})$$

$$+\frac{1}{4}L_{z10}^2(k_{D1x} + k_{D2x} + k_{D3x} + k_{D4x}) + \frac{1}{4}L_{x7}^2(k_{D1z} + k_{D2z} + k_{D3z} + k_{D4z})$$

$$k_{2105} = \frac{1}{2}L_{x2}(k_{A1y} + k_{A2y} - k_{A3y} - k_{A4y})$$

$$k_{2106} = -\frac{1}{2}L_{x2}(k_{A1y} + k_{A2y} - k_{A3y} - k_{A4y})$$

$$k_{2113} = -\frac{1}{4}L_{x2}L_{z4}(k_{A1y} - k_{A2y} + k_{A3y} - k_{A4y})$$

$$k_{2114} = \frac{1}{4}L_{x2}L_{z4}(k_{A1y} - k_{A2y} + k_{A3y} - k_{A4y})$$

$$k_{2121} = \frac{1}{4}L_{x2}^2(k_{A1y} + k_{A2y} + k_{A3y} + k_{A4y})$$

$$k_{2205} = -\frac{1}{2}L_{x2}(k_{A1y} + k_{A2y} - k_{A3y} - k_{A4y}) - L_{x3}(k_{A1y} + k_{A2y} + k_{A3y} + k_{A4y})$$

$$k_{2206} = \frac{1}{2}L_{x2}(k_{A1y} + k_{A2y} - k_{A3y} - k_{A4y}) + L_{x3}(k_{A1y} + k_{A2y} + k_{A3y} + k_{A4y}) + \frac{1}{2}L_{x4}(k_{B1y} + k_{B2y} - k_{B3y} - k_{B4y})$$

$$k_{2207} = -\frac{1}{2}L_{x4}(k_{B1y} + k_{B2y} - k_{B3y} - k_{B4y})$$

$$k_{2213} = \frac{1}{4}L_{x2}L_{z4}(k_{A1y} - k_{A2y} + k_{A3y} - k_{A4y}) + \frac{1}{2}L_{x3}L_{z4}(k_{A1y} - k_{A2y} - k_{A3y} + k_{A4y})$$

$$k_{2214} = -\frac{1}{4}L_{z6}L_{x4}(k_{B1y} - k_{B2y} + k_{B3y} - k_{B4y}) - \frac{1}{4}L_{x2}L_{z4}(k_{A1y} - k_{A2y} + k_{A3y} - k_{A4y}) - \frac{1}{2}L_{x3}L_{z4}(k_{A1y} - k_{A2y} - k_{A3y} + k_{A4y})$$

$$k_{2215} = \frac{1}{4}L_{z6}L_{x4}(k_{B1y} - k_{B2y} + k_{B3y} - k_{B4y})$$

$$k_{2221} = -\frac{1}{4}L_{x2}^2(k_{A1y} + k_{A2y} + k_{A3y} + k_{A4y}) - \frac{1}{2}L_{x2}L_{x3}(k_{A1y} + k_{A2y} - k_{A3y} - k_{A4y})$$

$$k_{2222} = \frac{1}{4} L_{x2}^2 (k_{A1y} + k_{A2y} + k_{A3y} + k_{A4y}) + L_{x3}^2 (k_{A1y} + k_{A2y} + k_{A3y} + k_{A4y}) + L_{x2} L_{x3} (k_{A1y} + k_{A2y} - k_{A3y} - k_{A4y})$$

$$+ \frac{1}{4} L_{x4}^2 (k_{B1z} + k_{B2z} + k_{B3z} + k_{B4z})$$

$$k_{2303} = \frac{1}{2} L_{y7} (k_{C1x} + k_{C2x} - k_{C3x} - k_{C4x} + k_{C5x} + k_{C6x} - k_{C7x} - k_{C8x})$$

$$k_{2304} = -\frac{1}{2} L_{y7} (k_{C1x} + k_{C2x} - k_{C3x} - k_{C4x} + k_{C5x} + k_{C6x} - k_{C7x} - k_{C8x})$$

$$k_{2306} = \frac{1}{2} L_{x4} (-k_{B1y} - k_{B2y} + k_{B3y} + k_{B4y})$$

$$k_{2307} = -\frac{1}{2} L_{x4} (-k_{B1y} - k_{B2y} + k_{B3y} + k_{B4y}) - \frac{1}{2} L_{x5} (-k_{C2y} - k_{C3y} + k_{C5y} + k_{C8y}) - \frac{1}{2} L_{x6} (-k_{C1y} - k_{C4y} + k_{C6y} + k_{C7y})$$

$$k_{2308} = \frac{1}{2} L_{x5} (-k_{C2y} - k_{C3y} + k_{C5y} + k_{C8y}) + \frac{1}{2} L_{x6} (-k_{C1y} - k_{C4y} + k_{C6y} + k_{C7y})$$

$$k_{2314} = \frac{1}{4} L_{z6} L_{x4} (k_{B1y} - k_{B2y} + k_{B3y} - k_{B4y})$$

$$k_{2315} = -\frac{1}{4} L_{z6} L_{x4} (k_{B1y} - k_{B2y} + k_{B3y} - k_{B4y}) - \frac{1}{2} L_{x6} L_{y7} (-k_{C1y} - k_{C4y} + k_{C6y} + k_{C7y}) - \frac{1}{2} L_{x5} L_{y7} (-k_{C2y} - k_{C3y} + k_{C5y} + k_{C8y})$$

$$k_{2316} = \frac{1}{2} L_{x6} L_{z9} (-k_{C1y} - k_{C4y} + k_{C6y} + k_{C7y}) + \frac{1}{2} L_{x5} L_{z9} (-k_{C2y} - k_{C3y} + k_{C5y} + k_{C8y})$$

$$k_{2319} = -\frac{1}{2} L_{y7} L_{z7} (-k_{C1x} - k_{C2x} + k_{C3x} + k_{C4x} - k_{C5x} - k_{C6x} + k_{C7x} + k_{C8x})$$

$$k_{2320} = \frac{1}{2} L_{y7} L_{z9} (-k_{C1x} - k_{C2x} + k_{C3x} + k_{C4x} - k_{C5x} - k_{C6x} + k_{C7x} + k_{C8x})$$

$$k_{2322} = -\frac{1}{4} L_{x4}^2 (k_{B1y} + k_{B2y} + k_{B3y} + k_{B4y})$$

$$k_{2323} = \frac{1}{4} L_{x4}^2 (k_{B1y} + k_{B2y} + k_{B3y} + k_{B4y}) + \frac{1}{4} L_{x5}^2 (k_{C2y} + k_{C3y} + k_{C5y} + k_{C8y}) + \frac{1}{4} L_{x6}^2 (k_{C1y} + k_{C4y} + k_{C6y} + k_{C7y})$$

$$+ \frac{1}{4} L_{y7}^2 (k_{C1x} + k_{C2x} + k_{C3x} + k_{C4x} + k_{C5x} + k_{C6x} + k_{C7x} + k_{C8x})$$

$$k_{2403} = -L_{y11} (k_{C3x} + k_{C4x} + k_{C7x} + k_{C8x}) - L_{y12} (k_{C1x} + k_{C2x} + k_{C5x} + k_{C6x})$$

$$k_{2404} = L_{y11} (k_{C3x} + k_{C4x} + k_{C7x} + k_{C8x}) + L_{y12} (k_{C1x} + k_{C2x} + k_{C5x} + k_{C6x})$$

$$k_{2407} = L_{x8} (-k_{C1y} - k_{C4y} + k_{C6y} + k_{C7y}) + L_{x9} (-k_{C2y} - k_{C3y} + k_{C5y} + k_{C8y})$$

$$k_{2408} = \frac{1}{2} L_{x7} (k_{D1y} + k_{D2y} - k_{D3y} - k_{D4y}) - L_{x8} (-k_{C1y} - k_{C4y} + k_{C6y} + k_{C7y}) - L_{x9} (-k_{C2y} - k_{C3y} + k_{C5y} + k_{C8y})$$

$$k_{2415} = L_{x8} L_{z7} (-k_{C1y} - k_{C4y} + k_{C6y} + k_{C7y}) + L_{x9} L_{z7} (-k_{C2y} - k_{C3y} + k_{C5y} + k_{C8y})$$

$$k_{2416} = -\frac{1}{4} L_{x7} L_{z10} (k_{D1y} - k_{D2y} + k_{D3y} - k_{D4y}) - L_{x8} L_{z9} (-k_{C1y} - k_{C4y} + k_{C6y} + k_{C7y}) - L_{x9} L_{z9} (-k_{C2y} - k_{C3y} + k_{C5y} + k_{C8y})$$

$$k_{2419} = -L_{y11} L_{z7} (k_{C3x} + k_{C4x} + k_{C7x} + k_{C8x}) - L_{y12} L_{z7} (k_{C1x} + k_{C2x} + k_{C5x} + k_{C6x})$$

$$k_{2420} = L_{y11} L_{z9} (k_{C3x} + k_{C4x} + k_{C7x} + k_{C8x}) + L_{y12} L_{z9} (k_{C1x} + k_{C2x} + k_{C5x} + k_{C6x})$$

$$k_{2423} = -\frac{1}{2} L_{x6} L_{x8} (k_{C1y} + k_{C4y} + k_{C6y} + k_{C7y}) - \frac{1}{2} L_{x5} L_{x9} (k_{C2y} + k_{C3y} + k_{C5y} + k_{C8y}) - \frac{1}{2} L_{y12} L_{y7} (k_{C1x} + k_{C2x} + k_{C5x} + k_{C6x})$$

$$+ \frac{1}{2} L_{y11} L_{y7} (k_{C3x} + k_{C4x} + k_{C7x} + k_{C8x})$$

$$k_{2424} = L_{x8}^2 (k_{C1y} + k_{C4y} + k_{C6y} + k_{C7y}) + L_{x9}^2 (k_{C2y} + k_{C3y} + k_{C5y} + k_{C8y}) + L_{y11}^2 (k_{C3x} + k_{C4x} + k_{C7x} + k_{C8x})$$

$$+ L_{y12}^2 (k_{C1x} + k_{C2x} + k_{C5x} + k_{C6x}) + \frac{1}{4} L_{x7}^2 (k_{D1y} + k_{D2y} + k_{D3y} + k_{D4y})$$

The non-zeros elements of the Force matrix are:

$$Q_1 = F_x \sin(w_x t)$$
$$Q_5 = F_y \sin(w_y t) - F_m$$
$$Q_9 = F_z \sin(w_z t)$$
$$Q_{13} = F_y \sin(w_y t)(L_{z1} + L_{z2}) + F_m L_{z2}$$
$$Q_{17} = F_x \sin(w_x t)(L_{z1} + L_{z2})$$
$$Q_{21} = T_z \sin(w_{Tz} t)$$

# APPENDIX B

# VALUES OF STATE SPACE A, B, C, AND D

# MATRICES

$$A_{0102} = 1$$

$$A_{0201} = -\frac{1}{M_A} \times k_{0101}$$
$$A_{0202} = -\frac{1}{M_A} \times C_{0101}$$
$$A_{0203} = -\frac{1}{M_A} \times k_{0102}$$
$$A_{0204} = -\frac{1}{M_A} \times C_{0102}$$
$$A_{0233} = -\frac{1}{M_A} \times k_{0117}$$
$$A_{0234} = -\frac{1}{M_A} \times C_{0117}$$
$$A_{0235} = -\frac{1}{M_A} \times k_{0118}$$
$$A_{0236} = -\frac{1}{M_A} \times C_{0118}$$

$A_{0304}$=1;

$$A_{0401} = -\frac{1}{M_B} \times k_{0201}$$
$$A_{0402} = -\frac{1}{M_B} \times C_{0201}$$
$$A_{0403} = -\frac{1}{M_B} \times k_{0202}$$
$$A_{0404} = -\frac{1}{M_B} \times C_{0202}$$
$$A_{0405} = -\frac{1}{M_B} \times k_{0203}$$
$$A_{0406} = -\frac{1}{M_B} \times C_{0203}$$
$$A_{0433} = -\frac{1}{M_B} \times k_{0217}$$
$$A_{0434} = -\frac{1}{M_B} \times C_{0217}$$
$$A_{0435} = -\frac{1}{M_B} \times k_{0218}$$
$$A_{0436} = -\frac{1}{M_B} \times C_{0218}$$
$$A_{0437} = -\frac{1}{M_B} \times k_{0219}$$
$$A_{0438} = -\frac{1}{M_B} \times C_{0219}$$

$A_{0506}$ = 1;

$$A_{0603} = -\frac{1}{M_C} \times k_{0302}$$
$$A_{0604} = -\frac{1}{M_C} \times C_{0302}$$
$$A_{0605} = -\frac{1}{M_C} \times k_{0303}$$
$$A_{0606} = -\frac{1}{M_C} \times C_{0303}$$
$$A_{0607} = -\frac{1}{M_C} \times k_{0304}$$
$$A_{0608} = -\frac{1}{M_C} \times C_{0304}$$
$$A_{0635} = -\frac{1}{M_C} \times k_{0318}$$
$$A_{0636} = -\frac{1}{M_C} \times C_{0318}$$
$$A_{0637} = -\frac{1}{M_C} \times k_{0319}$$
$$A_{0638} = -\frac{1}{M_C} \times C_{0319}$$
$$A_{0639} = -\frac{1}{M_C} \times k_{0320}$$
$$A_{0640} = -\frac{1}{M_C} \times C_{0320}$$
$$A_{0645} = -\frac{1}{M_C} \times k_{0323}$$
$$A_{0646} = -\frac{1}{M_C} \times C_{0323}$$
$$A_{0647} = -\frac{1}{M_C} \times k_{0324}$$
$$A_{0648} = -\frac{1}{M_C} \times C_{0324}$$

$A_{0708}$ = 1;

$$A_{0805} = -\frac{1}{M_D} \times k_{0403}$$
$$A_{0806} = -\frac{1}{M_D} \times C_{0403}$$

$$A_{0807} = -\frac{1}{M_D} \times k_{0404}$$
$$A_{0808} = -\frac{1}{M_D} \times C_{0404}$$
$$A_{0837} = -\frac{1}{M_D} \times k_{0419}$$
$$A_{0838} = -\frac{1}{M_D} \times C_{0419}$$
$$A_{0839} = -\frac{1}{M_D} \times k_{0420}$$
$$A_{0840} = -\frac{1}{M_D} \times C_{0420}$$
$$A_{0845} = -\frac{1}{M_D} \times k_{0423}$$
$$A_{0846} = -\frac{1}{M_D} \times C_{0423}$$
$$A_{0847} = -\frac{1}{M_D} \times k_{0424}$$
$$A_{0848} = -\frac{1}{M_D} \times C_{0424}$$

$A_{0910} = 1;$

$$A_{1009} = -\frac{1}{M_A} \times k_{0505}$$
$$A_{1010} = -\frac{1}{M_A} \times C_{0505}$$
$$A_{1011} = -\frac{1}{M_A} \times k_{0506}$$
$$A_{1012} = -\frac{1}{M_A} \times C_{0506}$$
$$A_{1025} = -\frac{1}{M_A} \times k_{0513}$$
$$A_{1026} = -\frac{1}{M_A} \times C_{0513}$$
$$A_{1027} = -\frac{1}{M_A} \times k_{0514}$$
$$A_{1028} = -\frac{1}{M_A} \times C_{0514}$$
$$A_{1041} = -\frac{1}{M_A} \times k_{0521}$$
$$A_{1042} = -\frac{1}{M_A} \times C_{0521}$$
$$A_{1043} = -\frac{1}{M_A} \times k_{0522}$$
$$A_{1044} = -\frac{1}{M_A} \times C_{0522}$$

$A_{1112} = 1;$

$$A_{1209} = -\frac{1}{M_B} \times k_{0605}$$
$$A_{1210} = -\frac{1}{M_B} \times C_{0605}$$
$$A_{1211} = -\frac{1}{M_B} \times k_{0606}$$
$$A_{1212} = -\frac{1}{M_B} \times C_{0606}$$
$$A_{1213} = -\frac{1}{M_B} \times k_{0607}$$
$$A_{1214} = -\frac{1}{M_B} \times C_{0607}$$
$$A_{1225} = -\frac{1}{M_B} \times k_{0613}$$
$$A_{1226} = -\frac{1}{M_B} \times C_{0613}$$
$$A_{1227} = -\frac{1}{M_B} \times k_{0614}$$
$$A_{1228} = -\frac{1}{M_B} \times C_{0614}$$
$$A_{1241} = -\frac{1}{M_B} \times k_{0621}$$
$$A_{1242} = -\frac{1}{M_B} \times C_{0621}$$
$$A_{1243} = -\frac{1}{M_B} \times k_{0622}$$
$$A_{1244} = -\frac{1}{M_B} \times C_{0622}$$
$$A_{1245} = -\frac{1}{M_B} \times k_{0623}$$
$$A_{1246} = -\frac{1}{M_B} \times C_{0623}$$

$A_{1314} = 1;$

$$A_{1411} = -\frac{1}{M_C} \times k_{0706}$$
$$A_{1412} = -\frac{1}{M_C} \times C_{0706}$$
$$A_{1413} = -\frac{1}{M_C} \times k_{0707}$$
$$A_{1414} = -\frac{1}{M_C} \times C_{0707}$$
$$A_{1415} = -\frac{1}{M_C} \times k_{0708}$$
$$A_{1416} = -\frac{1}{M_C} \times C_{0708}$$
$$A_{1427} = -\frac{1}{M_C} \times k_{0714}$$
$$A_{1428} = -\frac{1}{M_C} \times C_{0714}$$
$$A_{1431} = -\frac{1}{M_C} \times k_{0716}$$
$$A_{1432} = -\frac{1}{M_C} \times C_{0716}$$
$$A_{1443} = -\frac{1}{M_C} \times k_{0722}$$
$$A_{1444} = -\frac{1}{M_C} \times C_{0722}$$
$$A_{1445} = -\frac{1}{M_C} \times k_{0723}$$
$$A_{1446} = -\frac{1}{M_C} \times C_{0723}$$
$$A_{1447} = -\frac{1}{M_C} \times k_{0724}$$
$$A_{1448} = -\frac{1}{M_C} \times C_{0724}$$

$A_{1516} = 1;$

$$A_{1613} = -\frac{1}{M_D} \times k_{0807}$$
$$A_{1614} = -\frac{1}{M_D} \times C_{0807}$$
$$A_{1615} = -\frac{1}{M_D} \times k_{0808}$$
$$A_{1616} = -\frac{1}{M_D} \times C_{0808}$$
$$A_{1631} = -\frac{1}{M_D} \times k_{0816}$$
$$A_{1632} = -\frac{1}{M_D} \times C_{0816}$$
$$A_{1645} = -\frac{1}{M_D} \times k_{0823}$$
$$A_{1646} = -\frac{1}{M_D} \times C_{0823}$$
$$A_{1647} = -\frac{1}{M_D} \times k_{0824}$$
$$A_{1648} = -\frac{1}{M_D} \times C_{0824}$$

$A_{1718} = 1;$

$$A_{1817} = -\frac{1}{M_A} \times k_{0909}$$
$$A_{1818} = -\frac{1}{M_A} \times C_{0909}$$
$$A_{1825} = -\frac{1}{M_A} \times k_{0913}$$
$$A_{1826} = -\frac{1}{M_A} \times C_{0913}$$
$$A_{1827} = -\frac{1}{M_A} \times k_{0914}$$
$$A_{1828} = -\frac{1}{M_A} \times C_{0914}$$
$$A_{1833} = -\frac{1}{M_A} \times k_{0917}$$
$$A_{1834} = -\frac{1}{M_A} \times C_{0917}$$
$$A_{1835} = -\frac{1}{M_A} \times k_{0918}$$
$$A_{1836} = -\frac{1}{M_A} \times C_{0918}$$

$A_{1920} = 1;$

$$A_{2017} = -\frac{1}{M_B} \times k_{1009}$$
$$A_{2018} = -\frac{1}{M_B} \times C_{1009}$$
$$A_{2019} = -\frac{1}{M_B} \times k_{1010}$$
$$A_{2020} = -\frac{1}{M_B} \times C_{1010}$$
$$A_{2021} = -\frac{1}{M_B} \times k_{1011}$$
$$A_{2022} = -\frac{1}{M_B} \times C_{1011}$$
$$A_{2025} = -\frac{1}{M_B} \times k_{1013}$$
$$A_{2026} = -\frac{1}{M_B} \times C_{1013}$$
$$A_{2027} = -\frac{1}{M_B} \times k_{1014}$$
$$A_{2028} = -\frac{1}{M_B} \times C_{1014}$$
$$A_{2029} = -\frac{1}{M_B} \times k_{1015}$$
$$A_{2030} = -\frac{1}{M_B} \times C_{1015}$$
$$A_{2033} = -\frac{1}{M_B} \times k_{1017}$$
$$A_{2034} = -\frac{1}{M_B} \times C_{1017}$$
$$A_{2035} = -\frac{1}{M_B} \times k_{1018}$$
$$A_{2036} = -\frac{1}{M_B} \times C_{1018}$$
$$A_{2037} = -\frac{1}{M_B} \times k_{1019}$$
$$A_{2038} = -\frac{1}{M_B} \times C_{1019}$$

$A_{2122} = 1;$

$$A_{2219} = -\frac{1}{M_C} \times k_{1110}$$
$$A_{2220} = -\frac{1}{M_C} \times C_{1110}$$
$$A_{2221} = -\frac{1}{M_C} \times k_{1111}$$
$$A_{2222} = -\frac{1}{M_C} \times C_{1111}$$
$$A_{2223} = -\frac{1}{M_C} \times k_{1112}$$
$$A_{2224} = -\frac{1}{M_C} \times C_{1112}$$
$$A_{2227} = -\frac{1}{M_C} \times k_{1114}$$
$$A_{2228} = -\frac{1}{M_C} \times C_{1114}$$
$$A_{2229} = -\frac{1}{M_C} \times k_{1115}$$
$$A_{2230} = -\frac{1}{M_C} \times C_{1115}$$
$$A_{2231} = -\frac{1}{M_C} \times k_{1116}$$
$$A_{2232} = -\frac{1}{M_C} \times C_{1116}$$
$$A_{2235} = -\frac{1}{M_C} \times k_{1118}$$
$$A_{2236} = -\frac{1}{M_C} \times C_{1118}$$
$$A_{2237} = -\frac{1}{M_C} \times k_{1119}$$
$$A_{2238} = -\frac{1}{M_C} \times C_{1119}$$
$$A_{2239} = -\frac{1}{M_C} \times k_{1120}$$
$$A_{2240} = -\frac{1}{M_C} \times C_{1120}$$

$A_{2324} = 1;$

$$A_{2421} = -\frac{1}{M_D} \times k_{1211}$$
$$A_{2422} = -\frac{1}{M_D} \times C_{1211}$$
$$A_{2423} = -\frac{1}{M_D} \times k_{1212}$$
$$A_{2424} = -\frac{1}{M_D} \times C_{1212}$$
$$A_{2429} = -\frac{1}{M_D} \times k_{1215}$$
$$A_{2430} = -\frac{1}{M_D} \times C_{1215}$$
$$A_{2431} = -\frac{1}{M_D} \times k_{1216}$$
$$A_{2432} = -\frac{1}{M_D} \times C_{1216}$$
$$A_{2437} = -\frac{1}{M_D} \times k_{1219}$$
$$A_{2438} = -\frac{1}{M_D} \times C_{1219}$$
$$A_{2439} = -\frac{1}{M_D} \times k_{1220}$$
$$A_{2440} = -\frac{1}{M_D} \times C_{1220}$$

$A_{2526} = 1;$

$$A_{2609} = -\frac{1}{I_{Ax}} \times k_{1305}$$
$$A_{2610} = -\frac{1}{I_{Ax}} \times C_{1305}$$
$$A_{2611} = -\frac{1}{I_{Ax}} \times k_{1306}$$
$$A_{2612} = -\frac{1}{I_{Ax}} \times C_{1306}$$
$$A_{2617} = -\frac{1}{I_{Ax}} \times k_{1309}$$
$$A_{2618} = -\frac{1}{I_{Ax}} \times C_{1309}$$
$$A_{2619} = -\frac{1}{I_{Ax}} \times k_{1310}$$
$$A_{2620} = -\frac{1}{I_{Ax}} \times C_{1310}$$
$$A_{2625} = -\frac{1}{I_{Ax}} \times k_{1313}$$
$$A_{2626} = -\frac{1}{I_{Ax}} \times C_{1313}$$
$$A_{2627} = -\frac{1}{I_{Ax}} \times k_{1314}$$
$$A_{2628} = -\frac{1}{I_{Ax}} \times C_{1314}$$
$$A_{2633} = -\frac{1}{I_{Ax}} \times k_{1317}$$
$$A_{2634} = -\frac{1}{I_{Ax}} \times C_{1317}$$
$$A_{2635} = -\frac{1}{I_{Ax}} \times k_{1318}$$
$$A_{2636} = -\frac{1}{I_{Ax}} \times C_{1318}$$
$$A_{2641} = -\frac{1}{I_{Ax}} \times k_{1321}$$
$$A_{2642} = -\frac{1}{I_{Ax}} \times C_{1321}$$
$$A_{2643} = -\frac{1}{I_{Ax}} \times k_{1322}$$
$$A_{2644} = -\frac{1}{I_{Ax}} \times C_{1322}$$

$$A_{2728} = 1$$

$$A_{2809} = -\frac{1}{I_{Bx}} \times k_{1405}$$
$$A_{2810} = -\frac{1}{I_{Bx}} \times C_{1405}$$
$$A_{2811} = -\frac{1}{I_{Bx}} \times k_{1406}$$
$$A_{2812} = -\frac{1}{I_{Bx}} \times C_{1406}$$
$$A_{2813} = -\frac{1}{I_{Bx}} \times k_{1407}$$
$$A_{2814} = -\frac{1}{I_{Bx}} \times C_{1407}$$
$$A_{2817} = -\frac{1}{I_{Bx}} \times k_{1409}$$
$$A_{2818} = -\frac{1}{I_{Bx}} \times C_{1409}$$
$$A_{2819} = -\frac{1}{I_{Bx}} \times k_{1410}$$
$$A_{2820} = -\frac{1}{I_{Bx}} \times C_{1410}$$
$$A_{2821} = -\frac{1}{I_{Bx}} \times k_{1411}$$
$$A_{2822} = -\frac{1}{I_{Bx}} \times C_{1411}$$
$$A_{2825} = -\frac{1}{I_{Bx}} \times k_{1413}$$
$$A_{2826} = -\frac{1}{I_{Bx}} \times C_{1413}$$
$$A_{2827} = -\frac{1}{I_{Bx}} \times k_{1414}$$
$$A_{2828} = -\frac{1}{I_{Bx}} \times C_{1414}$$
$$A_{2829} = -\frac{1}{I_{Bx}} \times k_{1415}$$
$$A_{2830} = -\frac{1}{I_{Bx}} \times C_{1415}$$
$$A_{2833} = -\frac{1}{I_{Bx}} \times k_{1417}$$
$$A_{2834} = -\frac{1}{I_{Bx}} \times C_{1417}$$
$$A_{2835} = -\frac{1}{I_{Bx}} \times k_{1418}$$
$$A_{2836} = -\frac{1}{I_{Bx}} \times C_{1418}$$
$$A_{2837} = -\frac{1}{I_{Bx}} \times k_{1419}$$
$$A_{2838} = -\frac{1}{I_{Bx}} \times C_{1419}$$

$$A_{2841} = -\frac{1}{I_{Bx}} \times k_{1421}$$
$$A_{2842} = -\frac{1}{I_{Bx}} \times C_{1421}$$
$$A_{2843} = -\frac{1}{I_{Bx}} \times k_{1422}$$
$$A_{2844} = -\frac{1}{I_{Bx}} \times C_{1422}$$
$$A_{2845} = -\frac{1}{I_{Bx}} \times k_{1423}$$
$$A_{2846} = -\frac{1}{I_{Bx}} \times C_{1423}$$

$$A_{2930} = 1$$

$$A_{3019} = -\frac{1}{I_{Cx}} \times k_{1510}$$
$$A_{3020} = -\frac{1}{I_{Cx}} \times C_{1510}$$
$$A_{3021} = -\frac{1}{I_{Cx}} \times k_{1511}$$
$$A_{3022} = -\frac{1}{I_{Cx}} \times C_{1511}$$
$$A_{3023} = -\frac{1}{I_{Cx}} \times k_{1512}$$
$$A_{3024} = -\frac{1}{I_{Cx}} \times C_{1512}$$
$$A_{3027} = -\frac{1}{I_{Cx}} \times k_{1514}$$
$$A_{3028} = -\frac{1}{I_{Cx}} \times C_{1514}$$
$$A_{3029} = -\frac{1}{I_{Cx}} \times k_{1515}$$
$$A_{3030} = -\frac{1}{I_{Cx}} \times C_{1515}$$
$$A_{3031} = -\frac{1}{I_{Cx}} \times k_{1516}$$
$$A_{3032} = -\frac{1}{I_{Cx}} \times C_{1516}$$
$$A_{3035} = -\frac{1}{I_{Cx}} \times k_{1518}$$
$$A_{3036} = -\frac{1}{I_{Cx}} \times C_{1518}$$
$$A_{3037} = -\frac{1}{I_{Cx}} \times k_{1519}$$
$$A_{3038} = -\frac{1}{I_{Cx}} \times C_{1519}$$
$$A_{3039} = -\frac{1}{I_{Cx}} \times k_{1520}$$
$$A_{3040} = -\frac{1}{I_{Cx}} \times C_{1520}$$
$$A_{3043} = -\frac{1}{I_{Cx}} \times k_{1522}$$
$$A_{3044} = -\frac{1}{I_{Cx}} \times C_{1522}$$
$$A_{3045} = -\frac{1}{I_{Cx}} \times k_{1523}$$
$$A_{3046} = -\frac{1}{I_{Cx}} \times C_{1523}$$
$$A_{3047} = -\frac{1}{I_{Cx}} \times k_{1524}$$
$$A_{3048} = -\frac{1}{I_{Cx}} \times C_{1524}$$

$$A_{3132} = 1$$

$$A_{3213} = -\frac{1}{I_{Dx}} \times k_{1607}$$
$$A_{3214} = -\frac{1}{I_{Dx}} \times C_{1607}$$
$$A_{3215} = -\frac{1}{I_{Dx}} \times k_{1608}$$
$$A_{3216} = -\frac{1}{I_{Dx}} \times C_{1608}$$
$$A_{3221} = -\frac{1}{I_{Dx}} \times k_{1611}$$
$$A_{3222} = -\frac{1}{I_{Dx}} \times C_{1611}$$
$$A_{3223} = -\frac{1}{I_{Dx}} \times k_{1612}$$
$$A_{3224} = -\frac{1}{I_{Dx}} \times C_{1612}$$
$$A_{3229} = -\frac{1}{I_{Dx}} \times k_{1615}$$
$$A_{3230} = -\frac{1}{I_{Dx}} \times C_{1615}$$
$$A_{3231} = -\frac{1}{I_{Dx}} \times k_{1616}$$
$$A_{3232} = -\frac{1}{I_{Dx}} \times C_{1616}$$
$$A_{3237} = -\frac{1}{I_{Dx}} \times k_{1619}$$
$$A_{3238} = -\frac{1}{I_{Dx}} \times C_{1619}$$
$$A_{3239} = -\frac{1}{I_{Dx}} \times k_{1620}$$
$$A_{3240} = -\frac{1}{I_{Dx}} \times C_{1620}$$
$$A_{3245} = -\frac{1}{I_{Dx}} \times k_{1623}$$
$$A_{3246} = -\frac{1}{I_{Dx}} \times C_{1623}$$
$$A_{3247} = -\frac{1}{I_{Dx}} \times k_{1624}$$
$$A_{3248} = -\frac{1}{I_{Dx}} \times C_{1624}$$

$$A_{3334} = 1$$

$$A_{3401} = -\frac{1}{I_{Ay}} \times k_{1701}$$
$$A_{3402} = -\frac{1}{I_{Ay}} \times C_{1701}$$
$$A_{3403} = -\frac{1}{I_{Ay}} \times k_{1702}$$
$$A_{3404} = -\frac{1}{I_{Ay}} \times C_{1702}$$
$$A_{3417} = -\frac{1}{I_{Ay}} \times k_{1709}$$
$$A_{3418} = -\frac{1}{I_{Ay}} \times C_{1709}$$

$$A_{3419} = -\frac{1}{I_{Ay}} \times k_{1710}$$
$$A_{3420} = -\frac{1}{I_{Ay}} \times C_{1710}$$
$$A_{3425} = -\frac{1}{I_{Ay}} \times k_{1713}$$
$$A_{3426} = -\frac{1}{I_{Ay}} \times C_{1713}$$
$$A_{3427} = -\frac{1}{I_{Ay}} \times k_{1714}$$
$$A_{3428} = -\frac{1}{I_{Ay}} \times C_{1714}$$
$$A_{3433} = -\frac{1}{I_{Ay}} \times k_{1717}$$
$$A_{3434} = -\frac{1}{I_{Ay}} \times C_{1717}$$
$$A_{3435} = -\frac{1}{I_{Ay}} \times k_{1718}$$
$$A_{3436} = -\frac{1}{I_{Ay}} \times C_{1718}$$

$$A_{3536} = 1$$

$$A_{3601} = -\frac{1}{I_{By}} \times k_{1801}$$
$$A_{3602} = -\frac{1}{I_{By}} \times C_{1801}$$
$$A_{3603} = -\frac{1}{I_{By}} \times k_{1802}$$
$$A_{3604} = -\frac{1}{I_{By}} \times C_{1802}$$
$$A_{3605} = -\frac{1}{I_{By}} \times k_{1803}$$
$$A_{3606} = -\frac{1}{I_{By}} \times C_{1803}$$
$$A_{3617} = -\frac{1}{I_{By}} \times k_{1809}$$
$$A_{3618} = -\frac{1}{I_{By}} \times C_{1809}$$
$$A_{3619} = -\frac{1}{I_{By}} \times k_{1810}$$
$$A_{3620} = -\frac{1}{I_{By}} \times C_{1810}$$
$$A_{3621} = -\frac{1}{I_{By}} \times k_{1811}$$
$$A_{3622} = -\frac{1}{I_{By}} \times C_{1811}$$
$$A_{3625} = -\frac{1}{I_{By}} \times k_{1813}$$
$$A_{3626} = -\frac{1}{I_{By}} \times C_{1813}$$
$$A_{3627} = -\frac{1}{I_{By}} \times k_{1814}$$
$$A_{3628} = -\frac{1}{I_{By}} \times C_{1814}$$
$$A_{3629} = -\frac{1}{I_{By}} \times k_{1815}$$
$$A_{3630} = -\frac{1}{I_{By}} \times C_{1815}$$
$$A_{3633} = -\frac{1}{I_{By}} \times k_{1817}$$
$$A_{3634} = -\frac{1}{I_{By}} \times C_{1817}$$
$$A_{3635} = -\frac{1}{I_{By}} \times k_{1818}$$
$$A_{3636} = -\frac{1}{I_{By}} \times C_{1818}$$
$$A_{3637} = -\frac{1}{I_{By}} \times k_{1819}$$
$$A_{3638} = -\frac{1}{I_{By}} \times C_{1819}$$

$$A_{3738} = 1$$

$$A_{3803} = -\frac{1}{I_{Cy}} \times k_{1902}$$
$$A_{3804} = -\frac{1}{I_{Cy}} \times C_{1902}$$
$$A_{3805} = -\frac{1}{I_{Cy}} \times k_{1903}$$
$$A_{3806} = -\frac{1}{I_{Cy}} \times C_{1903}$$
$$A_{3807} = -\frac{1}{I_{Cy}} \times k_{1904}$$
$$A_{3808} = -\frac{1}{I_{Cy}} \times C_{1904}$$
$$A_{3819} = -\frac{1}{I_{Cy}} \times k_{1910}$$
$$A_{3820} = -\frac{1}{I_{Cy}} \times C_{1910}$$
$$A_{3821} = -\frac{1}{I_{Cy}} \times k_{1911}$$
$$A_{3822} = -\frac{1}{I_{Cy}} \times C_{1911}$$
$$A_{3823} = -\frac{1}{I_{Cy}} \times k_{1912}$$
$$A_{3824} = -\frac{1}{I_{Cy}} \times C_{1912}$$
$$A_{3827} = -\frac{1}{I_{Cy}} \times k_{1914}$$
$$A_{3828} = -\frac{1}{I_{Cy}} \times C_{1914}$$
$$A_{3829} = -\frac{1}{I_{Cy}} \times k_{1915}$$
$$A_{3830} = -\frac{1}{I_{Cy}} \times C_{1915}$$
$$A_{3831} = -\frac{1}{I_{Cy}} \times k_{1916}$$
$$A_{3832} = -\frac{1}{I_{Cy}} \times C_{1916}$$
$$A_{3835} = -\frac{1}{I_{Cy}} \times k_{1918}$$
$$A_{3836} = -\frac{1}{I_{Cy}} \times C_{1918}$$

$$A_{3837} = -\frac{1}{I_{Cy}} \times k_{1919}$$
$$A_{3838} = -\frac{1}{I_{Cy}} \times C_{1919}$$
$$A_{3839} = -\frac{1}{I_{Cy}} \times k_{1920}$$
$$A_{3840} = -\frac{1}{I_{Cy}} \times C_{1920}$$
$$A_{3845} = -\frac{1}{I_{Cy}} \times k_{1923}$$
$$A_{3846} = -\frac{1}{I_{Cy}} \times C_{1923}$$
$$A_{3847} = -\frac{1}{I_{Cy}} \times k_{1924}$$
$$A_{3848} = -\frac{1}{I_{Cy}} \times C_{1924}$$

$$A_{3940} = 1$$

$$A_{4005} = -\frac{1}{I_{Dy}} \times k_{2003}$$
$$A_{4006} = -\frac{1}{I_{Dy}} \times C_{2003}$$
$$A_{4007} = -\frac{1}{I_{Dy}} \times k_{2004}$$
$$A_{4008} = -\frac{1}{I_{Dy}} \times C_{2004}$$
$$A_{4021} = -\frac{1}{I_{Dy}} \times k_{2011}$$
$$A_{4022} = -\frac{1}{I_{Dy}} \times C_{2011}$$
$$A_{4023} = -\frac{1}{I_{Dy}} \times k_{2012}$$
$$A_{4024} = -\frac{1}{I_{Dy}} \times C_{2012}$$
$$A_{4029} = -\frac{1}{I_{Dy}} \times k_{2015}$$
$$A_{4030} = -\frac{1}{I_{Dy}} \times C_{2015}$$
$$A_{4031} = -\frac{1}{I_{Dy}} \times k_{2016}$$
$$A_{4032} = -\frac{1}{I_{Dy}} \times C_{2016}$$
$$A_{4037} = -\frac{1}{I_{Dy}} \times k_{2019}$$
$$A_{4038} = -\frac{1}{I_{Dy}} \times C_{2019}$$
$$A_{4039} = -\frac{1}{I_{Dy}} \times k_{2020}$$
$$A_{4040} = -\frac{1}{I_{Dy}} \times C_{2020}$$
$$A_{4045} = -\frac{1}{I_{Dy}} \times k_{2023}$$
$$A_{4046} = -\frac{1}{I_{Dy}} \times C_{2023}$$
$$A_{4047} = -\frac{1}{I_{Dy}} \times k_{2024}$$
$$A_{4048} = -\frac{1}{I_{Dy}} \times C_{2024}$$

$$A_{4142} = 1$$

$$A_{4209} = -\frac{1}{I_{Az}} \times k_{2105}$$
$$A_{4210} = -\frac{1}{I_{Az}} \times C_{2105}$$
$$A_{4211} = -\frac{1}{I_{Az}} \times k_{2106}$$
$$A_{4212} = -\frac{1}{I_{Az}} \times C_{2106}$$
$$A_{4225} = -\frac{1}{I_{Az}} \times k_{2113}$$
$$A_{4226} = -\frac{1}{I_{Az}} \times C_{2113}$$
$$A_{4227} = -\frac{1}{I_{Az}} \times k_{2114}$$
$$A_{4228} = -\frac{1}{I_{Az}} \times C_{2114}$$
$$A_{4241} = -\frac{1}{I_{Az}} \times k_{2121}$$
$$A_{4242} = -\frac{1}{I_{Az}} \times C_{2121}$$
$$A_{4243} = -\frac{1}{I_{Az}} \times k_{2122}$$
$$A_{4244} = -\frac{1}{I_{Az}} \times C_{2122}$$

$$A_{4344} = 1$$

$$A_{4409} = -\frac{1}{I_{Bz}} \times k_{2205}$$
$$A_{4410} = -\frac{1}{I_{Bz}} \times C_{2205}$$
$$A_{4411} = -\frac{1}{I_{Bz}} \times k_{2206}$$
$$A_{4412} = -\frac{1}{I_{Bz}} \times C_{2206}$$
$$A_{4413} = -\frac{1}{I_{Bz}} \times k_{2207}$$
$$A_{4414} = -\frac{1}{I_{Bz}} \times C_{2207}$$
$$A_{4425} = -\frac{1}{I_{Bz}} \times k_{2213}$$
$$A_{4426} = -\frac{1}{I_{Bz}} \times C_{2213}$$
$$A_{4427} = -\frac{1}{I_{Bz}} \times k_{2214}$$
$$A_{4428} = -\frac{1}{I_{Bz}} \times C_{2214}$$
$$A_{4429} = -\frac{1}{I_{Bz}} \times k_{2215}$$
$$A_{4430} = -\frac{1}{I_{Bz}} \times C_{2215}$$
$$A_{4441} = -\frac{1}{I_{Bz}} \times k_{2221}$$
$$A_{4442} = -\frac{1}{I_{Bz}} \times C_{2221}$$

$$A_{4443} = -\frac{1}{I_{Bz}} \times k_{2222}$$
$$A_{4444} = -\frac{1}{I_{Bz}} \times C_{2222}$$
$$A_{4445} = -\frac{1}{I_{Bz}} \times k_{2223}$$
$$A_{4446} = -\frac{1}{I_{Bz}} \times C_{2223}$$

$$A_{4546} = 1$$

$$A_{4605} = -\frac{1}{I_{Cz}} \times k_{2303}$$
$$A_{4606} = -\frac{1}{I_{Cz}} \times C_{2303}$$
$$A_{4607} = -\frac{1}{I_{Cz}} \times k_{2304}$$
$$A_{4608} = -\frac{1}{I_{Cz}} \times C_{2304}$$
$$A_{4611} = -\frac{1}{I_{Cz}} \times k_{2306}$$
$$A_{4612} = -\frac{1}{I_{Cz}} \times C_{2306}$$
$$A_{4613} = -\frac{1}{I_{Cz}} \times k_{2307}$$
$$A_{4614} = -\frac{1}{I_{Cz}} \times C_{2307}$$
$$A_{4615} = -\frac{1}{I_{Cz}} \times k_{2308}$$
$$A_{4616} = -\frac{1}{I_{Cz}} \times C_{2308}$$
$$A_{4627} = -\frac{1}{I_{Cz}} \times k_{2314}$$
$$A_{4628} = -\frac{1}{I_{Cz}} \times C_{2314}$$
$$A_{4629} = -\frac{1}{I_{Cz}} \times k_{2315}$$
$$A_{4630} = -\frac{1}{I_{Cz}} \times C_{2315}$$
$$A_{4631} = -\frac{1}{I_{Cz}} \times k_{2316}$$
$$A_{4632} = -\frac{1}{I_{Cz}} \times C_{2316}$$
$$A_{4637} = -\frac{1}{I_{Cz}} \times k_{2319}$$
$$A_{4638} = -\frac{1}{I_{Cz}} \times C_{2319}$$
$$A_{4639} = -\frac{1}{I_{Cz}} \times k_{2320}$$
$$A_{4640} = -\frac{1}{I_{Cz}} \times C_{2320}$$
$$A_{4643} = -\frac{1}{I_{Cz}} \times k_{2322}$$
$$A_{4644} = -\frac{1}{I_{Cz}} \times C_{2322}$$
$$A_{4645} = -\frac{1}{I_{Cz}} \times k_{2323}$$
$$A_{4646} = -\frac{1}{I_{Cz}} \times C_{2323}$$
$$A_{4647} = -\frac{1}{I_{Cz}} \times k_{2324}$$
$$A_{4648} = -\frac{1}{I_{Cz}} \times C_{2324}$$

$$A_{4748} = 1$$

$$A_{4805} = -\frac{1}{I_{Dz}} \times k_{2403}$$
$$A_{4806} = -\frac{1}{I_{Dz}} \times C_{2403}$$
$$A_{4807} = -\frac{1}{I_{Dz}} \times k_{2404}$$
$$A_{4808} = -\frac{1}{I_{Dz}} \times C_{2404}$$
$$A_{4813} = -\frac{1}{I_{Dz}} \times k_{2407}$$
$$A_{4814} = -\frac{1}{I_{Dz}} \times C_{2407}$$
$$A_{4815} = -\frac{1}{I_{Dz}} \times k_{2408}$$
$$A_{4816} = -\frac{1}{I_{Dz}} \times C_{2408}$$
$$A_{4829} = -\frac{1}{I_{Dz}} \times k_{2415}$$
$$A_{4830} = -\frac{1}{I_{Dz}} \times C_{2415}$$
$$A_{4831} = -\frac{1}{I_{Dz}} \times k_{2416}$$
$$A_{4832} = -\frac{1}{I_{Dz}} \times C_{2416}$$
$$A_{4837} = -\frac{1}{I_{Dz}} \times k_{2419}$$
$$A_{4838} = -\frac{1}{I_{Dz}} \times C_{2419}$$
$$A_{4839} = -\frac{1}{I_{Dz}} \times k_{2420}$$
$$A_{4840} = -\frac{1}{I_{Dz}} \times C_{2420}$$
$$A_{4845} = -\frac{1}{I_{Dz}} \times k_{2423}$$
$$A_{4846} = -\frac{1}{I_{Dz}} \times C_{2423}$$
$$A_{4847} = -\frac{1}{I_{Dz}} \times k_{2424}$$
$$A_{4848} = -\frac{1}{I_{Dz}} \times C_{2424}$$

```
B_Matrix(2,2) = (1/M_A) * F_X;
B_Matrix(10,10) = (1/M_A) * (F_Y - F_M);
B_Matrix(18,18) = (1/M_A) * F_Z;
B_Matrix(26,26) = (1/I_Ax) * (F_M * L_z2 + F_Y * (L_z1 + L_z2));
B_Matrix(34,34) = (1/I_Ay) * F_X * (L_z1 + L_z2);
B_Matrix(42,42) = (1/I_Az) * T_Z;


C_Matrix(1,1) = 1;
C_Matrix(2,3) = 1;
C_Matrix(3,5) = 1;
C_Matrix(4,7) = 1;
C_Matrix(5,9) = 1;
C_Matrix(6,11) = 1;
C_Matrix(7,13) = 1;
C_Matrix(8,15) = 1;
C_Matrix(9,17) = 1;
C_Matrix(10,19) = 1;
C_Matrix(11,21) = 1;
C_Matrix(12,23) = 1;
C_Matrix(13,25) = 1;
C_Matrix(14,27) = 1;
C_Matrix(15,29) = 1;
C_Matrix(16,31) = 1;
C_Matrix(17,33) = 1;
C_Matrix(18,35) = 1;
C_Matrix(19,37) = 1;
C_Matrix(20,39) = 1;
C_Matrix(21,41) = 1;
C_Matrix(22,43) = 1;
C_Matrix(22,45) = 1;
C_Matrix(24,47) = 1;
```

# APPENDIX C

# DETAILED MACHINE PART LIST AND ADDED

# FIXTURES

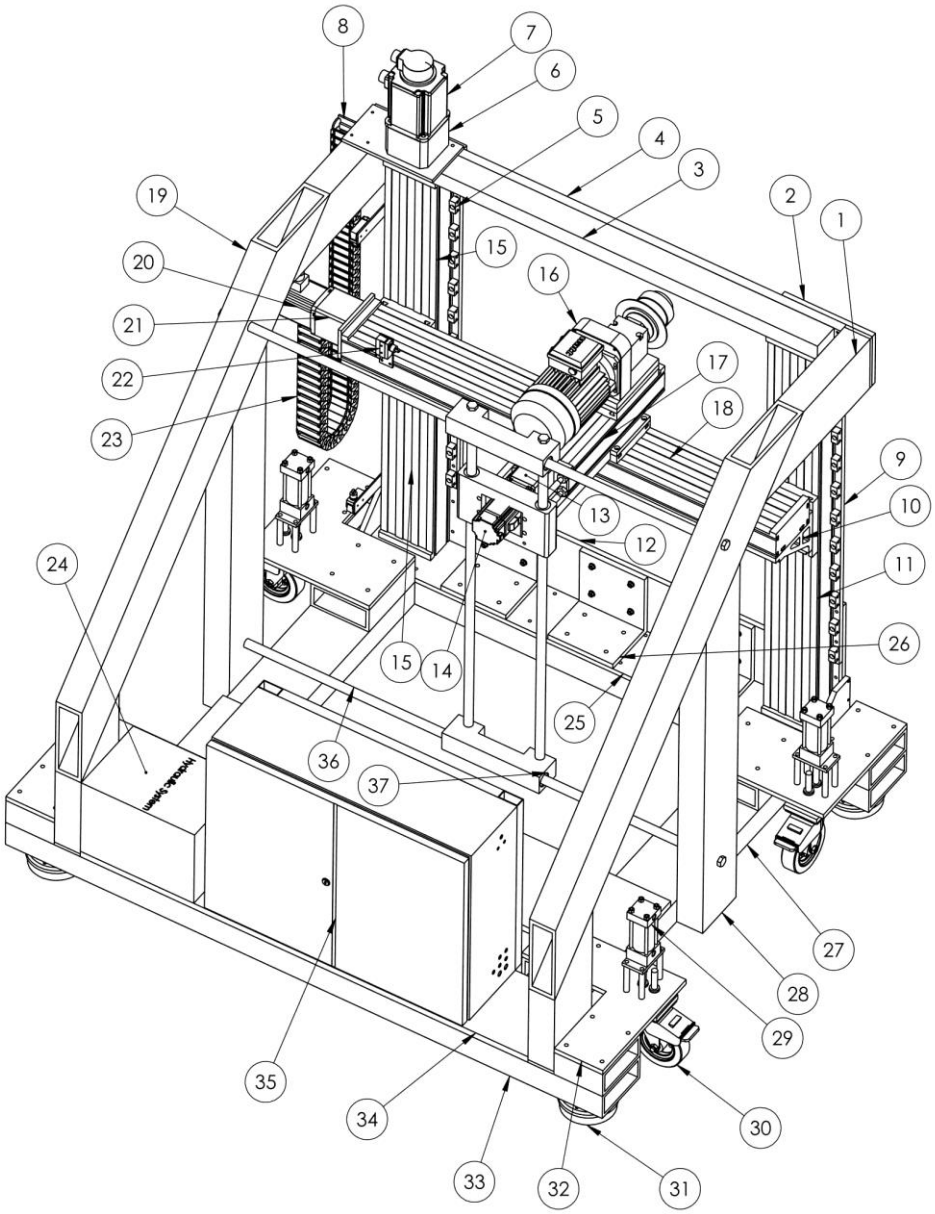


**Figure C-1: Detailed Machine Part List**

The fully assembled machine is seen in Figure C-1 with the detailed machine part list with balloon numbering attached to each part. The name of each part is displayed in Table C-1.

**Table C-1: Machine Parts List**

| No. | Part Name | Material | Dimensions [mm] (length × width × thickness × height) |
|---|---|---|---|
| 1 | Rectangular Profile | Carbon steel | 80×180×10×400 |
| 2 | Plate | Carbon steel | 280×180×15 |
| 3 | Timing belt assembly(T13081 1380) | - | - |
| 4 | Plate | Carbon steel | 1380×50×20 |
| 5 | Mounting Block | - | - |
| 6 | Motor 1 Flange | Carbon steel | - |
| 7 | Motor 1(Servo Motor) | - | - |
| 8 | Plate | Carbon steel | 300×150×10 |
| 9 | Plate | Alloyed steel | 1180×200×15 |
| 10 | Angle Holder (42003 length 1340) | Aluminum | - |
| 11 | Mechanical Linear Motion Module (DLK16010000001380) | - | - |
| 12 | Plate | Carbon steel | 1380×200×15 |
| 13 | Motor 3 Flange | - | - |
| 14 | Motor 3(Servo Motor) | - | - |
| 15 | Mechanical Linear Motion Module (DLK16010000001380) | - | - |
| 16 | Spindle Motor with Cooled Tool Holder | - | - |

| | | | |
|---|---|---|---|
| 17 | Mechanical Linear Motion Module (DSK1601000000460) | - | - |
| 18 | Mechanical Linear Motion Module (DSK16010000001340) | - | - |
| 19 | Rectangular Profile | Carbon steel | 80×180×10×1805 |
| 20 | Motor 2(Servo Motor) | - | - |
| 21 | Motor 2 Flange | - | - |
| 22 | Omron Limit Switch | - | |
| 23 | Electrical Wires Support Chain | - | - |
| 24 | Hydraulic System Box | - | - |
| 25 | Plate | Carbon steel | 1380×200×15 |
| 26 | Angle | Carbon steel | 200×165×16×200 |
| 27 | Rectangular Profile | Carbon steel | 80×180×10×1145 |
| 28 | Rectangular Profile | Carbon steel | 80×180×10×1000 |
| 29 | Hydraulic Cylinder | - | - |
| 30 | Mobility Wheel | - | - |
| 31 | Leveler Foot | Carbon steel | 200×165×16×200 |
| 32 | Plate | Carbon steel | 350×400×10 |
| 33 | Rectangular Profile | Carbon steel | 80×180×10×1840 |
| 34 | Plate | Aluminum 6061 Alloy | 1380×285×15 |
| 35 | Electrical Cabinet | Stainless Steel | - |
| 36 | Rods | Chrome Vanadium Steel | 1380×OD25 |
| 37 | Slider Bearing (LPAR25) | Alloyed Steel | -ID25 |

Figure C-2 show the added fixtures to enhance the machine's x-directional displacements. The machine is more rigid but at the expense of its total volume and weight. The fixtures can be detached and reattached when needed.

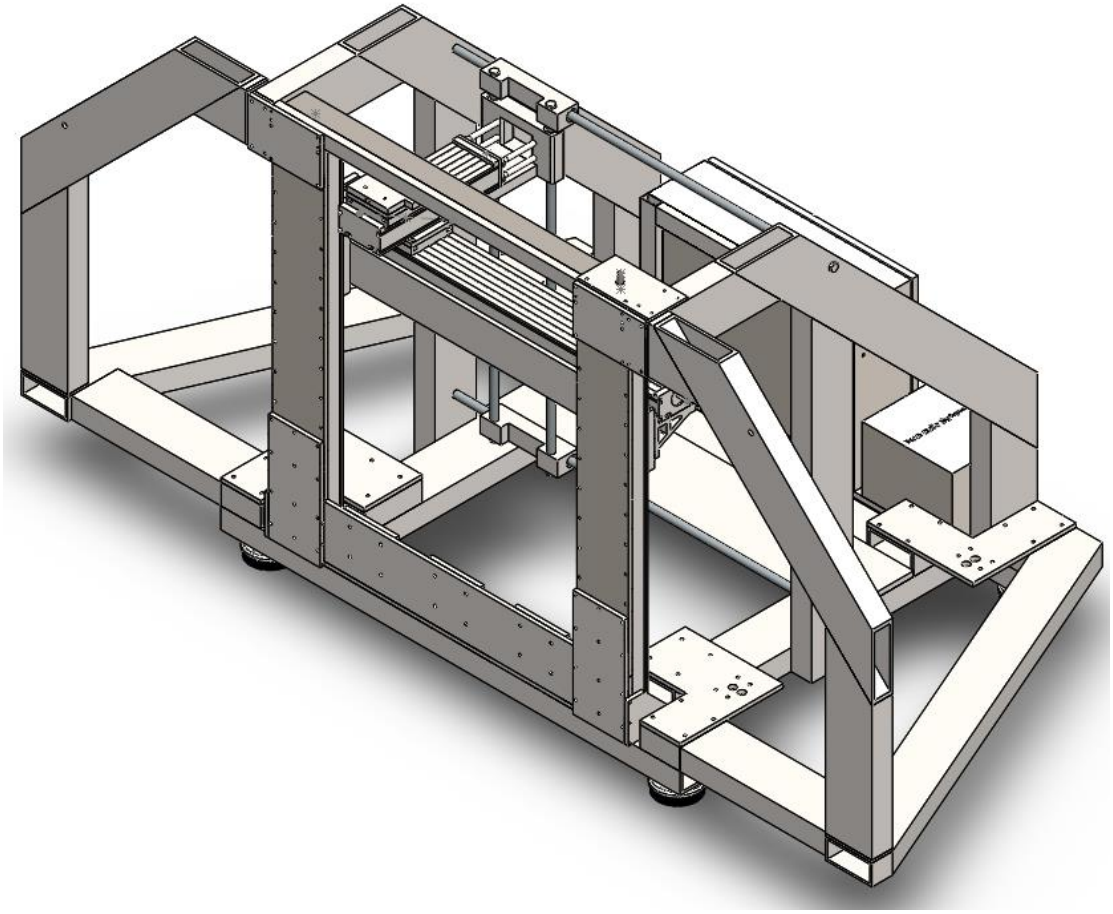

**Figure C-2: Addition of Fixtures**

# APPENDIX D

# SIMPLIFIED EQUATIONS OF MOTION

**Equation 1:**

$$M\ddot{x} + k_{1x}\left(x + \frac{L_x}{2}(tan\theta_1)\theta_y - \frac{L_x}{2}(tan\theta_2)\theta_z\right) + k_{2x}\left(x + \frac{L_x}{2}(tan\theta_1)\theta_y + \frac{L_x}{2}(tan\theta_2)\theta_z\right) + k_{3x}\left(x + \frac{L_x}{2}(tan\theta_1)\theta_y + \frac{L_x}{2}(tan\theta_2)\theta_z\right) + k_{4x}\left(x + \frac{L_x}{2}(tan\theta_1)\theta_y - \frac{L_x}{2}(tan\theta_2)\theta_z\right) = f_X sin\omega_X t$$

**Equation 2:**

$$M\ddot{y} + k_{1y}\left(y + L_z\theta_x + \frac{L_x}{2cos\theta_2}\theta_z\right) + k_{2y}\left(y + L_z\theta_x + \frac{L_x}{2cos\theta_2}\theta_z\right) + k_{3y}\left(y + L_z\theta_x - \frac{L_x}{2cos\theta_2}\theta_z\right) + k_{4y}\left(y + L_z\theta_x - \frac{L_x}{2cos\theta_2}\theta_z\right) = f_y sin\omega_y t$$

**Equation 3:**

$$M\ddot{z} + k_{1z}\left(z - \frac{L_y}{2}\theta_x - \frac{L_x}{2cos\theta_1}\theta_y\right) + k_{2z}\left(z + \frac{L_y}{2}\theta_x - \frac{L_x}{2cos\theta_1}\theta_y\right) + k_{3z}\left(z + \frac{L_y}{2}\theta_x + \frac{L_x}{2cos\theta_1}\theta_y\right) + k_{4z}\left(z - \frac{L_y}{2}\theta_x + \frac{L_x}{2cos\theta_1}\theta_y\right) = f_z sin\omega_z t$$

**Equation 4:**

$$I_x\ddot{\theta}_x + L_z k_{1y}\left(y + L_z\theta_x + \frac{L_x}{2cos\theta_2}\theta_z\right) + L_z k_{2y}\left(y + L_z\theta_x + \frac{L_x}{2cos\theta_2}\theta_z\right) + L_z k_{3y}\left(y + L_z\theta_x - \frac{L_x}{2cos\theta_2}\theta_z\right) + L_z k_{4y}\left(y + L_z\theta_x - \frac{L_x}{2cos\theta_2}\theta_z\right) - \frac{L_y}{2}k_{1z}\left(z - \frac{L_y}{2}\theta_x - \frac{L_x}{2cos\theta_1}\theta_y\right) + \frac{L_y}{2}k_{2z}\left(z + \frac{L_y}{2}\theta_x - \frac{L_x}{2cos\theta_1}\theta_y\right) + \frac{L_y}{2}k_{3z}\left(z + \frac{L_y}{2}\theta_x + \frac{L_x}{2cos\theta_1}\theta_y\right) - \frac{L_y}{2}k_{4z}\left(z - \frac{L_y}{2}\theta_x + \frac{L_x}{2cos\theta_1}\theta_y\right) = 0$$

**Equation 5:**

$$I_y\ddot{\theta}_y + \frac{L_x}{2}(tan\theta_1)k_{1x}\left(x + \frac{L_x}{2}(tan\theta_1)\theta_y - \frac{L_x}{2}(tan\theta_2)\theta_z\right) + \frac{L_x}{2}(tan\theta_1)k_{2x}\left(x + \frac{L_x}{2}(tan\theta_1)\theta_y + \frac{L_x}{2}(tan\theta_2)\theta_z\right) + \frac{L_x}{2}(tan\theta_1)k_{3x}\left(x + \frac{L_x}{2}(tan\theta_1)\theta_y + \frac{L_x}{2}(tan\theta_2)\theta_z\right) + \frac{L_x}{2}(tan\theta_1)k_{4x}\left(x + \frac{L_x}{2}(tan\theta_1)\theta_y - \frac{L_x}{2}(tan\theta_2)\theta_z\right) - \frac{L_x}{2cos\theta_1}k_{1z}\left(z - \frac{L_y}{2}\theta_x - \frac{L_x}{2cos\theta_1}\theta_y\right) - \frac{L_x}{2cos\theta_1}k_{2z}\left(z + \frac{L_y}{2}\theta_x - \frac{L_x}{2cos\theta_1}\theta_y\right) + \frac{L_x}{2cos\theta_1}k_{3z}\left(z + \frac{L_y}{2}\theta_x + \frac{L_x}{2cos\theta_1}\theta_y\right) + \frac{L_x}{2cos\theta_1}k_{4z}\left(z - \frac{L_y}{2}\theta_x + \frac{L_x}{2cos\theta_1}\theta_y\right) = 0$$

**Equation 6:**

$$
\begin{aligned}
I_z\ddot{\theta}_z + \frac{L_x}{2}(tan\theta_2)k_{1x}\left(x + \frac{L_x}{2}(tan\theta_1)\theta_y - \frac{L_x}{2}(tan\theta_2)\theta_z\right) \\
+ \frac{L_x}{2}(tan\theta_2)k_{2x}\left(x + \frac{L_x}{2}(tan\theta_1)\theta_y + \frac{L_x}{2}(tan\theta_2)\theta_z\right) \\
+ \frac{L_x}{2}(tan\theta_2)k_{3x}\left(x + \frac{L_x}{2}(tan\theta_1)\theta_y + \frac{L_x}{2}(tan\theta_2)\theta_z\right) \\
+ \frac{L_x}{2}(tan\theta_2)k_{4x}\left(x + \frac{L_x}{2}(tan\theta_1)\theta_y - \frac{L_x}{2}(tan\theta_2)\theta_z\right) \\
+ \frac{L_x}{2cos\theta_2}k_{1y}\left(y + L_z\theta_x + \frac{L_x}{2cos\theta_2}\theta_z\right) \\
+ \frac{L_x}{2cos\theta_2}k_{2y}\left(y + L_z\theta_x + \frac{L_x}{2cos\theta_2}\theta_z\right) \\
+ \frac{L_x}{2cos\theta_2}k_{3y}\left(y + L_z\theta_x - \frac{L_x}{2cos\theta_2}\theta_z\right) \\
+ \frac{L_x}{2cos\theta_2}k_{4y}\left(y + L_z\theta_x - \frac{L_x}{2cos\theta_2}\theta_z\right) = T_z sin\omega_{zT}t
\end{aligned}
$$

# References


1. Shah, S. and S. Tosunoglu. *Friction stir welding: current state of the art and future prospects*. in *16th World Multi-Conference on Systemics, Cybernetics and Informatics, Orlando, Florida*. 2012.
2. Company, O. *Orbitalum Cutting and Welding*. [cited 2015 10/12]; Available from: http://www.orbitalum.de/en/home.html.
3. Company, A. *Axxair Inovative Orbital Solutions*. [cited 2015 10/12]; Available from: http://www.axxair.com/en/.
4. MegaStir. *MegaStir a Venture of Schlumberger and Advanced Metal Products*. [cited 2015 10/12]; Available from: http://www.slb.com/services/megastir.aspx.
5. Technologies, G. *Gatwick Technologies Special Joining and Forming Processes*. [cited 2015 10/12]; Available from: http://www.gatwicktechnologies.com/.
6. Masithulela, F., *Conceptual design of a friction stir welding machine for joining rails*. 2010.
7. Murali, S. and Y.B. Rao, *A Simple Tubesheet Layout Program for Heat Exchangers.* American Journal of Engineering and Applied Sciences, 2008. **1**(2).
8. Kim, S.-T., S.-Y. Kim, I.-S. Lee, Y.-S. Park, M.-C. Shin, and Y.-S. Kim, *Effects of shielding gases on the microstructure and localized corrosion of tube-to-tube sheet welds of super austenitic stainless steel for seawater cooled condenser*. Corrosion Science, 2011. **53**(8): p. 2611-2618.
9. Moorthy, V., S. Vaidyanathan, T. Jayakumar, and B. Raj, *Evaluation of post-weld heat treatment in 2.25 Cr–1Mo steel tube to tube sheet welded joints using magnetic Barkhausen noise measurements.* Materials Science and Technology, 1997. **13**(7): p. 614-617.
10. Gibson, B., D. Lammlein, T. Prater, W. Longhurst, C. Cox, M. Ballun, K. Dharmaraj, G. Cook, and A. Strauss, *Friction stir welding: process, automation, and control.* Journal of Manufacturing Processes, 2014. **16**(1): p. 56-73.
11. Burford, D.A., E.H. Fenn, D.R. High, and R.M. Kay, *System and associated friction stir welding (FSW) assembly, controller and method for performing a friction stir welding operation*. 2007, Google Patents.
12. Cook, G.E., R. Crawford, D.E. Clark, and A.M. Strauss, *Robotic friction stir welding.* Industrial Robot: An International Journal, 2004. **31**(1): p. 55-63.
13. De Backer, J., A.-K. Christiansson, J. Oqueka, and G. Bolmsjö, *Investigation of path compensation methods for robotic friction stir welding.* Industrial Robot: An International Journal, 2012. **39**(6): p. 601-608.
14. Smith, C.B. *Robotic friction stir welding using a standard industrial robot*. in *2nd International Friction Stir Welding Symposium, Gothenburg, Sweden, TWI, Published on CD*. 2000. Citeseer.
15. Kusuda, Y., *Honda develops robotized FSW technology to weld steel and aluminum and applied it to a mass-production vehicle.* Industrial Robot: An International Journal, 2013. **40**(3): p. 208-212.

16. Fan, X., C. Xu, Z. Zhang, and X. Jin, *Vibration Testing and Analysis of Dynamic Characteristics of a Reconfigurable Turn-Milling Machine Tool.* 2010: p. 898-902.
17. Ebrahimi, M. and R. Whalley, *Analysis, modeling and simulation of stiffness in machine tool drives.* Computers & industrial engineering, 2000. **38**(1): p. 93-105.
18. Beltrán Carbajal, F., E. Chávez Conde, A. Favela Contrera, and R.F. Vázquez Bautista, *Active Perturbation Rejection in Motion Control of Milling Machine Tools.* Revista Facultad de Ingeniería, 2014(69): p. 193-204.
19. Morar, L., L.-C. Pop, and M.-Z. Ciortea. *A comparative approach to the NC axis dynamic behaviour modelling*. in *Management and Control of Production and Logistics*. 2007.
20. Sciavicco, L. and B. Siciliano, *Modelling and control of robot manipulators*. 2000: Springer Science & Business Media.
21. Chen, W., *Dynamic modeling of multi-link flexible robotic manipulators.* Computers & Structures, 2001. **79**(2): p. 183-195.
22. Le, A.Y., J.K. Mills, and B. Benhabib, *Dynamic modeling and control design for a parallel-mechanism-based meso-milling machine tool.* Robotica, 2014. **32**(04): p. 515-532.
23. Huo, D., K. Cheng, and F. Wardle, *Design of a five-axis ultra-precision micro-milling machine—UltraMill. Part 2: integrated dynamic modelling, design optimisation and analysis.* The International Journal of Advanced Manufacturing Technology, 2010. **47**(9-12): p. 879-890.
24. Hung, J.-P., Y.-L. Lai, C.-Y. Lin, and T.-L. Lo, *Modeling the machining stability of a vertical milling machine under the influence of the preloaded linear guide.* International Journal of Machine Tools and Manufacture, 2011. **51**(9): p. 731-739.
25. Tian, H., B. Li, H. Liu, K. Mao, F. Peng, and X. Huang, *A new method of virtual material hypothesis-based dynamic modeling on fixed joint interface in machine tools.* International Journal of Machine Tools and Manufacture, 2011. **51**(3): p. 239-249.
26. Mendes, N., P. Neto, A. Loureiro, and A.P. Moreira, *Machines and control systems for friction stir welding: a review.* Materials & Design, 2016. **90**: p. 256-265.
27. Okawa, Y., M. Taniguchi, H. Sugii, and Y. Marutani. *Development of 5-axis friction stir welding system*. in *SICE-ICASE, 2006. International Joint Conference*. 2006. IEEE.
28. Lijin, F. and S. Longfei, *Design of a novel robotic arm with non-backlash driving for friction stir welding process.* The International Journal of Advanced Manufacturing Technology, 2017: p. 1-14.
29. Batistoni, M. and A. Georges, *Method of automatic welding*. 1984, Google Patents.
30. Monley, R.E., *Method for continuously welding a plurality of tubes disposed in multiple rows to a tube sheet*. 1982, Google Patents.
31. Eller, M.R. and L. Zhixian, *Method and apparatus for friction stir welding tube ends for a heat exchanger*. 2015, Google Patents.
32. Al-Badour, F.A., N. Merah, A. Shuaib, and A. Bazoune, *Experimental Investigation of Friction Stir Seal Welding of Tube–Tubesheet Joints.* Journal of Pressure Vessel Technology, 2015. **137**(1): p. 011402.

33. Shuaib, A.R., F. Al-Badour, and N. Merah. *Friction Stir Seal Welding (FSSW) Tube-Tubesheet Joints Made of Steel*. in *ASME 2015 Pressure Vessels and Piping Conference*. 2015. American Society of Mechanical Engineers.
34. Shuaib, A.N., N. Merah, F.A. Al-Badour, and A. Bazoune, *Apparatus for joint sealing using tube expansion and friction welding*. 2015, Google Patents.
35. Al-Badour, F., *Numerical and Experimental Investigations of Friction Stir Welding of Tube-Tubesheet Joints*, in *Department of Mechanical Engineering*. May 2012, King Fahd University of Petroleum and Minerals: Dhahran.
36. Shuaib, A., Merah, N. and Bazoune, A., *Developing A Friction Stir Welding Process For Joining Similar And Dissimilar Materials In Heat Transfer Equipment.* NSTIP project # 08-ADV66-4-4, 2013.
37. Burford, D., C. Widener, and B. Tweedy. *Advances in friction stir welding for aerospace applications*. in *6th AIAA Aviation Technology, Integration and Operations Conf.(ATIO)*. 2006.
38. Modultechnik, B. *Linear Drives*. 2018; Available from: https://www.bahr-modultechnik.de/de/dl-rollenfuehrung.
39. Delta, *Servo Motor*. 2017.
40. Rao, S.S. and F.F. Yap, *Mechanical Vibrations*. 2011: Prentice Hall.
41. Rao, S.S. and F.F. Yap, *Mechanical vibrations*. Vol. 4. 2011: Prentice Hall Upper Saddle River.
42. DELTA. *CNC Machine Tool Solutions*. 2017; Available from: http://www.deltaww.com/Products/CategoryListT1.aspx?CID=060202&PID=787&hl=en-US&Name=CNC%20Machine%20Tool%20Solutions.
43. Crawford, R., G.E. Cook, A.M. Strauss, and D.A. Hartman, *Modelling of friction stir welding for robotic implementation.* International Journal of Modelling, Identification and Control, 2006. **1**(2): p. 101-106.
44. Systèmes, D., *Solidworks*. 2015.
45. Crandall, S.H. and W.D. Mark, *Random vibration in mechanical systems*. 2014: Academic Press.

# VITAE


| | |
|---|---|
| Name | :Mohammedanas Tuffaha |
| Nationality | :Palestinian |
| Date of Birth | :8/7/1989 |
| Email | :tuffahamech@gmail.com |
| Address | :Hebron, Palestine |
| Academic Background | :BSc. In Mechanical Engineer |